Dr.-ing. thesis

Tor Anders Hauge

Roll-out of Model Based Control with Application to Paper Machines

Tor Anders Hauge

NTNU Trondheim
Norwegian University of
Science and Technology

Dr.-ing. thesis 2003:31
Telemark University College
Faculty of Technology

Dr.-ing. thesis 2003:31

NTNU

ISBN 82-471-5581-8
ISSN 0809-103X

Roll-out of model based control with application to paper machines

Tor Anders Hauge
Telemark University College
Faculty of Technology
Porsgrunn, Norway

Thesis submitted to the
Norwegian University of Science and Technology
for the degree of Dr.ing.

Contents

Preface and acknowledgments

This thesis is submitted in partial fulfillment of the requirements for the degree of *doktor ingeniør* (dr.ing.) at the Norwegian University of Science and Technology (NTNU) and Telemark University College (HIT). The work is carried out with financial support from the Research Council of Norway through project 134557/432, and Norske Skog Saugbrugs through the project "Stabilization of the wet end at PM6". This financial support is gratefully acknowledged.

In 1999, the intention of this work was to investigate "*Methods for efficient roll-out of robust model based control in the process industry*"[1], i.e. how do we efficiently develop and apply a model based controller for a number of similar processes or process units. Four terms were to be focused on: modeling, robust control, roll-out, and a case study. The reader of this thesis will find lots of pages on modeling and model predictive control (MPC), none on robust control, some pages on roll-out, and almost all pages related to the case study: paper machines. Although it was not the intention to have such a strong focus on the case study, it seemed that with such practical issues as modeling, control and roll-out in the process industry, it was beneficial to discuss an actual industrial plant rather than some fabricated model. Thus, the title of this thesis was changed to "*Roll-out of model based control with application to paper machines*" to better reflect the focus of this work. Nevertheless, it is my hope and belief that this work should also be of interest beyond the pulp and paper community, as modeling, control, and roll-out have many similarities across various process industries.

I have spent the time from September 1999 to December 2002 working on this thesis, and I have had the pleasure of meeting and interacting with so many brilliant and nice persons from both industry and colleges/universities. A number of them deserve special recognition.

First I would like to thank my supervisor associate professor Bernt Lie, at Telemark University College (HIT). Thank you for encouraging me to study for the degree of dr.ing, for providing financial funding for my study, and for guidance, tips, hints, corrections, and valuable discussions along the way. It is funny, and a bit frustrating, thinking how I imagined that I would really be an expert in a niche after finishing my doctoral degree, only to find out that I still have "a world" to learn before I have the wealth of knowledge that you have.

I deeply appreciated having two co-supervisors with great professional skill to rely

[1] Working title for this thesis.

on. Thank you associate professor Rolf Ergon (HIT) for always being helpful and interested in my work, for functioning as supervisor while Bernt was on sabbatical leave, for collaboration on two M.Sc. theses and one conference article, and for pleasant lunch breaks and discussions. Although my contact with dr. Steinar Sælid (Prediktor) has been less frequent, I want to thank him for his tips and comments on modeling and his repeated comment "make the model simpler" which I know have been very important.

The person that I have had most professional contact with during these years is Mr. Roger Slora from Norske Skog Saugbrugs. He took the initiative to, and is the project leader for, the "Stabilization of the wet end at PM6" project at Norske Skog Saugbrugs. I am very grateful that I was given the opportunity to work in this exiting project, with its enthusiastic, positive, and technically skilled leader. And I feel privileged to have had an industrial partner so eager to turn theoretical studies into practical implementations. I would also like to thank the other project members: Mr. Jan Tore Gjøby (specialist on the Saugbrugs DCS system), Mr. Øystein Jonassen (specialist on the Saugbrugs measurement devices), Mr. Hans Erik Høydahl (chemistry specialist from Norske Skog Research), and Mr. Hans Hoel (chemistry specialist from Norske Skog Research), as well as managers at Saugbrugs that dared to invest time and money in the project; specifically Mr. Eilert Vikesland (Development Manager), Mr. Per Ivar Berg (now Mill Manager at Norske Skog Follum), and Mr. Vidar Backstrøm (Senior Production Manager).

A couple of years ago, associate professor Bernt Lie and his doctoral students formed The Cybernetics Research Group (CYNERG at www.hit.no/cynerg) at Telemark University College (www.hit.no). As of today the CYNERG doctoral students are Glenn-Ole Kaasa (whom I shared office with), Martha Dueñas Díez, and Beathe Furenes. Thank you fellow CYNERG doctoral students for warm and joyful memories, for making the lunch break a highlight of the day, and for friendship and support during good and hard times.

I would also like to thank Dr. Hong Wang for being my kind host during my short visit to UMIST Department of paper science in December 2001, associate professor David Di Ruscio at HIT for help on system identification issues, Anders Veberg from Prediktor AS for MPC collaboration, Glenn-Ove Forsland and Ståle Enes for their contributions through their M.Sc. theses, process engineer Tor Gunnar Heggli at Norske Skog Skogn for providing data and information about PM3, colleagues in the department of process automation at HIT for providing a fine working environment, the administration at the faculty of technology at HIT (Trine Ellefsen, Stig F. Nilsen, Eldrid Eilertsen, and more) for always being helpful with keeping account of my income and expenditure, paying my bills, and other non-technical problems, and the library personnel at HIT, Porsgrunn campus, for providing any obscure article that I have requested.

Finally, I am indebted to my wife Randi Katrine for her support during these years, and to our children Daniel and Emilie for keeping my mind off of modeling and control for at least a few hours every day.

Porsgrunn, December 2002
Tor Anders Hauge

Summary and conclusions

Abstract A mechanistic nonlinear model of the wet end of paper machine 6 (PM6) at Norske Skog Saugbrugs, Norway has been developed, and used in an MPC application. The MPC provides reduced variability in many key variables, and better efficiency through faster grade changes, start ups, and improved control during periods of poor measurements. The model and controller can be rolled-out to other paper machines, as found by studying and fitting the model to data from PM4 at Norske Skog Saugbrugs, and PM3 at Norske Skog Skogn, Norway. No changes to the model, except for parameter values, were introduced, and still the validation results were good. The time spent on fitting and validating the PM6 model to PM4 and PM3 are approximately 1% of the time spent on developing the original model. This should be a strong incentive for focusing on mechanistic modeling in industries were there are many similar production lines or units.

Motivation Many large- and medium sized industry companies have a number of more or less similar process-units for processing of raw materials or production of finished products. An industrial company which has invested, or is about to invest, in advanced model based control in one of their units / factories, would benefit economically if the model and controller could be efficiently rolled-out at similar units. The main idea of this thesis is to develop a model and a controller for an industrial process, and then investigate how the model and controller can be applied to similar processes. Paper machine 6 (PM6) at Norske Skog Saugbrugs, Norway, is used as a case study for modeling and control throughout the thesis, and the PM6 model is also applied at Norske Skog Saugbrugs PM4, and PM3 at Norske Skog Skogn, Norway.

The papermaking process is the only process studied in this thesis, however the field of roll-out should be of interest also to other industries. For example Borealis (www.borealisgroup.com) has many polymer reactors for producing plastics raw materials, Norsk Hydro (www.hydro.com) has many plants for fertilizer production, and Icopal (www.icopal.com) has many production lines for extrusion of plastic pipes. The idea of efficient roll-out of models is not entirely new, e.g. (Glemmestad, Ertler & Hillestad 2002) emphasize the advantage of reusing the models developed at Borealis, and many commercial simulators include model libraries of process units intended for reuse.

The control method chosen in this work is model predictive control (MPC). The reason for choosing MPC is that it is perhaps the only advanced model based control

scheme used to any extent in the industry, there are commercially available software systems for implementation, and the reported payback time is low (e.g. 3 months in (Bassett & Van Wijck 1999)).

Modeling Two basic modeling approaches are *mechanistic* modeling and *empiric* modeling. An empiric model is entirely based on experimental data and an appropriate model structure, and often requires little knowledge of the system to be modeled. A mechanistic model is a model built from basic principles of physics, chemistry, biology, etc., by writing down conservation or balance equations. Obviously this requires extensive knowledge of the process to be modeled. Emphasis has been on mechanistic modeling of PM6, however empiric modeling is also carried out and described in this thesis.

A high order mechanistic model of PM6 was developed and implemented in Matlab. The objective was to make a model of a limited part of PM6, which were suitable for model predictive control (MPC) , captured the essential dynamic behavior of the process, and was applicable over a wide range of operating conditions. The output variables are the basis weight, the paper ash content and the white water total concentration. To make the model suitable for model based control, reduced order models were developed and fitted to experimental and operational mill data. The fitted models where validated with historical operational data.

An augmented suboptimal Kalman filter has been developed at PM6 for estimating the states and some of the parameters in the paper machine model. Three biases have been selected for on-line estimation in the paper machine model. The first two are biases in the estimated total- and filler thick stock consistencies. These disturbances are estimated using a ballistic estimator, and thus they are assumed to be good candidates for having time-varying biases. The third bias estimated on-line is for the total wire tray concentration, i.e. a bias in one of the outputs. In theory, and in the true Kalman filter, the noise characteristics of the process should be found and used in the Kalman filter equations. However, these characteristics are hard, if not impossible, to find. Thus, a suboptimal Kalman filter was identified, where the noise characteristics where used as tuning parameters until satisfactory Kalman filter performance was obtained.

MPC The MPC was installed at PM6 in March 2002. During the first two months, the MPC, the Kalman filter and the model were continuously tuned, retuned, and validated in open and closed loop. Some structural changes were also made during these months. From May 2002, the MPC has been in operation more or less continuously. The process operators still have the original "pre-MPC era" control configuration available, but the MPC has been the preferred choice from the beginning. Furthermore, the operators have been very active in making suggestions for improvements and new features in the system. Some of these suggestions are implemented, and others are being considered for implementation.

A specific feature of the MPC implemented at PM6 is that the setpoints for new grades can be submitted to the MPC some time before the grade change. The operators can specify a grade change e.g. half an hour into the future, and see how

the MPC will achieve the change: how the inputs will be manipulated to reach the new setpoints. In terms of gaining operator acceptance for the MPC, this feature of previewing the action taken by the controller has been very helpful.

Results The work carried out on modeling and MPC of PM6 has been part of a project called "Stabilization of the wet end at PM6". The main objective of the project was to increase the total efficiency by 0.47%. This is an objective that is hard to measure, due to many factors affecting the total efficiency. Thus, several sub-goals were defined which were assumed easier to measure and validate. The sub-goals, and results, concerning reduced variability are:

Variable	**Sub-goal (red. std. dev.)**	**Result**
Total cons. in the wire tray	60%	Achieved
Filler cons. in the wire tray	50%	Achieved
Total cons. in the headbox	50%	Achieved
Filler cons. in the headbox	35%	Achieved
Basis weight	20%	Not achieved
Paper ash	20%	Achieved
Paper moisture	20%	Achieved

These sub-goals were defined in 1999 when the project was initiated. In 2001 a new scanning device for measuring e.g. basis weight and paper ash was installed at PM6. This significantly improved the control of the basis weight using the "old" controllers. The results in the table above are calculated with the measurement devices as of 2002, comparing the old control configuration with the MPC control configuration. Exact numbers for the reduction in standard deviation are not given, as they vary from day to day, and from operator to operator.

In addition to reducing the variation in key paper machine variables, several other benefits are obtained using MPC. Some of these benefits arise from utilizing the developed model, not only for control purposes, but also as a replacement for measurements when these are not available or not trustworthy.

Previously, grade changes were carried out manually or partly manually (the setpoints were changed a number of times before they were equal to the new grade) by the operators. With a mechanistic model, applicable over a wide range of operating conditions, the grade changes are carried out using the MPC. This has resulted in faster grade changes and operator independent grade changes. During larger grade changes, the use of MPC results in less off-spec paper being produced during the change. Using a single mechanistic model, the grade change is handled in a straight forward fashion, as there is no need to switch between various local models.

The basis weight and paper ash outputs can not be measured during sheet breaks. Previously during sheet breaks, the flow of thick stock and filler were frozen at the value they had immediately prior to the break. Usually the sheet breaks last less than half an hour, and the output variables are not far from target values when the paper is back on the reel. However, occasionally the sheet breaks last longer periods and there may be e.g. velocity changes during the break, leading to off-spec paper

being produced for a period after the paper is back on the reel. Another frequently experienced problem are large measurement errors immediately after a sheet break. With the MPC, the Kalman filter estimates the basis weight and paper ash during sheet breaks, and these estimates are used in the MPC as if no break had taken place. Thus, when the paper is back on the reel, the outputs are close to their setpoints.

Previously, the controllers were not set to automatic mode before the outputs were close to the setpoints, following a start up. With a model based controller using a mechanistic model with a wide operating range, the MPC is set to automatic mode early during start ups. This results in faster start ups, and less off-spec paper being produced.

Occasionally a special filler is added to the stock, to increase the brightness of the paper. During these periods the consistency measurements are not trustworthy as they are based on optical measurement methods. This problem is solved within the MPC / Kalman filter framework by neglecting the measured consistency, relying on the estimate alone. For each output, there is an option within the MPC to neglect the updating of states based on this output. This is done based on experience with periods of poor measurements, even when only standard filler is used.

The Kalman filter estimates are used in the MPC instead of the measurements. This leads to smoother controller action, and eliminates the need for additional filtering.

The model is augmented so that some key parameters/biases are updated automatically. This reduces the need for model maintenance off-line. However, should there be larger changes in the process, such as if the white water tank is removed, or a new retention aid is used, then it will probably be necessary to re-tune the model and controller.

Roll-out The possibility of reusing the PM6 model at other paper machines is investigated. The paper machines studied are PM4 at Norske Skog Saugbrugs, and PM3 at Norske Skog Skogn, Norway. PM6 is a new and modern paper machine producing SC (Super Calendered) magazine paper. PM4 also produce SC paper but the machine is older and smaller than PM6. PM3 produce newsprint and has a size comparable with that of PM6. Fitting and validation of the model to PM4 and PM3 were very promising. No changes to the model, except for parameter values, were introduced and still the validation results were good. The time spent on fitting and validating the PM6 model to PM4 and PM3 are approximately 1% of the time spent on developing the original model. This should be a strong incentive for focusing on mechanistic modeling in industries were there are many similar production lines or units.

Part I

Overview

Chapter 1

Introduction

1.1 Problem description

Many large- and medium sized industry companies have a number of more or less similar process-units for processing of raw materials or production of finished products. An industrial company which has invested, or is about to invest, in advanced model based control in one of their units / factories, would benefit economically if the model and controller could be efficiently rolled-out on similar units. The main idea of this thesis is to develop a model and a controller for an industrial process, and then investigate how the model and controller can be applied to similar processes. Paper machine 6 (PM6) at Norske Skog Saugbrugs, Norway, is used as a case study for modeling and control throughout the thesis, and the PM6 model is also applied at Norske Skog Saugbrugs PM4, and PM3 at Norske Skog Skogn, Norway. Pulp and paper is one of the largest and most important industries in Norway. In 2001, a total of 25 pulp and paper mills, and 7,300 employees contributed with aggregate sales of about NOK[1] 19,000 million. Approximately 90% of the Norwegian made paper and boards are exported, mostly to EU countries, but also to North America, Asia, Oceania, Eastern Europe, Latin America, and Africa (NPPA (The Norwegian Pulp and Paper Association) 2002) (Statistics Norway 2002*b*) (Statistics Norway 2002*a*).

The papermaking process is the only process studied in this thesis, however the field of roll-out should be of interest also to other industries. For example Borealis (www.borealisgroup.com) has many polymer reactors for producing plastics raw materials, Norsk Hydro (www.hydro.com) has many plants for fertilizer production, and Icopal (www.icopal.com) has many production lines for extrusion of plastic pipes.

The control method chosen in this work, is model predictive control (MPC). The reason for choosing MPC is that it is perhaps the only advanced model based control scheme used to any extent by the industry, there are commercially available software systems for implementation, and the reported payback time is low (e.g. 3 months in (Bassett & Van Wijck 1999)).

[1] NOK is the Norwegian currency. 1 Euro equals NOK 7.3, and 1 U.S. dollar equals NOK 7.3, November 22, 2002.

1.2 Previous work

There exists very little published material focusing on how to efficiently roll-out models and controllers in the industry. However, the idea of efficient roll-out of models is not entirely new, e.g. (Glemmestad et al. 2002) emphasize the advantage of reusing the models developed at Borealis, and many commercial simulators include model libraries of process units intended for reuse.

Empirical modeling or system identification of paper machines are reported in several papers and books. Some of these focus on so-called cross-directional (CD) modeling, i.e. a model for the profile across the paper web, e.g. (Featherstone, VanAntwerp & Braatz 2000), (Campbell 1997) and (Heaven, Manness, Vu & Vyse 1996). Others focus on the machine-direction (MD), i.e. changes in average values across the web, e.g. (Menani, Koivo, Huhtelin & Kuusisto 1998), (Noreus & Saltin 1998), and Papers A–B in this thesis. Note that only the MD modeling and control problem is studied in this thesis.

The reported works on mechanistic modeling of paper machines are in most cases constrained to smaller parts of the paper machine. However, (Rao, Xia & Ying 1994), (Larsson & Olsson 1996) and (Hagberg & Isaksson 1993) consider a larger part of the paper machine, e.g. the wet end and the wire, press, and dryer sections, although the chemistry involved in papermaking is not considered at all. Mechanistic models of a larger part of a paper machine which includes chemical modeling is found in (Shirt 1997), and Papers A–C in this thesis. In Shirt's work both chemical aspects, which include adsorption and flocculation, and physical aspects, which include drainage on the wire, refining, tanks, headbox, wire section, etc., are part of the overall model, although transportation delays in pipelines are neglected and not all aspects are presented in detail.

Several MPC implementations using multivariable empiric paper machine models are reported, e.g. (McQuillin & Huizinga 1995), (Lang, Tian, Kuusisto & Rantala 1998), (Mack, Lovett, Austin, Wright & Terry 2001), (Kosonen, Fu, Nuyan, Kuusisto & Huhtelin 2002), and (Austin, Mack, Lovett, Wright & Terry 2002). To the best of the author's knowledge, there exists no reported industrial MPC implementations utilizing a multivariable mechanistic model of the wet-end of the paper machine. Some industrial implementations of MPC with mechanistic models are known in other industry areas, e.g. (Qin & Badgwell 1998) and (Badgwell & Qin 2001) have reported a few implementations. Papers describing industrial implementations of MPC with mechanistic models are few, however (Hillestad & Andersen 1994) and (Glemmestad et al. 2002) report several applications to industrial polymer reactors. Several simulated examples exist, e.g. (Lee, Lee, Yang & Mahoney 2002), (Prasad, Schley, Russo & Bequette 2002), (Amin, Mehra & Arambel 2001), and (Schei & Singstad 1998), and also some applications to experimental test stands, e.g. (Ahn, Park & Rhee 1999) and (Park, Hur & Rhee 2002).

1.3 Outline of thesis

This thesis is composed of two parts. Part I basically gives an overview of the results obtained in the papers provided in Part II. However, a few results in Part I are not presented in any paper, either because they did not fit with the scope of the papers or because the results were not ready at the time of submission or publishing. Due to the structure of the thesis, some pieces of information are necessarily repeated several times; for example most papers have a section on description of the process. Also, some papers have similar scopes, notably papers A–C, and thus some information is repeated. Note that the papers in Part II are not entirely reproduced from the original source. In most papers a few corrections are made, e.g. pure spelling errors are corrected, and some papers are extended by adding material that was thought to be of interest in this thesis. The character of the modifications for each paper are given in Chapter 6 as well as at the start of each paper.

Chapter 2 gives an introduction to paper production. Some facts and statistics for the pulp and paper industry are given, and the production line from tree to paper is explained. Modeling aspects are discussed in Chapter 3, and results from the modeling of PM6 is summarized. Chapter 4 concentrates on model predictive control (MPC). The chapter consists of a short introduction to MPC, as well as results from the implementation at PM6, Norske Skog Saugbrugs, Norway. Chapter 5 summarizes the results from applying the PM6 model to other paper machines. Chapter 6 lists the papers appearing in the thesis, and Chapter 7 lists contributions not included in the thesis.

Abstract of Paper A A mechanistic model of order 528 of PM6 is implemented in Matlab. It is shown how the full scale model can be reduced by both system identification techniques and by utilizing physical knowledge about the process. The long term prediction abilities of the various reduced order models are compared with the output from the 528 order model, highlighting some distinct features of the various models.

Abstract of Paper B This paper summarize some of the results from Paper A, and also provides results from using industrial data from PM6. Closed loop experiments on PM6 is described and carried out, and empiric models are identified and validated. A solution for estimating missing measurements during sheet breaks is presented and demonstrated with simulations.

Abstract of Paper C Details of the mechanistic model of PM6 is presented. The model is developed as a foundation for the control of three selected variables, the basis weight, the paper ash content and the white water total concentration. The model is of high order and reduced order models are developed and fitted to experimental mill data. The fitted models are validated with historical operational data.

Abstract of Paper D Results from a controllability analysis, based on a linearized PM6 model, is given. The analysis indicates the necessity of process operators acting on measured disturbances to avoid input saturation. A commercially available MPC algorithm based on a linear model is modified to handle the nonlinear model, and to allow for future setpoint changes.

Abstract of Paper E Four quadratic programming (QP) formulations of model predictive control (MPC) are compared with regards to ease of formulation, memory requirement, and numerical properties. The comparison is based on two example processes: A linearized PM6 model, and a model of the Tennessee Eastman challenge process; the number of free variables range from 150–1400. Five commercial QP solvers are compared. Preliminary results indicate that dense solvers still are the most efficient, but sparse solvers hold great promise.

Abstract of Paper F The PM6 model is used in an MPC implementation. The MPC uses an infinite horizon criterion, successive linearization of the model, and estimation of states and parameters by an augmented Kalman filter. Variation in important quality variables and consistencies in the wet end have been reduced substantially, compared to the variation prior to the MPC implementation. The MPC also provides better efficiency through faster grade changes, control during sheet breaks and start ups, and better control during periods of poor measurements. From May 2002 the MPC has been the preferred controller choice for the process operators at PM6.

Abstract of Paper G The possibility of reusing the PM6 model at other paper machines is investigated. The paper machines studied are PM4 at Norske Skog Saugbrugs, and PM3 at Norske Skog Skogn, Norway. PM6 is a new and modern paper machine producing SC (Super Calendered) magazine paper. PM4 also produce SC paper but the machine is older and smaller than PM6. PM3 produce newsprint and has a size comparable with that of PM6. Fitting and validation of the model to PM4 and PM3 data were very promising. No changes to the model, except for parameter values, were introduced and still the validation results were good. The time spent on fitting and validating the PM6 model to PM4 and PM3 data are approximately 1% of the time spent on developing the original model. This should be a strong incentive for focusing on mechanistic modeling in industries were there are many similar production lines or units.

1.4 Main contributions

The main contributions of this thesis are:

- A mechanistic model of the wet end of a paper machine is developed, fitted with data, and validated: Chapter 3, and Papers A–C.

- Extensions to a previously published infinite horizon criterion by (Muske & Rawlings 1993). Extensions include e.g. the possibility to specify future reference changes, direct input to output term, and inclusion of measured disturbances. Chapter 4, and Papers D–F.
- Algorithm for nonlinear infinite horizon MPC, based on successive linearization of mechanistic model: Chapter 4, and Paper F.
- Industrial application of nonlinear MPC with a mechanistic model: Chapter 4, and Paper F.
- Investigation of the roll-out potential of the mechanistic model: Chapter 5, and Paper G.

Chapter 2

Paper production

2.1 Facts and statistics

Pulp and paper industry in Norway and worldwide (Sources: (NPPA (The Norwegian Pulp and Paper Association) 2002), (Statistics Norway 2002*b*), and (Statistics Norway 2002*a*))

Pulp and paper is one of the largest and most important industries in Norway. In 2001, a total of 25 pulp and paper mills, and 7,300 employees contributed with aggregate sales of about NOK[1] 19,000 million. Approximately 90% of the Norwegian made paper and boards are exported, mostly to EU countries, but also to North America, Asia, Oceania, Eastern Europe, Latin America, and Africa.

On a worldwide basis, the production of paper and boards in Norway is not large. The total world production of paper and board in the year 2000 was 323 million tons, and the Norwegian share was "only" 2.4 million tons. The largest producer is by far USA with a production of 85.5 million tons, with other large producers being Japan, and Canada. Finland and Sweden are also large on a world wide basis, producing above 10 million tons each.

Norske Skog (Source: (Norske Skog 2002))

The Norske Skog group is the world's second largest producer of newsprint, and the world's third largest supplier of printing paper. Norske Skog employs 14,000 people in 24 production units (full- and part-owner) spread around Europe, North and South America, Asia and Oceania. The operating revenue for 2001 exceeded NOK 30,000 million, and the earnings were close to NOK 2,500 million. In terms of area, the European revenue accounts for nearly half the total revenue. In terms of product, the newsprint is by far the largest contributor accounting for 68% of the revenue, and pulp and SC[2] magazine paper accounts for 10% each.

[1] NOK is the Norwegian currency. 1 Euro equals NOK 7.3, and 1 U.S. dollar equals NOK 7.3, November 22, 2002.

[2] SC = Super Calendered

Norske Skog Saugbrugs (Source: (Sandersen 1999))

Founded in 1859, and a part of the Norske Skog group since 1989, Norske Skog Saugbrugs is today one of the world's leading producers of SC magazine paper. Saugbrugs has a market share in Europe and USA of about 10%. As much as 99% of the paper is sold for export, and the turnover is approximately NOK $2,500$ million. The total production capacity at the Saugbrugs mill is $550,000$ tons, and PM6 (Paper Machine 6) accounts for more than half the total capacity. PM6 was build by Valmet and started up in 1993. The production speed is around 1500 m/min, and the paper width is 8.62 m. Many different grades are produced, e.g. the basis weight[3] range from 40-60 g/m^2.

2.2 From tree to paper

2.2.1 The PM6 production line

Figure 2.1 shows the PM6 production line. The trees are transported from the woodyard to the groundwood mill and TMP (Thermo Mechanical Pulp) plant, where pulp[4] is produced. The stone groundwood mill produce pulp by pressing a piece of wood lengthwise against a wetted, roughened grinding stone revolving at high speed. In the TMP plant, pulp is produced from chips of wood by pressurized steam pretreatment and shredding, and defibering between rotating discs in refiners. The pulp is bleached and stored in large tanks. The pulp is then transported to the wire section and blended with chemical pulp, clay (filler particles), color, and other chemicals on the way. Most of the fiber and filler particles are retained on the wire where they form a thin mat. The mat becomes the paper sheet when water is pressed out of it in the press section, and dried in the dryer section. The paper sheet is then accumulated on the pope (or reel), and transported to the super calenders where properties like smoothness and gloss are added. The paper sheet is cut into appropriate size, wrapped and transported to the end-users (publishing companies, printing offices, etc.).

A proper introduction to the various stages in papermaking, and other issues as well, can be found in e.g. (Smook 1992). Books more focused on chemical issues in papermaking are e.g. (Roberts 1996*a*), and (Roberts 1996*b*).

The content of this thesis focuses on the PM6 production line approximately from the outlets of the storage tanks and to the paper is rolled-up on the pope. This sub-process is described next.

2.2.2 The thick stock and short circulation of PM6

A simplified drawing of the thick stock and short circulation of PM6 is shown in Figure 2.2. Cellulose, TMP (thermomechanical pulp) and broke (repulped fibers and filler from sheet breaks and edge trimmings) are blended in the mixing chest. The stock is

[3] Basis weight is the weight per area of finished paper.
[4] Pulp is a fibrous mass.

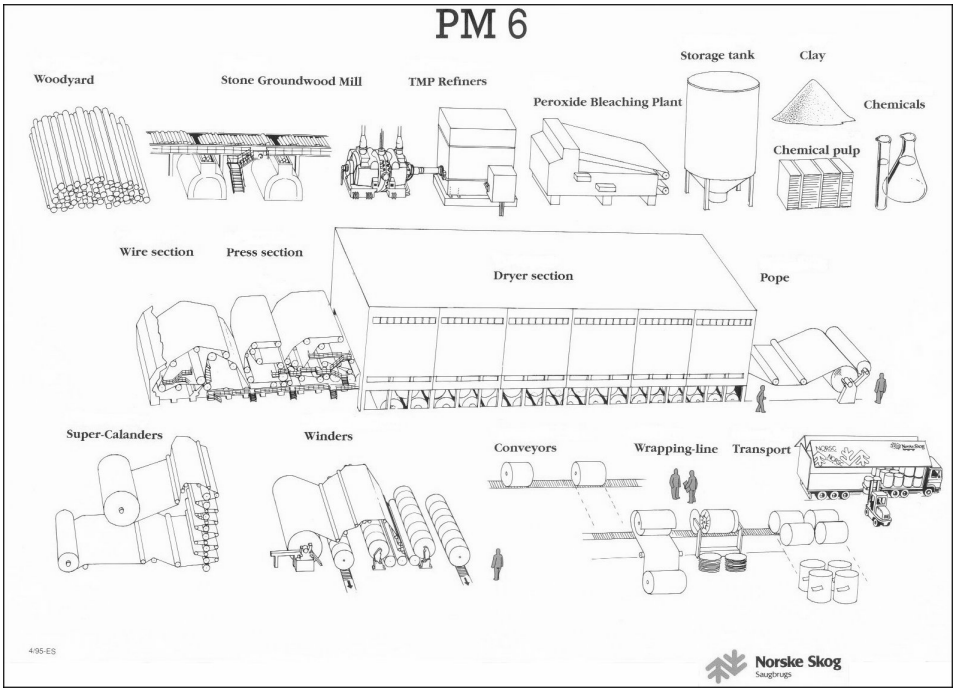

Figure 2.1: PM6 production line (From Norske Skog Saugbrugs leaflet).

fed to the machine chest with a controlled total consistency[5]. Filler is added between the mixing and machine chests. The fillers used in paper production depend on the end-user requirements; typical fillers are kaolin, chalk, talc, and titanium dioxide (Bown 1996). About two thirds of the filler particles used at PM6 are added to the thick stock; the rest is added at the outlet of the white water tank. The flow to the machine chest is large in order to keep the level of the machine chest constant, and an overflow is returned to the mixing chest. The total consistency in the mixing and machine chests are typically around 3 – 4%, which is considerably higher than consistencies later on in the process, and thus the stock from the machine chest is denoted the "thick stock".

The thick stock enters the "short circulation" in the white water tank. Here, the thick stock is diluted to 1-1.5% total consistency by white water[6] and a recirculation flow from the deculator. Filler is added to the stock just after the white water tank. The first cleaning process is a five stage hydrocyclone arrangement, mainly intended to separate heavy particles (e.g. sand and stones) from the flow. The *accept* from the first stage of the hydrocyclones goes to the deculator where air is separated from the stock. The second cleaning process consists of two parallel screens, which separate larger particles (e.g. bark) from the stock. Retention aid is added to the stock at the outlet of the screens. The retention aid is a cationic polymer which, amongst others, adsorb onto anionic fibers and filler particles and cause them to flocculate. The flocculation is a key process for retaining small filler particles and small fiber fragments on the wire, although the significance of mechanical entrapment of non-flocculated filler and fines seems to be somewhat controversial in the literature. For example (Van de Ven 1984) found (theoretically) that mechanical entrapment was low, while (Bown 1996) reports that mechanical entrapment can be a dominant mechanism. In the headbox, the pulp is distributed evenly onto the finely meshed woven wire cloth. Most of the water in the pulp is recirculated to the white water tank, while a share of fiber material and filler particles form a network on the wire which will soon become the paper sheet. The pulp flow from the white water tank, through the hydrocyclones, deculator, screens, headbox, onto the wire and back to the white water tank is denoted the "short circulation".

In the wire section, most of the water is removed by drainage. In the press section, the paper sheet is pressed between rotating steel rolls, thus making use of mechanical forces for water removal. Finally, in the dryer section, the paper sheet passes over rotating and heated cast iron cylinders, and most of the water left in the sheet is removed by evaporation. The paper is then rolled up on the reel before it is moved on to further processing.

[5] The total consistency is the weight of solids (i.e. filler particles and fiber) divided by the total weight of solids and water.

[6] White water, which is stored in the white water tank, is the drainage from the wire.

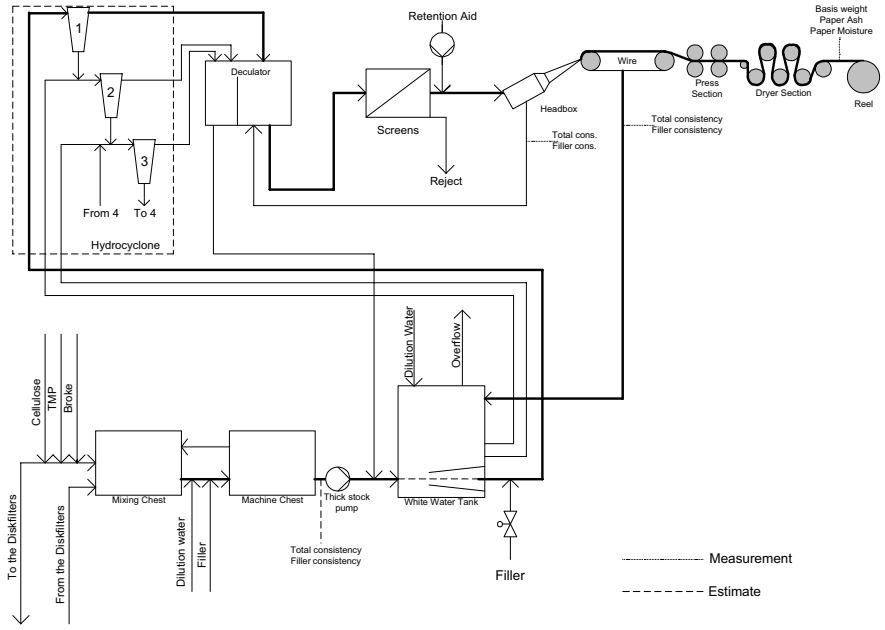

Figure 2.2: A simplified drawing of the thick stock and short circulation of PM6. More details are available in Paper C.

Chapter 3

Modeling

A model of the process is the foundation for every advanced control algorithm. Given a good model of a process, there are probably a number of algorithms that will provide excellent control of the process, and given a poor model of a process, there are probably no algorithms that will provide good control of the process. Also, given a good advanced control algorithm, there are often no models available for the specific process or process unit of concern. Thus, today the key factor for success in advanced control is the development of a reliable and good process model, or as the following closing sentence in a paper put it:

> Nowadays control is easy, modelling will always be the nut to crack...
> (Richalet, Estival & Fiani 1995, page 942)

It should be emphasized that even if a perfect model is available, several limitations to control performance may occur. These limitations may arise from e.g. input constraints, and right half plane (RHP) zeros (Skogestad & Postlethwaite 1996). In practice, the model is not perfect, and additional limitations due to model uncertainty are always present.

Two basic modeling approaches are *mechanistic* modeling and *empiric* modeling. Next, these approaches are presented in more detail.

3.1 Empiric modeling

3.1.1 Introduction

An empiric model is entirely based on experimental data and an appropriate model structure, and often requires little knowledge of the system to be modeled. In the literature one often encounters terms like black box modeling, system identification, time series analysis, and behavioral modeling. All these terms basically mean the same as empiric modeling, the term which is used in this thesis. Introductory and advanced text books on empiric modeling are e.g. (Nelles 2001), (Ljung 1999), (Walter & Pronzato 1997), (Söderström & Stoica 1989), and (Box, Jenkins & Reinsel 1994).

Empiric modeling methods can be further categorized in nonparametric and parametric methods.

Nonparametric methods Nonparametric methods typically provide a pictorial representation of the model. These methods provide information about the process, but the models need to be converted to parametric models before they can be useful for e.g. control purposes. Two common nonparametric methods are, see e.g. (Ljung 1999) and (Söderström & Stoica 1989):

- Transient analysis – Plots of impulse responses or step responses provide information about the delay, gain, and time constants of simple systems.
- Frequency analysis – Sinusoidal input signals are applied to the process, and phase and amplitude are calculated. Various frequencies are applied and the result is plotted in e.g. a Bode diagram.

Parametric methods Although an iterative procedure, several steps in building a parametric empiric model can be identified. The steps below are not necessarily performed successively, see e.g. (Ljung 1999) and (Walter & Pronzato 1997):

1. Choose inputs and outputs
2. Collect experimental data
3. Pretreatment of data, search for outliers, and trends.
4. Choose model structure (state space model, neural net, transfer function, etc.)
5. Choose model order
6. Choose criterion for optimization of model fit
7. Calculate parameters in model, based on optimization of the criterion
8. Validate model

Within the control community, the prediction error method (PEM) is probably the best known criterion:

$$\hat{\theta}_{PEM} = \arg\min_{\theta} J_{PEM}(\theta), \tag{3.1}$$

where $\hat{\theta}_{PEM}$ is the estimated parameter vector that minimize the criterion $J_{PEM}(\theta)$. The criterion is a function of the l-step-ahead prediction error

$$\varepsilon = \hat{y}(k|k-l) - y(k), \tag{3.2}$$

where $\hat{y}(k|k-l)$ are the predicted outputs at time k based on data up to time $k-l$, and $y(k)$ are the measured outputs at time k. Typically the squared prediction error is used

$$J_{PEM}(\theta) = \sum_{k=0}^{N-1} \varepsilon^T Q_k \varepsilon, \tag{3.3}$$

where Q_k is a weight matrix. One-step-ahead predictions are often preferred for models for control, while $l = k + 1$ is commonly used when long term prediction abilities are required, such as in model predictive control. Note that setting $l = k+1$ means pure curve fitting, i.e. fitting the simulated model output to the measured data. Normally one need to use some iterative search algorithm, like e.g. Gauss-Newton, to find the optimal parameter vector, however if the model is linear in the parameters then the optimal parameters can be found without iterations by the least squares method.

A statistically founded competitor to PEM is the maximum likelihood method (MLM):

$$\hat{\theta}_{MLM} = \arg\max_{\theta} J_{MLM}(\theta), \tag{3.4}$$

where $\hat{\theta}_{MLM}$ is the estimated parameter vector that maximizes the criterion $J_{MLM}(\theta)$. The criterion is the likelihood function, reflecting the likelihood of the measured data. If the measured data are independent random variables, then the likelihood is the joint probability density function of these data

$$J_{MLM}(\theta) = f_y(y_{\text{obs}}|\theta), \tag{3.5}$$

where y_{obs} is the measured data, and $f_y(y_{\text{obs}}|\theta)$ is the probability that the observations y_{obs} should take place with a given parameter vector θ. For a dynamic system, the observations are usually dependent. However, using an estimator, the prediction errors are assumed independent and with a certain probability density function. In such a case the MLM can be seen as a special case of the PEM.

Subspace methods Subspace methods are parametric methods, as the output from such methods are state space models. However, the subspace methods have some distinct features and it makes sense to present them as a unique method. (Ljung 1996) characterize subspace system identification as the most interesting development in system identification in the past decade. There are a number of different subspace algorithms available, such as DSR, CVA, N4SID, and PO-MOESP. Complete linear state space models are identified without prior parametrization, except for the system order which can be decided upon by studying singular values, and without iteration (Di Ruscio 1997), (Van Overschee & De Moor 1996). The algorithms are very fast and reliable because no iterations are performed.

The probably best known algorithm is N4SID due to its inclusion in the Matlab System Identification Toolbox (Ljung 2000). However, in (Di Ruscio 1997) N4SID is criticized for finding the erroneous column space for the extended observability matrix[1] when colored noise enters the process, as opposed to DSR, CVA and PO-MOESP. Based on the results in Papers A – B this may very well be correct as it was experienced that N4SID always found a much higher model order than the DSR algorithm, without in general improving the model fit.

While e.g. PEM use an iterative search for optimal parameter values, subspace algorithm use linear algebra to find the parameters without iteration. Uncorrelated

[1] Estimation of the extended observability matrix is the first and common step in most subspace algorithms. From this matrix we can find the order n of the system and the A and C model matrices.

noise and inputs are a basic assumption in subspace algorithms, and thus used in a straight forward fashion these algorithms will not yield consistent estimates when closed loop data are used. For PEM, the use of closed loop data is in most cases un-problematic (Ljung 1999).

3.1.2 Empiric modeling of PM6

Empiric modeling of PM6 are covered in more detail in Papers A – B. In Paper A a high order mechanistic model is used as starting point for the empiric modeling, while in B both empiric modeling from experimentation on the high order mechanistic model and on the real process is carried out. The main results from empiric modeling of the real paper machine process are presented next.

The manipulated inputs u and the outputs y are

$$u = \begin{bmatrix} u_{TS} \\ u_F \\ u_{RA} \end{bmatrix}, \; y = \begin{bmatrix} y_{BW} \\ y_{PA} \\ y_{WC} \end{bmatrix}, \tag{3.6}$$

where the inputs u are the amount of *thick stock*, *filler* added at the outlet of the white water tank, and *retention aid* added at the outlet of the screens, and where the outputs y are the *basis weight* (weight per area), *paper ash* content (content of filler in the paper), and *wire tray consistency* in the recirculation flow from the wire to the white water tank. The basis weight and paper ash outputs are direct quality variables, while the wire tray consistency is an indirect quality variable having significant effect on variation in other short circulation variables (see Figure 2.2).

Identification of models with the subspace methods DSR and N4SID for model orders 1-30, and for various user defined parameters were carried out. The raw data observations were not equally spaced in time and a linear interpolation routine in Matlab was used for creating time series with five seconds sampling intervals, the sampling interval was approximately two seconds in the raw data. The identifications were repeated for data without pretreatment, data which were centered, and for data which were centered and scaled. The centering was carried out by subtracting the value of the first element in each input and output series[2], and the scaling was carried out by dividing each series with its standard deviation. Note that no particular consideration was given to the fact that the basis weight and paper ash measurements are updated less frequently than other variables.

A root mean square error (RMSE) criterion was used for comparing the identification and validation of the various models

$$RMSE_i = \sqrt{\frac{1}{N}\sum_{k=1}^{N}\left(\hat{y}_i(k|0) - y_i(k)\right)^2}, \tag{3.7}$$

where N is the number of observations, $y_i(k)$ is the measured output i at time k, and $\hat{y}_i(k|0)$ is the simulated output i at time k from the empiric model. The i's in the

[2] Centering may also be carried out e.g. by subtracting the mean of the series.

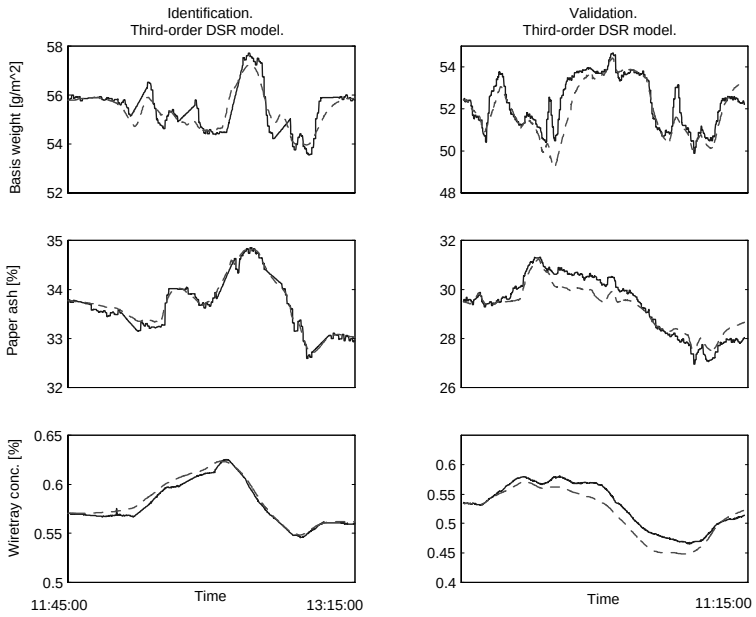

Figure 3.1: Real data (solid lines) and simulated data (dashed lines). Data set for identification collected at September 19. 2000, and data set for validation collected at October 27. 2000. Identification was carried out on centered data.

RMSE's are denoted as *weight* (basis weight), *ash* (paper ash content) or *conc.* (wire tray concentration). The simulated $\hat{y}_i$ are centered so that they have the same mean value as the measured responses y_i, before the RMSE's are calculated.

A third-order model with centered data was identified with the DSR method. Several higher order DSR models were identified, but non of these improved the validation RMSE values. The results from the identification and validation of this model is shown in Figure 3.1, and Table 3.1 gives the RMSE values.

With N4SID a fifth-order centered and scaled model was identified, in addition to several higher order models (11^{th} to 23^{rd} order models) with RMSE values comparable to those of the DSR models. The validation gave higher RMSE values for the fifth-order N4SID model than for the third-order DSR model. None of the higher order

Table 3.1: RMSE values for third-order DSR model.

	Identification	Validation
$\text{RMSE}_{\text{weight}}$	0.410	0.697
RMSE_{ash}	0.095	0.410
$\text{RMSE}_{\text{conc.}}$	0.0043	0.0173

N4SID models improved all three RMSE values at validation. The RMSE values for the basis weight were improved and the RMSE values for the wire tray consistency were poorer for all these models compared to the third-order DSR model.

All identified DSR and N4SID models were used as initial values for a corresponding PEM method. Some minor improvements on some of the DSR models were obtained at identification, however no validation improvements were found.

Individual[3] gains and time constants in the empiric models are far from the expected ones, the ones seen in step tests, or the ones in the mechanistic model implemented at PM6. This may be due to the experiments not being informative enough (Ljung 1999), and it suggests that quite extensive experimentation is needed in order to obtain a multivariable empiric model. It is however interesting to note that the validation results based on RMSE values seem to be quite good despite the poorly identified dynamics of the system.

3.2 Mechanistic modeling

3.2.1 Introduction

A mechanistic model is a model built from basic principles of physics, chemistry, biology, etc., by writing down conservation or balance equations. Obviously this requires extensive knowledge of the process to be modeled. In the literature one sometimes encounters terms like white-, and grey box modeling, see e.g. (Sohlberg 1998). White box models are mechanistic models based on complete knowledge of the process, i.e. where both equations governing the behavior and the associated parameters are known a priori. Obviously, such models are rarely found. A grey box model is a mechanistic model where the equations governing the behavior are assumed known, but parameter values need to be estimated using experimental or historical data. Throughout this thesis grey box models are included in mechanistic models.

There is a vast amount of literature on mechanistic modeling. Most sources deal with specific processes or process units, such as this thesis. However, studying a new process unit one often finds out that similar but not entirely the same units have been modeled, and often the models available are developed with another scope. A search for most of the known processes or process units in a data base will result in numerous hits.

In subsection 3.1.1 a procedure for parametric empiric modeling was outlined. Similar procedures for mechanistic modeling may also be found, e.g. in (Foss, Lohmann & Marquardt 1998), (Sohlberg 1998), and (Sælid 1984). The procedures for empiric and mechanistic modeling are similar to some extent, but with some exceptions:

- There are probably many more iterations and unstructured patterns of the iterations for mechanistic modeling compared to empiric modeling (Foss et al. 1998).
- Conceptual modeling enters as a step in the mechanistic modeling procedure. This step includes e.g. dividing the problem into several subproblems, making

[3] From **one** input to **one** output.

a list of relevant phenomena, and searching for literature (Foss et al. 1998), (Sælid 1984).

- Model simplifications enters as a step in the mechanistic modeling procedure (Sælid 1984).
- For a mechanistic model, the model structure and model order are chosen by formulating the physical laws and balances describing the process.

3.2.2 Mechanistic modeling of PM6

Mechanistic modeling of PM6 are covered in more detail in Papers A – C. In Papers A – B the model is not presented in detail, and neither is it fitted to real time data, nor is it validated with real time data. In Paper C the model is presented in detail, and it is also fitted to and validated with real time data. Thus, Paper C should be considered the main source of information about the mechanistic model developed for PM6. Probably, the most important reference used in the development of the PM6 model was (Shirt 1997):

> ... this work develops the first large scale dynamic simulation of a paper machine wet end which incorporates chemical phenomena (Shirt 1997, page 6).

More references can be found in Papers A – C. Despite the work carried out in (Shirt 1997), there seems to exist some resistance to mechanistic modeling of paper machines:

> The greatest problem here (concerning wet-end chemistry control. Authors note) is that it is not yet, nor is it likely to be, possible to generate a comprehensive physico-chemical model for the description of the adsorption, retention and other processes operative at the wet end of a multi-component additive system. However, some success in control has been achieved with more empirical approaches (Roberts 1996*b*, page 8).

> The wet end of the paper machine is perhaps the most complex and important part of the paper making process, but can also be described as being one of the least understood sections as well. ... The physical modelling approach was thought to offer the best possible method for the papermachine [Humphrey 1986, Nicholson 1980]. However, the loss of material through the wire into the backwater was thought to be far too complex for purely physical modelling alone (Rooke 1999, page 31 and 104).

These claims are probably correct, and the objective of the mechanistic modeling of PM6 was not to make a detailed all-including model which in all aspects had the correct physical structure. The objective was to make a model of a limited part of PM6, which were suitable for model predictive control (MPC), captured the essential

dynamic behavior of the process, and was applicable over a wide range of operating conditions. A similar thought is presented in (Scott 1996, page 136) which state that a comprehensive wet end control scheme will not work, and that the solution is to divide the overall process into subsystems and strive to reduce variability in each of them.

The deterministic model Some modifications have been introduced to the model detailed in Paper C, as compared to the model implemented at PM6. The most prominent modification is that a first order empiric model that was added to capture neglected and unknown dynamics in the process, has been removed.

The deterministic model was originally developed with several ordinary and partial differential equations. The model was then simplified, and eventually fitted to experimental and operational mill data. The implemented PM6 model consists of a third order nonlinear mechanistic model based on physical and chemical laws. The structure of the developed process model is

$$\begin{aligned} \dot{\bar{x}} &= \bar{f}(\bar{x}, \bar{u}, \bar{d}, \bar{\theta}) \\ \bar{y} &= \bar{g}(\bar{x}, \bar{u}, \bar{d}, \bar{\theta}), \end{aligned} \tag{3.8}$$

with $\bar{x} \in \mathbb{R}^n = \mathbb{R}^3$, $\bar{y} \in \mathbb{R}^m = \mathbb{R}^3$, $\bar{u} \in \mathbb{R}^r = \mathbb{R}^3$ and $\bar{d} \in \mathbb{R}^g = \mathbb{R}^4$. The bar above the variable names indicates that these are the variables in their original units and coordinate system. $\bar{\theta}$ consists of several model parameters, tuned to fit the model outputs to experimental and operational data.

The inputs and outputs are as shown in eq. 3.6. In the mechanistic model the states and measured disturbances are

$$\begin{aligned} \bar{x}^T &= \begin{bmatrix} \bar{C}_{R,fil}, & \bar{C}_{WT,fil}, & \bar{C}_{D,fib} \end{bmatrix} \\ \bar{d}^T &= \begin{bmatrix} \bar{C}_{\mathrm{TS,tot}}, & \bar{C}_{\mathrm{TS,fil}}, & \bar{v}, & \bar{f} \end{bmatrix}, \end{aligned} \tag{3.9}$$

where $\bar{C}_{R,fil}$ is the concentration of filler in a *reject tank* in the hydrocyclones, $\bar{C}_{WT,fil}$ is the concentration of filler in the *white water tank*, and $\bar{C}_{D,fib}$ is the concentration of fiber in the *deculator*. The measured disturbances accounted for in the mechanistic model, are the total and filler thick stock concentrations $\bar{C}_{\mathrm{TS,tot}}$ and $\bar{C}_{\mathrm{TS,fil}}$, the paper machine velocity $\bar{v}$, and the paper moisture percentage $\bar{f}$.

Note that the total- and filler concentrations in the thick stock flow are called "measured disturbances", although they are not measured. A model of the thick stock area has been developed (Slora 2001), and implemented at PM6, providing *estimates* of total- and filler concentrations in the thick stock.

Parameter estimation in the deterministic model The model implemented at PM6 has many parameters. These parameters have physical interpretations and thus it should be possible to measure them (e.g. the volumes) or estimate them one by one from local measurements (e.g. measure the flows and concentrations in each stage of the hydrocyclones and calculate the associated parameters). This approach would require a very large and detailed model, probably not suitable for on-line use.

Table 3.2: Parameters estimated in PM6 model.

Name	Description	Unit
α_{filler}	conversion from total flow [l/s] to filler flow [kg/s]	kg/l
$\alpha_{\text{filler,Wire}}$	share of non-flocculated filler retained on the wire	–
$\alpha_{Cy1,\text{inject}}$	inject flow to first stage, relative to flow onto the wire	–
$\alpha_{Cy1,\text{filler}}$	filler accepted in first stage, relative to filler in inject flow	–
$\alpha_{Cy1,\text{fiber}}$	fiber accepted in first stage, relative to fiber in inject flow	–
$\alpha_{Cy2,\text{filler}}$	filler accepted in second stage, relative to filler in inject flow	–
$\alpha_{Cy2,\text{fiber}}$	fiber accepted in second stage, relative to fiber in inject flow	–
$\alpha_{\text{fiber,Wire}}$	share of non-flocculated fiber retained on the wire	–
$\theta_{T.S.\text{total}}$	bias on estimated thick stock total concentration	–
$\theta_{T.S.\text{filler}}$	bias on estimated thick stock filler share	–
k_{filler}	flocculation constant for filler	1/s
k_{fiber}	flocculation constant for fiber	1/s
$k_{\text{fiber-filler}}$	flocculation constant for filler	1/s
V_{Dr}	volume of deculator (right chamber)	m^3
V_R	volume of reject tank	m^3
V_{WT}	volume of white water tank	m^3
$x_{1,\text{initial}}$	initial value for filler concentration in reject tank	–
$x_{2,\text{initial}}$	initial value for filler concentration in white water tank	–
$x_{3,\text{initial}}$	initial value for fiber concentration in deculator	–

The model implemented at PM6 is a simple approximation of a complex process and the parameters in the model, although they have a physical interpretation, should not be measured and/or estimated one by one due to the poor input-output properties of the resulting model. Consider e.g. the deculator volume, which is important for characterizing the time constant for the sub-model between the thick stock and the basis weight. The real volume of the deculator is approximately $17\,\text{m}^3$ (right chamber), however in the model it is many times larger. The deculator volume in the model should be regarded as a lumped volume and not a single physical volume. The most important properties of the model are the input-output properties, i.e. the response on the outputs from changes in inputs. Thus, we want to estimate the parameters in the model so that these properties are good. In principle we would therefore like to tune the parameters so that the model outputs are equal to measured outputs. However, due to the large number of parameters in the model we set some parameters equal to values that seem reasonable, and estimate the rest. The parameters that we have chosen to estimate are shown in Table 3.2.

The function `lsqnonlin` in the Matlab Optimization toolbox (The MathWorks, Inc. 2000) is used for solving the minimization problem defined in eq. 3.1 – 3.3. The prediction errors ε are calculated by simulating the system, with only the initial conditions given, i.e. with $l = k + 1$ in eq. 3.2. In addition the optimization has been subject to the constraints

$$\theta_{\min} \leq \hat{\theta} \leq \theta_{\max}, \tag{3.10}$$

Traditional system identification (see e.g. (Ljung 1999)) is in most cases carried

out using a one-step-ahead predictor, corresponding to $l = 1$, however in our case we wish to emphasize the need for a model with good long term prediction abilities. The reason for this is that the model will be used for model predictive control (MPC). Then, it seems natural to use the simulation approach in the parameter estimation algorithm.

The concept of scaling is very important for robust and rapid convergence to the optimal parameter values (Betts 2001). Here, we will point at two simple methods for scaling; scaling of parameters and scaling of the simulation error. Scaling of the parameters can be done by introducing

$$\theta = S \times \tilde{\theta}, \tag{3.11}$$

where $\tilde{\theta}$ is the scaled parameter vector, θ is the original non-scaled parameter vector, S is a scaling vector, and $\times$ is the Hadamard product (an element by element multiplication). The scaling vector S may be chosen so that the assumed scaled parameter values are close to unity. Consider e.g. the following assumed parameter vector

$$\theta = [10^{-5}, 10^{8}].$$

Choosing

$$S = [10^{-5}, 10^{8}],$$

gives the following scaled parameter vector

$$\tilde{\theta} = [1, 1].$$

Any constraints or bounds on the parameters must be scaled accordingly.

The simulation error is defined in equation 3.2 by setting $l = k + 1$. The basis weight is measured in $\mathrm{g/m^2}$ and has a value typically around $50\,\mathrm{g/m^2}$, paper ash is measured in % and has a value typically around 30%, and the wire tray concentration in measured in % has a value of approximately 0.6%. Based on this, it is easy to understand that the error for the wire tray concentration is very small compared to the other two errors, thus any model fitting routine would more or less ignore the wire tray concentration and concentrate on fitting the basis weight and paper ash. To compensate for this one may scale the simulation error or outputs, simply by multiplying with a weight. If all outputs are regarded equally important, one may weight them so that the outputs are approximately equal. For example, the wire tray could be multiplied by 50 to make it approximately equal to the paper ash. However, in our case we define the most important output to be the basis weight, the second most important output to be the paper ash, and the least important output is the wire tray concentration. This ranking of importance should thus also be reflected in the weighting of the outputs.

Validation and re-tuning of deterministic model Validation is the method of checking how good the model really is. One may find a model fitted almost perfectly to one data set, and totally failing to explain (failing to simulate outputs close to measured outputs) another data set. Many methods for validation exist, however

if possible a proper validation should include testing of the model with a new data set. Using one half of the data set for model fitting and one half for validation is not an equally proper method, as slow varying disturbances and parameters , drifts, and trends, will be very hard to discover. Ideally, data sets spanning all operating conditions of the process should be used for validation, thus one would have a fair chance to find areas where the model is not functioning properly.

In subsection 3.1.1 a procedure for parametric empiric modeling is outlined, and in subsection 3.2.1 some similarities and differences between the empiric modeling procedure and a procedure for mechanistic modeling is pointed at. A similar procedure as the ones found in subsections 3.1.1 and 3.2.1 has been used for the PM6 model, although with some changes. Validating a model by comparing simulated and real outputs, is in general not enough when the model should be used for control. The individual responses from each input to each output are also very important. A procedure is presented next, which is used at PM6 and found to work well, for model fitting, validation and re-tuning of the model. The procedure is also pictorially presented in Figure 3.2.

1. Make model.
2. Collect several data sets, at least one for model fitting and one for validation. The data set used for model fitting should contain well excited data. The data set for validation must also to some extent be excited. The length of the data sets obviously depends on the process and size of the model. For the PM6 work, the data sets ranged from 2 hours to several days. It is usually not important wether the data are collected in open or closed loop since "*a directly applied prediction error method – applied as if any feedback did not exist – will work well and give optimal accuracy if the true system can be described within the chosen model structure*" (Ljung 1999, page 434). Check the data for outliers and that the units are correct, and also consider filtering of the data.
3. Set up tables of approximately expected gains and time constants from inputs and measured disturbances, to outputs. These gains and time constants could be found from discussions with process operators and engineers alone, but should be supported by step tests carried out on the process, if possible.
4. Choose initial parameter values and fit the model to the data. Several re-optimizations may be needed. For example if the optimal parameter values are very different from the initial values, then the optimal values should be used as initial values and optimized again (thus, a re-scaling is also carried out). Other reasons for re-optimizing may be to try other initial parameter values, or other parameter bounds. If reasonably good model fit is *not* obtained, changing the model equations may eventually be necessary.
5. Validate the model by comparing simulated and measured outputs, using a different data set than the one used for model fitting. If the result is not satisfactory one should probably return to point 4, and try different initial values or parameter bounds. Eventually one may need to change the model equations if reasonable validation results are not obtained.

Table 3.3: RMSE values for mechanistic PM6 models.

	Fitting M1	Fitting/re-tuning M2	Val. M1	Val. M2
Basis weight	0.21	0.25	1.00	0.71
Paper ash	0.24	0.40	0.87	1.20
Wire tray conc.	0.024	0.020	0.0496	0.042

Table 3.4: Gain ratios (M1/M2) for mechanistic PM6 models.

	Thick stock	Filler	Ret.aid
Basis weight	0.130 / 0.135	1.25 / 1.85	2.98 / 3.98
Paper ash	-0.023 / -0.022	1.63 / 2.40	1.66 / 5.10
Wire tray conc.	-0.00022 / -0.00057	0.081 / 0.11	-0.18 / -0.21

6. Simulate step tests on the fitted model, and compare the gains and time constants with the expected results as found in point 3. If the gains and time constants are reasonably close to the expected ones, the model fitting and validation is finished.

7. If the gains and time constants in point 6 are too far from the expected values, re-tune the model by changing parameter values that move the gains and time constants towards the expected ones. When reasonable gains and time constants are found, go to point 5 and compare simulated and measured outputs. Eventually one may need to change the model equations if reasonable gains and time constants are not found.

Figure 3.3 shows the validation result after fitting the model to an experimental data set, and Figure 3.4 shows the validation result after re-tuning to obtain expected gains and time constants. A comparison of the fitting and validation results are also given in Tables 3.3 and 3.4, based on the root mean square error values as defined in eq. 3.7 and the gains found in a specific operating point. In the tables we denote the fitted model by *M1*, and the fitted and re-tuned model by *M2*, i.e. the implemented model is denoted *M2*.

Comparing the RMSE values in Table 3.3, it seems that the basis weight fit became somewhat poorer after re-tuning the model, but the validation result improved significantly. The paper ash RMSE values became poorer after the re-tuning, while the wire tray total concentration RMSE values were improved. Studying the gain matrix in Table 3.4, it is seen that some gains changed dramatically, e.g. the gain between the thick stock and wire tray concentration more than doubled after the re-tuning. Similar results are found for the gains from the filler to the paper ash, and from the retention aid to the basis weight and paper ash.

Both models, M1 and M2, have been tested in MPC applications at PM6. It was observed that MPC with M1 resulted in e.g. poor grade changes due to the erroneous gains. These results are in accordance with the results from empiric modeling of PM6 in subsection 3.1.2. For the identified empiric model, the validation results were reasonably good, and it seemed that a model suitable for control was obtained.

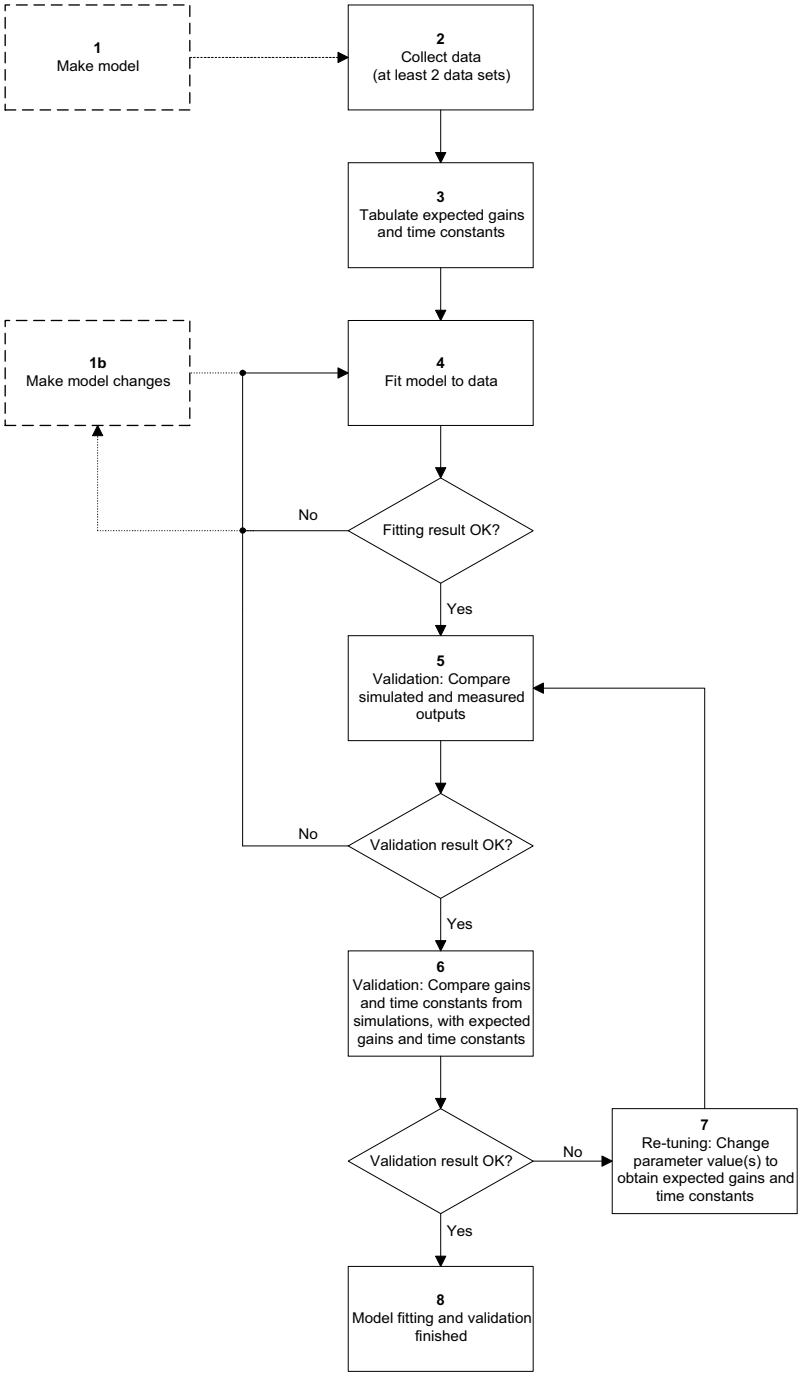

Figure 3.2: Procedure for model fitting and validation.

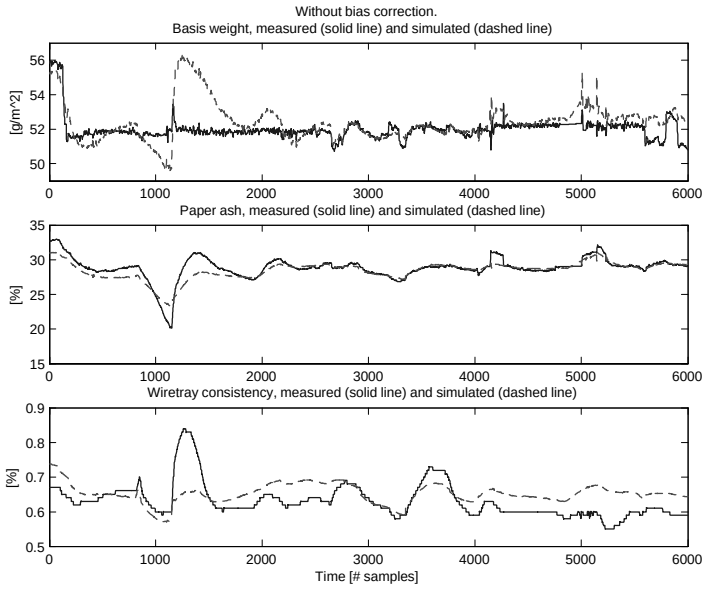

Figure 3.3: Validation of the model after fitting with `lsqnonlin`.

However studying the individual gains and time constants suggested that the model would probably work poorly for control applications due to large differences between model dynamics and dynamics in the real process.

Identification and tuning of stochastic model An augmented suboptimal Kalman filter is used at PM6 for estimating the states and some of the parameters in the paper machine model. As pointed out in (Muske & Badgwell 2002), only a limited number of parameters can be estimated on-line, thus the choice of which parameters or biases to estimate must be based on experience with the process and model. Three biases have been selected for on-line estimation in the paper machine model. The first two are biases on the estimated total- and filler thick stock consistencies (see eq. 3.9). These disturbances are estimated using a ballistic estimator (Slora 2001), and thus they are assumed to be good candidates for having time-varying biases. The third bias estimated on-line is for the total wire tray concentration, i.e. a bias in one of the outputs.

In theory, and in the true Kalman filter, the noise characteristics of the process should be found and used in the Kalman filter equations. However, these characteristics are hard, if not impossible, to find. Thus, one often aims for a suboptimal Kalman filter, where the noise characteristics are used as tuning parameters until satisfactory Kalman filter performance is obtained. Specifically, the tuning parameters are the augmented process noise covariance matrix, $\tilde{Q}_k$, and the measurement

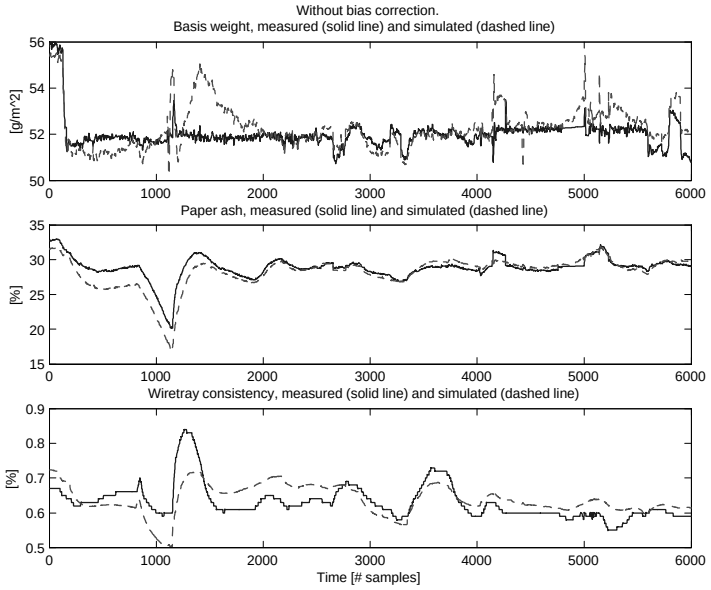

Figure 3.4: Validating the model after fitting with `lsqnonlin`, and re-tuning to obtain expected gains and time constants.

noise covariance matrix, R_k. Often, it is assumed that only diagonal elements are non-zero. Thus, for the paper machine model there are three diagonal elements in R_k (three outputs), and six diagonal elements in $\tilde{Q}_k$ (three states plus three estimated parameters).

When tuning and validating the (suboptimal) Kalman filter at PM6, a few facts and rules of thumb have been used, e.g.:

- The tuning and validation (with different data sets) should aim at
  - good tracking properties, i.e. the estimated outputs should follow the measured outputs to some extent;
  - good filtering properties, i.e. the estimated outputs should not track measurement noise;
  - a sound balance between the updating of states and updating of parameters, e.g. the parameters should not vary a lot while the states are more or less resting.
- It can be shown that it is the ratio of the various variances that determines the performance of the Kalman filter. Thus, one needs not be careful about finding realistic variance values.
- It is possible to estimate the variances, using a parameter estimation method. This is carried out for a constant gain Kalman filter (i.e. the individual variances are not estimated, but the Kalman filter gain matrix is estimated) in (Hauge & Lie 2002). The drawback with this method is that the Kalman filter will be rather aggressive, and some de-tuning procedure is needed (but it may give a good starting point).
- Start the tuning by finding approximate values for the various variances. The measurement variances can be approximately found by visually studying the random variations in the measurements. It is harder to find suitable starting values for the process noise variances and the parameter estimate variances. However, the expected state and parameter values will give good indications of reasonable starting values. Consider e.g. a concentration that is expected to have a value around 0.05 (5%). If one assumes that the noise entering this state is approximately 1% of the state value, we see that the variance will be a very small number. In the Kalman filter used at PM6, the measurement variances are much larger than the process and parameter variances (around 10^8 larger).
- In general, increasing the measurement variances leads to a slower updating of state estimates. The same result is obtained by decreasing the process variance. Thus, decreasing the process variance leads to a slower updating of state estimates.
- Since the parameters are augmented states, changing the parameter variances has much of the same effect as changing the state variances. Increasing the parameter variances leads to a faster updating of parameter estimates, thus

also leading to a faster elimination of estimation error (the difference between estimated outputs and measured outputs).

Refining versus lumping approach Studying Papers A – C, it is obvious that the mechanistic PM6 model has been developed basically in a *lumping approach*[4]: a large complex model was developed first, and simplifications were then carried out to establish a smaller and less complex model suitable for model based control. A *refining approach*[5] would include developing a coarse model, and then gradually refine the structure by introducing new elements.

In (Sohlberg 1998) a refining approach to modeling of a rinsing process within the steel industry can be followed closely. A basic model is developed first, consisting of only one unknown parameter. The model is fitted to data and refined in several stages before the final model, consisting of nine parameters, is achieved. The refining approach seems to be the preferred method amongst experienced modelers, although a certain mixture of the two approaches seems likely to occur in most projects (Foss et al. 1998). This mixing of approaches is also the case for the PM6 model. Even though the lumping approach is very pronounced, some elements of refining can be identified.

Two interesting questions are then: if a refining approach had been used for the PM6 model, (i) would the result be any different, and (ii) would the time spent on modeling be any different? (Sælid 1984, page 6) argues that if a too detailed model is developed, then much time and work is more or less wasted. This is probably correct for an experienced modeler having some knowledge about the process to be modeled, as (s)he will have an *a priori* feeling of the important phenomena and simplifications that can be carried out. For an unexperienced modeler, unfamiliar with the process (s)he is about to model, it will probably be much harder to identify sensible simplifying assumptions *a priori*. Consider e.g. the question of whether flocculation at PM6 takes place throughout the whole short circulation or only between the screens and the headbox. In the first model developed, the flocculation was assumed to take place in the whole short circulation, while the flocculation was constrained to take place only in the pipeline between the screens and the headbox in later versions of the model. This simplifying assumption was based on results from simulation, and sources such as (Shirt 1997), (Pelton 1984), (Koethe & Scott 1993), and (Gregory 1988). Next, consider a simpler example of how to model a pipeline. Assume for simplicity that no flocculation takes place within the pipeline, thus one expects that a very reliable model for the concentration in the pipeline is a partial differential equation (PDE)

$$\frac{\partial C}{\partial t} = -v\frac{\partial C}{\partial x}, \tag{3.12}$$

where v is the velocity of the mass inside the pipeline, and x is the variable corresponding to the direction along the pipeline. Using the method of lines (MOL) for discretization (Schiesser 1991), the choice of discretization level is a trade-off between

[4] Also called a bottom-up approach.
[5] Also called a top-down approach.

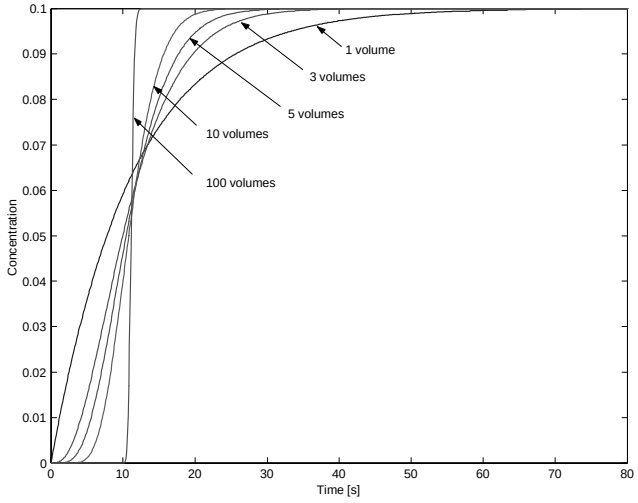

Figure 3.5: Step responses at the outlet of a pipeline (40 m length, 0.7 m^2 cross sectional area, 2500 kg/ s mass flow). Discretization carried out with various numbers of ideally stirred volumes.

factors such as accuracy, complexity and numerical properties. With an increasing number of volumes, the model is more accurate but also more complex and the stiffness of the overall system is increased. The trade-off can be studied from the responses in Figure 3.5, where a step change (from 0 to 0.1) in the initial concentration is applied to the pipeline between the screens and the headbox. The pipeline is 40 m long, it has a cross section area of 0.7 m^2 and a mass flow of 2500 kg/ s. A density of $\rho = 1000\,\mathrm{kg/\,m^3}$ is assumed. If the pipeline is a pure time delay then the step change would appear at the outlet at $t = L/(w/(A\rho)) = 11.2\,\mathrm{s}$, where L is the length of the pipeline. For the original PM6 model there were 100 pipelines included in the model. One advantage of using the lumping approach to modeling is then that the various choices of discretization can be easily studied using simulation, and one will have good control of which simplifications are negligible and not. In Paper A various simplified models are compared with a large basic model, showing that for the PM6 model all PDE's can be simplified to one ordinary differential equation (ODE) each without affecting the properties of the model to any large extent.

To sum up some thoughts and experiences: The refining approach is used by most experienced modelers in the field, however combined with some elements of the lumping approach. It is hard to find arguments supporting that a model will be better or worse using one approach or the other, however the time spent using the lumping approach may be longer than for the refining approach. For a novice in mechanistic modeling, the lumping approach may be more valuable in terms of gaining modeling

experience.

3.2.3 Linearized PM6 state space model

In this subsection, a typical example of a linearized PM6 state space model is given. The structure of the linearized model is

$$\begin{aligned} x_{k+1} &= Ax_k + Bu_k + Ed_k \\ y_k &= Cx_k + Du_k + Fd_k, \end{aligned} \tag{3.13}$$

where the sample time is 30 seconds, and the states, inputs, outputs, and measured disturbances are as described in eqs. 3.6 and 3.9. Typical model matrices are

$$\begin{aligned} A &= \begin{bmatrix} 0.9702 & 0.3283 & 0 \\ 0.0018 & 0.9596 & -0.0197 \\ 0 & 0 & 0.8661 \end{bmatrix} \\ B &= \begin{bmatrix} 1.3 & 160.1 & 0.2 \\ 0.1 & 10.1 & -33.4 \\ 1.3 & 0 & -0.7 \end{bmatrix} \\ E &= \begin{bmatrix} 0.0247 & 0.0023 & 0 & 0 \\ 0.0016 & 0.0001 & 0 & 0 \\ 0.0134 & -0.0007 & 0 & 0 \end{bmatrix} \\ C &= \begin{bmatrix} 61 & 727 & 13,109 \\ 83 & 986 & -1692 \\ 3 & 34 & -32 \end{bmatrix} \\ D &= \begin{bmatrix} 0.0029 & 0.3544 & 5.3831 \\ 0.0040 & 0.4815 & 7.1769 \\ 0.0001 & 0.0166 & -0.0554 \end{bmatrix} \\ F &= \begin{bmatrix} 54.5613 & 5.1415 & -1.9777 & 51.0179 \\ 74.1090 & 6.9836 & 0 & -30.6923 \\ 2.5519 & 0.2405 & 0 & 0 \end{bmatrix} \end{aligned} \tag{3.14}$$

3.3 Mechanistic versus empiric models

Table 3.5 summarizes some general properties of mechanistic and empiric models, although exceptions can easily be found.

The perhaps strongest argument for using an empiric model is that the time for building such a model is much lower than for a mechanistic model. In (Foss et al. 1998) it is indicated that the development cost for an empiric model is about 1/10 compared to a mechanistic model. This was indicated by a person experienced with mechanistic modeling, and for the paper machine modeling in Papers A – C the ratio is probably closer to 1/100. Another positive feature of empiric models are that they often have a simple structure (linear and time invariant) which leads to quick and easy simulation, analysis, and design of control algorithms. If one has access to experimental data,

Table 3.5: Mechanistic versus empiric models. Partly reproduced from Støle-Hansen 1998, and Walter & Pronzato 1997.

Properties	**Mechanistic**	**Empiric**
Utilize physical knowledge and insight	yes	no
The parameters have known range	yes	no
Number of unknown parameters	low	high
Time needed to develop a model	high	low
Resources needed to maintain a model	low	high
Easy to use for complex/unknown processes	no	yes
Amount of data needed	low	high
Applicability to control and training	yes	yes
Applicability to design	yes	no
Extrapolation properties	good*	bad
Increases process knowledge	yes	no
Complex	yes (non-linear)	no (often linear)
Simulation	long/difficult	quick/easy
Possible roll-out of model	yes	no

*if structure is correct.

and the operating region of the process is only moderately nonlinear, then it seems reasonable to first try an empiric model.

The strength of a mechanistic model lies in its ability to capture known nonlinear phenomena and thereby having extraordinary extrapolating properties, and the possible reuse of the model on similar processes. This and other features are emphasized in the following quotation:

> ..., a model based on first principles can operate in a larger domain than a black-box model. A model based on first principles will in general contain fewer parameters and will therefore be more parsimonious. From the parsimony principle we know that the best model is the simplest model that adequately describes the process, since overparameterization will in general lead to poor generalization. A consequence of fewer parameters, a model based on first principles will need fewer experiments to be identified. On the other hand, a black-box structure is easier to develop. ... To identify our model (a mechanistic model. Authors note) we have only used history data from the plant. (Hillestad & Andersen 1994, page 42 and 45)

Consider the paper machine model implemented at PM6. This model has 19 parameters, including two biases and three initial ODE values, which is tuned to fit the model to data. The model has three inputs, three outputs, three states, and four measured disturbances. A linear (empiric) state space model of the same dimension would consist of 63 parameters, including direct input to output matrix and three initial ODE values. An empiric transfer matrix model would consist of *minimum* 42 parameters, corresponding to pure first order elements, i.e. one parameter for

the time constant, and one for the gain, in each element. If a step response model or impulse response model is used, the number of parameters would increase even more. In addition, the empiric models mentioned here have a limited operating range and must either be adaptive or a set of models is needed. In (Kosonen et al. 2002) an approach where a set of adaptive empiric models are used to cover the operating region of the paper machine is described.

A point made by (Ogunnaike & Wright 1997, page 49), is that mechanistic modeling results in a small number of parameters that can intuitively be understood, thus reducing long term support cost. Industrial processes do not remain static and it is likely that the model, whether empiric or mechanistic, will degrade with time. Another point, which is often neglected in the literature, is that the un-manipulatable nature of most measured disturbances makes it impossible to model their effect on the model outputs empirically. The empiric PM6 model developed in subsection 3.1.2 consists of none measured disturbances. Submodels from measured disturbances to model outputs can in some cases be identified from experimental data, however in most cases the data will not be informative enough and physical knowledge and insight must be used. For example the thick stock total consistency could be incorporated in the model by assuming that it affected the outputs similarly to the thick stock input.

Chapter 4

Model Predictive Control

4.1 Introduction

Readers not familiar with model predictive control (MPC) may consult one of the many texts on the subject. Introductory textbooks on MPC are e.g. (Maciejowski 2002) focusing on MPC with state space models, and (Camacho & Bordons 1999) focusing on MPC with transfer function models. A tutorial is given in (Rawlings 2000), and survey papers focusing on both theory and practice are e.g. (Garcia, Prett & Morari 1989), (Mayne, Rawlings, Rao & Scokaert 2000), (Qin & Badgwell 1997), and (Qin & Badgwell 1998).

In model predictive control (MPC) one calculates optimal inputs in a receding horizon fashion. The inputs at time k are calculated by minimizing a criterion aiming at keeping control errors small, the inputs close to some preferred values, the input changes small, and the inputs, outputs, and input changes within some predefined bounds. A typical mathematical formulation of the criterion may be

$$\min_{\mathcal{U}_k} J_k = \min_{\mathcal{U}_k} \sum_{j=0}^{\infty} \left[e_{k+j}^T Q e_{k+j} + \tilde{u}_{k+j}^T R \tilde{u}_{k+j} + \Delta u_{k+j}^T S \Delta u_{k+j} \right], \tag{4.1}$$

constrained by the definitions

$$\begin{aligned} e_{k+j} &= y_{k+j} - r_{k+j}^y \\ \tilde{u}_{k+j} &= u_{k+j} - r_{k+j}^u \\ \Delta u_{k+j} &= u_{k+j} - u_{k+j-1}, \end{aligned} \tag{4.2}$$

the model of the process, e.g.

$$\begin{aligned} x_{k+1+j} &= f(x_{k+j}, u_{k+j}, d_{k+j}) \\ y_{k+j} &= g(x_{k+j}, u_{k+j}, d_{k+j}), \end{aligned} \tag{4.3}$$

and the bounds

$$\begin{aligned} u_{k+j}^{\min} \leq u_{k+j} \leq u_{k+j}^{\max} \\ y_{k+j}^{\min} \leq y_{k+j} \leq y_{k+j}^{\max} \\ \Delta u_{k+j}^{\min} \leq \Delta u_{k+j} \leq \Delta u_{k+j}^{\max}, \end{aligned} \tag{4.4}$$

where y and r^y are the outputs and output targets, u and r^u are the inputs and input targets, x are the states, d are the disturbances acting on the system, and Q, R, and S are weighting matrices. The input sequence $\mathcal{U}_k$ covers the inputs from the present time and N steps into the future, however only the first input is applied to the process. At the next time instant, the computation is carried out again with the same length N of the horizon, giving another input to apply to the process. Thus, the inputs are computed in a receding horizon fashion, and MPC is occasionally called receding horizon (optimal) control.

The basic MPC principle is shown in Figure 4.1. Here, the principle is illustrated using only one input and one output (the basis weight of a paper machine), although a major advantage of MPC is its ability to handle multivariable systems in a straightforward fashion. In the figure, the reference changes 15 minutes into the future, giving the process operators time to evaluate the controller action. Even though this functionality is available and described in many introductory texts on MPC (Camacho & Bordons 1999) (Maciejowski 2002), most commercial MPC's have not implemented this facility. Instead, the change takes place immediately, or a trajectory is calculated from the present setpoint to the new setpoint.

Linear model predictive control, i.e. MPC with linear models, is the only advanced control method used to any extent by the industry. The main reasons for its success are probably

- Intuitive and attractive concept.
- Constraints are handled in an elegant fashion.
- Compensates for dead time.
- Handles measured disturbances by feed forward control.
- Handles coupled multivariable systems with elegancy.
- Short payback time is reported, e.g. 3 months in (Bassett & Van Wijck 1999).
- Commercial MPC software packages are available.
- Linear empiric models can be developed efficiently, with or without commercial software.

Nonlinear model predictive control, with mechanistic models, is not reported used in many industrial applications. The reason for this is probably that the modeling procedure is more expensive and time consuming, and that many of the larger vendors only support linear models in their MPC's. However, there are cases where it seems reasonable to use nonlinear MPC with a mechanistic model, e.g. when:

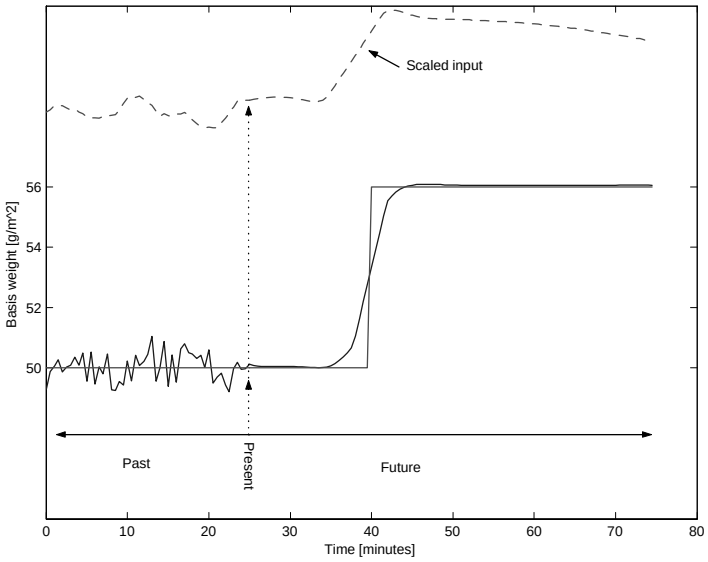

Figure 4.1: Basic MPC principle.

- The process is nonlinear, with wide operating range or several grades.
- Limited experimentation can be carried out on the process. Less experimentation is needed for fitting a mechanistic model compared to an empiric model, e.g. (Hillestad & Andersen 1994) reports that their mechanistic model is identified purely from historical data.
- There are a number of similar processes or process units, which the controller is sought applied to.

Algorithm for MPC with mechanistic model Here, an algorithm for MPC with a mechanistic model is suggested. The algorithm is detailed in Paper F.

The basic idea of the algorithm is that the nonlinear mechanistic model can be approximated by a linear model which is updated at each sample, thus using successive linearization, extended Kalman filter, and a linear MPC framework. Similar approaches are also suggested in (Lee & Ricker 1994), although with a finite horizon criterion, and (Gattu & Zafiriou 1992), with computation of the steady state Kalman gain at each sample.

At time k we have available the process model (eq. 3.8) in its discrete version

$$\begin{aligned} \bar{x}_{k+1} &= f(\bar{x}_k, \bar{u}_k, \bar{d}_k, \bar{\theta}_k) \\ \bar{y}_k &= g(\bar{x}_k, \bar{u}_k, \bar{d}_k, \bar{\theta}_k), \end{aligned} \tag{4.5}$$

as well as the following past measurements and estimates

$$\left.\begin{array}{c}\bar{u}_{k-i}\\ \bar{y}_{k-i}\\ \bar{d}_{k-i}\\ \widehat{\bar{x}}_{k-i+1}\end{array}\right\}, \forall i = 1, 2, 3..., \tag{4.6}$$

where $\widehat{\bar{x}}$ is an estimated state vector. The following step by step algorithm for controlling the process is suggested, assuming the present time to be k.

1. Linearization of model based on conditions at time $k-1$.

   The linearization is based on the most up-to-date information about the process, i.e. the variable values at time $k-1$. Note that we have no information about $\bar{u}_k$ yet, so we can not linearize based on variable values at time k. The resulting model is

   $$\begin{aligned}\bar{\bar{x}}_{k+1} &= A_k\bar{\bar{x}}_k + B_k\bar{\bar{u}}_k + E_k\bar{\bar{d}}_k \\ \bar{\bar{y}}_k &= C_k\bar{\bar{x}}_k + D_k\bar{\bar{u}}_k + F_k\bar{\bar{d}}_k.\end{aligned} \tag{4.7}$$

2. Obtain current measured disturbances and future setpoints and disturbances.

   The measured disturbances obtained from the process are $\bar{d}_k$. The future disturbances and references are

   $$\begin{aligned}&\bar{r}_{k+j},\ j = 0, ..., N-1 \\ &\bar{d}_{k+j},\ j = 0, ..., N-1,\end{aligned} \tag{4.8}$$

   which must be provided by the process operators or simply taken as an extension of the present values into the future.

3. Shift variables, i.e. change variable coordinates, corresponding to the linearized model.

   The references, disturbances, and constraints will be used with the linearized model in eq. 4.7 for calculation of target or steady state values. The references, disturbances, and constraints must then be shifted along with the model so that all variables have compatible origins before the calculation of target values.

4. Calculate steady state values.

   The calculation of steady state values is carried out for several reasons. The steady state values are used as targets in the optimization criterion. One could use e.g. reference values directly as targets in the criterion. However, the calculation of steady state values is a way of ensuring that the targets are feasible. In addition, by calculating steady state values one has the opportunity to add e.g. an economic type criterion if there are additional degrees of freedom. Finally, for the special case of an infinite horizon criterion with possibility of changing future references and measured disturbances, we need the steady state values at the end of the horizon in order to shift the origin of the model.

5. Shift the origin of the model to the steady state values at time $k+N-1$.

   The model origin is shifted so that the variables in the criterion converge exponentially to a zero steady state, thus avoiding an infinite value of the criterion in eq. 4.1. The resulting model is

$$\begin{aligned} x_{k+1} &= A_k x_k + B_k u_k + E_k d_k \\ y_k &= C_k x_k + D_k u_k + F_k d_k. \end{aligned} \tag{4.9}$$

6. Shift measured and estimated variables.

   The variables must be shifted along with the model so that they have the same origin.

7. Update MPC matrices and vectors.

   The matrices and vectors in the MPC formulation that contain time variant variables, such as linear model matrices, input variables, estimated states, etc., must be updated.

8. Optimization.

   An optimization algorithm is used to calculate optimal inputs.

9. Apply $\bar{u}_k$ to the process.

   Note that only the first input is used.

10. Obtain $\bar{y}_k$ from the process.

11. Estimate $\widehat{\bar{x}}_{k+1}$.

    Unless all states are measured, we need to estimate them (or some of them). Typically an extended Kalman filter is used for this purpose.

12. Set $k := k+1$ and go to step 1

Note that variables in original units, i.e. unscaled and unshifted, are denoted by a bar above the variable, e.g. $\bar{x}$ and $\bar{u}$. Variables in the linearized model, i.e. variables that have origin corresponding to the center of linearization are denoted by a double bar above the variable, e.g. $\bar{\bar{x}}$ and $\bar{\bar{u}}$. Finally, variables shifted first by linearization and then by the steady state values at time $k+N-1$ are shown as e.g. x and u.

Computational efficiency Consider the criterion and constraints in eqs. 4.1 – 4.4. The choice of unknown variables are here given as the future input sequence $\mathcal{U}_k$. By extensive manipulation (see Paper F) the criterion and constraints can be formulated as the following quadratic programming (QP) problem

$$\min_{\mathcal{U}_k} J_k = \min_{\mathcal{U}_k} \left(\frac{1}{2} \mathcal{U}_k^T H_k \mathcal{U}_k + c_k^T \mathcal{U}_k \right), \tag{4.10}$$

subject to

$$b_{L,k} \leq \begin{bmatrix} \mathcal{U}_k \\ \bar{A}_k \mathcal{U}_k \end{bmatrix} \leq b_{U,k}, \tag{4.11}$$

which can be solved by commercial QP software. This choice of unknowns in the optimization criterion is by no means the only one, however in Paper E it is shown that reducing the number of variables to a minimum often is beneficial for the computation time. It is also shown that the efficiency of commercially available QP solvers varies quite much. Consider a simulated case using the mechanistic model of PM6 and the MPC algorithm above. The number of variables are down to a minimum, i.e. only future input variables are computed, and we simulate 100 samples (50 minutes), with a rather short horizon $N = 20$ samples. After 20 samples a step change in the reference values occur. The change is known to the MPC from the start of the simulation. One instance of outputs from such a simulation are shown in Figure 4.2, and the computation time using `qpopt` (Holmström 2001) and `quadprog` (The MathWorks, Inc. 2000) are shown in Figures 4.3 - 4.4 respectively. It is clear that `qpopt` is superior to `quadprog` when it comes to computing efficiency. No difference in computing accuracy has been found between the two solvers in this study. Some statistics from the two simulations are:

Solver	mean comp. time	1.opt. comp. time	mean(2:end) comp. time
`qpopt`	0.013 s	0.11 s	0.012 s
`quadprog`	0.616 s	14.52 s	0.476 s

Here, "mean comp. time" is the average computation time for all 100 samples, "1.opt. comp. time" is the computation time for the first optimization carried out, and "mean(2:end) comp. time" is the average computation time for all 100 samples except for the first.

4.2 Model predictive control at PM6

Model predictive control at PM6 is covered in more detail in Paper F.

Motivation for multivariable model based control Magazine paper is characterized by its glossy appearance due to a high content of filler in the paper. The finished magazine paper typically consists of 65% fiber, 30% filler, and 5% water. The main difference between magazine paper and e.g. newsprint is the high content of filler. For newsprint, the amount of filler is typically 0-10%. Due to the high filler content in magazine paper, the couplings between important input and output variables are relatively strong. The project "Stabilization of the wet end at PM6" was initiated in 1999 based on the experience of strong couplings and oscillating behavior in the process. A key goal was to reduce variation in certain variables, such as consistencies in the short circulation, basis weight, filler content, and more. Based on experience and reported results from competitive mills (e.g. (McQuillin & Huizinga 1995), and (Lang et al. 1998)), it was decided to develop a model of the

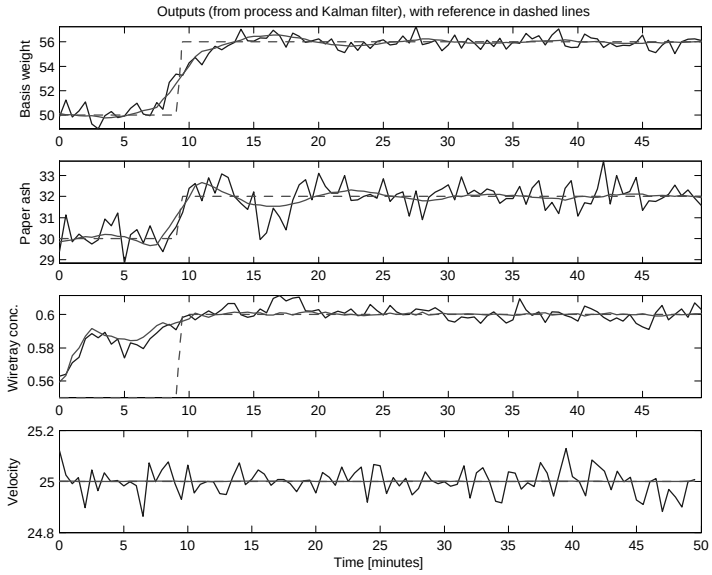

Figure 4.2: Outputs (measured, estimated and reference) after simulation of 100 samples, with horizon $N = 20$. A change in reference values occurs after 10 minutes.

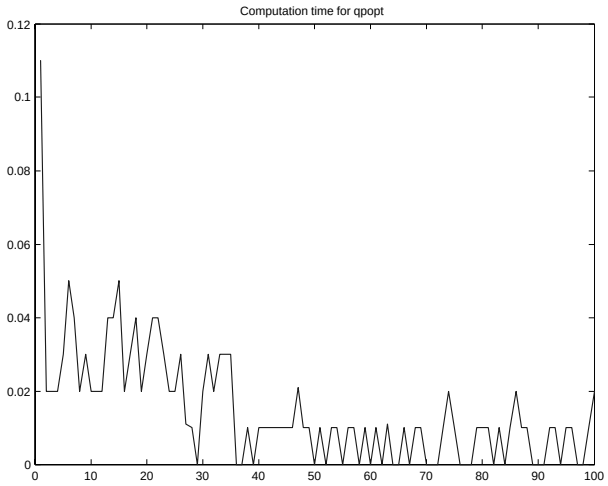

Figure 4.3: Optimization time using qpopt. Simulation carried out with 100 samples, and with horizon $N = 20$. A change in reference values occurs after 10 minutes (20 samples).

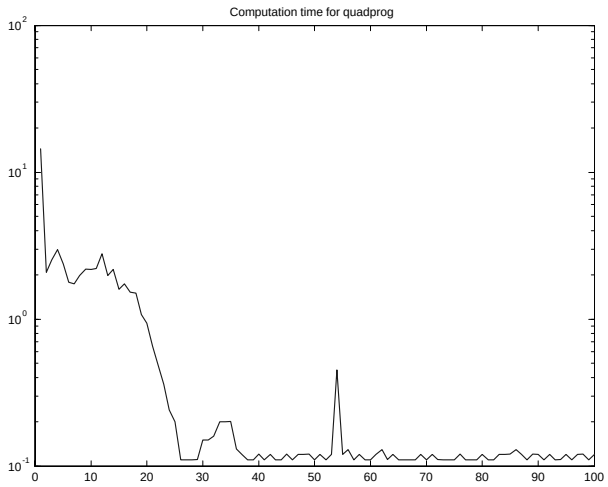

Figure 4.4: Optimization time using quadprog. Simulation carried out with 100 samples, and with horizon $N = 20$. A change in reference values occurs after 10 minutes (20 samples).

process and utilize this in a model predictive controller. Input, output, and measured disturbance variables were selected as shown in eqs. 3.6 and 3.9.

Before the project started, single loop controllers and manual control were used. Grade changes were carried out manually or partly manually by the operators: the setpoints were changed a number of times before they were equal to the new grade. During start ups, the controllers were kept in manual mode until the measurements were close to the desired specifications. In addition, during sheet breaks the basis weight and paper ash measurements were lost and the inputs controlling these variables were set equal to the values that they had prior to the sheet break. The controllers were kept in manual mode until the paper was back on the reel. Thus, it was also a key goal in the project to be able to have the controllers in automatic mode during grade changes, sheet breaks, and start ups.

APIS MPC A commercial MPC developed by Prediktor AS (www.prediktor.no), was chosen by Norske Skog for implementation. The choice of MPC was based on (i) cost, and (ii) the ability to add and develop certain features that were important. Special features that were important were the abilities to

- utilize the non-linear model;
- specify future reference changes. This means that the process operators can specify a setpoint change some time into the future, see how the controller will respond, and let the controller do the grade change if they are satisfied with the response. In many systems, the setpoint is constant into the future, so once a change in setpoint is made, the controller will respond immediately, giving the operators no time to consider how wise the response is;
- make an interface suitable for gaining operator acceptance of the MPC;
- use the MPC during grade changes, sheet breaks, and start ups.

The commercial MPC is part of a software package named Apis (Advanced Process Improvement System), which also consists of a Kalman filter, subspace system identification, and more. The Apis MPC was intended for linear models, based on the infinite horizon objective function presented in (Muske & Rawlings 1993). For the predictive controller implemented at PM6, several extensions were made to the original MPC, such as

- on-line linearization at each sample;
- on-line estimation of key model parameters/biases;
- future setpoint changes, i.e. the process operators can submit new setpoints to the controller some time before the actual grade change;
- addition of a direct input to output term;
- inclusion of measured disturbances.

The use of MPC, a nonlinear model, extended Kalman filter, and linearization at each sample, has also been suggested by (Lee & Ricker 1994), although with a finite horizon criterion. Similarly, (Gattu & Zafiriou 1992) proposed an algorithm for nonlinear MPC, with linearization at each sample, but with computation of the steady state Kalman gain at each sample.

Implementation and interface The MPC was installed at PM6 in March 2002. During the first two months, the MPC, the Kalman filter and the model were continuously tuned, retuned, and validated in open and closed loop. Some structural changes were also made during these months. From May 2002, the MPC has been in operation more or less continuously. The process operators still have the original "pre-MPC era" control configuration available, but the MPC has been the preferred choice from the beginning. Furthermore, the operators have been very active in making suggestions for improvements and new features in the system. Some of these suggestions are implemented, and others are being considered for implementation.

In addition to discussing with and involving the operators in the project from the beginning, it seems that the MPC interface has been very important for the positive operator attitude. Figure 4.5 shows part of the MPC interface at PM6. The upper row in the figure shows the basis weight, setpoint for basis weight, and the flow of thick stock. The middle row shows the paper ash, setpoint for paper ash, and the flow of filler added to the short circulation. The lower row shows the total concentration in the wire tray, the corresponding setpoint, and the flow of retention aid added to the short circulation. The interface and pairing of inputs and outputs are based on the pre-MPC era control configuration, basically because this is how the operators and engineers at PM6 are used to see it. The vertical dashed line in the middle of each row is the current time. When Figure 4.5 was captured, the paper machine was in the middle of a grade change, and studying the figure carefully, one may see the setpoints change at the current time. The setpoints for the new grade were submitted to the MPC some time before the grade change, so at the time of the grade change the outputs are actually half way to the new setpoints. In terms of gaining operator acceptance for the MPC, this feature of previewing the action taken by the controller has been very helpful. The operators can specify a grade change e.g. half an hour into the future, and see how the MPC will achieve the change: how the inputs will be manipulated to reach the new setpoints.

Reduction of variation An important objective with the MPC was to reduce variation in consistencies, basis weigh, paper ash, paper moisture, and more. Figure 4.6 shows an example with the wire tray concentration and the paper ash. The bottom line indicates whether the MPC is on (at 1) or off (at 0). When the controller is off, the original control configuration is used. The MPC provides a distinct effect of reduced variation in these two outputs.

The main objective of the project "Stabilization of the wet end at PM6" was to increase the total efficiency by 0.47%. This is an objective that is hard to measure, due to many factors affecting the total efficiency. Thus, several sub-goals were defined which were assumed easier to measure and validate. The sub-goals, and results,

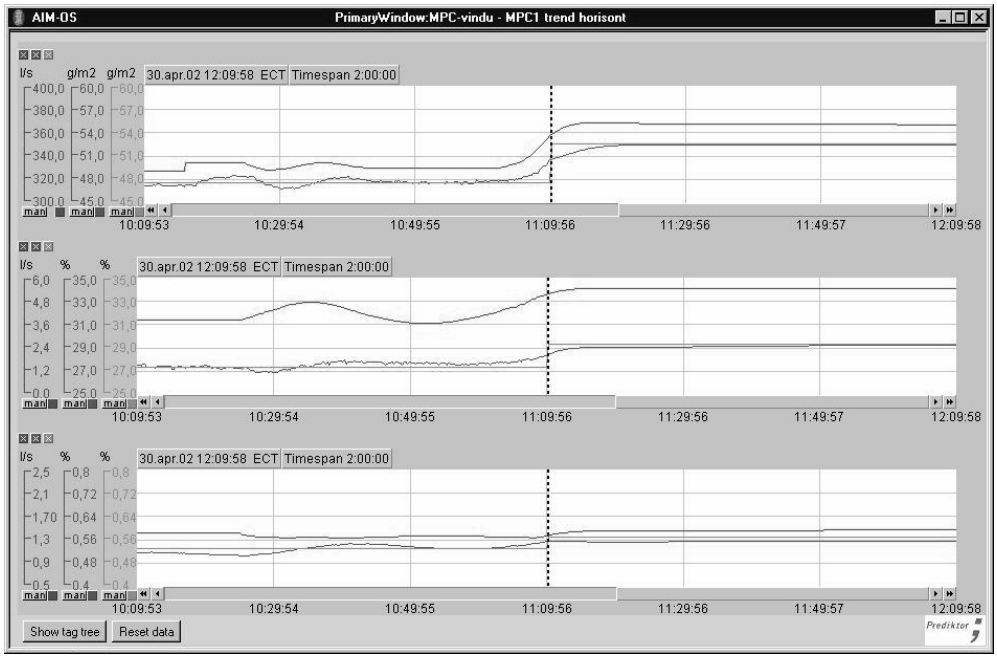

Figure 4.5: Part of the MPC interface at PM6.

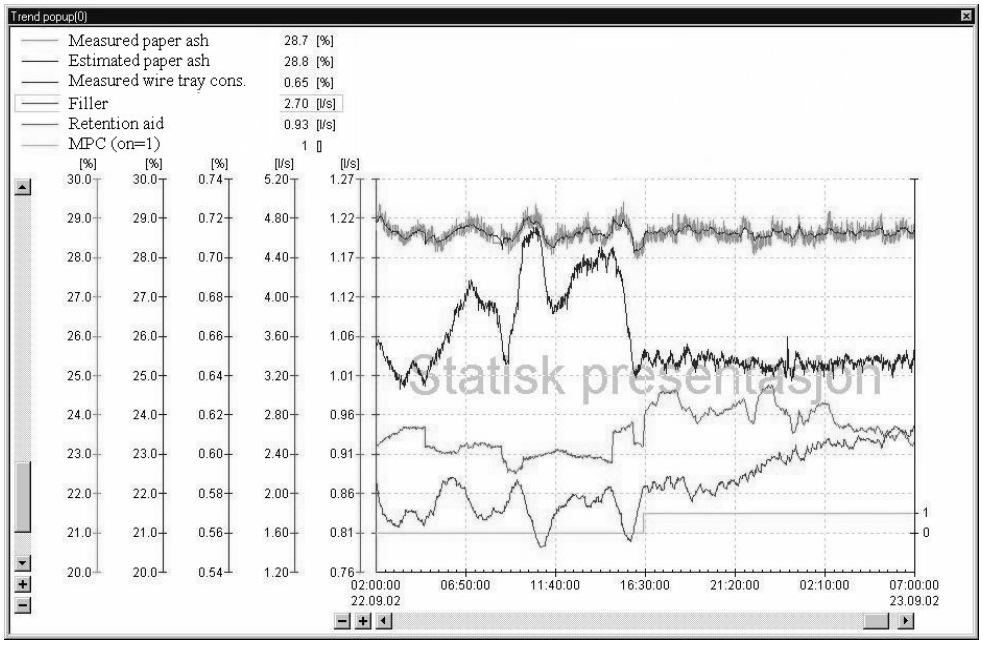

Figure 4.6: Wire tray concentration and paper ash, with (bottom line is 1) and without (bottom line is 0) MPC. From top to bottom the following variables are shown: Measured and estimated paper ash (overlapping), wire tray total concentration, retention aid, filler, and MPC on/off indication.

concerning reduced variability are:

Variable	Sub-goal (red. std. dev.)	Result
Total cons. in the wire tray	60%	Achieved
Filler cons. in the wire tray	50%	Achieved
Total cons. in the headbox	50%	Achieved
Filler cons. in the headbox	35%	Achieved
Basis weight	20%	Not achieved
Paper ash	20%	Achieved
Paper moisture	20%	Achieved

These sub-goals were defined in 1999 when the project was initiated. In 2001 a new scanning device for measuring e.g. basis weight and paper ash was installed at PM6. This significantly improved the control of the basis weight using the "old" controllers. The results in the table above are calculated with the measurement devices as of 2002, comparing the old control configuration with the MPC control configuration. Exact numbers for the reduction in standard deviation are not given, as they vary from day to day, and from operator to operator.

Other benefits of MPC In addition to reducing the variation in key paper machine variables, several other benefits are obtained using MPC. Some of these benefits arise from utilizing the developed model, not only for control purposes, but also as a replacement for measurements when these are not available or not trustworthy:

- Previously, grade changes were carried out manually or partly manually; the setpoints were changed a number of times before they were equal to the new grade. With a mechanistic model, applicable over a wide range of operating conditions, the grade changes are carried out using the MPC (see Figure 4.5). This has resulted in faster grade changes and operator independent grade changes. During larger grade changes, the use of MPC results in less off-spec paper being produced during the change. Using one mechanistic model, the grade change is handled in a straight forward fashion, as there is no need to switch between various local models.

- The basis weight and paper ash outputs can not be measured during sheet breaks. Previously, during sheet breaks the flow of thick stock and filler were frozen at the value they had immediately prior to the break. Usually the sheet breaks last less than half an hour, and the output variables are not far from target values when the paper is back on the reel. However, occasionally the sheet breaks last longer periods and there may be e.g. velocity changes during the break, leading to off-spec paper being produced for a period following the break. Another frequently experienced problem are large measurement errors immediately after a sheet break. With the MPC, the Kalman filter estimates the basis weight and paper ash during sheet breaks, and these estimates are used in the MPC as if no break had taken place. Thus, when the paper is back on the reel, the outputs are close to their setpoints.

- Previously, the controllers were not set to automatic mode before the outputs were close to the setpoints, following a start up. With a model based controller using a mechanistic model with a wide operating range, the MPC is set to automatic mode early during start ups. This results in faster start ups, and less off-spec paper being produced.

- Occasionally a special filler is added to the stock, to increase the brightness of the paper. During these periods the consistency measurements are not trustworthy as they are based on optical measurement methods. This problem is solved within the MPC / Kalman filter framework by neglecting the updates of the consistency estimate, relying on the estimate alone. For each output, there is an option within the MPC to neglect the updating of states based on this output. This is done based on experience with periods of poor measurements, even when only standard filler is used.

- The Kalman filter estimates are used in the MPC instead of the measurements. This leads to smoother controller action, and eliminates the need for additional filtering.

- The model is augmented so that some key parameters/biases are updated automatically. This reduces the need for model maintenance off-line. However, should there be larger changes in the process, such as if the white water tank is removed, or a new retention aid is used, then it will probably be necessary to re-tune the model and controller.

Further MPC refinements Based on inputs from amongst others the process operators, some refinements have been carried out. One of these are the inclusion of the paper machine velocity as both an input and an output in the model formulation. A change in paper machine velocity has a direct and distinct effect on the basis weight. Previously, the velocity was implemented as a measured disturbance in the MPC. Thus, when a change in the velocity occurred this lead to a deviation in the basis weight which it took some time to compensate for. Now, the process operators can submit a new velocity and the time for the velocity change to the MPC. The MPC will then know about this change in advance and take corrective action to prevent disturbance in the other outputs. This is illustrated in a simulated example in Figures 4.7-4.8. The velocity change was submitted to the MPC at the start of the simulation, and due to constraints on the allowed change per sample, the velocity approach the new setpoint in a ramp. The other outputs are more or less unaffected because the controller starts to compensate before the velocity change has actually happened.

In Figures 4.9 – 4.11 a sequence of screen dumps from part of the operator interface is shown. The sequence shows a grade change at October 7th, 2002, and it shows the paper machine velocity included in the interface in the fourth row.

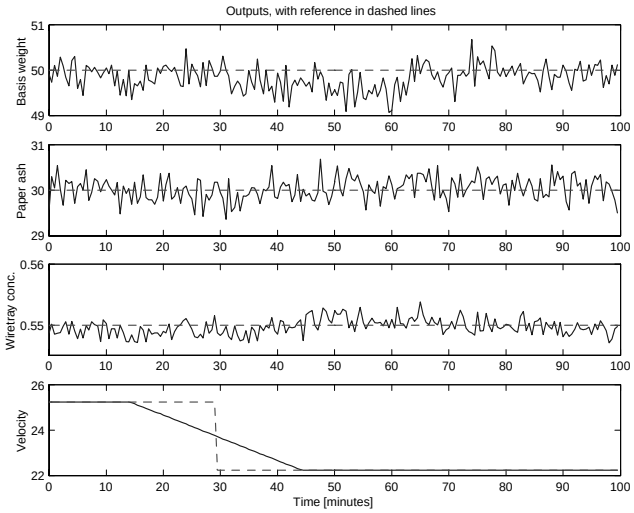

Figure 4.7: Outputs during simulation of velocity change from 25 m/ s to 22 m/ s.

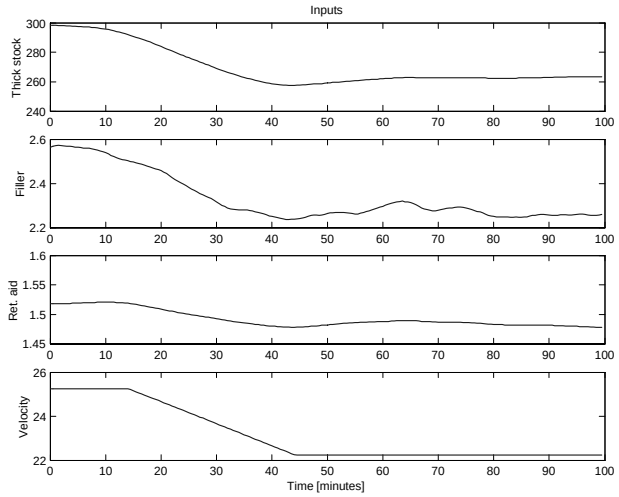

Figure 4.8: Inputs during simulation of velocity change from 25 m/ s to 22 m/ s.

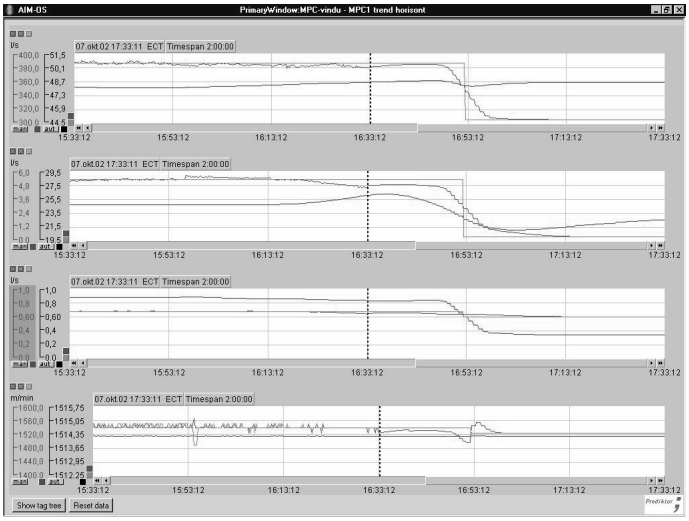

Figure 4.9: New setpoints for grade change at October 7th, 2002, have just been submitted.

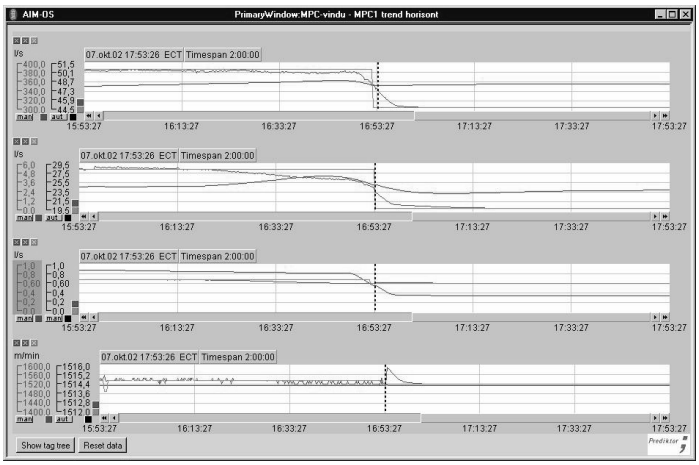

Figure 4.10: In the middle of a grade change at October 7th, 2002.

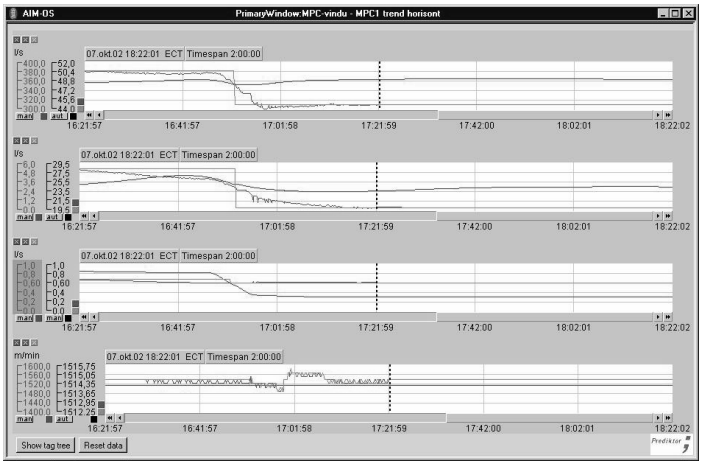

Figure 4.11: Grade change at October 7th, 2002, is finished.

Chapter 5

Roll-out of model based control

5.1 Introduction

Many large- and medium sized industry companies have a number of more or less similar process-units for processing of raw materials or production of finished products. An industrial company which has invested, or is about to invest, in advanced model based control in one of their units / factories, would benefit economically if the model and controller could be efficiently rolled-out at similar units.

The mechanistic model of PM6 at Norske Skog Saugbrugs, Norway, has been developed , and used in a model predictive control (MPC) implementation, and it is of interest to investigate if the model can be applied to other paper machines. At the beginning of Chapter 3, it was argued that the development of a reliable model was the key factor for success in advanced control. Thus, the reuse of the PM6 model to other paper machines is the main focus of this chapter. Specifically, it is investigated if and how the model can be reused at PM4, Norske Skog Saugbrugs, and PM3, Norske Skog Skogn, Norway.

There exists very little published material focusing on how to efficiently roll-out models and controllers in the industry. However, the idea of efficient roll-out of models is not entirely new, e.g. (Glemmestad et al. 2002) emphasize the advantage of reusing the models developed at Borealis, and many commercial simulators include model libraries of process units intended for reuse.

5.2 Roll-out at PM4, Norske Skog Saugbrugs

Process description PM4 at Norske Skog Saugbrugs in Halden, Norway, produce super calendered magazine paper. PM4 started up in 1963 and was rebuild during a period between 1987 to 1993. The production capacity is $125,000$ ton per year, with paper width of 4.65 meters and with a typical velocity of $1,250$ meters per minute

(Sandersen 1999). Both PM6 and PM4 at Norske Skog Saugbrugs produce super calendered magazine paper, but PM6 is 30 years younger, and has more than twice the production capacity of PM4.

The largest differences between PM4 and PM6 are probably found in the thick stock area. At PM4, no filler is added to the thick stock. Thus the only filler present in the thick stock area comes with the flow of broke and recovered stock. At PM6 disc filters are used to reclaim usable fiber and filler particles from the white water tank overflow, while another technology is used at PM4. Starch is a polymer of glucose derived from e.g. corn and potatoes (Scott 1996). Starch is added to the thick stock of PM4 through the TMP flow, while no starch is added at PM6. Starch is mainly added to improve the dry-strength of the paper, however it may also improve fines retention and drainage on the wire, and it may have a negative effect on paper formation[1] (Marton 1996). At PM6 the thick stock pump is manipulated to control the flow of thick stock, while at PM4 the thick stock pump is set at a constant speed and a thick stock valve is manipulated. This difference should be of no concern since the measured flow of thick stock is the flow entering the white water tank in both cases, and the MPC calculates the setpoint for this flow. Whether the lower level controller manipulates a pump or valve to obtain the setpoint, is irrelevant for the MPC.

The accept from the second and third stages of the hydrocyclone arrangement goes to the inlet of the white water tank via the deculator (left chamber) at PM6. At PM4 the accept goes straight to the inlet of the white water tank. This is probably not an important difference since the volume of the left chamber of the deculator is very small. Finally, a difference in the number of stages in the hydrocyclone arrangement can be found; at PM6 a five stage arrangement is used, while it is a seven stage arrangement at PM4.

Model fitting results Open loop experiments were carried out during a 5-hour period on the 10th of December 2002. These experiments were used to find approximate values for gains and time constants in the process, and for model fitting, as described in subsection 3.2.2 and Figure 3.2. Another data set was collected on the 12th of December 2002 for validation of the model. The validation data set was collected partly in open loop and with the process operators manually carrying out some step changes and a grade change. The measured and simulated outputs during validation are shown in Figure 5.1. Note that no state updating takes place during the validation, and only the initial values are given. Some statistics from the validation are given in Table 5.1. The term RMSE in Table 5.1 denotes the Root Mean Square Error value defined by

$$\mathrm{RMSE}_i = \sqrt{\frac{1}{N}\sum_{t=1}^{N}(y_i(t) - \hat{y}_i(t))^2}, \tag{5.1}$$

where N is the number of observations, $y_i(t)$ is the measured value of output i at time t, and $\hat{y}_i(t)$ is the predicted or simulated value of output i at time t.

[1] The distribution of fibres in the paper sheet.

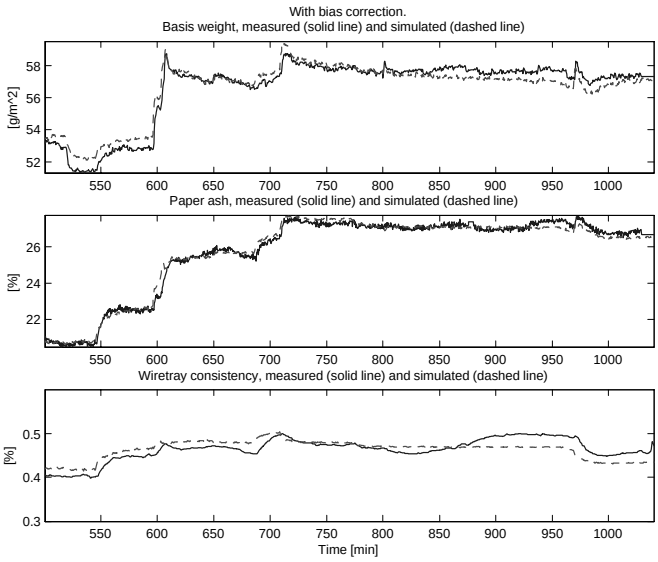

Figure 5.1: Validation of fitted model. The outputs were collected at PM4 on the 12th of December 2002. The validation is carried out by simulating the system with only the initial state values given.

Table 5.1: Statistics from validation of model with PM4 data.

Properties	**Basis weight**	**Paper ash**	**W.t. conc.**
Bias	−0.52	0.97	0.04
RMSE*	0.37	0.19	0.013

*Bias corrected

5.3 Roll-out at PM3, Norske Skog Skogn

Process description Norske Skog Skogn is the largest producer of newsprint in Norway. The production of newsprint started in 1966, and the mill has three paper machines as of today. PM3 is the largest and most modern paper machine at the Skogn mill. The production capacity of PM3 is 227,000 ton per year, with paper width of 8.47 meters, and with a typical velocity of 1,350 meters per minute. The basis weight has a more limited range than the Saugbrugs machines; typical values are 42.5, 45, and 48.8 $\mathrm{g/m^2}$. PM3 started up in 1981 and had a major rebuild/updating in 1995. PM3 is the only paper machine in Norway using DIP[2] for production of newsprint. The DIP content, or the amount of recycled fiber, is approximately 50-55% (Norske Skog 2002), (Heggli 2002). Note that PM3 in Skogn produce newsprint while both PM6 and PM4 at Saugbrugs produce super calendered magazine paper. In terms of production capacity and paper width, PM3 at Skogn, and PM6 at Saugbrugs are comparable.

Filler is added via the DIP and broke flows, thus no other filler is added to the thick stock or short circulation. The thick stock flow is manipulated through the thick stock valve, with the thick stock pump set to a constant speed. The number of stages in the hydrocyclones are 6. The accept from the second stage of the hydrocyclones goes to the inlet of the white water tank, and the accept from the third stage goes to the white water tank. At PM6, the accept from the second and third stage goes to the left chamber of the deculator. The screens and the deculator appear in reverse order at PM3, compared to PM6 and PM4 at Saugbrugs. Also, the retention aid is added before the screens, and not after as is done at PM6.

Model fitting results Figure 5.2 shows the first attempt to fit the PM6 Saugbrugs model to data collected at PM3 Skogn during December, 4th, 2002. The basis weight is the only output excited to any extent in this data set, the paper ash and wire tray concentration being more or less at rest. This is a general feature of PM3 due to the low filler content in the stock. Thus, the multivariable PM6 model does not come to full appraisal at PM3 yet, however there is an increasing trend of using more filler in newsprint, and test runs at PM3 with filler added to the short circulation will soon take place (Heggli 2002).

Studying data from PM3, it is clear that there is not much to gain in terms of stabilizing the process during normal operation. However, during start ups, sheet breaks, and grade changes, efficiency may be improved. Figure 5.3 shows the validation of the model during a grade change. At the beginning of the grade change a sheet break occur. This is recognized in Figure 5.3 by the basis weight and paper ash outputs being frozen at the values that they had immediately prior to the break. When the paper is back on the reel, the measured basis weight is $52\,\mathrm{g/m^2}$, while the setpoint is $48.8\,\mathrm{g/m^2}$. The simulated basis weight is close to the measured basis weight when the paper is back on the reel, and the simulated basis weight follows the measured basis weight closely during the whole simulation. The bias in the basis weight is approximately $0.25\,\mathrm{g/m^2}$. If the controller had relied on the simulated model output during

[2] DIP = De-Inked Pulp, i.e. pulp produced from recovered paper.

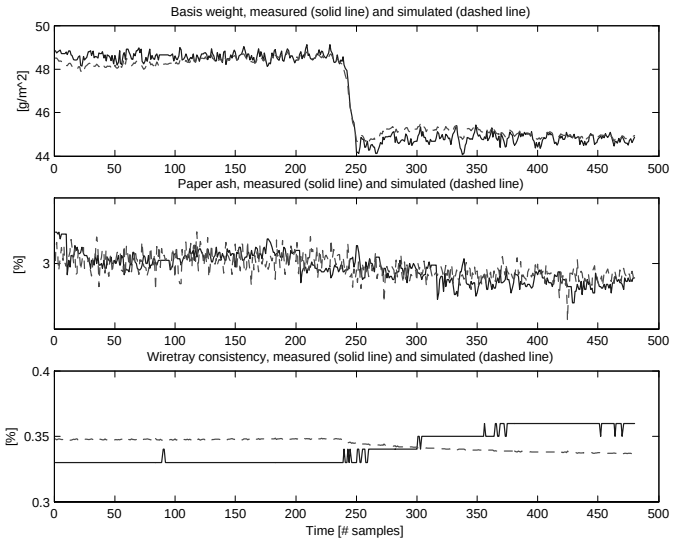

Figure 5.2: First trial fitting of PM6 Saugbrugs model to data from PM3 Skogn. Data collected at 4th of December, 2002, with 30 seconds sampling time (resampled from 5 seconds sampling time).

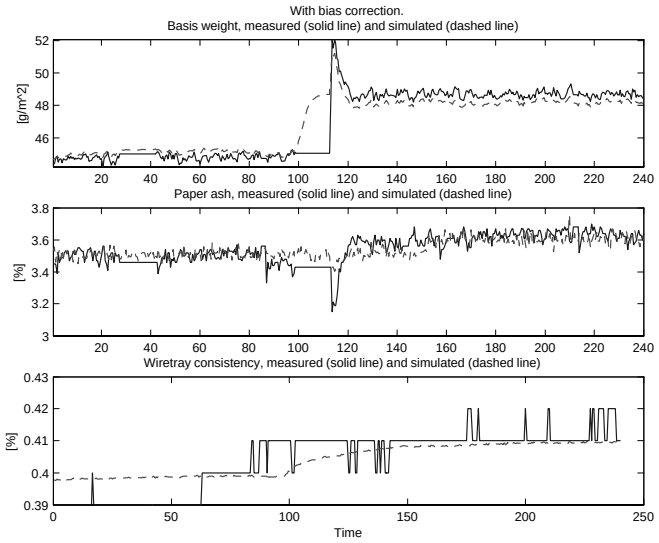

Figure 5.3: Validation of fitted model. The outputs were collected at Norske Skog Skogn PM3 on the 12th of December 2002 during a grade change. The validation is carried out by simulating the system with only the initial state values given.

the combined grade change and sheet break, the basis weight would probably have been close to the setpoint when the paper was back on the reel. Thus, less off-spec paper would be produced.

Figure 5.4 shows the basis weight and wire tray concentration outputs during a start up. The basis weight measurement is frozen at $44.8\,\mathrm{g/m^2}$ during the first 330 minutes. In Figure 5.5, it is shown in detail what happens to the basis weight measurement and simulated output when the paper is back on the reel for the first time after the start up. The measured basis weight is close to $49\,\mathrm{g/m^2}$, with the setpoint being $45\,\mathrm{g/m^2}$. This deviation was more or less predicted by the model simulation, thus the basis weight could have been much closer to the setpoint after the start up if the controller had relied on the simulated model outputs when the measurements were not available.

5.4 Comments on roll-out of PM6 model

Data and information from PM4 at Norske Skog Saugbrugs, and PM3 at Norske Skog Skogn were gathered in order to investigate the possibility to roll-out the PM6 model at other paper machines. Fitting and validation of the model are very promising. No changes to the model were carried out, except for tuning of parameter values, and still the validation results are good. The time spent on fitting and validating the

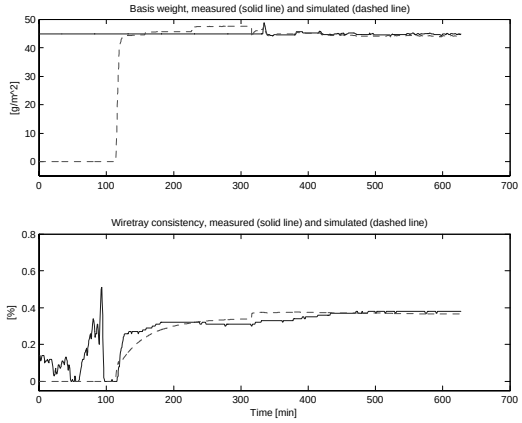

Figure 5.4: Validation of fitted model. The outputs were collected at Norske Skog Skogn PM3 on the 11th and 12th of December 2002 during a start up. The validation is carried out by simulating the system with only the initial state values given. During the first 330 minutes paper is not produced and the basis weight measurement is frozen at $44.8\,\mathrm{g/\,m^2}$.

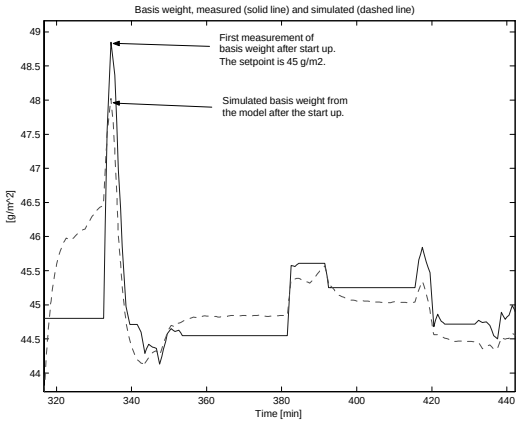

Figure 5.5: Validation of basis weight during start up. The outputs were collected at Norske Skog Skogn PM3 on the 11th and 12th of December 2002. The validation is carried out by simulating the system with only the initial state values given. During the first 330 minutes paper is not produced and the basis weight measurement is frozen at $44.8\,\mathrm{g/\,m^2}$.

PM6 model to PM4 and PM3 are approximately 1% of the time spent on developing the original model. This should be a strong incentive for focusing on mechanistic modeling in industries were there are many similar production lines or units.

Chapter 6

List of papers in thesis

A. Hauge, T.A. and Lie, B. (2000). *Simulation for Advanced Control of a Paper Machine: Model Complexity and Model Reduction*, in proceedings of the 41st SIMS simulation Conference, September 18-19, 2000, Technical University of Denmark, Kgs. Lyngby, Denmark, p 135-154.

A few corrections are made to the original paper.

B. Hauge, T.A., Ergon, R., Forsland, G.O., Slora, R. and Lie, B. (2000). *Modeling, Simulation and Control of Paper Machine Quality Variables at Norske Skog Saugbrugs, Norway*, in proceedings of the PIRA conference "Scientific & Technological Advances in the Measurement & Control of Papermaking", December 11-12, 2000, Edinburgh, UK.

A few corrections are made to the original paper.

C. Hauge, T.A. and Lie, B. (2001). *Paper Machine Modeling at Norske Skog Saugbrugs: A Mechanistic Approach*, in proceedings of the 42nd SIMS Simulation Conference, October 8-9, 2001, Telemark University College, Porsgrunn, Norway, p 119-154.

Also in *Modeling, Identification and Control*, 23(1), p 27-52. (An updated and condensed version of the SIMS 2001 paper).

The version given here is the SIMS paper with updates from the MIC paper, but not condensed.

D. Hauge, T.A., Slora, R. and Lie, B. (2002). *Model Predictive Control of a Norske Skog Saugbrugs Paper Machine: Preliminary Study*, in proceedings of Control Systems 2002, June 3-5, Stockholm, Sweden, p 75-79.

Extended version.

E. Lie, B., Dueñas Díez, M., and Hauge, T. A. (2002). *A Comparison of Implementation Strategies for MPC*, in Proceedings of International Symposium on Advanced Control of Industrial Processes, June 10-11, 2002, Kumamoto, Japan.

A few corrections are made to the original paper.

F. Hauge, T.A., Slora, R., and Lie, B. (2002). *Application of a Nonlinear Mechanistic Model and an Infinite Horizon Predictive Controller on Paper Machine 6 at Norske Skog Saugbrugs*, Submitted to Journal of Process Control.

   Extended version.

G. Hauge, T.A., Slora, R., and Lie, B. (2002). *Roll-out of model based control with application to paper machines*, Submitted to Journal of Process Control.

   Extended version.

Chapter 7

List of other contributions

1. Hauge, T.A. (2002). Modeling and control of PM6 at Norske Skog Saugbrugs, Invited lecture at MSc. course "Modeling of dynamic systems" at Telemark University College, Norway, November 18, 2002 (in Norwegian).

2. Hauge, T.A. and Lie, B. (2002). Stabilization of the Wet End at PM6. Part 3: Modeling, Model Fitting, and Tuning of a Kalman Filter at PM6, Norske Skog Saugbrugs, Norway, Norske Skog Saugbrugs A-rapport no. TAH20201 (confidential report).

3. Lie, B., Hauge, T.A., and Dueñas Diez, M. (2002). Trenger avanserte etterlikninger, Teknisk Ukeblad, No. 07, 2002, p. 22-23 (popular science in Norwegian)

4. Hauge, T. A., and Slora, R. (2002). Improved quality and efficiency by model based control: Example from PM6, Norske Skog Saugbrugs, Presentation at Norske Skog Research's joint meeting between NSE mechanical pulp- and papermaking contact fora and global optimization TMP knowledge network, Norske Skog Follum, Norway, September 24-26 2002.

5. Hauge, T. A., and Slora, R. (2002). Control of the Wet End: Examples from PM6, Norske Skog Saugbrugs, Lecture at up-grading course at the Norwegian Pulp and Paper Research Institute, Trondheim, Norway, February 6th, 2002.

6. Slora, R. and Hauge, T. A. (2001). Control of the wet end at Norske Skog Saugbrugs PM6, Presentation at Norske Skog Research's Contact Forum for Paper Making 2-2001, Trondheim, Norway, November 6-7 2001.

7. Hauge, T.A. and Lie, B. (2000). Stabilization of the Wet End at PM6. Part 2: Introductory Process Description and Modeling, Norske Skog Saugbrugs A-rapport no. TAH20001 (confidential report in Norwegian).

8. Hauge, T.A. (2000). Poster at the "Research days", September 25-27, 2000, Telemark University College.

Bibliography

Ahn, S., Park, M. & Rhee, H. (1999), 'Extended Kalman filter-based nonlinear model predictive control for a continuous MMA polymerization reactor', *Ind. Eng. Chem. Res.* **38**(10), 3942–3949.

Amin, J., Mehra, R. K. & Arambel, P. (2001), Coordinated dynamic positioning of a multi-platform mobile offshore base using nonlinear model predictive control, *in* 'Eleventh (2001) International Offshore and Polar Engineering Conference'. Stavanger, Norway, June 17-22, 2001.

Austin, P., Mack, J., Lovett, D., Wright, M. & Terry, M. (2002), Improved wet end stability of a paper machine using model predictive control, *in* 'Control Systems 2002', STFi and SPCI, pp. 80–84. June 3-5, 2002, Stockholm, Sweden.

Badgwell, T. A. & Qin, S. J. (2001), Review of nonlinear model predictive control applications, *in* 'IEE Control Engineering Series', Vol. 61, pp. 3–32.

Bassett, S. & Van Wijck, M. (1999), 'Application of predictive control technology at BP's crude oil terminal at grangemouth', *IEE Colloquium Digest* (95).

Betts, J. T. (2001), *Practical Methods for Optimal Control Using Nonlinear Programming*, SIAM.

Bown, R. (1996), Physical and chemical aspects of the use of fillers in paper, *in* J. Roberts, ed., 'Paper Chemistry', 2 edn, Chapman and Hall, chapter 11.

Box, G. E. P., Jenkins, G. M. & Reinsel, G. C. (1994), *Time Series Analysis, Forecasting and Control*, third edn, Prentice-Hall, Inc.

Camacho, E. F. & Bordons, C. (1999), *Model Predictive Control*, Springer-Verlag London.

Campbell, J. C. (1997), Modelling, Estimation, and Control of Sheet and Film Forming Processes, PhD thesis, University of Wisconsin-Madison.

Di Ruscio, D. (1997), A method for identification of combined deterministic stochastic systems, *in* M. Aoki & A. Havenner, eds, 'Applications of Computer Aided Time Series Modeling', Springer.

Featherstone, A. P., VanAntwerp, J. G. & Braatz, R. D. (2000), *Identification and Control of Sheet and Film Processes*, Springer-Verlag London.

Foss, B. A., Lohmann, B. & Marquardt, W. (1998), 'A field study of the industrial modeling process', *Journal of Process Control* **8**, 325–338.

Garcia, C. E., Prett, D. M. & Morari, M. (1989), 'Model predictive control: Theory and practice – a survey', *Automatica* **25**(3), 335–348.

Gattu, G. & Zafiriou, E. (1992), 'Nonlinear quadratic dynamic matrix control with state estimation', *Ind. Eng. Chem. Res.* **31**(4), 1096–1104.

Glemmestad, B., Ertler, G. & Hillestad, M. (2002), Advanced process control in a Borstar PP plant, *in* 'ECOREPII, 2nd European Conference on the Reaction Engineering of Polyolefins. Lyon, France, 1-4 July 2002'.

Gregory, J. (1988), 'Polymer adsorption and flocculation in sheared suspensions', *Colloids and Surfaces* **31**, 231–250.

Hagberg, M. & Isaksson, A. (1993), 'A paper machine benchmark for control systems 94', Available at ftp://ftp.e.kth.se/pub/control/benchmark/bench.ps.

Hauge, T. A. & Lie, B. (2002), 'Paper machine modeling at Norske Skog Saugbrugs: A mechanistic approach', *Modeling, Identification and Control* **23**(1), 27–52.

Heaven, E. M., Manness, M. A., Vu, K. M. & Vyse, R. N. (1996), 'Application of systems identification to paper machine model development and simulation', *Pulp and Paper Canada* **97**(4), 49–54.

Heggli, T. G. (2002). Personal communication with process engineer T. G. Heggli at Norske Skog Skogn.

Hillestad, M. & Andersen, K. S. (1994), Model predictive control for grade transitions of a polypropylene reactor, *in* 'ESCAPE4, 4th European Symposioum on Computer Aided Process Engineering, Dublin, March 1994'.

Holmström, K. (2001), The TOMLAB optimization environment v3.0 user's guide, Technical report, HKH MatrisAnalys AB.

Koethe, J. L. & Scott, W. E. (1993), 'Polyelectrolyte interactions with papermaking fibers: The mechanism of surface-charge decay', *Tappi Journal* **76**(12), 123–133.

Kosonen, M., Fu, C., Nuyan, S., Kuusisto, R. & Huhtelin, T. (2002), Narrowing the gap between theory and practice: Mill experiences with multivariable predictive control, *in* 'Control Systems 2002', STFi and SPCI, pp. 54–59. June 3-5, 2002, Stockholm, Sweden.

Lang, D., Tian, L., Kuusisto, R. & Rantala, T. (1998), Multivariable predictive control for the wet end, *in* 'Measurement and Control of Papermaking, Edinburgh, Scotland', Pira International.

Larsson, J. E. & Olsson, T. (1996), Styrning av utstromningshastighet ur innlopp-slada, Master's thesis, Tekniska Hogskolan i Lulea.

Lee, J. H. & Ricker, N. L. (1994), 'Extended Kalman filter based nonlinear model predictive control', *Ind. Eng. Chem. Res.* **33**(6), 1530–1541.

Lee, K., Lee, J. H., Yang, D. R. & Mahoney, A. W. (2002), 'Integrated run-to-run and on-line model-based control of particle size distribution for a semi-batch precipitation reactor', *Computers and chemical engineering* **26**(7-8), 1117–1131.

Ljung, L. (1996), Development of system identification, Technical Report LiTH-ISY-R-1910, Department of Electrical Engineering, Linköping University, Sweden.

Ljung, L. (1999), *System Identification, Theory for the User*, second edn, Prentice Hall PTR.

Ljung, L. (2000), 'System identification toolbox for use with matlab, user's guide (version 5)'.

Maciejowski, J. (2002), *Predictive Control with Constraints*, Prentice Hall, Harlow, England.

Mack, J., Lovett, D., Austin, P., Wright, M. & Terry, M. (2001), Connoisseur model predictive control of a paper machine's wet-end., *in* 'ICHEME - Advances in Process Control'. York, UK, 24-25 September 2001.

Marton, J. (1996), Dry-strength additives, *in* J. C. Roberts, ed., 'Paper Chemistry', Chapman and Hall, chapter 6.

Mayne, D. Q., Rawlings, J. B., Rao, C. V. & Scokaert, P. O. M. (2000), 'Constrained model predictive control: Stability and optimality', *Automatica* **36**, 789–814.

McQuillin, D. L. & Huizinga, P. W. (1995), Reducing grade change time through the use of predictive multi-variable cotrol, *in* 'ECOPAPERTECH', pp. 73–82. Helsinki, Finland.

Menani, S., Koivo, H. N., Huhtelin, T. & Kuusisto, R. (1998), Dynamic modelling of paper machine from grade change data, *in* 'Control Systems 98, Helsinki', pp. 79–85.

Muske, K. R. & Badgwell, T. A. (2002), 'Disturbance modeling for offset-free linear model predictive control', *Journal of Process Control* **12**, 617–632.

Muske, K. R. & Rawlings, J. B. (1993), 'Model predictive control with linear models', *AIChE Journal* **39**(2), 262–287.

Nelles, O. (2001), *Nonlinear System Identification*, Springer.

Noreus, O. & Saltin, J. (1998), Dynamic modelling of wet-end on paper machine, *in* 'Control Systems 98, Helsinki', pp. 104–110.

Norske Skog (2002), Norske Skog internet page at www.norske-skog.com.

NPPA (The Norwegian Pulp and Paper Association) (2002), 'Key figures 2001', NPPA internet page at www.pulp-and-paper.no.

Ogunnaike, B. A. & Wright, R. A. (1997), Industrial applications of nonlinear control, *in* 'AIChE Symposium Series; 1997; Issue 316', pp. 46–59.

Park, M. J., Hur, S. M. & Rhee, H. K. (2002), 'Online estimation and control of polymer quality in a copolymerization reactor', *AIChE Journal* **48**(5), 1013–1021.

Pelton, R. H. (1984), 'The influence of hydrodynamic forces on retention aid performance: Model experiments', *Tappi Journal* **67**(9), 116–118.

Prasad, V., Schley, M., Russo, L. P. & Bequette, B. W. (2002), 'Product property and production rate control of styrene polymerization', *Journal of Process Control* **12**(3), 353–372.

Qin, S. J. & Badgwell, T. A. (1997), An overview of industrial model predictive control technology, *in* 'AIChE Symposium Series, No. 316', pp. 232–256.

Qin, S. J. & Badgwell, T. A. (1998), An overview of nonlinear model predictive control applications, *in* 'Nonlinear Model Predictive Control Workshop - Assessment and Future Directions'. Ascona, Switzerland, June 3-5, 1998.

Rao, M., Xia, Q. & Ying, Y. (1994), *Modeling and Advanced Control for Process Industries: Applications to Paper Making Processes*, Springer-Verlag London.

Rawlings, J. B. (2000), 'Tutorial overview of model predictive control', *IEEE Control Systems Magazine* pp. 38–52.

Richalet, J., Estival, J. L. & Fiani, P. (1995), Industrial applications of predictive functional control to metallurgical industries, *in* 'In Proceedings of the 4th IEEE Conference on Control Applications', pp. 934–942. Albany, N.Y.

Roberts, J. C. (1996*a*), *The Chemistry of Paper*, The Royal Society of Chemistry.

Roberts, J. C., ed. (1996*b*), *Paper Chemistry*, 2 edn, Blackie, London.

Rooke, P. E. (1999), Applying Combined Neural Network and Physical Modelling to Retention Processes in Papermaking, PhD thesis, UMIST, Department of Paper Science.

Sælid, S. (1984), Forelesningsnotater i modellering av dynamiske prosesser, Technical Report 84-2-X, Division of Engineering Cybernetics, NTH, Norway. (in Norwegian).

Sandersen, E. (1999), 'Guide. Norske Skog Saugbrugs'. (Booklet).

Schei, T. S. & Singstad, P. (1998), Nonlinear model predictive control of a batch polymerization process, *in* 'American Control Conference'. Philadelphia, Pennsylvania, June 1998.

Schiesser, W. E. (1991), *The Numerical Method of Lines: Integration of Partial Differential Equations*, Academic Press, Inc.

Scott, W. E. (1996), *Principles of Wet End Chemistry*, Tappi Press, Atlanta.

Shirt, R. W. (1997), Modelling and Identification of Paper Machine Wet End Chemistry, PhD thesis, The University of British Columbia, Dep. of Electrical and Computer Engineering, Canada.

Skogestad, S. & Postlethwaite, I. (1996), *Multivariable Feedback Control: Analysis and Design*, John Wiley & Sons Ltd.

Slora, R. (2001), Stabilization of the wet end at PM6. part 1: Developing controllers for the thick stock, Technical Report A-rapport RSL20001, Norske Skog Saugbrugs. (confidential and in Norwegian).

Smook, G. A. (1992), *Handbook for Pulp and Paper Technologists*, 2nd edn, Angus Wilde Publications Inc., Vancouver.

Söderström, T. & Stoica, P. (1989), *System Identification*, Prentice Hall International.

Sohlberg, B. (1998), *Supervision and Control for Industrial Processes*, Springer.

Statistics Norway (2002*a*), 'Industrial statistics. structural data, 2000', Statistics Norway internet page at www.ssb.no/english.

Statistics Norway (2002*b*), 'Manufacturing statistics. commodity figures, 2001', Statistics Norway internet page at www.ssb.no/english.

Støle-Hansen, K. (1998), Studies of some Phenomena in Control Engineering Projects - With Application to Precipitation Processes, PhD thesis, Norwegian University of Science and Technology.

The MathWorks, Inc. (2000), 'Optimization toolbox for use with matlab, user's guide (version 2)'.

Van de Ven, T. G. M. (1984), 'Theoretical aspects of drainage and retention of small particles on the fourdrinier', *Journal of Pulp and Paper Science* **10**(3), 57–63.

Van Overschee, P. & De Moor, B. (1996), *Subspace Identification for Linear Systems*, Kluwer Academic Publishers.

Walter, E. & Pronzato, L. (1997), *Identification of Parametric Models from Experimental Data*, Springer.

Part II

Published and Submitted Papers

Paper A

Simulation for Advanced Control of a Paper Machine: Model Complexity and Model Reduction

Hauge, T.A. and Lie, B. (2000). *Simulation for Advanced Control of a Paper Machine: Model Complexity and Model Reduction*, in proceedings of the 41st SIMS simulation Conference, September 18-19, 2000, Technical University of Denmark, Kgs. Lyngby, Denmark, p 135-154.

A few corrections are made to the original paper.

Simulation for Advanced Control of a Paper Machine: Model Complexity and Model Reduction

T. A. Hauge and B. Lie
Telemark University College
Kjolnes Ring 56
3914 Porsgrunn
Norway

Abstract

A 528 order mechanistic model of a paper machine is implemented in Matlab. The model has been developed for advanced control of three key quality variables, and it is desirable to reduce the size and complexity of the full scale model. It is shown how the full scale model can be reduced by both system identification techniques and by utilizing our physical knowledge about the process. The prediction abilities of the various reduced order models are compared with the output from the 528 order model, highlighting some distinct features of the various models.

Keywords: Paper machine, dynamic model, model complexity, model reduction, system identification

1 Introduction

The world's second largest manufacturer of uncoated magazine paper (SC) is Norske Skog Saugbrugs, at Halden, Norway (Norske Skog 2000). Magazine paper is characterized by its glossy appearance due to the high content of filler (usually clay). Typically 30% (weight %) of the paper consists of filler, 65% of fibers and 5% of water. The filler is added for improving certain properties of the paper, such as brightness and smoothness, and also often to reduce the production costs. The Saugbrugs mill incorporates three paper machines (PM), in which PM6 is the largest and most modern one (build in the 1990's). A paper machine is in general a multivariable non-linear complex mixture of mechanical and chemical processes. A model of such a machine must capture the essential behavior with respect to a set of chosen variables. Typically the term "essential" will have different meaning to scientists working in different areas. A model for control should have input-output properties reasonably close to the input-output properties of the true system, while still be simple enough for implementation and use in real-time applications. There are basically two different approaches to modeling for control: i) Mechanistic modeling, in which physics,

material balances, etc. form the basis of the model, and ii) Empirical modeling, in which collected input-output data are used to fit a non-physical model structure to the data. The two approaches have some distinct features which will be discussed later.

At Norske Skog Saugbrugs, a project has been initiated to implement advanced model based control for some key paper quality variables at PM6. A mechanistic model of PM6, with three selected output variables and three selected input variables, has been developed and implemented in MATLAB. This work is thoroughly described in (Hauge & Lie 2000). The model, which is a non-linear state-space model, is quite large and complex, and perhaps not a good candidate for model based control. Input-output data are collected from the process and these indicate that first- or second-order submodels with time delays may be sufficient to describe the process behavior (at a given operating condition) (Slora 1999). Thus, the problem is to reduce the complexity of the model so that it is more suitable for advanced control purposes.

There are many benefits of simplified models, e.g. less computational time, and easier analysis, interpretation and controller design. However, the accuracy of a simplified model will in general decrease. A lot of work has been done in the area of model reduction - see e.g. (Öhman 1998), (Andersson 1997) and (Diwekar 1994). These references focus on e.g. model reduction within specified error bounds or along known trajectories. In this paper we approach the simplification problem by i) system identification methods - i.e. we identify empirical "low order" models by various well established methods, and ii) physical knowledge - i.e. we utilize our physical knowledge about the process to reduce the model. Finally, we compare the various reduced models and test their prediction abilities at different operating conditions.

The full scale mechanistic model will be used as a reference for comparison with models of reduced complexity. The comparison will be done by simulation studies, and we will investigate how the reduced complexity influence on the input-output behavior of the system. Thus, we only consider the $\hat{y}_{k|0}$ predictor in this paper, i.e. the predicted output $\hat{y}$ at time k, given y at time 0. Another well known predictor is the one-step-ahead predictor $\hat{y}_{k+1|k}$.

2 The Process

A simplified overview of PM6 is given in Figure 1. Cellulose, TMP (thermomechanical pulp) and broke (repulped fibers and filler from sheet breaks and edge trimmings) are blended in the mixing chest. The stock is fed to the machine chest with a controlled total consistency[1]. Between the mixing and machine chests, filler is added at a constant rate. The filler is usually clay, but occasionally another kind of filler is added when high whiteness is required. The flow to the machine chest is large in order to keep the level of the machine chest constant, and an overflow is returned to the mixing chest. The total consistency in the mixing and machine chests are typically around

[1] The total consistency is the weight of solids (i.e. filler, fiber and fines) divided by the total weight of solids and water.

3 to 4%, which is considerably higher than consistencies later on in the process, and thus the stock from the machine chest is denoted as the "thick stock".

The thick stock enters the "short circulation" in the white water tank. Here, the thick stock is diluted to 1-1.5% total consistency by white water[2] and a recirculation flow from the deculator. More filler is added to the stock just after the white water tank. The first cleaning process is a five stage hydrocyclone arrangement, mainly intended to separate heavy particles from the flow. The accept from the first stage of the hydrocyclones goes to the deculator where air is separated from the stock. The second cleaning process is two parallel screens, which separates larger particles from the stock. Retention aid is added to the stock at the outlet of the machine screens. The retention aid is a cationic polymer which, amongst others, adsorb onto anionic fibers and filler particles and cause them to flocculate. The flocculation mechanism is the key for retaining small fiber fragments (fines) and filler particles on the wire. Non-flocculated filler particles will in general be to small to be retained on the wire, although mechanical entrapment of particles can be a significant mechanism (Bown 1996). In the headbox the pulp is distributed evenly onto the fine mesh, woven wire cloth. Most of the water in the pulp is recirculated to the white water tank, while a share of fiber material and filler particles form a network on the wire which will soon become the paper sheet. The pulp flow from the white water tank, through the hydrocyclones, deculator, screens, headbox, onto the wire and back to the white water tank is denoted the "short circulation".

In the wire section, most of the water is removed by draining. In the press section, the paper sheet is pressed between rotating steel rolls, thus making use of mechanical forces for water removal. Finally, in the dryer section the paper sheet passes over rotating and heated cast iron cylinders, and most of the water left in the sheet is removed by evaporation. The paper is then accumulated on the reel before it is moved on to further processing.

3 The Full Scale Model

A black-box overview of the system is given in Figure 2. The manipulated inputs to the system are the amount of thick stock (u_t), the amount of filler added to the short circulation (u_c), and the amount of retention aid (u_r). The outputs from the system are the basis weight (y_w), the paper ash content (y_a), and the white water total consistency (y_c). The basis weight and the paper ash content are measured between the dryer section and the reel, while the white water total consistency is measured in the flow from the wire to the white water tank. The paper ash content is the amount of filler in the paper (the weight of the ash from a burned piece of paper approximately equals the weight of filler in the paper).

The model is basically covering those elements (chests, tanks, pipes, etc.) found in Figure 1. Typically, there are mass-balances of (longer) fiber, fiber fines, and the

[2] White water is the drainage from the wire. It is stored in the white water tank.

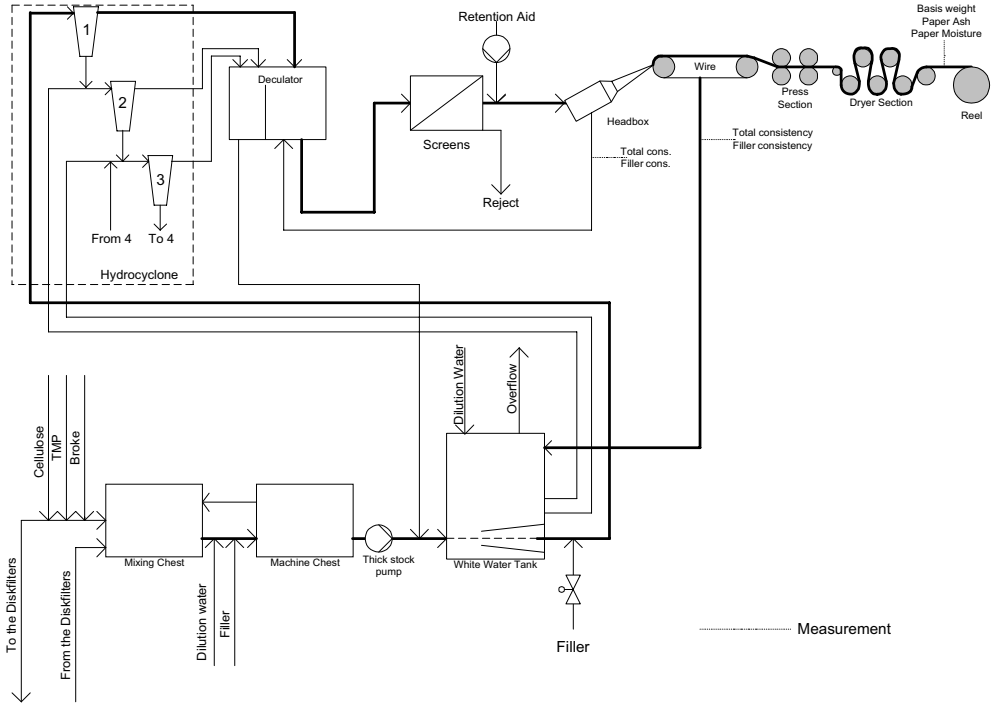

Figure 1: An overview of the paper machine.

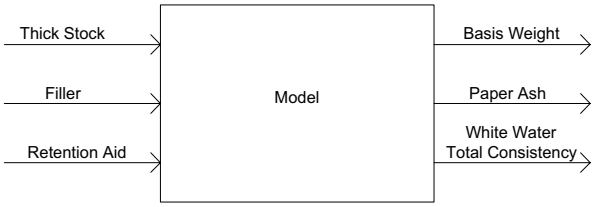

Figure 2: Inputs and outputs from the model.

two filler types for every significant volume, i.e.

$$\frac{dm_i}{dt} = \sum_j w_{i,j}, \tag{1}$$

where m_i is mass of component i in some volume, and $w_{i,j}$ is mass flow j of component i into this volume. In the short circulation there are also mass-balances for flocculated components and retention aid. Most pipelines are modeled by partial differential equations (time delays), i.e.

$$\frac{\partial C_i}{\partial t} = -v \cdot \frac{\partial C_i}{\partial x}, \tag{2}$$

where C_i is the concentration of component i, and v is the velocity of mass flow in the pipeline. The addition of retention aid causes fibers and fillers to flocculate. The flocculation takes place in the short circulation, and is here modeled by second order kinetic equations like

$$\frac{\partial C_{floc,i}}{\partial t} = -v \cdot \frac{\partial C_{floc,i}}{\partial x} + \frac{k_i}{\rho} \cdot C_i \cdot C_{ret.aid}, \tag{3}$$

where $C_{floc,i}$ is the concentration of flocculated mass of component i, C_i is the concentration of component i (non-flocculated), k_i is a flocculation constant, ρ is the density of the mass flow, and $C_{ret.aid}$ is the concentration of retention aid. Elements like the screens, headbox and wire are basically modeled with static/algebraic equations, considering the relatively small volumes involved.

The number of ordinary differential equations (ODE) is 34, and there are 104 partial differential equations (PDE). The PDE's are discretized in x-direction, bringing the total number of ODE's to 554. In this paper we omit the model for the thick stock, thus the system to study is between the thick stock pump and the reel. The reason for this being that new measurements for total consistency and ash consistency in the thick stock will be installed at PM6, thus making the thick stock model superfluous. The number of ODE's and PDE's are down to respectively 28 and 100, making the total number of ODE's (after discretization) 528.

4 Complexity Reduction

4.1 Input signals

Filtered PRBS's (Pseudo Random Binary Signals) are used as test and identification inputs to the system, and are shown in Figure 3. This type of input is widely used in identification experiments for linear systems/models (Ljung 1999) (Söderström & Stoica 1989).

The data are collected in the neighborhood of a typical operating condition of the paper machine. The most important variables defining this operating condition are given in Table 1.

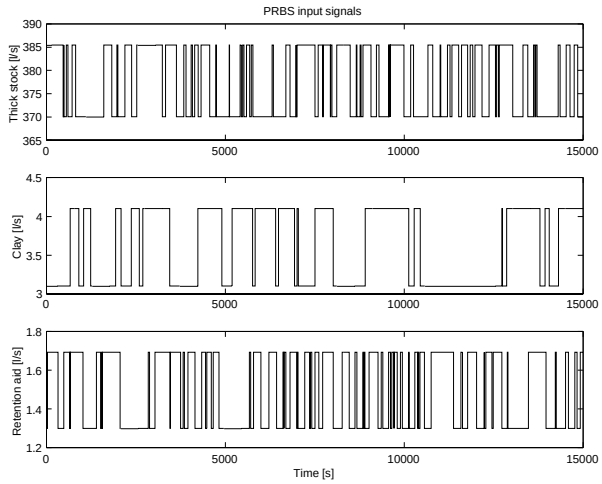

Figure 3: The filtered PRBS input signals used for identification and model reduction.

Table 1: Variable values describing the operating condition for identification.

Thick stock, flow	370 l/ s
Thick stock, total consistency	3.72%
Thick stock, filler consistency	1.47%
Addition of filler to the short circulation	3.1 l/ s
Addition of retention aid to the short circulation	1.3 l/ s
Basis weight	49.2 g/ m^2
Paper ash content	29.9%
Wire tray, total consistency	0.78%
Wire tray, ash consistency	0.61%
Headbox, total consistency	1.47%
Headbox, ash consistency	0.83%
Machine velocity	1500 m/min

Table 2: Sum of squared errors for mechanistic models.

Order	38^3	38	87	161
SSE_w	40	89	18.5	5.4
SSE_a	10.8	28	2.7	1.2
SSE_c	0.011	0.025	0.03	$8.5 \cdot 10^{-4}$

4.2 Measuring the error

The test signals are the filtered PRBS signals of Figure 3, and the calculated sum of squared errors (SSE)

$$SSE_i = \sum_{k=1}^{N} (\hat{y}_{i,k} - y_{i,k})^2, \tag{4}$$

is used as a measure of the error introduced by the simplifications. Here, $\hat{y}_i$ is the simulated i^{th} output from the reduced order model, y_i is the simulated i^{th} output from the full scale model, and N is the number of samples. The i's in the SSE's are denoted as w (basis weight), a (paper ash content) or c (wiretray concentration). The predictions $\hat{y}_i$ are centered so that they have the same mean value as the full scale model responses y_i, before the SSE's are calculated.

In this paper we only consider horizons in which only the initial values are known. This is often written as $\hat{y}_{k|0}$, i.e. the predicted output $\hat{y}$ at time k, given y at time 0. Another well known predictor is the one-step-ahead predictor $\hat{y}_{k+1|k}$.

4.3 Reduced mechanistic models

The full scale model is based on physical and chemical laws and balances. In this section we use our physical knowledge about the process, along with common sense, to reduce the complexity and size of the model.

In Figure 4 the full scale model responses are shown along with a 38^{th} order model. Based on the observed sum of squared errors (SSE) for various reduced models, it is chosen to concentrate on a 38^{th} order model, an 87^{th} order model and a 161^{th} order model for the comparison with other models. For the 38^{th} order model it is also chosen to optimize the behavior by tuning some key parameters in the model. These parameters are the volumes in the deculator, and in a reject tank between the fourth and fifth stage of the hydrocyclones, and the clay and fines flocculation constants. The physical insight of the model is only negligibly degraded by the optimization, although e.g. the optimized volumes no longer have the correct physical value. The sum of squared errors (SSE) are given in Table 2.

The reduction in computation time from the 161^{th} order model to the 38^{th} order model was approximately 50%, while the reduction from the full scale model to the 38^{th} order model was more than 80%.

[3] Optimized.

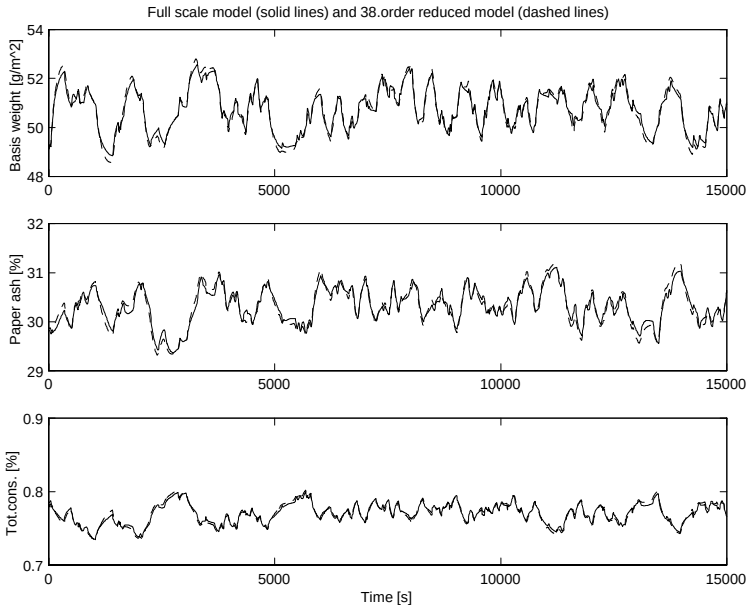

Figure 4: The responses of the full scale model (solid lines) and of a 38^{th} order reduced mechanistic model (dashed lines). The PRBS input signals are shown in Figure 3.

4.3.1 The simplifications

In a model reduction effort it is natural to look at the discretization of the PDE's. In the full scale model each pipeline is discretized into 5 volumes making the pipeline delays the largest contributor to the number of states in the model. Simulation showed that by replacing every PDE outside of the main flow (thick line in Figure 1) by one ODE, the model behavior was essentially the same. This immediately reduced the number of states from 528 to 256. In addition the pipelines between the machine chest and white water tank and between the white water tank and the first stage of the hydrocyclones could also be discretized into one volume without affecting the model behavior too much. These simplifications combined with several lumped volumes in the hydrocyclones, and the inclusion of the volume of the pipeline between the deculator (left side) and the white water tank into the deculator (left side) gave the 161^{th} order reduced model.

The 87^{th} order model is the result of a continuation of reductions and simplifications on the 161^{th} order model:

- The pipeline between the deculator (right side) and the screens are discretized into one volume
- The wire-, press- and dryer sections are discretized into one "volume"
- Several pipeline volumes in the hydrocyclone arrangement are included in a reject tank between the fourth and fifth stage
- Several pipeline volumes are included in the deculator:
  - The pipeline volume between the headbox and the deculator
  - The pipeline volume between the machine chest and the white water tank
  - The pipeline volume between the hydrocyclones first stage and second stage pump
  - The pipeline volume between the hydrocyclones second stage pump and the second stage
  - The pipeline volume between the hydrocyclones second stage and third stage pump
  - The pipeline volume between the hydrocyclones third stage pump and third stage
  - The pipeline volume between the hydrocyclones fourth stage and third stage pump.

The 38^{th} order model results from a continuation of reductions and simplifications on the 87^{th} order model:

- The pipeline volume between the deculator (right side) and the screens, is included in the deculator

- The pipeline volume between the white water tank and the first stage of the hydrocyclones, is included in the deculator
- The pipeline between the screens and the headbox is discretized into one volume.

4.4 Reduced empiric (black-box) models

In this section, several black-box identification schemes will be used to identify "simple" linear models. Input-output data from the full scale model are collected, and models will be identified by prediction error and subspace methods. The data are collected in the neighborhood of a typical operating condition of the paper machine. The most important variables defining this operating condition are given in Table 1.

4.4.1 Transfer matrix models

The responses of the process to step inputs are saved on file. In turn, the data from one input and one output are used to fit the parameters in a first- and second-order model (transfer function) with time delay:

$$y(s) = \frac{K}{\tau_1 s + 1} e^{-\tau_3 s} \cdot u(s) \tag{5}$$

$$y(s) = \frac{K}{(\tau_1 s + 1) \cdot (\tau_2 s + 1)} e^{-\tau_3 s} \cdot u(s) \tag{6}$$

The time delays are found visually, while the process gains and time constants are found by applying

$$K = \frac{\lim_{k\to\infty} y_k - y_{k=0}}{U} \qquad \text{(process gain)} \tag{7}$$

$$\hat{\tau}_1 = \arg\min_{\tau_1} \sum_k e_k^2 \qquad \text{(time constant, first-order model)}$$

$$[\hat{\tau}_1, \hat{\tau}_2] = \arg\min_{[\tau_1,\tau_2]} \sum_k e_k^2 \qquad \text{(time constants, second-order model)} \tag{8}$$

where $y_{k=0}$ is the initial output value, U is the step input size, and e_k is the error between the simulated model output and the output on file, at time k.

A first-order model is preferred whenever the fit of the second-order model is only negligibly[4] better. The transfer matrix is found to be:

$$\begin{bmatrix} y_w \\ y_a \\ y_c \end{bmatrix} = \begin{bmatrix} \frac{0.1020}{(169s+1)} e^{-50s} & \frac{0.5583}{(1831s+1)(617s+1)} e^{-50s} & \frac{2.7726}{32^2 s^2+2\cdot 0.5\cdot 32 s+1} e^{-12s} \\ \frac{-0.0221}{31^2 s^2+2\cdot 0.5\cdot 31 s+1} e^{-35s} & \frac{0.7051}{(1867s+1)(549s+1)} e^{-40s} & \frac{1.6916}{119^2 s^2+2\cdot 0.37\cdot 119 s+1} e^{-12s} \\ \frac{0.0013}{(203s+1)} e^{-20s} & \frac{0.020}{(1826s+1)(623s+1)} e^{-20s} & \frac{-0.1455}{(301s+1)} e^{-7s} \end{bmatrix} \cdot \begin{bmatrix} u_t \\ u_c \\ u_r \end{bmatrix} \tag{9}$$

[4] That is, when the difference in SSE (sum of squares) is zero for a rounded three digit number.

Table 3: Sum of squared errors for N4SID models.

Order	7	28
SSE_w	19.69	9.78
SSE_a	24.15	11.64
SSE_c	0.0126	0.0054

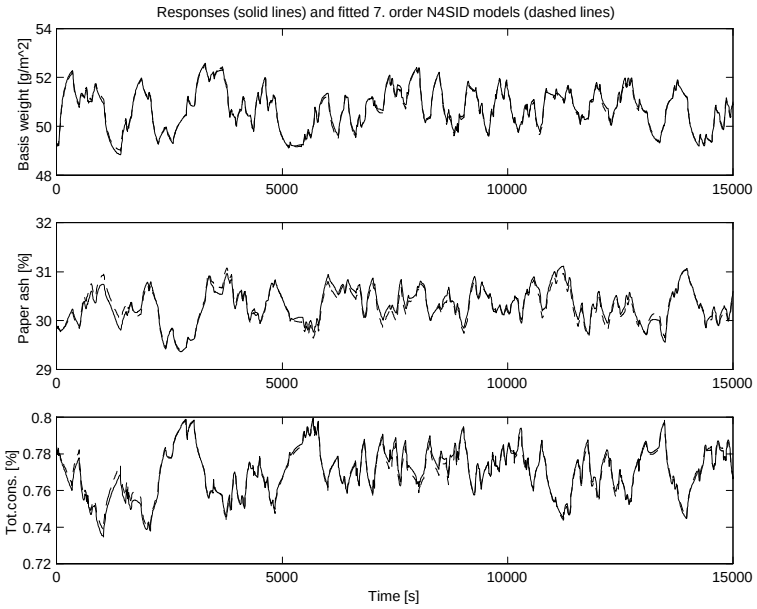

Figure 5: The responses of the full scale model (solid lines) and of a fitted 7^{th} order N4SID model (dashed lines). The PRBS input signals are shown in Figure 3.

4.4.2 N4SID subspace method

The "Numerical algorithms for Subspace State Space System Identification" method (N4SID) belongs to the subspace system identification family (Van Overschee & De Moor 1996). The method is an integrated part of the system identification toolbox (Ljung 1997) in Matlab. The data are pretreated by centering and scaling before entered into the N4SID function.

The input signals are shown in Figure 3. In Figure 5 the responses are shown along with a fitted 7^{th} order model. Based on the observed sum of squared errors (SSE) for various model orders, it is chosen to concentrate on the 7^{th} order model and a 28^{th} order model for the comparison with other models. The sum of squared errors, SSE (see Equation 4), are given in Table 3.

Table 4: Sum of squared errors for DSR models.

Order	3	7
SSE_w	46.19	16.98
SSE_a	28.13	20.81
SSE_c	0.0211	0.0156

4.4.3 DSR subspace method

The "combined Deterministic and Stochastic system identification and Realization" method (DSR) belongs to the subspace system identification family (Di Ruscio 1997). The method and software (Di Ruscio 1996) are easy to use, requiring only the data and an additional parameter to be specified. A singular value plot is supplied for helping to determine the model order. When the model order is specified, the program returns a state-space model (including the Kalman filter gain matrix, and the innovations covariance matrix) along with the initial conditions. The data are pretreated by centering and scaling before entered into the DSR program.

The input signals are shown in Figure 3. In Figure 6 the responses are shown along with a fitted 7^{th} order model. It is chosen to concentrate on a third order model and a 7^{th} order model for the comparison with other models. The sum of squared errors, SSE (see Equation 4), are shown in Table 4.

4.4.4 Prediction error method (PEM)

The celebrated prediction error method (Ljung 1999) (Söderström & Stoica 1989) is an integrated part of Matlab's System Identification toolbox (Ljung 1997). It offers a vast amount of possibilities regarding linear model structures, such as ARMAX, BJ, FIR and state-space models. However, for MIMO (multi-input multi-output) systems, the ARMAX-type of models get complicated and they are perhaps not very suitable for such systems. The state-space model, is however often preferred for representation of MIMO systems.

Unlike the subspace methods, the PEM is an iterative method, based on minimization of the prediction error. The fact that it is iterative limits the possible number of free parameters in the model structure dramatically, and one should not expect to be able to identify high order models (even when one is using a canonical form). A recommended method (Ljung 1997) for identifying MIMO models is to use a subspace method (such as N4SID or DSR) to identify an initial model, and use the parameters of this model as initial values for the PEM method. This approach is taken here, although the 7^{th} and 28^{th} order models where not improved by the PEM method, probably due to too many free parameters involved. The third order DSR model where improved by the PEM method, and the sum of squares (see Equation 4) are as given in Table 5.

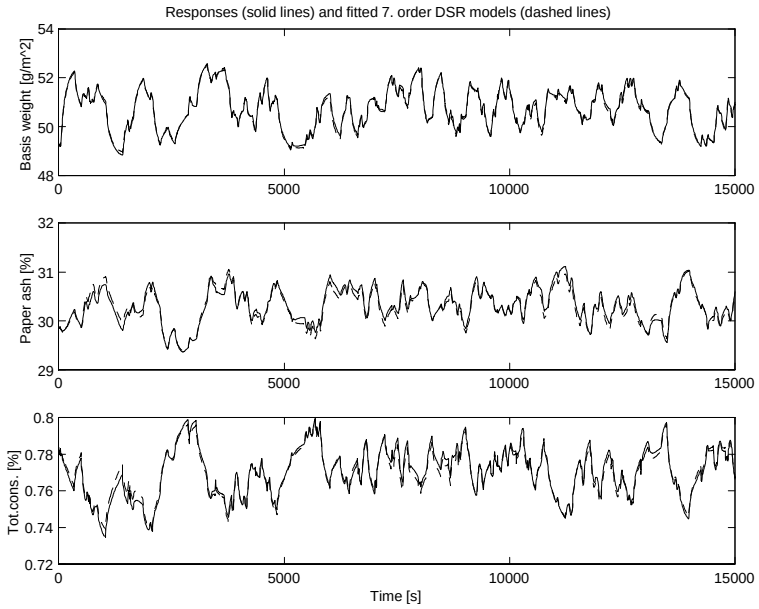

Figure 6: The responses of the full scale model (solid lines) and of a fitted 7^{th} order DSR model (dashed lines). The PRBS input signals are shown in Figure 3.

Table 5: Sum of squared errors for PEM model.

Order	3
SSE_w	41.02
SSE_a	21.81
SSE_c	0.01716

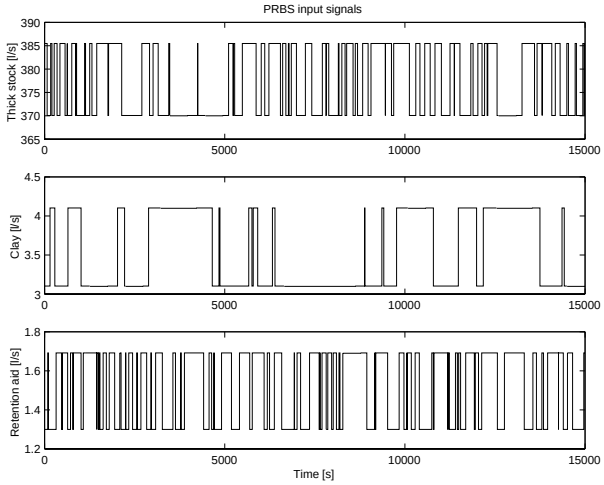

Figure 7: The filtered PRBS signals used for validation of the models. The overall operating condition of the paper machine is the same as when the models where identified.

5 Comparison of the Models: Prediction Ability

5.1 Prediction of future outputs without change in operating condition

New input signals are designed and applied to the full scale model. The levels of the input signals are such that the overall operating condition of the paper machine is in the neighborhood of that given by the variables in Table 1. The new input signals are shown in Figure 7.

The SSE's (see Equation 4) for the empirically identified and reduced mechanistic models are given in Table 6.

The PEM, DSR and N4SID models have good prediction ability, although the SSE's have increased significantly as compared to the identification. The SSE's of the mechanistic models are in some cases lower (better), and in some cases higher than in Chapter 4.3.

5.2 Prediction of future outputs with change in operating condition

Yet another set of input signals are designed, differing from previously used signals such that the overall operating condition of the paper machine is changed. The most

[5] Time delays are not included.
[6] Optimized.

Table 6: Sum of squared errors for reduced and identified models. The operating condition is comparable to that at the time of identification.

Method	Order	SSE_w	SSE_a	SSE_c
TM*	15[5]	266	76	0.046
PEM	3	76	32	0.036
DSR	3	82	46	0.043
DSR	7	47	29	0.041
N4SID	7	55	32	0.034
N4SID	28	36	12	0.018
Mech.[6]	38	41	11	0.011
Mech.	38	75	25	0.021
Mech.	87	18	2.2	0.003
Mech.	161	5	0.9	$8 \cdot 10^{-4}$

*Transfer Matrix

Table 7: Variable values describing a new operating condition for validation.

Thick stock, flow	436 l/ s
Thick stock, total consistency	3.72%
Thick stock, filler consistency	1.47%
Addition of filler to the short circulation	5.95 l/ s
Addition of retention aid to the short circulation	2.01/ s
Basis weight	56 g/ m^2
Paper ash content	32%
Wire tray, total consistency	0.78%
Wire tray, ash consistency	0.62%
Headbox, total consistency	1.47%
Headbox, ash consistency	0.85%
Machine velocity	1650 m/min

important variables to describe this new operating condition are given in Table 7.

The input signals are shown in Figure 8, and the SSE's (see Equation 4) for the empirically identified and reduced mechanistic models are given in Table 8.

The PEM, DSR and N4SID models are identified at a different operating condition, and thus it is not a surprise that the prediction ability is decreased (except for some of the y_c outputs, for which the ability has improved). The mechanistic models are producing better predictions than previously (with a few exceptions).

Figure 9 shows the responses from the full scale model and the third order DSR predictions.

[7] Time delays are not included.
[8] Optimized.

Table 8: Sum of squared errors for reduced and identified models. The operating condition is different from what was used for identification.

Method	Order	SSE_w	SSE_a	SSE_c
TM*	15[7]	275	57	0.050
PEM	3	110	60	0.035
DSR	3	148	101	0.074
DSR	7	93	63	0.032
N4SID	7	98	59	0.030
N4SID	28	74	31	0.016
Mech.[8]	38	40	8	0.0078
Mech.	38	43	13	0.011
Mech.	87	17	3	0.0022
Mech.	161	6.5	0.8	$8.5 \cdot 10^{-4}$

*Transfer Matrix

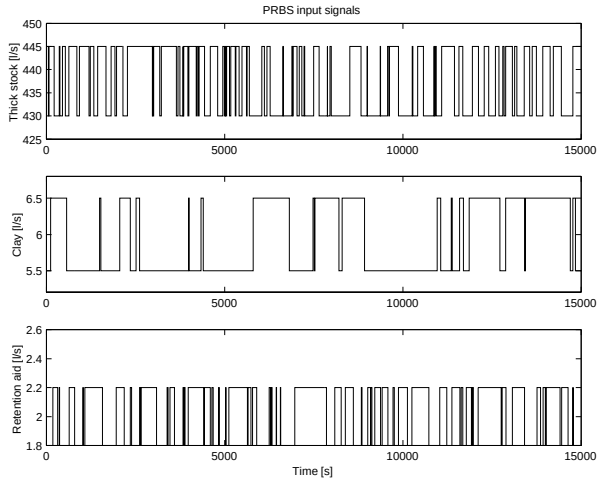

Figure 8: The filtered PRBS signals used for validation of the models. The overall operating condition of the paper machine is different from what was used for model identification and reduction.

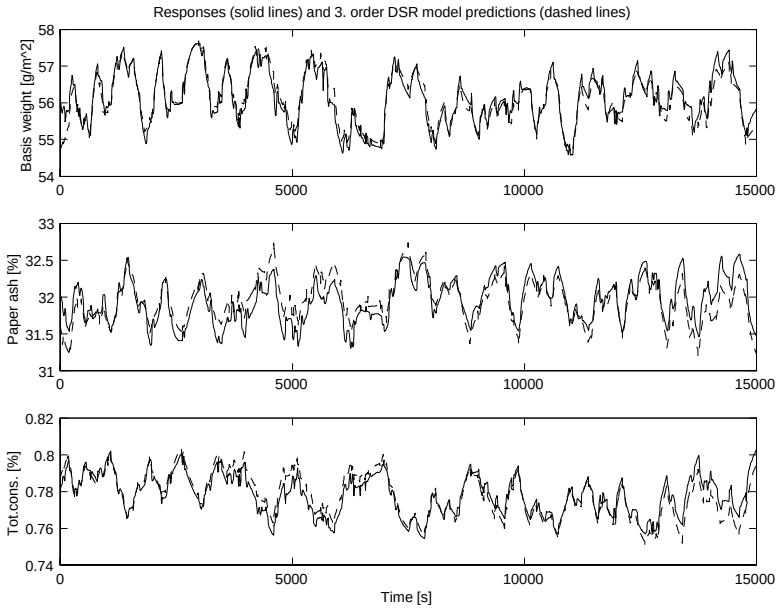

Figure 9: Full scale model responses (solid lines) and third order DSR model predictions (dashed lines), after change in operating condition.

6 Conclusions

The efforts made in this paper has been to study the possibilities for reducing the complexity of a paper machine model, and how the reduction affects the prediction abilities. The predictions for the various models are compared to the output from a mechanistic model of 528 ordinary differential equations (ODE). One should be aware that the full scale mechanistic model by no means represents the true system, although it is considered to do so in the comparisons of this paper.

For three different sets of input-output data, it is shown that the 528 order mechanistic model can be reduced to a 161 order mechanistic model with negligible effect. Mechanistic models using 87 and 38 ODE's are also validated with three different data sets, as are empiric models of order between 3 and 28. The mechanistic models in this paper are distinguished from the empiric models in several ways:

- The empiric models are much simpler than the mechanistic models. The empiric models usually have low order and they are linear, while the mechanistic models are of higher order and they are non-linear.
- The simulation time for the empiric models are much shorter than for the mechanistic models.
- It takes much more effort to develop a mechanistic model of a paper machine than it does to find an empiric model. However, to find a high order empiric model demands extensive experimentation on the paper machine, which is often impossible.
- The prediction ability of the empiric models strongly depends on the operating condition of the paper machine, compared to the operating condition at which the model was identified. The prediction ability at the same operating condition as in the identification, is generally very good. The prediction ability deteriorates as the operating condition is shifted away from the condition at the time of identification.
- The prediction abilities of the mechanistic models are (close to) constant, and are in most cases only negligibly affected by changes in the operating condition.

It is not possible, nor was it the intention with this paper, to conclude which model or model type is best for advanced control purposes. The various models has their specific attributes which are summarized in the list above, and it will be necessary to run tests on the real paper machine before one decides which model is best suited for the purpose.

Acknowledgments The authors would like to thank the employees at PM6, and especially Roger Slora, for their cooperation in providing information for this paper and for their general helpfulness. We also wish to express our thanks to associate professor Rolf Ergon for taking time to examine and pointing at errors in an earlier

version of this paper, and to associate professor David Di Ruscio and Finn Haugen for LaTeX help. The work of Tor Anders Hauge is financially supported by the Research Council of Norway (project number 134557/410) with additional financial support by Norske Skog Saugbrugs.

References

Andersson, L. (1997), Comparison and simplification of uncertain models, Licentiate thesis, Department of Automatic Control, Lund Institute of Technology.

Bown, R. (1996), Physical and chemical aspects of the use of fillers in paper, *in* J. Roberts, ed., 'Paper Chemistry', 2 edn, Chapman and Hall.

Di Ruscio, D. (1996), 'DSR toolbox for MATLAB'. Copyright, Fantoft Process, Norway.

Di Ruscio, D. (1997), A method for identification of combined deterministic stochastic systems, *in* M. Aoki & A. Havenner, eds, 'Applications of Computer Aided Time Series Modeling', Springer Verlag, New York.

Diwekar, U. M. (1994), 'How simple can it be? - a look at the models for batch distillation', *Computers & chemical Engineering* **18**, S451–S457.

Hauge, T. A. & Lie, B. (2000), Stabilization of the wet end at PM6. part 2: Introductory process description and modeling, A-rapport TAH20001, Norske Skog Saugbrugs, Halden, Norway (confidential and in Norwegian).

Ljung, L. (1997), *System Identification Toolbox - For Use with Matlab*, The MathWorks, Inc.

Ljung, L. (1999), *System Identification. Theory for the User*, 2 edn, Prentice Hall PTR.

Norske Skog (2000), Norske Skog internet page at www.norske-skog.com.

Öhman, M. (1998), Trajectory-based model reduction of nonlinear systems, Licentiate thesis, Department of Automatic Control, Lund Institute of Technology.

Slora, R. (1999), Wire tray consistency control at PM6, PM6-Rapport RSL9904, Norske Skog Saugbrugs, Halden, Norway (confidential and in Norwegian).

Söderström, T. & Stoica, P. (1989), *System Identification*, Prentice Hall International.

Van Overschee, P. & De Moor, B. (1996), *Subspace Identification for Linear Systems*, Kluwer Academic Publishers.

Paper B

Modeling, Simulation and Control of Paper Machine Quality Variables at Norske Skog Saugbrugs, Norway

Hauge, T.A., Ergon, R., Forsland, G.O., Slora, R. and Lie, B. (2000). *Modeling, Simulation and Control of Paper Machine Quality Variables at Norske Skog Saugbrugs, Norway*, in proceedings of the PIRA conference "Scientific & Technological Advances in the Measurement & Control of Papermaking", December 11-12, 2000, Edinburgh, UK.

A few corrections are made to the original paper.

Modeling, Simulation and Control of Paper Machine Quality Variables at Norske Skog Saugbrugs, Norway

T. A. Hauge[*], R. Ergon[*], G. O. Forsland[†], R. Slora[‡] and B. Lie[*]

Abstract

In this paper we focus on an ongoing project at Norske Skog Saugbrugs, Norway, for stabilization of the wet end of paper machine 6 (PM6). A high-order order mechanistic model is developed, and model reduction is studied by simulation. Closed loop experiments on PM6 is described and carried out, and empiric models are identified and validated. The models will be used in a model predictive control (MPC) structure. A solution for estimating missing measurements during sheet breaks is presented and demonstrated with simulations.

Keywords: Paper machine, dynamic model, optimal estimation, system identification, closed loop identification, model reduction, model predictive control

1 Introduction

At Norske Skog Saugbrugs, Norway, a project has been initiated to stabilize the wet end of paper machine 6 (PM6). Norske Skog Saugbrugs is the world's second largest manufacturer of uncoated magazine paper (SC) (Norske Skog 2000), and the mill incorporates three paper machines, of which PM6 is the largest and most modern one (build in the 1990's). The project "Stabilization of the wet end of PM6" will be described in some detail here, focusing on the results so far and also briefly discussing future actions.

The objects of the project are to reduce the number of sheet breaks, reduce the down time when sheet breaks occur and to substantially reduce the variability in key variables such as basis weight, paper ash, white water consistencies, etc. Another important objective is to investigate how the methods developed in this project can be efficiently applied on other paper machines within Norske Skog.

[*]Telemark University College, PB 203, 3901 Porsgrunn, Norway.
[†]Sonton Teknologi, Porsgrunn, Norway.
[‡]Norske Skog Saugbrugs, 1756 Halden, Norway

The basic idea is to model selected parts of the paper machine and use model predictive control (MPC) for improving the stability of selected variables. A similar approach is reported in (Lang, Tian, Kuusisto & Rantala 1998), although there are several important differences, notably the use of a mechanistic model in this project. The selected variables are the basis weight, the paper ash content and the white water total consistency.

There are basically two different approaches to modeling for control: i) Mechanistic modeling, in which physics, material balances, etc. form the basis of the model, and ii) Empirical modeling, in which collected input-output data are used to fit a non-physical model structure to the data. Both mechanistic and empiric models are presented in this paper and the two approaches have some distinct features which will be discussed later. The mechanistic model of PM6, with the three selected output variables and three selected input variables, is implemented in MATLAB. This work is thoroughly described in (Hauge & Lie 2000*b*). The model, which is a non-linear state-space model, is quite large and complex, and perhaps not a good candidate for model based control. Input-output data are collected from the process and these indicate that a transfer matrix with elements consisting of first- or second-order models with time delays may be sufficient to describe the process behavior at a given operating condition (Slora 1999). Thus, we wish to reduce the complexity of the mechanistic model so that it is more suitable for advanced control purposes. In this paper we approach the simplification problem by i) system identification methods - i.e. we identify empirical "low-order" models by various well established methods, and ii) physical knowledge - i.e. we utilize our physical knowledge about the process to reduce the model. This leads to a set of models of various size and complexity, and these are compared by their prediction abilities at different operating conditions.

Included in this paper are also results from identification and validation of dynamic models from real time data. The experiments were carried out in September-October, 2000, and in this paper we chose to focus on empirical models, saving the mechanistic model fitting for future work. Experiment design problems are addressed and discussed to some extent. Closed loop data are used with various identification methods, giving low-order linear models.

During sheet breaks the basis weight and paper ash measurements are lost, leading to serious problems for the controller. An alternative to "freezing" the controlled inputs is to estimate the missing measurements and let the controller use the estimates during sheet breaks. An estimator could be mechanistic or empiric, and in this paper we focus on a theoretically optimal empiric estimator. The estimator utilizes system inputs and also secondary measurements (measurements which are of less importance) as estimator inputs. The optimal estimator is based on an underlying Kalman filter and an output error (OE) model structure (Ergon 1999*b*).

The paper is organized as follows: In Section 2 an overview of PM6 is presented. Section 3 elaborates on mechanistic and empiric modeling of PM6 using simulated data, while real-time data are used in Section 4. Section 5 deals with an optimal solution for estimation of missing measurements during sheet breaks. In Section 6 a possible future model predictive control structure of PM6 is presented in addition

to several ongoing projects for disturbance rejection in connection with the models. Finally, Section 7 summarizes this paper and presents some conclusions.

2 The Process

A simplified description of the paper machine is given in Figure 1. A short description of some important aspects is given next, while a more thorough description is found in (Hauge & Lie 2000*a*) and (Hauge & Lie 2000*b*).

Filler is added both to the thick stock and to the short circulation. Various types of fillers are added depending on the required properties for the finished paper. The behavior of the various kinds of fillers is very distinct, at least regarding the retention aid. However, these differences will not be seen in the present paper, as only one kind of filler is added to the stock during experimentation and simulation.

The first cleaning process is a five stage hydrocyclone arrangement, mainly intended to separate heavy particles from the flow. The accept from the first stage of the hydrocyclones goes to the deculator where air is separated from the stock. The second cleaning process consists of two parallel screens, which separates larger particles from the stock. Retention aid is added to the stock at the outlet of the machine screens. The retention aid is a cationic polymer which, amongst others, adsorb onto anionic fibers and filler particles and cause them to flocculate. The flocculation mechanism is the key for retaining small fiber fragments (fines) and filler particles on the wire. Non-flocculated fines and filler particles will in general be too small to be retained on the wire, although mechanical entrapment can be a significant mechanism (Bown 1996), (Orccotoma, Paris & Perrier 1999).

3 Modelling and identification from simulated data

3.1 A mechanistic approach

A black-box overview of the system is given in Figure 2. The manipulated inputs to the system are the amount of thick stock (u_t), the amount of filler added to the short circulation (u_f), and the amount of retention aid (u_r). The outputs from the system are the basis weight (y_w), the paper ash content (y_a), and the white water total consistency (y_c). The basis weight and the paper ash content are measured between the dryer section and the reel, while the white water total consistency is measured in the flow from the wire to the white water tank.

The model is basically covering the elements (chests, tanks, pipes, etc.) found in Figure 1. Typically, there are mass-balances of (longer) fiber, fiber fines, and various kinds of fillers for every significant volume, i.e.

$$\frac{dm_i}{dt} = \sum_j w_{i,j}, \tag{1}$$

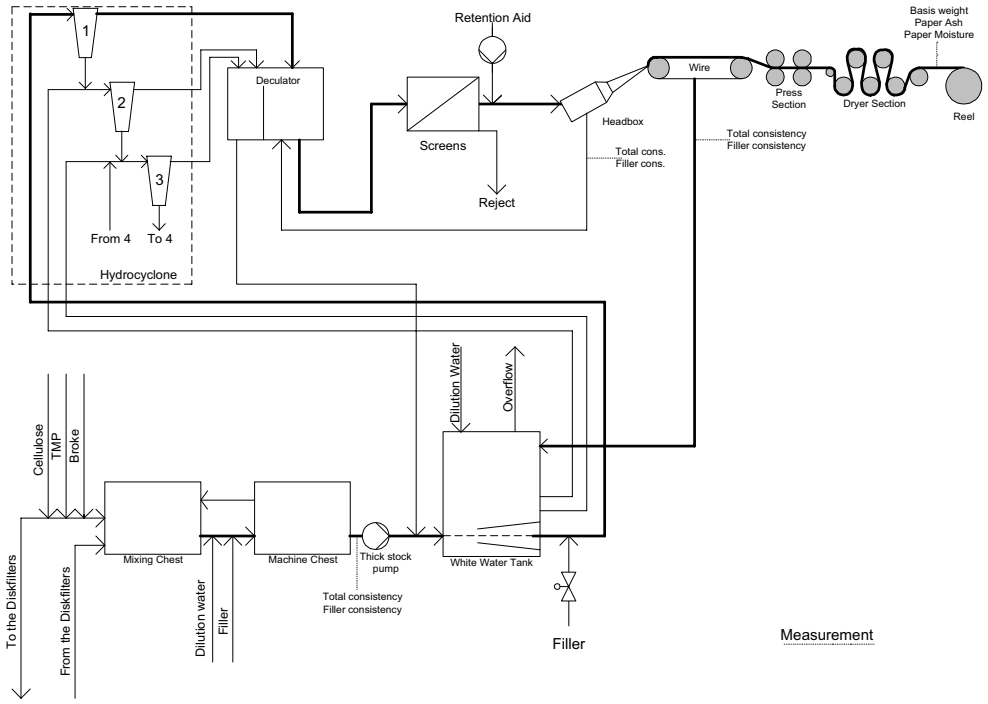

Figure 1: Simplified sketch of the paper machine.

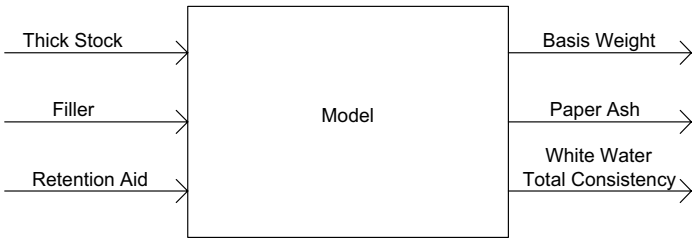

Figure 2: Inputs and outputs from the model.

where m_i is mass of component i in some volume, and $w_{i,j}$ is mass flow j of component i into this volume. In the short circulation there are also mass-balances for flocculated components and retention aid. Most pipelines are modeled by partial differential equations (time delays), i.e.

$$\frac{\partial C_i}{\partial t} = -v \cdot \frac{\partial C_i}{\partial x}, \tag{2}$$

where C_i is the concentration of component i, and v is the velocity of mass flow in the pipeline. The addition of retention aid causes fibers and fillers to flocculate. The flocculation takes place in the short circulation, and is here modeled by second-order kinetic equations like

$$\frac{\partial C_{\text{floc},i}}{\partial t} = -v \cdot \frac{\partial C_{\text{floc},i}}{\partial x} + \frac{k_i}{\rho} \cdot C_i \cdot C_{\text{ret.aid}}, \tag{3}$$

where $C_{floc,i}$ is the concentration of flocculated mass of component i, C_i is the concentration of component i (non-flocculated), k_i is a flocculation constant, ρ is the density of the mass flow, and $C_{ret.aid}$ is the concentration of retention aid. The flocculation term in Equation 3 is obviously too simple for describing the complicated flocculation (and adsorption) process, but it may be sufficient for a model for control. The mechanistic model is not yet validated with real data, and should the validation fail then there are some alternative, and more complicated, flocculation terms which can be derived from the literature. Several sources, e.g. (Swerin, Ödberg & Wågberg 1996) and (Moudgil, Shah & Soto 1987), state that the flocculation rate can be expressed as

$$F = kEN_0^2, \tag{4}$$

where k is a rate constant, E is a flocculation efficiency factor often modelled by $E = \theta(1-\theta)$ where θ is the fractional coverage of the solid surface by polymer, and where finally N_0 is the number of particles. (Shirt 1997) uses the following second-order kinetic equation in his dynamic simulation model

$$\begin{aligned} \frac{dC_{ij}}{dt} &= k^{ij} C_i C_j \theta_i^+ \theta_j^- \left(\frac{V_i V_j}{V_i + V_j} \right), \\ \frac{d\theta}{dt} &= k_{\text{att}}(n_0 - \theta)(1-\theta) - k_{\text{det}}\theta, \end{aligned} \tag{5}$$

where C_{ij} is consistency of flocs formed from components i and j, C_i and C_j are consistencies of component i and j, θ_i^+ is the fractional coverage of component i by cationic polymer, θ_j^- is fractional coverage of component j by anionic polymer, V_i and V_j are volumes of individual component particles i and j, k_{att} and k_{det} are attachment and detachment rate constants respectively, and finally n_0 is the dosage of polymer relative to the amount required to completely cover the particle surface. Shirt's model is based on a retention aid system with one anionic polymer and one cationic polymer, and is not directly applicable to the PM6 model where only cationic polymer is used. However, from experiments carried out in this project it is observed that certain important aspects which are covered by Shirt's model (Equation 5) are

hardly explained by the flocculation term in Equation 3. It is, for example, observed that the wire tray consistency is reduced when the thick stock flow is increased. This can not be explained by a flocculation term as in Equation 3, and a certain modification is probably necessary.

Elements like the screens, headbox and wire are basically modeled with static/algebraic equations, considering the relatively small volumes involved.

The number of ordinary differential equations (ODE) is 34, and there are 104 partial differential equations (PDE). The PDE's are discretized in x-direction into five ODE's each, bringing the total number of ODE's to 554. In this paper we omit the model for the thick stock, thus the system to study is between the thick stock pump and the reel. The reason for this being that new methods for controlling and calculating the total consistency and ash consistency in the thick stock are implemented at PM6 (more on this in Section 6), thus making the thick stock model superfluous. The number of ODE's and PDE's are thus down to respectively 28 and 100, making the total number of ODE's (after discretization) 528.

3.2 Reduced order mechanistic models

The full scale model is based on physical and chemical laws and balances. In this section we use our physical knowledge about the process, along with common sense, to reduce the complexity and size of the model. Filtered PRBS's (Pseudo Random Binary Signals) are used as test inputs to the system. This type of input is widely used in identification experiments for linear systems/models (Ljung 1999) (Söderström & Stoica 1989). The data are collected in the neighborhood of a typical operating condition of the paper machine.

An RMSE (root mean square error) criterion

$$RMSE_i = \sqrt{\frac{1}{N}\sum_{t=1}^{N}\left(y_i(t) - \hat{y}_i(t)\right)^2}, \tag{6}$$

were used for comparing the identification and validation of the various models. Equation 6 gives the RMSE for output i, N is the number of observations, $y_i(t)$ is the simulated output i from the full scale model at time t and $\hat{y}_i(t)$ is the simulated output i at time t from a reduced order model. The i's in the RMSE's are denoted as *weight* (basis weight), *ash* (paper ash content) or *conc.* (wire tray concentration). The simulated $\hat{y}_i$ are centered so that they have the same mean value as the full scale model responses y_i, before the RMSE's are calculated.

The RMSE is calculated for various reduced models, and we chose to concentrate on a 38^{th} order model, an 87^{th} order model and a 161^{th} order model for the comparison with other models. For the 38^{th} order model we also chose to optimize the behavior by tuning some key parameters in the model. These parameters are the volumes in the deculator and in a reject tank between the fourth and fifth stage of the hydrocyclones, and the filler and fines flocculation constants. The physical foundation of the model is only negligibly degraded by the tuning, although e.g. the optimized volumes no longer have the correct physical value.

The reduction in computational time from the 161^{th} order model to the 38^{th} order model was approximately 50%, while the reduction from the full scale model to the 38^{th} order model was more than 80%.

The simplifications In a model reduction effort it is natural to look at the discretization of the PDE's. In the full scale model each pipeline is discretized into 5 volumes making the pipeline delays the largest contributor to the number of state variables in the model. Simulation showed that by replacing every PDE outside of the main flow (thick line in Figure 1) by one ODE, the model behavior was essentially the same. This immediately reduced the number of states from 528 to 256. In addition the pipelines between the machine chest and white water tank and between the white water tank and the first stage of the hydrocyclones could also be discretized into one volume without affecting the model behavior too much. These simplifications combined with several lumped volumes in the hydrocyclones, and the inclusion of the volume of the pipeline between the deculator (left side) and the white water tank into the deculator (left side) gave the 161^{th} order reduced model.

The 87^{th} and 38^{th} order models are the results of a continuation of reductions and simplifications on the 161^{th} order model. Thus, in the 38^{th} order model the remaining volumes are the white water tank volume, a lumped hydrocyclone reject tank volume, lumped deculator volumes ("right" and "left" side volume) and the volume of the pipeline between the screens and the headbox. More details on the simplifications can be found in (Hauge & Lie 2000*a*).

Further model simplifications are hard to attain without degrading the physical foundation of the model to a larger extent. However, by allowing the model to be semi mechanistic it is possible to reduce the number of states considerably. A low-order semi mechanistic model is being developed at the moment.

3.3 Empiric models

In this section, several black-box identification schemes will be used to identify "simple" linear models. Input-output data from the full scale model are collected, and models will be identified by prediction error and subspace methods. The data are collected in the neighborhood of a typical operating condition of the paper machine.

Transfer matrix with first- or second-order elements with time delays The responses of the process to step inputs are saved on file. In turn, the data from one input and one output are used to fit the parameters in a first- or second-order model (transfer function) with time delay:

$$y(s) = \frac{K}{\tau_1 s + 1} e^{-\tau_2 s} \cdot u(s) \tag{7}$$

$$y(s) = \frac{K}{\tau_1^2 s^2 + 2\zeta\tau_1 s + 1} e^{-\tau_2 s} \cdot u(s) \tag{8}$$

The time delays are found visually, while the process gains, time constants and damping coefficients are found by applying

$$K = \frac{\lim_{k\to\infty} y_k - y_{k=0}}{U} \quad \text{(process gain)} \tag{9}$$

$$\hat{\tau}_1 = \arg\min_{\tau_1} \sum_k e_k^2 \quad \text{(time constant, first-order model)}$$

$$[\hat{\tau}_1, \hat{\zeta}] = \arg\min_{[\tau_1,\zeta]} \sum_k e_k^2 \quad \text{(time constant and damping coefficient, second-order model),} \tag{10}$$

where $y_{k=0}$ is the initial output value, U is the step input size, and e_k is the error between the simulated model output and the output on file, at time k.

A first-order model is preferred whenever the fit of the second-order model is only negligibly[1] better. The transfer matrix is found to be:

$$\begin{bmatrix} y_w \\ y_a \\ y_c \end{bmatrix} \tag{11}$$

$$= \begin{bmatrix} \frac{0.1020}{(169s+1)}e^{-50s} & \frac{0.5583}{(1831s+1)(617s+1)}e^{-50s} & \frac{2.7726}{32^2s^2+2\cdot0.5\cdot32s+1}e^{-12s} \\ \frac{-0.0221}{31^2s^2+2\cdot0.5\cdot31s+1}e^{-35s} & \frac{0.7051}{(1867s+1)(549s+1)}e^{-40s} & \frac{1.6916}{119^2s^2+2\cdot0.37\cdot119s+1}e^{-12s} \\ \frac{0.0013}{(203s+1)}e^{-20s} & \frac{0.020}{(1826s+1)(623s+1)}e^{-20s} & \frac{-0.1455}{(301s+1)}e^{-7s} \end{bmatrix} \begin{bmatrix} u_t \\ u_f \\ u_r \end{bmatrix}$$

N4SID subspace method The "Numerical algorithms for Subspace State Space System IDentification" method (N4SID) belongs to the subspace system identification family (Van Overschee & De Moor 1996). The method is an integrated part of the System Identification Toolbox for use in Matlab (Ljung 1997). The data are pretreated by centering and scaling before entered into the N4SID function.

The input signals are filtered PRBS's (Pseudo Random Binary Signals). Based on the observed RMSE (root mean square error) for various model orders, we chose to concentrate on a 7^{th} order model and a 28^{th} order model for the comparison with other models.

DSR subspace method The "combined Deterministic and Stochastic system identification and Realization" method (DSR) also belongs to the subspace system identification family (Di Ruscio 1997). The method and software (Di Ruscio 1996) are easy to use, requiring only the data and one parameter to be specified. A singular value plot is supplied for helping to determine the model order. When the model order is specified, the program returns a state-space model (including the Kalman filter gain matrix, and the innovations covariance matrix) along with the initial conditions. The data are pretreated by centering and scaling before entered into the DSR program.

[1] That is, when the difference in RMSE is zero for a rounded three digit number.

The input signals are the same filtered PRBS signals as were used for the N4SID algorithm. We chose to concentrate on a third-order model and a 7^{th} order model for the comparison with other models.

Prediction error method (PEM) The prediction error method (Ljung 1999) (Söderström & Stoica 1989) is an integrated part of Matlab's System Identification toolbox (Ljung 1997). It offers a vast amount of possibilities regarding linear model structures, such as ARMAX, BJ, FIR and state-space models. However, for MIMO (multi-input multi-output) systems, the ARMAX-type of models get complicated and they are perhaps not very suitable for such systems. The state-space model is therefore often preferred for representation of MIMO systems.

Unlike the subspace methods, the PEM is an iterative method, based on minimization of the prediction error. The fact that it is iterative limits the possible number of free parameters in the model structure dramatically, and one should not expect to be able to identify high-order models (even when one is using a canonical form). A recommended method (Ljung 1997) for identifying MIMO models is to use a subspace method (such as N4SID or DSR) to identify an initial model, and use the parameters of this model as initial values for the PEM method. This approach is taken here, although the 7^{th} and 28^{th} order models were not improved by the PEM method, probably due to too many free parameters involved. However, the third-order DSR model where slightly improved by the PEM method.

3.4 Comparison of the models

Without change in operating condition New input signals were designed and applied to the full scale model. The levels of the input signals are such that the overall operating condition of the paper machine is in the neighborhood of the condition at the time of identification.

The RMSE's (see Equation 6) for the empirically identified and reduced mechanistic models are given in Table 1.

The PEM, DSR and N4SID models have good prediction[4] abilities, although the RMSE's have increased significantly as compared to the identification. The prediction abilities of the mechanistic models are in general good. The higher order mechanistic models have very good prediction abilities

With change in operating condition Yet another set of input signals were designed, differing from previously used signals such that the overall operating condition of the paper machine is changed. The change in operating condition include e.g. an increase in thick stock flow from around 370 l / s to about 436 l / s, an increase of about

[2] TM - Transfer Matrix (Equation 11). Time delays are not included in model order.

[3] Optimized.

[4] The $\hat{y}$'s are the simulated response from the deterministic part of the identified model, thus the phrase "prediction ability" does not mean that e.g. a Kalman filter is applied in the validation process.

Table 1: Root Mean Square Error (RMSE) for reduced and identified models. The operating condition is comparable to that at the time of identification.

Method	Order	$RMSE_{weight}$	$RMSE_{ash}$	$RMSE_{conc.}$
TM[2]	15	0.30	0.16	$3.9 \cdot 10^{-3}$
PEM	3	0.16	0.10	$3.46 \cdot 10^{-3}$
DSR	3	0.17	0.12	$3.79 \cdot 10^{-3}$
DSR	7	0.13	0.098	$3.70 \cdot 10^{-3}$
N4SID	7	0.14	0.10	$3.37 \cdot 10^{-3}$
N4SID	28	0.11	0.063	$2.45 \cdot 10^{-3}$
Mech.[3]	38	0.12	0.061	$1.91 \cdot 10^{-3}$
Mech.	38	0.16	0.091	$2.65 \cdot 10^{-3}$
Mech.	87	0.077	0.027	$1.00 \cdot 10^{-3}$
Mech.	161	0.041	0.017	$0.52 \cdot 10^{-3}$

Table 2: Root Mean Square Error (RMSE) for reduced and identified models. The operating condition is different from what was used for identification.

Method	Order	$RMSE_{weight}$	$RMSE_{ash}$	$RMSE_{conc.}$
TM[2]	15	0.30	0.14	$4.08 \cdot 10^{-3}$
PEM	3	0.19	0.14	$3.42 \cdot 10^{-3}$
DSR	3	0.22	0.18	$4.97 \cdot 10^{-3}$
DSR	7	0.18	0.14	$3.27 \cdot 10^{-3}$
N4SID	7	0.18	0.14	$3.16 \cdot 10^{-3}$
N4SID	28	0.16	0.10	$2.31 \cdot 10^{-3}$
Mech.[3]	38	0.12	0.052	$1.61 \cdot 10^{-3}$
Mech.	38	0.12	0.066	$1.91 \cdot 10^{-3}$
Mech.	87	0.075	0.032	$0.86 \cdot 10^{-3}$
Mech.	161	0.047	0.016	$0.53 \cdot 10^{-3}$

90% in filler added to the short circulation, an increase of about 50% of retention aid and an increase in machine velocity from 1500 m /min to 1650 m /min.

The input signals are shown in Figure 3, and the RMSE's (see Equation 6) for the empirically identified and reduced mechanistic models are given in Table 2.

The PEM, DSR and N4SID models are identified at a different operating condition, and thus it is not a surprise that the prediction ability is decreased (except for some of the y_c outputs, for which the ability has improved). The mechanistic models are producing better predictions than previously (with a few exceptions).

Figure 4 shows the responses from the full scale model and the third-order DSR model.

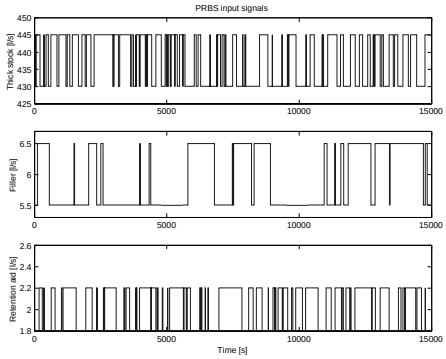

Figure 3: The filtered PRBS signals used for validation of the models. The overall operating condition of the paper machine is different from what was used for model identification and reduction.

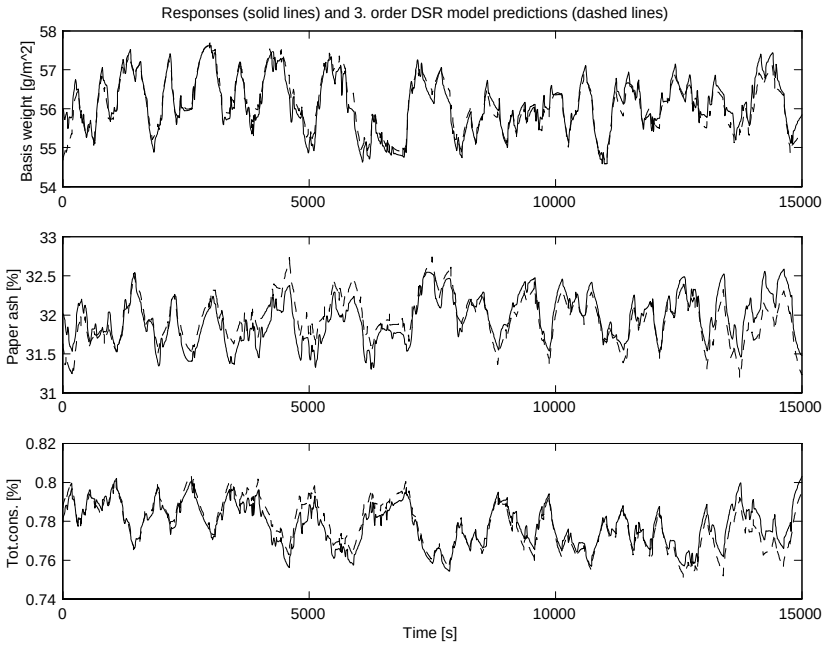

Figure 4: Full scale model responses (solid lines) and third-order DSR model responses (dashed lines), after change in operating condition.

4 Modeling and identification from real-time data

In Section 3, mechanistic models and empiric models of various orders and complexity were compared. In this section we will study some of the same concepts with real-time data. However, we confine ourselves to study empiric models. Fitting of mechanistic models to real-time data is more time consuming and is saved for future work.

4.1 Experiment design

One data set for identification and one data set for validation were collected. The type of experiments performed on the simulation model in Section 3 are impossible in reality, because step changes of a valve opening or a pump velocity are physically impossible. An approximation of the filtered PRBS signal is possible by changing the setpoints of the mass flows according to a PRBS scheme and let the valve and pump controllers work out the correct openings and velocities. However, on a paper machine even such an experiment is performed with high risk of poor paper quality or even sheet breaks. A solution to this problem is to perform closed loop experiments, i.e. in this case experiments where the basis weight, paper ash and wire tray total consistency controllers are in automatic mode. There is a vast amount of published material on closed loop system identification, and various approaches and algorithms are treated in more detail in e.g. (Ljung 1999), (Söderström & Stoica 1989) and (Forssell 1999). Our approach is the recommended one and it is often called "the direct approach" (Ljung 1999). In the direct approach we use the process inputs u and outputs y in the same way as for open loop identification, ignoring the feedback mechanisms and the reference signals.

Figure 5 shows the experimental plan with the changes in setpoints that the process operators should follow.

Figure 6 shows the resulting real-time input signals which is used together with the collected output signals for validation of models. Thus, the experiment plan gives filtered PRBS signals for the reference values, but only the process inputs (u) and outputs (y) are used for identification.

A similar procedure is used for collecting the identification data set.

4.2 Identification methods and closed loop data

It is well known that closed loop identification with the direct approach and a prediction error method (PEM) works very well (Ljung 1999), (Forssell 1999), (Söderström & Stoica 1989). However, problems may arise for poorly excited systems (this is also the case for open loop identification) and for systems with too simple controllers. The standard example of a closed loop identification failure uses a single-input-single-output ARX model with a proportional controller and with the reference value set to zero. This system is not identifiable in closed loop.

For subspace methods it is a fact that when applied in a straightforward fashion they do not yield consistent estimates in closed loop. This is due to the fact that the property of uncorrelated noise and system inputs is a basic assumption in these

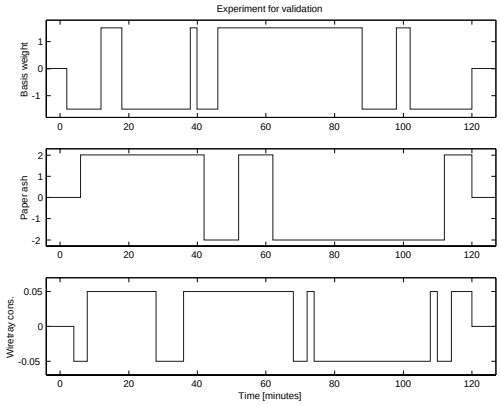

Figure 5: Experiment plan for the PM6 process operators. The plan shows the changes in setpoints for the validation data set.

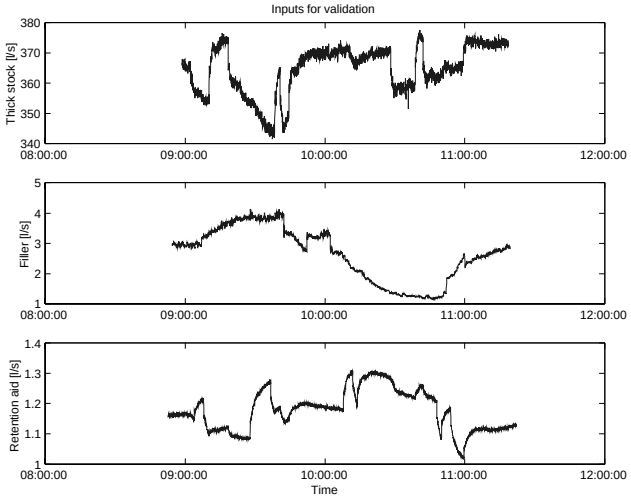

Figure 6: The resulting input signal with the experiment plan of Figure 5.

Table 3: RMSE values for third-order DSR model.

	Identification	Validation
$\text{RMSE}_{\text{weight}}$	0.410	0.697
RMSE_{ash}	0.095	0.410
$\text{RMSE}_{\text{conc.}}$	0.0043	0.0173

algorithms. As pointed out by e.g. (Forssell 1999) it is possible to use the reference signal instead of the input signal in the projection matrix which may cause problems in closed loop. However when using the subspace software packages in a straightforward fashion, a bias is introduced due to the correlation between noise and inputs. In practice this may not be a problem, due to the fact that all consistent system identification methods rely on several assumptions that do not hold, e.g. that the model structure equals the real structure. The question is to what extent a closed loop experiment invalidates the assumption of no correlation between noise and inputs, and to our knowledge there exist no results on this matter. However, it seems intuitively correct that the larger the signal-to-noise ratio is, the more insignificant is the closed loop problem. This is due to the fact that the correlation between noise and inputs will decrease with larger signal-to-noise ratio. Studying figures of inputs and outputs from experiments is perhaps the easiest way (perhaps not the most scientific way) of judging the size of the signal-to-noise ratio. In our case, the signal-to-noise ratio seems quite large, and subspace methods will be used along with the prediction error method.

4.3 Results

Identification of models with the subspace methods DSR and N4SID for model orders 1-30, and for various user defined parameters were carried out. The raw data observations were not equally spaced in time and a linear interpolation routine in Matlab was used for creating time series with five seconds sampling intervals (the sampling interval was approximately two seconds in the raw data). The identifications were repeated for data "without" pretreatment, data which were centered and for data which were centered and scaled. The centering was carried out by subtracting the value of the first element in each input and output series (centering may also be done by other methods, e.g. subtracting the mean of the series), and the scaling was carried out by dividing each series with its standard deviation. Note that no particular consideration was given to the fact that the basis weight and paper ash measurements are updated less frequently than other variables.

An RMSE (root mean square error) criterion, as in Equation 6, was used for comparing the identification and validation of the various models.

A third-order model with centered data was identified with the DSR method. Several higher order DSR models were identified, but non of these improved the validation RMSE values. The results from the identification and validation of this model is shown in Figure 7, and Table 3 gives the RMSE values.

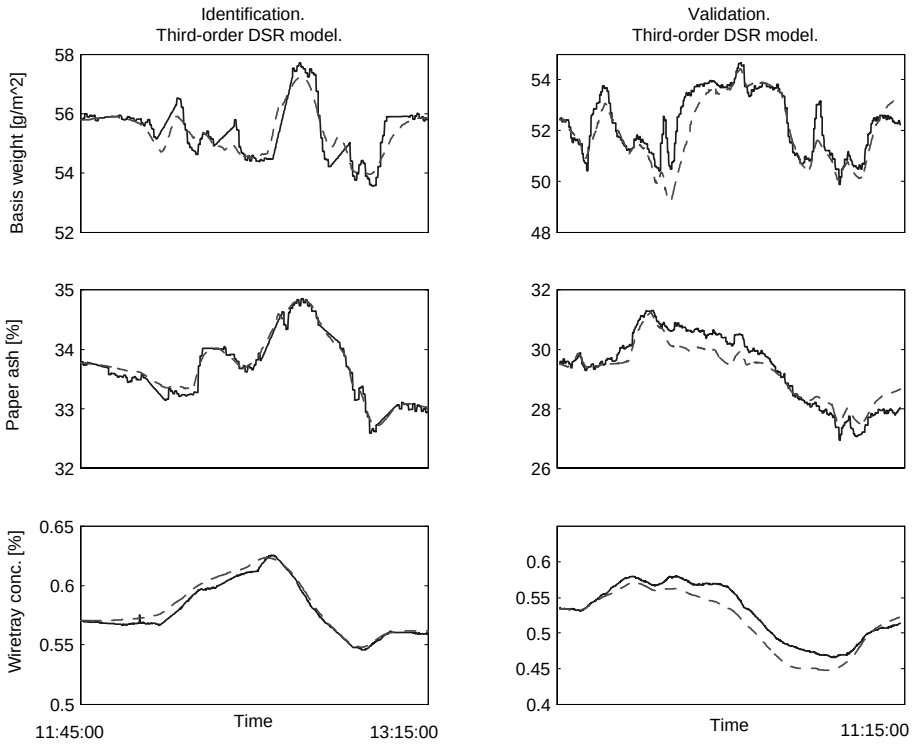

Figure 7: Real data (solid lines) and simulated data (dashed lines). Data set for identification collected at September 19. 2000, and data set for validation collected at October 27. 2000. Identification was carried out on centered data.

With N4SID we identified a fifth-order centered and scaled model, in addition to several higher order models (11^{th} to 23^{rd} order models) with RMSE values comparable to those of the DSR models. The validation gave higher RMSE values for the fifth-order N4SID model than for the third-order DSR model. None of the higher order N4SID models improved all three RMSE values at validation. The RMSE values for the basis weight were improved and the RMSE values for the wire tray consistency were poorer for all these models compared to the third-order DSR model.

All identified DSR and N4SID models were used as initial values for a corresponding PEM method. Some minor improvements on some of the DSR models were obtained at identification, however no validation improvements were found.

5 Calibration for estimation of quality variables

System structure Section 3 and 4 focus on various models for control. For these models we assumed that both the (controllable) inputs and outputs are measured, and are therefore known. A problem within the paper industry is that some of these measurements are lost when sheet breaks occur, and a standard solution to this problem is to "freeze" the corresponding inputs at their present values (the values at the time of the sheet break). This strategy will in most cases lead to drifts in e.g. headbox and white water consistencies. It seems more appropriate to estimate the missing measurements and Figure 8 shows how this may be arranged.

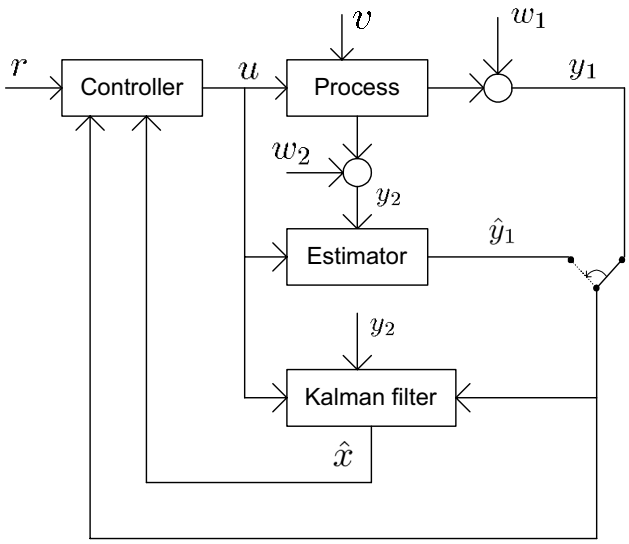

Figure 8: Arrangement for estimating missing measurements during sheet breaks.

In Figure 8 a distinction has been made between the primary y_1 outputs, which

Table 4: RMSE values for OE and DSR models.

	$RMSE_{weight}$	$RMSE_{ash}$
DSR	0.4123	0.3840
OE	0.3691	0.3504

correspond to the basis weight, paper ash and wire tray total consistency outputs, and secondary y_2 outputs which are used as inputs to the estimator. The secondary outputs are the wire tray filler consistency, the headbox total and filler consistency and the thick stock total and filler consistency. Note that for simplicity Figure 8 does not take into account that one of the primary outputs (the wire tray consistency) is available and used as estimator input even during sheet breaks. Whenever a sheet break occurs the primary measurements y_1 are replaced by estimates $\hat{y}_1$. The measurements or estimates are fed to the Kalman filter and the controller. The controller arrangement consists of e.g. model predictive control (MPC) and some single loop controllers (SLC) as further discussed in Section 6.

In Figure 8 the estimator and Kalman filter are represented by separate boxes. This is based on the assumption that the estimator is identified from process data with the aim of obtaining the best possible $\hat{y}_1$ estimates, while the Kalman filter is based on a mechanistic model with the aim of obtaining the best possible state estimates $\hat{x}$ for control purposes. The best $\hat{y}_1$ estimates will in fact be obtained by use of two separate estimators, one for each of the primary measurements that will be lost at a sheet break.

Estimator identification The estimators can be identified by use of a prediction error or subspace method using both the manipulated inputs u and the secondary process outputs y_2 as estimator inputs. Assuming a well known mechanistic process model, including noise covariances, the optimal estimator would be a Kalman filter driven by u and y_2 but not by y_1 (which is not available when the estimator is needed). This implies that an output error (OE) model structure should be specified for the identification, which can readily be done in the prediction error method (Ergon 1999*b*). It further implies that a direct subspace method (e.g. DSR) that make use of past y_1 values as estimator inputs will give theoretically non-optimal results, although the difference between OE and DSR results may not be of much practical importance.

Different identification methods have been tested by use of a mechanistic model similar to the one presented in Section 3, and noise covariances adjusted to achieve realistic output noise as compared with process measurement data (Forsland 2000). The estimator validation RMSE results were as given in Table 4, showing differences in line with the theoretical discussion above.

Figure 9 shows the validation responses for the paper weight based on a first-order OE estimator in the bracketed time period (from sample 20 to sample 320) and a first-order DSR estimator before and after this time period. Figure 10 shows the corresponding results for the paper ash content. A further investigation of this based on real data is part of the future work.

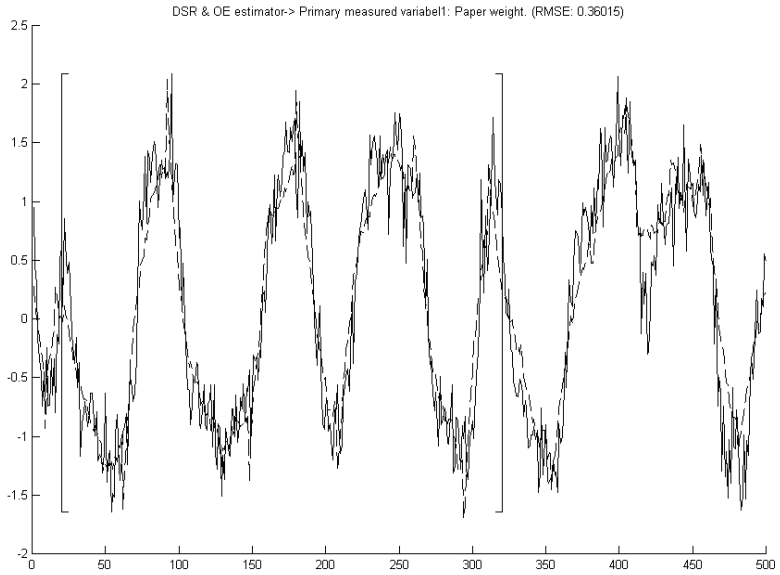

Figure 9: Basis weight. Mechanistic model output as solid line and estimator output as dashed line. First-order OE estimator in bracketed time period and first-order DSR estimator elsewhere. The data are centered and scaled.

Estimation based on multirate sampling data The primary output measurements are obtained with a lower sampling rate then the rest of the process signals, due to the scanner based sensor. The OE estimators may be identified also in this case, although some modifications of the Matlab identification functions are necessary (Ergon 1999*a*). A further investigation of this based on real data is also a part of the future work.

6 Control structure and related work

When a suitable model has been developed (possibly identified) it will be used in conjunction with model predictive control (MPC). MPC refers to a class of algorithms that compute a sequence of manipulated inputs in order to optimize a chosen criterion. The details of MPC algorithms are not discussed any further in this paper, and the interested reader is referred to e.g. (Camacho & Bordons 1999) or (Lie 1999). The interest in MPC has increased significantly since its introduction in the 1970's, and (Qin & Badgwell 1997) give an overview of commercial industrial solutions and implementations. The pulp and paper industry has also several reported MPC implementations, e.g. (Qin & Badgwell 1997) and (Lang et al. 1998).

A model structure has to be selected for the MPC, and commercial packages based

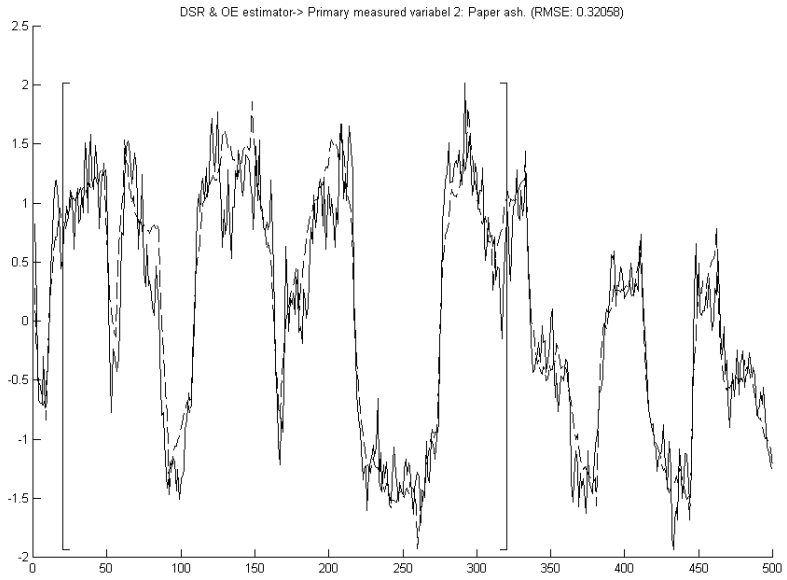

Figure 10: Paper ash. Mechanistic model output as solid line and estimator output as dashed line. First-order OE estimator in bracketed time period and first-order DSR estimator elsewhere. The data are centered and scaled.

on e.g. impulse response models, step response models, state space models and others are known to exist (Camacho & Bordons 1999). The development of a mechanistic model and the use of subspace identification techniques leads to state space models, and such models may be used in the MPC at PM6. An overview of the control structure is given in Figure 11.

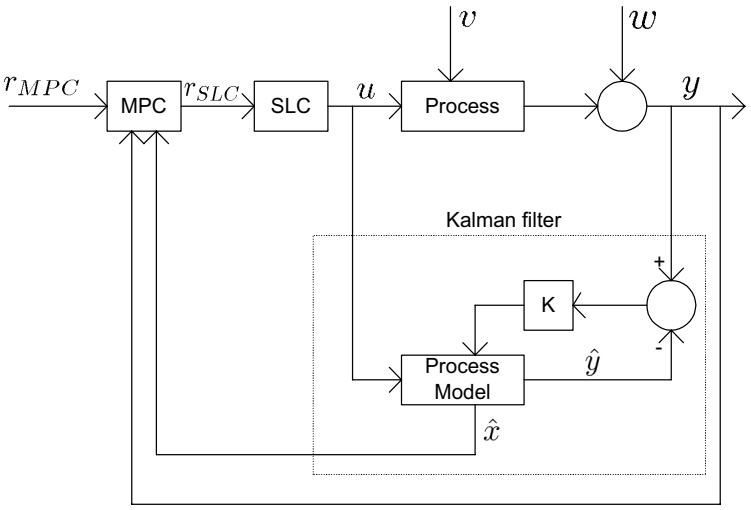

Figure 11: MPC and Kalman filter structure.

Here, a Kalman filter has been added for estimation of internal states that are not measured. In the figure, we use the abbreviation SLC for single loop controllers operating on the valves and pumps. Estimated states and outputs are $\hat{x}$ and $\hat{y}$ respectively. The following vectors are used:

$$r_{MPC} = \begin{bmatrix} r_{weight} \\ r_{ash} \\ r_{conc.} \end{bmatrix}, r_{SLC} = \begin{bmatrix} r_{thick\ stock} \\ r_{filler} \\ r_{retention\ aid} \end{bmatrix}$$

$$u = \begin{bmatrix} u_{thick\ stock} \\ u_{filler} \\ u_{retention\ aid} \end{bmatrix}, y = \begin{bmatrix} y_{weight} \\ y_{ash} \\ y_{conc.} \end{bmatrix}$$

Disturbances, v and w The mechanistic model which is developed and the empiric models which are identified can never cover every aspect of the process. The underlying physical phenomena are far too complex, and in many cases not known at all. It is therefore instrumental that those mechanisms that are not modelled but still affect the outputs, are not allowed to invalidate the model. Such phenomena are typically present in the process- and measurement noise v and w (see Figure 11).

At Saugbrugs several efforts focusing on these disturbances are initiated. A short description of the most prominent efforts will be given next.

Thick stock stabilization A sixth-order mechanistic model of the thick stock, including the mixing and machine chests, is developed and used for controlling the filler consistency. A Kajaani RMi measuring device for on line filler consistency measurements is installed and has been used for validation of the controller performance. The controller operates in a feedforward fashion, relying on the model and measured inputs only. The controller is working very well, although it is not operating in closed loop.

A feedforward controller which utilizes the measured total consistency between the mixing and machine chests, and compensates for any deviation from the setpoint by altering the speed of the thick stock pump, is also implemented. The feedforward controller is based on a dynamic model of the machine chest.

Charge measurement and control A project including Kemira (supplier of retention aid at PM6) and Neles Automation is initiated for, amongst others, investigating the need for measurement and control of charge. A Kajaani CATi measurement device is installed, and is currently being connected to the control system. One reason for this particular project is that it has been observed that in order to control the wire tray consistency the amount of retention aid often varies with $\pm 15\%$ at normal and stable conditions. Problems in the wet end when changes in the dosage of bleaching chemicals occur are often observed and are probably related to the charge of the stock. A cationic coagulant will be used for controlling the charge if the project concludes that this is beneficial.

pH variations and control Some variations in pH are observed, notably from about 4.4 to about 5.0. The models from Section 3 and 4 will be implemented in the control system, and on-line simulations in parallel with the process will show whether these variations in pH invalidate the models. Some preliminary investigations on control of pH has begun.

Air measurement and control A project for investigating the need for air measurement and control is (temporarily) finished, with no air found in the headbox. It may be interesting, at a later stage, to measure and control the air content in the headbox by acting on the amount of defoamer added to the white water tank.

Calibration of measurement devices An intensified calibration program is initiated, focusing especially on consistency measurement devices.

7 Conclusions

Various aspects of the project "Stabilization of the wet end of PM6" at Norske Skog Saugbrugs, Norway, are presented in this paper. The basic idea of the project is to use model predictive control (MPC) to achieve the objects of reducing the down time and reducing the variability in selected key variables. In the model structure, the chosen inputs are the thick stock pump, the addition of filler in the short circulation, and the addition of retention aid at the screens. The outputs are the basis weight, the paper ash content, and the wire tray concentration.

A 528 order mechanistic model is developed and an overview is presented. A lower order model is more beneficial for control purposes and model reduction and system identification techniques are used to arrive at several lower order models. These models are compared for their accuracy with respect to the full scale model (the 528 order model). Linear low order empiric models showed in general good accuracy, although depending on the operating condition of the paper machine. The reduced order mechanistic models are nonlinear and of higher order than the empiric models. The accuracies of these models were in general good and not depending on the operating condition of the paper machine.

Empiric models were also identified from real time data. Experiments were carried out in closed loop and subspace and prediction error methods were used for the identification. A third-order model (identified with the DSR subspace method) gave good accuracy at validation, and no higher order models were significantly better. For the validation, the operating condition of the paper machine were somewhat altered compared to the operating condition at the time of identification.

A solution to the problem of missing measurements during sheet breaks is proposed. One estimator for each of the measurements that are lost is identified, and at sheet breaks the estimate replaces the corresponding output. The estimator is based on an output error (OE) model structure and an underlying Kalman filter, and it utilizes other measurements as estimator inputs. Simulation results, with first-order estimators, are in line with the theoretical result that the OE model structure is the optimal one for these estimators.

A possible future model predictive control (MPC) structure is presented. It is vital that those mechanisms that are not modelled are not allowed to invalidate the model so that the MPC fails. A range of projects aiming at rejecting disturbances are established, focusing on thick stock stabilization, charge, pH, air, calibration routines, and more.

It is expected that the work on model reductions, model validation and identification of estimators will go on for a few months, and that a preliminary MPC controller will be implemented in 2001. The project at PM6 will run throughout 2002.

Acknowledgments The authors would like to thank the employees at PM6 for their cooperation in providing information and data for this paper and for their general helpfulness. We also wish to express our thanks to associate professor David Di Ruscio for comments on the subspace algorithms. The work of Tor Anders Hauge is financially

supported by the Research Council of Norway (project number 134557/410), with additional financial support by Norske Skog Saugbrugs.

References

Bown, R. (1996), Physical and chemical aspects of the use of fillers in paper, *in* J. Roberts, ed., 'Paper Chemistry', 2 edn, Chapman and Hall.

Camacho, E. F. & Bordons, C. (1999), *Model Predictive Control*, Advanced Textbooks in Control and Signal Processing, Springer, London.

Di Ruscio, D. (1996), 'DSR toolbox for MATLAB'. Copyright, Fantoft Process, Norway.

Di Ruscio, D. (1997), A method for identification of combined deterministic stochastic systems, *in* M. Aoki & A. Havenner, eds, 'Applications of Computer Aided Time Series Modeling', Springer Verlag, New York.

Ergon, R. (1999*a*), Dynamic System Multivariate Calibration for Optimal Primary Output Estimation, PhD thesis, Telemark University College & The Norwegian University of Science and Technology, Norway.

Ergon, R. (1999*b*), 'On primary output estimation by use of secondary measurements as input signals in system identification', *IEEE Transactions on Automatic Control* **44**(4), 821–825.

Forsland, G. O. (2000), Estimation and control of quality variables in a paper machine, Master's thesis, Telemark University College, Department of Technology, Porsgrunn, Norway.

Forssell, U. (1999), Closed-Loop Identification: Methods, Theory, and Applications, PhD thesis, Dep. of Electrical Engineering, Linköping University, Sweden.

Hauge, T. A. & Lie, B. (2000*a*), Simulation for advanced control of a paper machine: Model complexity and model reduction, *in* '41. SIMS Simulation Conference, Kgs. Lyngby, Denmark', SIMS, Scandinavian Simulation Society, pp. 135–154.

Hauge, T. A. & Lie, B. (2000*b*), Stabilization of the wet end at PM6. part 2: Introductory process description and modeling, A-rapport TAH20001, Norske Skog Saugbrugs, Halden, Norway (confidential and in Norwegian).

Lang, D., Tian, L., Kuusisto, R. & Rantala, T. (1998), Multivariable predictive control for the wet end, *in* 'Measurement and Control of Papermaking, Edinburgh, Scotland', Pira International.

Lie, B. (1999), 'An introduction to predictive control in the process industry', Lecture notes in Norwegian, Telemark University College, Porsgrunn, Norway.

Ljung, L. (1997), *System Identification Toolbox - For Use with Matlab*, The MathWorks, Inc.

Ljung, L. (1999), *System Identification. Theory for the User*, 2 edn, Prentice Hall PTR.

Moudgil, B. M., Shah, B. D. & Soto, H. S. (1987), 'Collision efficiency factors in polymer flocculation of fine particles', *Journal of colloid and interface Science* **119**(2), 466–473.

Norske Skog (2000), Norske Skog internet page at www.norske-skog.com.

Orccotoma, J. A., Paris, J. & Perrier, M. (1999), 'Dynamic analysis of fibrous material and dissolved solids distribution in the wet-end of a newsprint mill', *Appita* **52**(2), 105–113.

Qin, S. J. & Badgwell, T. A. (1997), An overview of industrial model predictive control technology, *in* '5. International Conference on Chemical Process Control, AlChE Symposium Series 316, 93', pp. 232–256.

Shirt, R. W. (1997), Modelling and Identification of Paper Machine Wet End Chemistry, PhD thesis, The University of British Columbia, Dep. of Electrical and Computer Engineering, Canada.

Slora, R. (1999), Wire tray consistency control at PM6, PM6-Rapport RSL9904, Norske Skog Saugbrugs, Halden, Norway (confidential and in Norwegian).

Söderström, T. & Stoica, P. (1989), *System Identification*, Prentice Hall International.

Swerin, A., Ödberg, L. & Wågberg, L. (1996), 'An extended model for the estimation of flocculation efficiency factors in multicomponent flocculant systems', *Colloids and Surfaces A: Physicochemical and Engineering Aspects* **113**, 25–38.

Van Overschee, P. & De Moor, B. (1996), *Subspace Identification for Linear Systems*, Kluwer Academic Publishers.

Paper C

Paper Machine Modeling at Norske Skog Saugbrugs: A Mechanistic Approach

Hauge, T.A. and Lie, B. (2001). *Paper Machine Modeling at Norske Skog Saugbrugs: A Mechanistic Approach*, in proceedings of the 42nd SIMS Simulation Conference, October 8-9, 2001, Telemark University College, Porsgrunn, Norway, p 119-154.

Hauge, T.A. and Lie, B. (2002). Paper Machine Modeling at Norske Skog Saugbrugs: A Mechanistic Approach, *Modeling, Identification and Control*, 23(1), p 27-52. (An updated and condensed version of the SIMS 2001 paper)

The version given here is the SIMS paper with updates from the MIC paper (but not condensed).

Paper Machine Modeling at Norske Skog Saugbrugs: A Mechanistic Approach

T. A. Hauge* and B. Lie†
Telemark University College
P.B. 203
3901 PORSGRUNN
Norway

Abstract

In this paper a mechanistic model of a paper machine is presented. The model is developed as a foundation for the control of three selected variables, the basis weight, the paper ash content and the white water total concentration. The model is of high order and reduced order models are developed and fitted to experimental mill data. The fitted models are validated with historical operational data.

Keywords: Paper machine, dynamic model, mechanistic model, model reduction, control, parameter estimation

1 Introduction

A paper machine is a complex process due to its multivariable nature and mixture of physical, chemical and mechanical sub-processes. Several researchers consider modeling of this process to be an impossible task (see e.g. (Roberts 1996*b*, page 8)), and no denying: an all-including model would not be possible given the present knowledge. The approach taken in this paper is one in which we focus on a mechanistic model[1] which will be used in an MPC (Model Predictive Control) application. There are three (manipulated) inputs and three outputs in the model. Several more inputs are present in the model and these will be considered as "measured disturbances". The model is simplified to make it more suitable for control purposes. It is beyond the scope of this paper to present a model which in all aspects have the correct physical structure, however it is important that the model captures the essential dynamic

*Tor.A.Hauge@hit.no
†Bernt.Lie@hit.no

[1] Also known as physical based model, knowledge based model, phenomenological model and/or first principle model.

behavior of the process and that it is applicable over a wider range of operating conditions than would be expected from an empiric model[2]. The manipulated inputs and outputs of the model are as shown in Figure 1.

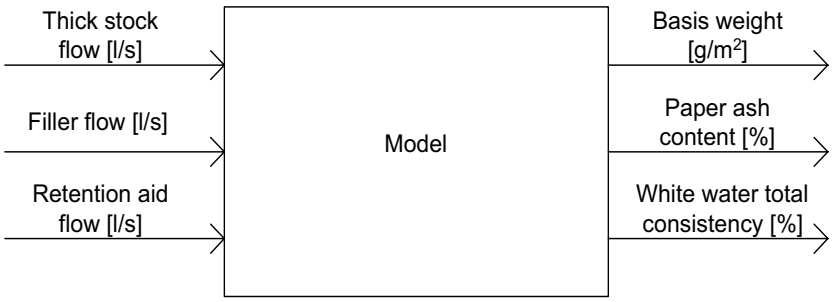

Figure 1: Manipulated inputs, and outputs of the model.

The modeling is part of a larger project for stabilization of the wet end of paper machine 6 (PM6) at Norske Skog Saugbrugs, Norway (Hauge, Ergon, Forsland, Slora & Lie 2000). Norske Skog Saugbrugs is the world's second largest manufacturer of uncoated super calendered magazine paper (Norske Skog 2000), and the mill incorporates three paper machines. PM6 is built in the early 1990's and is the largest and most modern papermachine at the Saugbrugs mill.

Empirical modeling or system identification of paper machines are reported in several papers and books. Some of these focus on so-called cross-directional (CD) modeling (i.e. a model for the profile across the paper web), e.g. (Featherstone, VanAntwerp & Braatz 2000), (Campbell 1997) and (Heaven, Manness, Vu & Vyse 1996), while others focus on the machine-direction (i.e. changes in average values across the web), e.g. (Hauge et al. 2000), (Hauge & Lie 2000), (Menani, Koivo, Huhtelin & Kuusisto 1998) and (Noreus & Saltin 1998).

The reported works on mechanistic modeling of paper machines are in most cases constrained to smaller parts of the paper machine. However, (Rao, Xia & Ying 1994), (Larsson & Olsson 1996) and (Hagberg & Isaksson 1993) consider a larger part of the paper machine, e.g. the wet end and the wire, press, and dryer sections, although the chemistry involved in papermaking is not considered at all. As far as we know, the only mechanistic models of a larger part of a paper machine which includes chemical modelling is found in (Shirt 1997), (Hauge et al. 2000) and (Hauge & Lie 2000). In Shirt's work both chemical aspects, which include adsorption and flocculation, and physical aspects, which include drainage on the wire, refining, tanks, headbox, wire section, etc., are part of the overall model, although transportation delays in pipelines are neglected and not all aspects are presented in detail. The mechanistic model in (Hauge et al. 2000) and (Hauge & Lie 2000) is in those papers not presented in detail, giving only an introduction to the equations used to describe the paper machine. In

[2] A model based on collected input-output data.

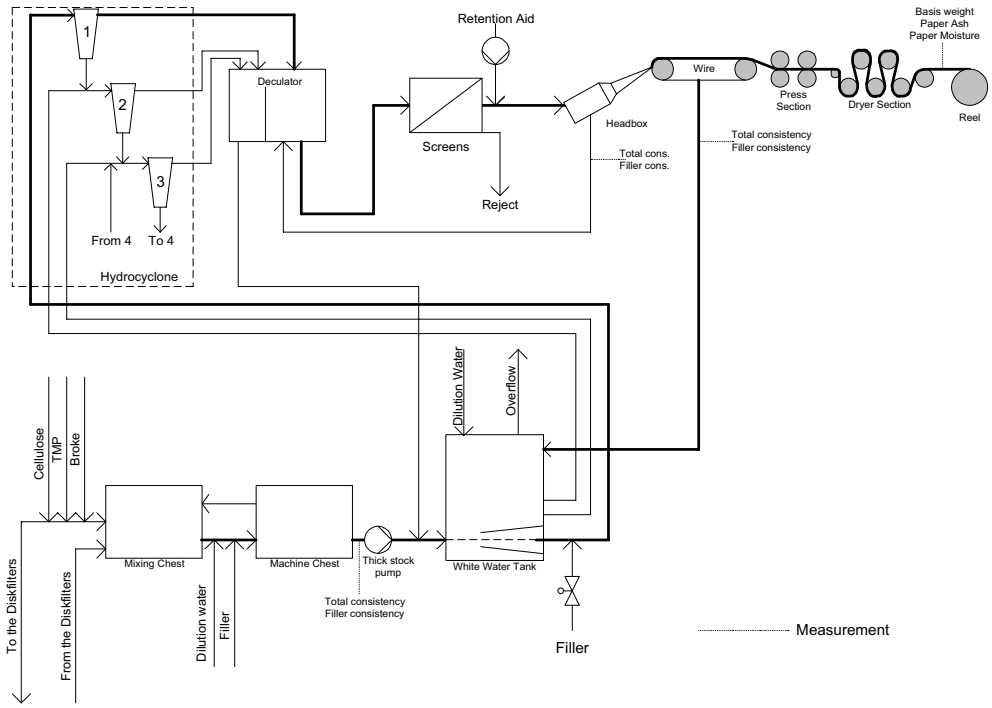

Figure 2: Simplified sketch of PM6.

neither of these latter references are the mechanistic models validated properly with real time data. The contributions in this paper are to bring more details on the model, to report on further refinements of the model, and to bring results from the model fitting and validation using experimental data.

A simplified overview of PM6 is given in Figure 2. Note that the developed models cover the process from the thick stock pump to the reel. A thick stock (lower left area of Figure 2, including the mixing- and machine- chests) model is developed in (Slora 2001), and this model is implemented in PM6 and provides estimates of total- and filler concentrations in the thick stock.

The paper is organized as follows: In Section 2 the paper machine sub-processes are discussed in detail and suggestions for equations describing them are given. In Section 3 we describe how simplified mechanistic models, more suitable for control purposes, may be obtained. In Section 4 we report on fitting and validation of the simplified models using real time process data. We improve the simplified mechanistic model by extending it with a first order empiric model in Section 5. In this section we also identify a Kalman filter and validate the model. Finally some conclusions are given in Section 6.

2 A Comprehensive Mechanistic Approach

The model described in this section consists of 28 ordinary differential equations (ODE), 100 partial differential equations (PDE) and hundreds of algebraic equations. For implementation in Matlab, each PDE is discretized by the method of lines (MOL) (see e.g. (Schiesser 1991)).

2.1 Chests and tanks

Chests and tanks are modelled as ideally stirred volumes, i.e.

$$\frac{dm_i}{dt} = \sum_j w_{i,j} + Vr_i \tag{1}$$

$$\Downarrow$$

$$\frac{dC_i}{dt} = \frac{1}{V}\sum_j C_{i,j}q_j + \frac{1}{\rho}r_i, \tag{2}$$

where m_i [kg] is mass of component i of some volume V [m^3], $w_{i,j}$ [kg / s] is mass flow j of component i into this volume, r_i [kg /(m^3 s)] is generation of component i in the volume, C_i [$-$] is the concentration of component i in the volume, $C_{i,j}$ is the concentration of component i in mass flow j into the volume, ρ [kg / m^3] is the density of the mass flow and q_j [m^3 / s] is the volumetric flow j into the volume. We will get back to the "ideally stirred" assumption when discussing the deculator and the white water tank, and the generation term when discussing the retention aid and flocculation.

2.2 Pipelines

Pipelines are modeled using partial differential equations (PDE's), i.e.

$$\frac{\partial C_i}{\partial t} = -v\frac{\partial C_i}{\partial x} + \frac{1}{\rho}r_i, \tag{3}$$

where v is the velocity of the mass inside the pipeline and x is the variable corresponding to the direction along the pipeline. Thus, the concentration is here a function of both time t and space x. When the reaction rates are small such that the advection term dominates, these models are notoriously difficult to discretize using the method of lines (MOL). With constant velocity v and $r_i = 0$, these models can be interpreted as time delays. For implementation, the partial differential equations are discretized into five ordinary differential equations each, i.e. a pipeline is approximated by dividing it into five ideally stirred volumes. The choice of discretization level is a trade-off between factors such as accuracy, complexity and numerical properties. With an increasing number of volumes, the model is more accurate but also more complex and the stiffness of the overall system is increased. Keeping in mind that the model is developed for control purposes, we found that the input-output properties of the

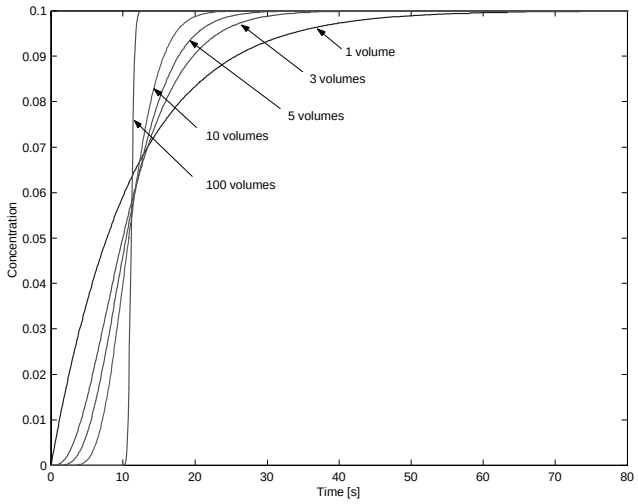

Figure 3: Step responses at the outlet of a pipeline (40 m length, 0.7 m^2 cross sectional area, 2500 kg / s mass flow). Discretization carried out with various numbers of ideally stirred volumes.

overall model, with a discretization level of five volumes, was very close to higher levels of discretization. The choice of five volumes was also convenient as a starting point with respect to model complexity. The trade-off can be studied from the responses in Figure 3, where a step change (from 0 to 0.1) in the initial concentration is applied to the pipeline between the screens and the headbox. The pipeline is 40 m long, it has a cross section area of 0.7 m^2 and a mass flow of 2500 kg / s. A density of $\rho = 1000\,\mathrm{kg}\,/\,\mathrm{m}^3$ is assumed. If the pipeline is a pure time delay then the step change would appear at the outlet at $t = L/(w/(A\rho)) = 11.2\,\mathrm{s}$, where L is the length of the pipeline.

2.3 Fibers and fillers

The finished paper typically consists of 65% (wood-) fibers, 30% filler particles and 5% water. The filler particles are added to improve certain properties of the paper, such as brightness and smoothness, and also often to reduce the production costs. At PM6 two different types of filler particles are used depending on the requirements from the end-user. One of these type of filler particles is used occasionally when particularly high brightness is required.

The fibers that enter the process come in a variety of dimensions, and may be crudely classified as fibers and fines where strict definitions of fines appear in the literature (Britt & Unbehend 1976). The fines are generated in the refining process

by the shearing action of the refiner bars upon the fiber cell walls (Roberts 1996*a*).

2.4 The thick stock

The thick stock area is the lower left area of Figure 2. Cellulose, thermomechanical pulp (TMP), broke (repulped fibers and fillers from sheet breaks and edge trimmings), recovered stock from the disk filters (thickened mixture of cellulose, white water, and more) and filler particles are the main additives, and they are blended in the mixing- and machine chests. These tanks have relatively large volumes for smoothing rapid changes in the additive flows. The stock is transported to the paper machine area (Figure 2, except for lower left area) by the thick stock pump. A mechanistic model of the thick stock area, estimating the total and filler consistencies in the flow to the paper machine, is developed and implemented at PM6 (Slora 2001).

The components in the flow from the thick stock pump are assumed to be fibers, fines and filler particles. The total-[3] and filler-concentrations are estimated by the thick stock model, and the concentration of fines is assumed to be

$$C_{\text{fines}} = \alpha_{\text{fines}}(C_{\text{total}} - C_{\text{filler}}), \tag{4}$$

where α_{fines} is a constant and C_{total} and C_{filler} are total- and filler-concentrations in the thick stock.

2.5 Retention aid and flocculation

The filler particles and fines are in general too small to be trapped on the wire (a fine meshed woven cloth) and one adds retention aid to help them flocculate, thus increasing the possibility of mechanical entrapment. The retention aid is also added for other reasons, such as improving the drainage from the sheet, but these effects will not be studied here; see e.g. (Roberts 1996*b*) for a general introduction to retention aids and flocculation.

Fibers and filler particles are mostly negatively charged, and at PM6 a two component cationic (positively charged) retention aid system is used. The two components have quite different charge densities and molecular weights. A low molecular weight, high charge density polymer is added first, mainly to fix or neutralize highly anionic (negatively charged) impurities in the stock but also to improve retention as illustrated in Figure 4. We will assume that the flocculation due to this polymer is negligible as is also experienced on the paper machine when the addition of this polymer is stopped. The addition of this polymer is now used in a control loop for stabilizing the charge (or cationic demand) of the stock at PM6.

The second polymer that is added has a low charge density and high molecular weight. This results in adsorption onto fibers and filler particles leaving "tails" which other fibers and filler particles may adsorb onto (see Figure 5). This is termed "bridging flocculation" and is assumed to be the main contributor to the flocculation in the process. The addition of this retention aid is located just after the screens as seen on Figure 2.

[3] The total concentration is the summed concentration of fibers, fines and filler particles.

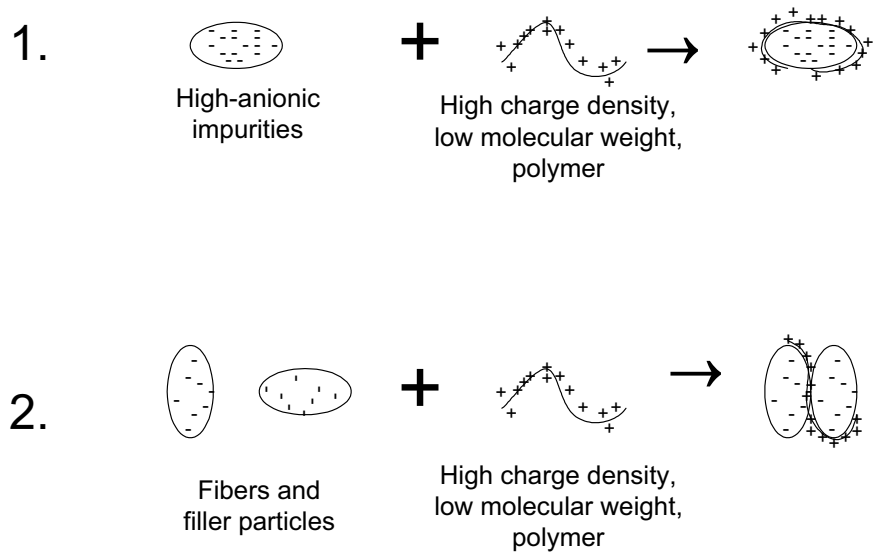

Figure 4: (1) The polymer adsorbs onto anionic impurities in the stock. (2) Flocculation caused by the polymer. Note the tight adsorption of the particles and the polymers due to the charge and weight characteristica of the polymer.

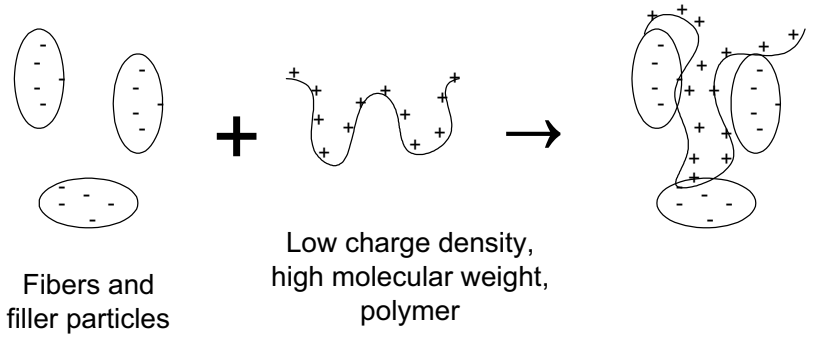

Figure 5: Bridging flocculation of fibers and fillers.

On a more microscopic level one may go on to describe the adsorption and flocculation of various components (e.g. adsorption of polymers onto fibers, fines and filler particles, and the flocculation of fibers with fibers, fibers with fines, filler particles with filler particles, etc.) as is found in e.g. (Van de Ven 1993) and (Shirt 1997). This, however requires many (ordinary and partial) differential equations, and a simpler solution was sought here. An equation for the concentration of flocculated component i that provided an overall good fit for the model, and which also was relatively simple was

$$\frac{\partial C_{\text{floc},i}}{\partial t} = -v\frac{\partial C_{\text{floc},i}}{\partial x} + \frac{1}{\rho}C_{\text{fiber}}(k_{i,\text{ret}}C_{\text{ret}}C_{\text{non-floc},i} + k_{i,\text{fiber}}). \tag{5}$$

This equation describes concentration of flocculated components in pipelines (following the convention of Equation 3), with obvious extensions to equations for chests and tanks as outlined in Equation 2. Component i is either filler particles or fines (we are not interested in flocculation of fibres as we assume later on that they will be retained on the wire in any case), $C_{\text{floc},i}$ is the concentration of flocculated component i, $C_{\text{non-floc},i}$ is the concentration of non-flocculated component i, $k_{i,\text{ret}}$ and $k_{i,\text{fiber}}$ are flocculation constants and C_{ret} and C_{fiber} are concentrations of retention aid and fibers, respectively. The reaction rate is empiric and should not be regarded as an attempt to explain the complicated process of flocculation. This is obvious considering that as long as there are fibers, the equation predicts a positive reaction rate even with no filler particles present in the system.

In addition to the flocculation equation (5) itself, there are several other issues which must be addressed. For example that the equation fails to account for several major disturbances on the flocculation. The temperature and charge are two of these disturbances and they are stabilized at PM6 by separate control loops. Another parameter which has tremendous effect on the flocculation is the pH (see e.g. (Horn & Linhart 1996)), and at PM6 the pH is observed for longer periods of time showing no dramatic variations.

The retention aid is added at the screens, and only seconds later it arrives at the wire section where obviously some of it must be recirculated through the wire cloth. We will get back to this issue in Section 2.11. The recirculated polymer will undergo a deactivation process in which it diffuses into the pores of the fibres (Koethe & Scott 1993) thus loosing some ability to cause flocculation (Pelssers, Cohen Stuart & Fleer 1989). In addition, the recirculated flocs must pass through a number of pumps and other process equipment (such as the hydrocyclones and the screens) with high shear rates, causing break-up of flocculated particles[4] (Gregory 1988). These facts caused (Shirt 1997), in his dynamic model, to assume that all particles which are recirculated through the white water system loose any active high molecular weight (low charge density) polymer coverage. In our model we allow for some flocculation to take place in the white water system, thus giving some initial concentrations (larger than zero) of flocs at the outlet of the screens where the retention aid is added.

[4] Bridging flocculation is typical for polymers with low charge density and high molecular weight. Flocs produced by bridging flocculation, and then broken at high shear rates, will not easily re-flocculate (Gregory 1988).

2.6 The white water tank

The white water tank is modeled as a perfectly stirred tank (Equation 2). The validity of this assumption may be questioned as the main input flow (the dewatering from the wire section) enters on top of the tank and the main output flow (the flow to the first stage of the hydrocyclones) leaves at the bottom of the tank, and there are no mixing arrangement present in this tank. The tank is however only moderately tall and the main input and output flows are quite large and have high velocities, so the turbulence inside the tank is assumed to blend the contents well. Another approach is taken in (Nissinen 1999) where the upper part of the tank is assumed perfectly mixed, and the lower part a plug flow.

2.7 The hydrocyclones

There are a total of five hydrocyclone stages and a tank between the fourth and fifth stage, as shown in Figure 6. Each stage consists of several units where the accept flow goes through the top of the cyclones and the reject flows out at the bottom. In the model we have neglected the time delays, or volumes, of the hydrocyclone units themselves, because these volumes are small compared to the pipeline volumes between the units. The pipelines are modeled as shown in Equation 3, and the cyclone units split the incoming flows into an accept flow and a reject flow. The concentrations in the accept flow will be lower than in the reject flow because gravitational forces are used to separate the two outlet flows and heavier particles will have a tendency to be rejected.

Equations like

$$w_{i,\text{accept}} = \alpha_{i,\text{accept}} \cdot w_{i,\text{inject}}, \tag{6}$$

are used for finding the accepted total mass flows in stage i ($i \in \{1, ..., 5\}$), and

$$C_{i,j,\text{accept}} = \alpha_{i,j,\text{accept}} \cdot C_{i,j,\text{inject}}, \tag{7}$$

are used for finding the concentration of component j in the accept flow at stage i. Component j is recirculated filler particles, "fresh" filler particles, fiber, fines, retention aid, flocculated fines or flocculated filler. Observations after step changes in the addition of filler particles indicate that recirculated and newly added filler behaves quite differently in the hydrocyclones, and this is the reason for treating them separately.

Due to high shear rates and deactivation (as explained in Section 2.5), it is assumed that no flocculation takes place in the fourth and fifth stage, and also that the polymer entering the fourth stage is completely inactive. The tank between the fourth and fifth stage is modeled by ordinary differential equations similar to Equation 2, but without the flocculation term, and only for the components filler, fiber and fines.

2.8 The deculator

The deculator is a relatively small two chamber tank whose purpose is to remove air bubbles from the stock. The "right side" chamber (refer to Figure 2) has the

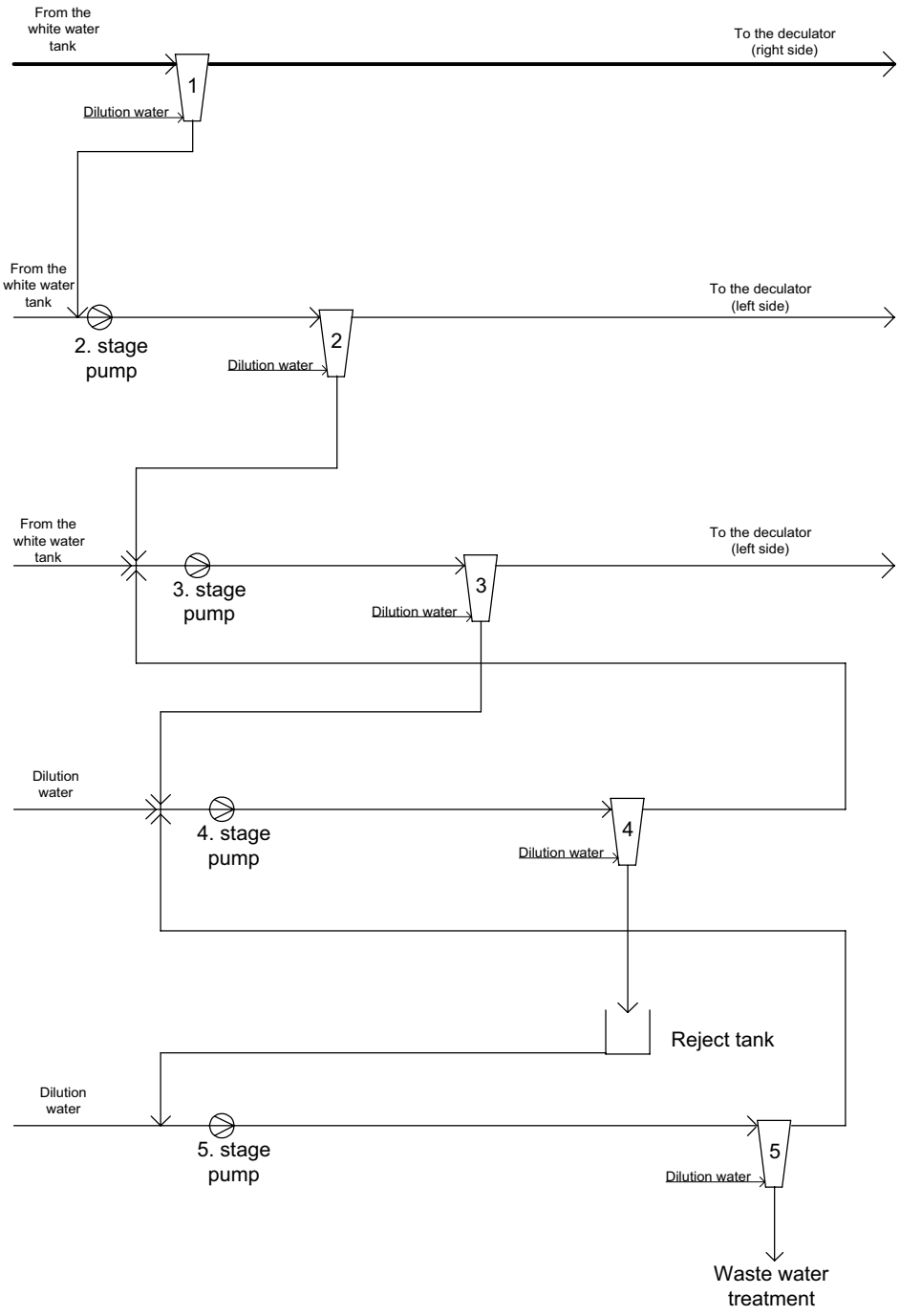

Figure 6: The five stage hydrocyclone arrangement.

largest volume and an overflow to the "left side" chamber keeps the level constant. The level on the "left" side is controlled and assumed constant. Equations similar to Equation 2 are used for both chambers. The assumption of ideally stirred masses in each chamber is probably good due to large masses entering and the small volumes involved. In addition, the "right" side chamber has an input flow (recirculated from the headbox) entering at the bottom which should make the assumption even better.

2.9 The screens

There are two screens in parallel, in addition to a reject system for recirculation of usable fibers and filler particles back into the white water tank. In the model the screens are seen as one unit, splitting the flow in a reject and an accept flow. The equations used are similar to those used for the hydrocyclones, thus ignoring the volume of the screens which are small. The reject system is not part of the model due to the reject flow and concentrations being small. The reject flow is about 2% of the inject flow and the concentrations are found by laboratory measurements to be no larger than the inject and accept concentrations.

2.10 The headbox

The headbox is modeled as a pure mass flow splitting unit. The two output flows, one recirculation flow to the deculator and one flow onto the wire, are assumed to have the same concentrations as the input flow. The mass flow to the wire section is calculated by

$$w_{H-W} = \alpha_I \cdot h_I \cdot \ell_I \cdot \sqrt{P_I}, \tag{8}$$

which can be derived from Bernoulli's equation, where w_{H-W} [kg / s] is the mass flow onto the wire, α_I [$\mathrm{kg}^{1/2}$ / $\mathrm{m}^{5/2}$] is a lumped constant (dependent on the geometry of the slice opening amongst others), h_I and ℓ_I are the height and length of the slice opening respectively and P_I [Pa] is the pressure inside the headbox. Note that the length of the slice opening is a constant while the height of the slice opening is used for controlling the cross directional (CD) profile. Thus the height varies across the slice opening and the average is used in the equation above. More detailed models of headboxes can be found in e.g. (Rao et al. 1994) and (Tuladhar, Davies, Yim & Woods 1997).

2.11 The wire, press, and dryer sections

Following (Shirt 1997) we assume that (long) fibers, flocculated fines and flocculated filler particles are retained on the wire[5]. In addition we allow for some filler particles

[5] Laboratory measurements at PM6 of the fiber (length) distribution in the headbox and in the flow from the wire section to the white water tank showed no clear distinction between fiber lengths being retained and fiber lengths being drained from the wire, although longer fibers seemed more likely to be retained.

to be mechanically entrapped, so that the component mass flows entrapped on the wire are

$$w_{W,\text{filler}} = w_{H-W} \cdot (C_{H,\text{flocculated filler}} + C_{H,\text{non-flocculated filler}} \cdot \alpha_{W,\text{filler}}) \quad (9)$$

$$w_{W,\text{fines}} = w_{H-W} \cdot C_{H,\text{flocculated fines}} \quad (10)$$

$$w_{W,\text{fiber}} = w_{H-W} \cdot C_{H,\text{fiber}}, \quad (11)$$

where $w_{W,i}$ [kg / s] are the component mass flows retained on the wire ($i \in \{\text{filler, fines, fiber}\}$), $C_{H,j}$ are the concentrations in the headbox ($j \in \{\text{flocculated filler, non-flocculated filler, flocculated fines, fiber}\}$), and $\alpha_{W,\text{filler}}$ is the fraction of non-flocculated filler mechanically entrapped on the wire. The significance of mechanical entrapment seems to be somewhat controversial in the literature. For example (Van de Ven 1984) found (theoretically) that mechanical entrapment was low, while (Bown 1996) reports that mechanical entrapment can be a dominant mechanism.

Most of the water is drained from the wire to the white water tank, and this is modeled by

$$w_{W-WWT} = \alpha_W \cdot w_{H-W}, \quad (12)$$

where w_{W-WWT} [kg / s] and w_{H-W} [kg / s] are total mass flows from the wire to the white water tank and from the headbox to the wire respectively, while α_W is the fraction (close to one) of mass flow out on the wire which is recirculated to the white water tank.

The concentrations of filler particles, fines and fibers in the mass flow from the wire section to the white water tank are easily calculated using Equations 8-12 and the concentrations in the headbox (the concentration of fibers in this flow is equal to zero). As explained in Section 2.5 we also allow for some recirculation of retention aid, and the concentration of retention aid in the flow from the wire to the white water tank is calculated as

$$C_{W-WWT,\text{ret.aid}} = \alpha_{\text{ret.aid}} \cdot C_{H,\text{ret.aid}}, \quad (13)$$

where $C_{W-WWT,\text{ret.aid}}$ and $C_{H,\text{ret.aid}}$ are concentrations of retention aid in the flow from the wire to the white water tank and in the headbox respectively, and $\alpha_{\text{ret.aid}}$ is the fraction of retention aid being recirculated. The parameter $\alpha_{\text{ret.aid}}$ may be viewed as a lumped parameter considering that we do not account for deactivation and destruction of polymers by shear rates elsewhere in the model. An exception is in the hydrocyclones, where we assume that polymer entering the fourth stage is completely inactive.

The transportation of the solids from the wire section, through the pressing and dryer section, and onto the reel is modeled by an advection equation

$$\frac{\partial w_{W-R,i}}{\partial t} = -v \cdot \frac{\partial w_{W-R,i}}{\partial x}, \quad (14)$$

where $w_{W-R,i}$ [kg / s] is the mass flow of component i (i =filler or solids (filler, fiber and fines added)) from the wire section to the reel, and v [m / s] is the paper machine velocity (near the reel). We do not model the filtration process or drainage process in any detail, and we only focus on the solids on the wire.

2.12 The output equations

The outputs are as shown in Figure 1, and the equations connecting the outputs to the internal states of the dynamic model are

$$y_{\text{basis weight}}(t) = \frac{1000 \cdot \alpha_{\text{edge trim}} \cdot w_{W-R,\text{solid}}(t, x = L_{\text{paper}})}{v(t) \cdot b_R \cdot (1 - f(t))} \tag{15}$$

$$y_{\text{paper ash}}(t) = \frac{100 \cdot w_{W-R,\text{filler}}(t, x = L_{\text{paper}}) \cdot (1 - f(t))}{w_{W-R,\text{solid}}(t, x = L_{\text{paper}})} \tag{16}$$

$$y_{\text{WW tot. conc.}}(t) = 100 \cdot (C_{W-WWT,\text{filler}}(t) + C_{W-WWT,\text{fines}}(t)), \tag{17}$$

where $y_{\text{basis weight}}(t)$ [g / m^2], $y_{\text{paper ash}}(t)$ [%], and $y_{\text{WW tot. conc.}}(t)$ [%] are the basis weight, paper ash content, and white water total concentration respectively. The basis weight and paper ash are measured by a scanning device between the dryer section and the reel. $\alpha_{\text{edge trim}}$ is a constant which adjusts for edge trimmings of the paper, $w_{W-R,i}(t, x = L_{\text{paper}})$ [kg / s] is the mass flow of component i (i = filler and/or solids (filler, fiber and fines added)) at the scanning device (L_{paper} indicates the length of the paper sheet from the wire section to the scanning device), $v(t)$ [m / s] is the paper machine velocity at the scanning device, b_R [m] is the width of the paper sheet at the scanning device and $f(t)$ is the measured moisture content in the paper at the scanning device. $C_{W-WWT,\text{filler}}(t)$ and $C_{W-WWT,\text{fines}}(t)$ are the concentrations of filler and fines in the flow from the wire section to the white water tank.

3 Model reduction

3.1 Finite dimensional models

Assume that we have an input-output model

$$\begin{aligned} \frac{dx}{dt} &= f(x, u) \\ y &= g(x, u), \end{aligned} \tag{18}$$

where $x \in \mathbb{R}^n$, $u \in \mathbb{R}^r$ and $y \in \mathbb{R}^m$. The dimension of the model is n, and we want to reduce the order of the model.

We illustrate the principle using a linear model:

$$\frac{dx}{dt} = Ax + Bu. \tag{19}$$

Assume that matrix A has a full set of eigenvectors such that there exist a non-singular matrix M and a diagonal matrix Λ such that $AM = M\Lambda$. We can then introduce a change of variables and let $z = M^{-1}x$ such that we find

$$\frac{dz}{dt} = \Lambda z + M^{-1}Bu. \tag{20}$$

Thus, we have a decoupled system:

$$\begin{aligned} \frac{dz_1}{dt} &= \lambda_1 z_1 + b_1^T u \\ &\vdots \\ \frac{dz_n}{dt} &= \lambda_n z_n + b_n^T u. \end{aligned} \tag{21}$$

The system is stable if $\forall i : \Re\lambda_i \leq 0$. For simplicity, assume that all eigenvalues λ_i are real, and that we have ordered the eigenvalues such that $\lambda_1 \leq \lambda_2 \leq \cdots \leq \lambda_n \leq 0$. If now for some k we have $\lambda_k \ll \lambda_{k+1}$, it is common to introduce the approximation $dz_i/dt \approx 0$ for $i \in \{1, \ldots, k\}$. Thus we have reduced the order of the model to $n - k$, and it is now:

$$\begin{aligned} \frac{dz_{k+1}}{dt} &= \lambda_{k+1} z_{k+1} + b_{k+1}^T u \\ &\vdots \\ \frac{dz_n}{dt} &= \lambda_n z_n + b_n^T u. \end{aligned} \tag{22}$$

In addition, we have the algebraic equations

$$\begin{aligned} 0 &= \lambda_1 z_1 + b_1^T u \\ &\vdots \\ 0 &= \lambda_k z_k + b_k^T u. \end{aligned} \tag{23}$$

A more formal analysis of this approximation can be performed using singular perturbation techniques, see e.g. (Hoppensteadt 2000).

The technique of singular perturbation is also applicable to nonlinear systems such as $dx/dt = f(x, u)$. However, for nonlinear systems, it is much more difficult to find a transformation of the state such that the transformed system is decoupled. Such a transformation would ideally have the form:

$$z = \phi(x, u), \tag{24}$$

where $z \in \mathbb{R}^n$, and ϕ is invertible yielding $x = \phi^{-1}(z, u)$. In that case, we would search for a transformation ϕ such that

$$\frac{dz}{dt} = \frac{\partial \phi}{\partial x} \cdot f\left(\phi^{-1}(z, u), u\right) + \frac{\partial \phi}{\partial u}\frac{du}{dt} = \tilde{f}(z, u), \tag{25}$$

where $\tilde{f}(z, u)$ has the following structure:

$$\tilde{f}_i(z, u) = \tilde{f}_i(z_i, u). \tag{26}$$

Assuming that such a transformation is available, the method of singular perturbation is readily applicable to the transformed system.

In practice, we can not expect to find such a decoupling transformation for nonlinear systems. A partial solution could be to linearize the model at an operating point, and then let $\phi(x,u) = M^{-1}x$ where M is the matrix of non-singular eigenvectors at this operating point. This would yield an approximate decoupling in the neighborhood of the operating point.

A simple case where we in fact have the desired decoupling, is in cascaded processes. This is relatively common, but feedback will then easily ruin the decoupling.

Even if there is no such natural decoupling, we may have an almost decoupled system. We may thus still try to use singular perturbation techniques on a system

$$\frac{dx_i}{dt} = f_i(x_1, \ldots, x_n, u), \tag{27}$$

and thus set $dx_i/dt \approx 0$, even if this approximation is not strictly correct.

The final word regarding what eigenvalue/mode of the system we can allow ourselves to set at steady state, will depend on the use of the model. If the model is used for control purposes, we will have to select the model reduction such that the input-output response is not severely changed. If we are interested in the accuracy of some state, however, we will have to make sure that this particular state is not severely changed.

3.2 Infinite dimensional models

Assume that we have an infinite dimensional model (i.e., the model includes PDEs) which we discretize using the Method of Lines (MOL) such that we arrive at a model

$$\begin{aligned} \frac{dx}{dt} &= f(x,u;N) \\ y &= g(x,u;N), \end{aligned} \tag{28}$$

where $\dim x$ depends on the discretization level N. This case can be treated just as in the previous subsection. The particular problem with infinite dimensional models is that as part of the model reduction, we have to decide the discretization level. If there are several PDEs in the model, these can in principle have individual discretization levels.

When using the model for control, a natural way to solve the problem of finding the appropriate discretization level is to vary N such that the input-output behavior is not severely changed from the infinitely (high) dimensional case. If we are particularly concerned with the approximating capabilities of an internal state, we should select the discretization level by making N as small as possible while retaining the accuracy of the state in question.

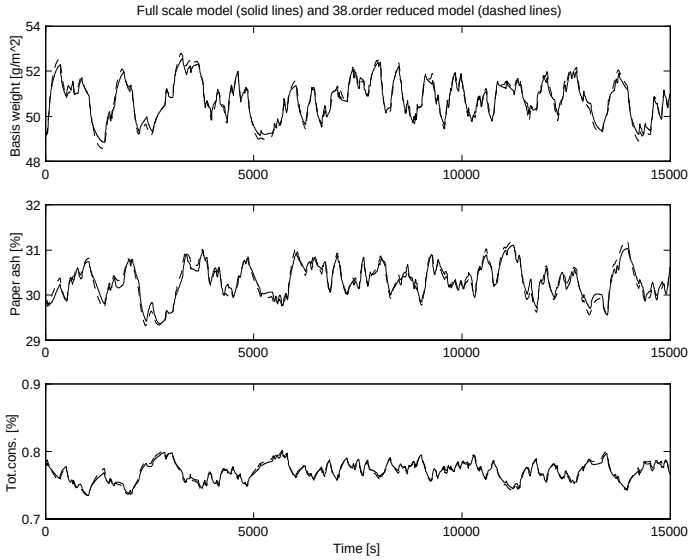

Figure 7: The responses of the full scale model (solid lines) and of the 38^{th} order simplified model (dashed lines).

3.3 A simplified paper machine model

In (Hauge & Lie 2000) it was shown, by simulation, that the full scale model described in Section 2 can be reduced to a much simpler and lower order model without affecting its properties to any large extent. The implemented full scale model is of order 528, and it was shown that a 38th order model have basically the same input-output properties. The simplifications were by and large carried out by lumping pipeline volumes into existing tanks, discretizing the remaining pipeline volume (the pipeline between the screens and the headbox) into one volume and discretizing the wire, press, and dryer sections into one "volume". The response from the full scale model and the simplified model, when filtered PRBSs (Pseudo Random Binary Signal) are applied to the inputs, is shown in Figure 7.

Further model reductions were obtained by e.g. comparing the responses of simplified models of various order, fitted to process data. The simplifications were carried out with a step by step approach in which the model was carefully studied after each phase of simplifications and model fitting. The model reductions culminated in a third order model which will be presented next.

In Figure 8, only elements relevant for the simplified model are shown. There are three lumped volumes, and these are the white water tank, the reject tank and the deculator ("right" side). Only two components are accounted for in the simplified model, and these are filler particles and fibers, thus no flocculated filler or fines concentrations are calculated throughout the white water system. We will go briefly

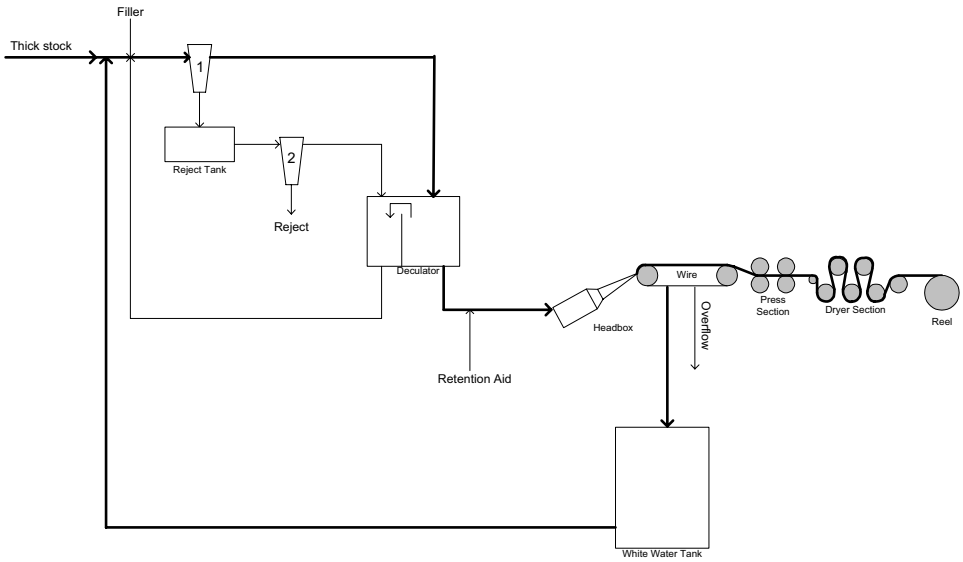

Figure 8: Sketch of PM6, according to the third order mechanistic model.

through the most important parts of the model, focusing on the differences between this simplified model and the more detailed model of section 2.

The thick stock The fiber and filler concentrations are estimated. In addition we calculate the concentration of "fresh" filler in the thick stock flow

$$C_{TS,\text{fresh filler}} = \alpha_{TS,\text{fresh filler}} \cdot C_{TS,\text{filler}}. \tag{29}$$

Here, only a share $\alpha_{TS,\text{fresh filler}}$ of the filler is assumed "fresh", while all the filler added at the outlet of the white water tank is assumed "fresh". The reason for this is that the filler from the thick stock is assumed better mixed when entering the hydrocyclone arrangement.

The white water tank The white water tank is modeled as a perfectly stirred tank with one flow entering (from the wire) and one flow leaving (to the hydrocyclones). The two components in the tank are filler particles and fiber, and the filler particles are modeled by an ODE (ordinary differential equation), while the fibers are at steady state.

The hydrocyclones The hydrocyclones consist of two stages and a reject tank between the two stages, as shown in Figure 8. The equations used to describe the hydrocyclones are equal to those presented in section 2.7, although fines, retention

aid, flocculated fines, and flocculated filler particles are not part of the model. In addition the ODE for fiber is at steady state, thus only the ODE for filler particles in the tank remain.

The deculator The ODEs in the "left" side are at steady state, and only the ODE for fiber in the "right" side remain.

The headbox The screens are neglected and the flow from the "right" side of the deculator goes directly to the headbox. Between the deculator and the headbox the retention aid is added, and the equation for flocculation of filler particles, as described in section 2.5, is at steady state. Since fines are no longer a component in the model, no equations for flocculated fines exist. The flow which is recirculated from the headbox to the deculator is removed from the model.

The wire We assume that a part $\alpha_{W,\text{fiber}}$ of the fibers are retained on the wire

$$w_{W,\text{fiber}} = \alpha_{W,\text{fiber}} \cdot w_{H-W} \cdot C_{H,\text{fiber}}, \tag{30}$$

where we follow the notational convention of section 2.11. Furthermore, we assume that flocculated filler particles are retained on the wire, in addition to some mechanical entrapment of non-flocculated filler particles

$$w_{W,\text{filler}} = w_{H-W} \cdot (C_{H,\text{flocculated filler}} + C_{H,\text{non-flocculated filler}} \cdot \alpha_{H,\text{filler}}). \tag{31}$$

The output equations The output equations are equal to those presented in section 2.12, except that the transportation delay through the wire, press, and dryer sections are neglected, and no fines are accounted for

$$y_{\text{basis weight}} = \frac{1000 \cdot \alpha_{\text{edge trim}} \cdot w_{W-R,\text{solid}}}{v \cdot b_R \cdot (1-f)} \tag{32}$$

$$y_{\text{paper ash}} = \frac{100 \cdot w_{W-R,\text{filler}} \cdot (1-f)}{w_{W-R,\text{solid}}} \tag{33}$$

$$y_{\text{WW tot. conc.}} = 100 \cdot (C_{W-WWT,\text{filler}} + C_{W-WWT,\text{fiber}}). \tag{34}$$

3.4 Summary of simplified third order model

The model equations are

$$\begin{aligned} \dot{x} &= f_1(x,u,d,z,\theta) \\ z &= f_2(x,u,d,z,\theta) \\ y &= g(x,u,d,z,\theta), \end{aligned} \tag{35}$$

where $z \in \mathbb{R}^{31}$ is a set of algebraic equations. The states are

$$x = \begin{bmatrix} C_{Re,\text{filler}} \\ C_{WWT,\text{filler}} \\ C_{Dr,\text{fiber}} \end{bmatrix}, \tag{36}$$

where $C_{Re,\text{filler}}$ is the concentration of filler in the reject tank, $C_{WWT,\text{filler}}$ is the concentration of filler in the white water tank, and $C_{Dr,\text{fiber}}$ is the concentration of fiber in the deculator ("right" side).

The inputs and outputs are

$$u = \begin{bmatrix} w_{TS} \\ w_{\text{filler}} \\ w_{\text{ret. aid}} \end{bmatrix}, y = \begin{bmatrix} y_{\text{basis weight}} \\ y_{\text{paper ash}} \\ y_{\text{WW tot. conc.}} \end{bmatrix}, \tag{37}$$

where w_{TS} is the flow of thick stock, w_{filler} is the flow of filler which is added at the outlet of the white water tank, $w_{\text{ret. aid}}$ is the flow of retention aid added at the outlet of the screens, and the outputs are as explained in section 2.12.

The measured disturbances, which are accounted for in the model, are

$$d = \begin{bmatrix} C_{TS,\text{total}} \\ C_{TS,\text{filler}} \\ S_{\text{1.stage pump}} \\ v \\ P_H \\ h_{\text{slice opening}} \\ f \end{bmatrix}, \tag{38}$$

where $C_{TS,\text{total}}$ and $C_{TS,\text{filler}}$ are total and filler thick stock concentrations, $S_{\text{1.stage pump}}$ is the speed of the pump between the white water tank and the first stage of the hydrocyclones, v is the machine velocity, P_H is the pressure inside the headbox, $h_{\text{slice opening}}$ is the height of the slice opening and f is the paper moisture percentage.

The parameter vector θ consists of various more or less unknown parameters, which we tune to fit the model to process data. Several other parameters exist, some which are known, and some which are set at fixed values due to identifiability considerations. The parameter vector then, is

$$\begin{aligned} \theta = \big[\; & \alpha_{1,\text{fresh filler,accept}} \quad \alpha_{1,\text{filler,accept}} \quad \alpha_{2,\text{filler,accept}} \quad \alpha_{1,\text{fiber,accept}} \quad \alpha_{2,\text{fiber,accept}} \\ & \alpha_{W,\text{fiber}} \quad \alpha_{W,\text{filler}} \quad \alpha_{TS,\text{fresh filler}} \quad V_{WWT} \quad V_{Re} \quad V_{Dr} \quad k_{\text{ret}} \quad k_{\text{fiber}} \; \big], \end{aligned} \tag{39}$$

where $\alpha_{i,j,\text{accept}}$ is the share of accepted component j (fresh filler, filler or fiber) at the i'th hydrocyclone stage, $\alpha_{W,\text{fiber}}$ and $\alpha_{W,\text{filler}}$ are shares of fiber and filler mechanically entrapped on the wire, $\alpha_{TS,\text{fresh filler}}$ is the share of fresh filler in the filler flow from the thick stock, V_i are the volumes of the white water tank, reject tank and deculator ("right" side), and k_j are flocculation constants for filler particles.

3.5 Implementation issues

The algebraic equations in the model are calculated in an order similar to the physical appearance of the variables in the process (e.g. algebraic equations associated with the first stage of the hydrocyclones are computed before equations associated with the reject tank and the second stage). The advantage of calculating them in this order is that the model file is well arranged, and changes in the model can be easily implemented and tested. The disadvantage is that due to several equations being mutually dependent, we can not compute all of them as they appear in the model equations. In the model file this is solved using shifted values for some variables, i.e.

$$\begin{aligned} x_{k+1} &= f_1(x_k, u_k, d_k, z_k, z_{k-1}, \theta) \\ z_k &= f_2(x_k, u_k, d_k, z_k, z_{k-1}, \theta) \\ y_k &= g(x_k, u_k, d_k, z_k, z_{k-1}, \theta). \end{aligned} \tag{40}$$

The method used here corresponds to the fixed-point iteration method (see e.g. (Gerald & Wheatley 1994)), using only one iteration. A simple explicit Euler method is used for discretizing the model in Equation 35. One reason for using the explicit Euler method, contrary to e.g. a Runge-Kutta method, is that it can be used in a straight forward manner, even though we use a fixed-point iteration method with one iteration to calculate some of the algebraic equations.

It is possible, by substitution, to eliminate the algebraic equations from the model. We have compared validation results (as in Section 4), using a model where the algebraic equations are eliminated, and a model where the fixed-point iteration method using one iteration is used. The two methods gave practically the same validation results and the model outputs were close to indistinguishable. The reason for this is that most of the variables in the process change slowly and thus the error of using a delayed value is small. The model file, when the algebraic equations are eliminated, consists of a few very large and complex equations. Changing the structure of the model would not be possible using this file, and in the remainder of this paper we use the model file where fixed-point iteration is used.

4 Parameter estimation and validation

4.1 Criterion and minimization algorithm

The least squares criterion is used for measuring the model fit

$$J(\theta) = e^T(\theta) \cdot Q \cdot e(\theta), \tag{41}$$

where e is a vector of errors and Q is a diagonal weighting matrix. The minimization algorithm's single task is to solve

$$\hat{\theta} = \arg\min_{\theta} J(\theta), \tag{42}$$

where $\hat{\theta}$ is the estimated parameter vector.

The function `lsqnonlin` in the Optimization toolbox (version 2) in Matlab (version 6) is used for solving the minimization problem. The function relies on the Levenberg-Marquardt algorithm in its search for the optimal parameter values (The MathWorks, Inc. 2000).

There are at least two alternatives when deciding how the errors e should be calculated. In the prediction error method (PEM) and in subspace methods one calculates the prediction error

$$\epsilon(t) = \hat{y}(t|t-1) - y(t), \tag{43}$$

where $y(t)$ is the measured output at time t, and $\hat{y}(t|t-1)$ is the predicted output at time t based on past input-output data, i.e. a one-step-ahead prediction. In this case the error vector would be e.g.

$$e^T(\theta) = \left[\begin{array}{cccccc} e_1^T(\theta) & e_2^T(\theta) & \cdots & e_{m-1}^T(\theta) & e_m^T(\theta) \end{array} \right], \tag{44}$$

with

$$e_i^T(\theta) = \left[\begin{array}{ccccccc} \epsilon_i(1) & \epsilon_i(2) & \cdots & \epsilon_i(t) & \cdots & \epsilon_i(N-1) & \epsilon_i(N) \end{array} \right], \tag{45}$$

where m is the number of outputs and N is the number of samples in the data set.

Another approach is to simulate the system, with only the initial conditions given. The error is then

$$\varepsilon(t) = \hat{y}(t|0) - y(t), \tag{46}$$

where $\hat{y}(t|0)$ is the model output at time t given only the initial conditions. The error vector for output i is then

$$e_i^T(\theta) = \left[\begin{array}{ccccccc} \varepsilon_i(1) & \varepsilon_i(2) & \cdots & \varepsilon_i(t) & \cdots & \varepsilon_i(N-1) & \varepsilon_i(N) \end{array} \right]. \tag{47}$$

Traditional system identification is carried out by using the one-step-ahead method, however in our case we wish to emphasize the need for a model with good long term prediction abilities. The reason for this is that the model will be used for model predictive control (MPC). Then, it seems natural to use the simulation approach in the parameter estimation algorithm. The simulation approach results in a deterministic model, and it will be necessary to identify or model the noise as well. We will return to this issue soon.

4.2 Experiment design and preprocessing of data

For a linear system, the concept of persistent excitation (see e.g. (Ljung 1999) and (Söderström & Stoica 1989)) provides an adequate characterization of the input signal needed to identify the model. The order of the excitation is dependent on the power spectrum of the signal only, and is independent of its shape (e.g. amplitude). This is not the case for a non-linear system; because such systems are amplitude dependent, i.e. the response to an input sequence $u(t)$ may be qualitatively very different from

that for $a \cdot u(t)$. One has the opportunity to design optimal experiments (Goodwin & Payne 1977)

$$\hat{\Xi} = \arg \underset{\Xi \in \digamma}{opt} \; J(\Xi), \tag{48}$$

where $\hat{\Xi}$ is the optimal experimental condition, e.g. shape of inputs and sampling times, $\digamma$ is the set of feasible values for Ξ, and $J(\Xi)$ is a scalar criterion. However, this approach is seldom practicable for mechanistic models due to a chain of assumptions which must be made, e.g. choosing nominal parameter values. Often, experiment design for non-linear systems is based on a few rules of thumb, e.g. to use an input sequence of several amplitude levels (Pearson & Ogunnaike 1997), and to excite the relevant frequency bands. On a paper machine an open loop experiment is carried out with high risk of poor paper quality or even sheet breaks. A solution to this problem is to perform closed loop experiments, i.e. in this case experiments where the basis weight, paper ash and wire tray (or white water) total consistency controllers are in automatic mode. There is a vast amount of published material on closed loop system identification, and various approaches and algorithms are treated in more detail in e.g. (Ljung 1999), (Söderström & Stoica 1989) and (Forssell 1999). Our approach is "the direct approach" (Ljung 1999) in which we use the process inputs u and outputs y in the same way as for open loop identification, ignoring the feedback mechanisms and the reference signals. We specify changes in the setpoints, thus forcing the inputs to perturb the process. For example a rough approximation of the filtered PRBS signal is possible by changing the setpoints of the mass flows according to a PRBS scheme and let the valve and pump controllers work out the correct openings and velocities. Such an experiment plan is shown in Figure 9. There is no need to introduce several amplitude levels in the plan, since the process inputs and outputs are far from typical binary signals. The resulting inputs and outputs are shown in Figures 10 and 11 respectively.

Filtered data are used when the deterministic model was identified, while the raw-data are used when the stochastic part of the model was identified. The filtering was carried out by a second order Butterworth filter, and as is seen in Figure 11, a cubic interpolation routine was applied to the paper ash data in a region near the 125th minute due to erroneous measurements.

4.3 Model fitting and validation of deterministic model

For comparison, we compute the value of a root mean square error (RMSE) criterion

$$\mathrm{RMSE}_i = \sqrt{\frac{1}{N} \sum_{t=1}^{N} (y_i(t) - \hat{y}_i(t))^2}, \tag{49}$$

where N is the number of observations, $y_i(t)$ is the measured value of output i at time t, and $\hat{y}_i(t)$ is the predicted or simulated value of output i at time t.

Optimal fitting of the mechanistic model to experimental data was carried out as described in section 4.1. The fitted model output is shown in Figure 12, along with

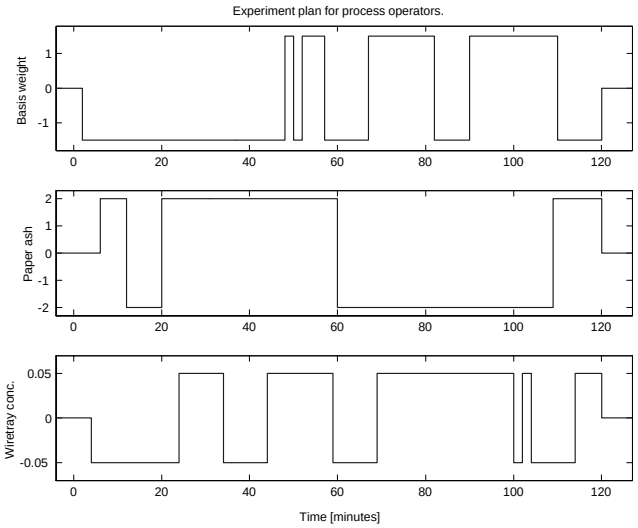

Figure 9: Experiment plan for the PM6 process operators. The plan shows the changes in setpoints carried out for the data set collected at February 28, 2001.

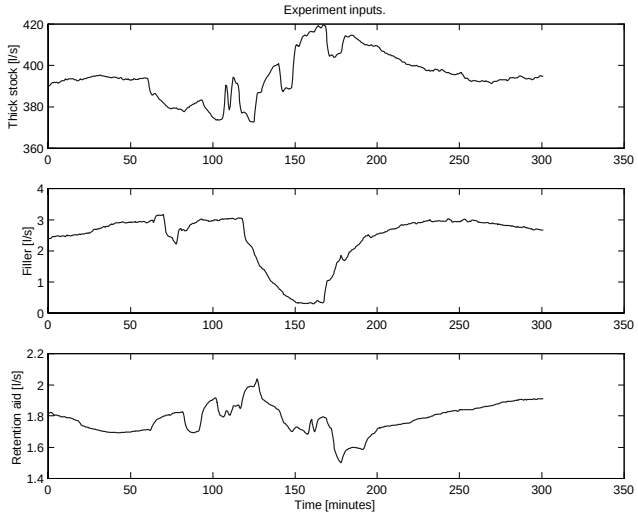

Figure 10: Experiment inputs applied to the process at February 28, 2001.

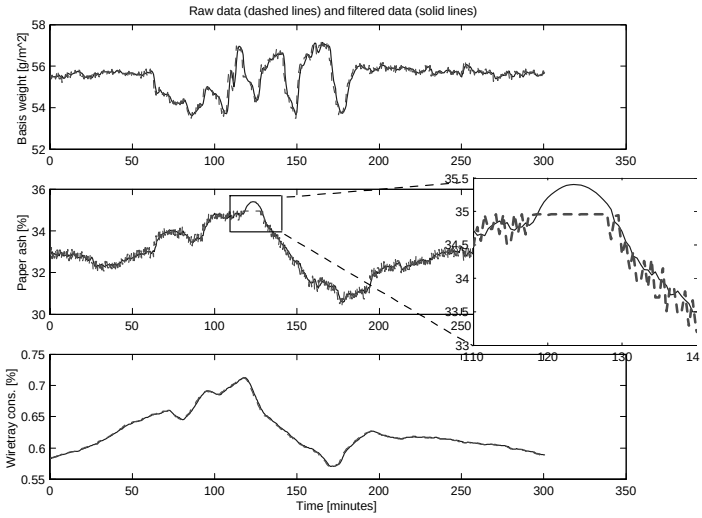

Figure 11: Process outputs during experimentation at February 28, 2001. Raw data are in dashed lines and filtered data are in solid lines. Note the erronous paper ash data around the 125th minute. A cubic interpolation function was applied to the data in the erronous region.

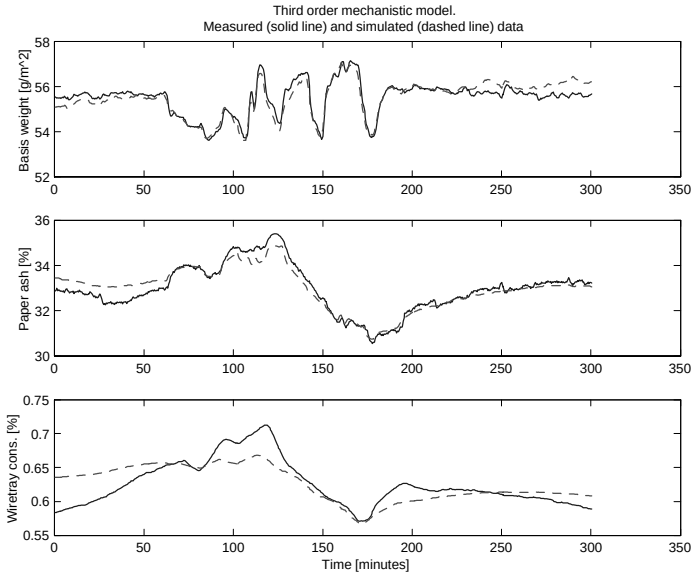

Figure 12: Third order mechanistic model fitted to experimental data. Experimental data collected at February 28th 2001.

the measured output. Note that only a *deterministic* model, or ballistic model, is used in this simulation. The basis weight and paper ash dynamics seem well captured by the model, while the wire tray concentration fit is less good. In addition to scaling of the parameters in Equation 39, the outputs in the criterion (Equation 41) where also scaled such that more weight was put on the wire tray concentration. Adding even more weight on the wire tray concentration did not improve the model fit for this particular output.

RMSE values for the fitted third order mechanistic model is shown below:

Basis weight	**Paper ash**	**Wire tray cons.**
0.30	0.33	0.022

For validation of the mechanistic model, three data sets containing operational data were used. The first data set was collected during March 8-11, 2001. Figure 13 shows the validation results, when the mechanistic model is simulated (ballistic) with the measured inputs. Although corrected for bias, the model fit for basis weight and paper ash seem reasonably good considering that the time span is more than 90 hours. The initial oscillations in the basis weight may be caused by large oscillations in the estimated thick stock consistencies at this time.

RMSE values for validation of the third order mechanistic model with operational data collected during March 8-11, 2001, are:

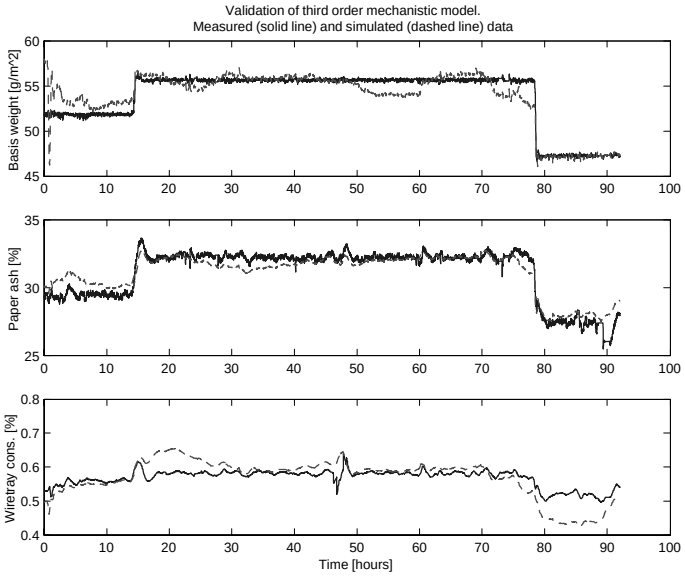

Figure 13: Validation of third order mechanistic model by simulation. Operational data collected during March 8-11, 2001. Simulated data are bias corrected.

Basis weight	**Paper ash**	**Wire tray cons.**
1.17	0.66	0.037

5 A Hybrid Extension

A hybrid model will be introduced in this section. The hybrid model consists of the third order mechanistic model and a first order empiric model. The empiric model is identified with the error signals in Equation 47 as outputs, u and various measured disturbance signals as inputs. Denote the output from the mechanistic model by $\hat{y}_{\text{mec}}$ and the output from the empiric model by $\hat{y}_{\text{emp}}$, then the hybrid model output is $\hat{y}_{\text{hyb}} = \hat{y}_{\text{mec}} - \hat{y}_{\text{emp}}$. The empiric model may be viewed as originating from neglected and unknown dynamics in the third order mechanistic model. The neglected dynamics typically arise from the model reductions carried out, but also from such sources as sensors and actuators. Unknown dynamics can e.g. be a filter in a measuring device with proprietary software, some physical unit not known to the person modelling the system or a general lack of understanding of the physical process.

We will start this section by fitting and validating a deterministic hybrid model. The validation will be carried out with operational data sets spanning several days. It is of course not realistic or the intention to use the models to predict several days ahead, so we will then identify a stochastic sub-model, and validate the combined deterministic and stochastic model. This validation will be carried out close to realistic conditions, validating the one-step ahead prediction abilities and the long-term prediction abilities.

5.1 Model fitting and validation of deterministic hybrid model

We use the experimental data set from February 28th, 2001, to identify the empiric model. The criterion and functions used are similar to those used with the mechanistic model (see Section 4.1). The model structure is

$$\begin{aligned} x_{\text{emp},k+1} &= Ax_{\text{emp},k} + Bu_k + Ed_k \\ y_{\text{emp},k} &= Cx_{\text{emp},k} + Du_k + Fd_k, \end{aligned} \tag{50}$$

with $x_{\text{emp}} \in \mathbb{R}^1$, $d \in \mathbb{R}^2$, $y_{\text{emp}} \in \mathbb{R}^3$ and $u \in \mathbb{R}^3$. The two sources of measured disturbances are the estimated thick stock concentrations. Although it would be preferable to add other disturbance sources, this is not possible using the February 28th, 2001, dataset due to lack of excitation from other sources. An alternative could be to use operational data spanning several days, such that more measured disturbances were excited. We will return to this issue soon, but point out that using operational data to identify e.g. the time constant of the process, which in this case is a simple transformation of A, in this case fails because the process itself is not properly excited. With operational data and a first order system, we found $A \approx 1$, which is an integrator. Validation of the model identified from operational data was not successful.

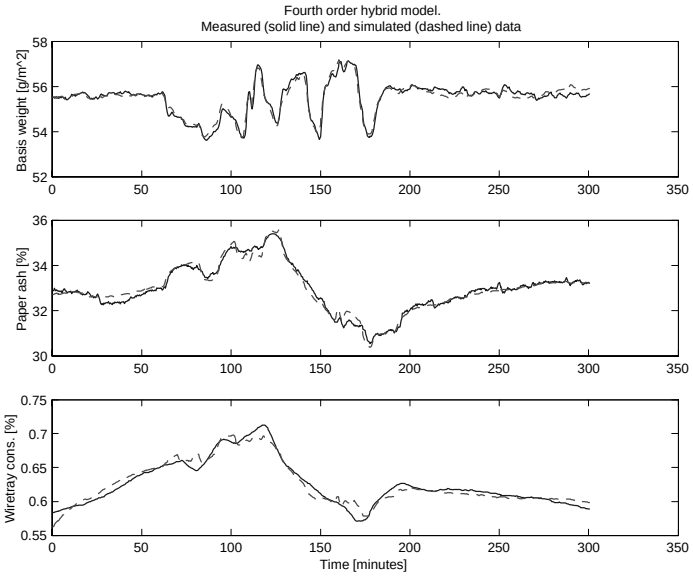

Figure 14: Fourth order hybrid model fitted to experimental data. Experimental data collected at February 28th 2001.

Figure 14 shows the fitted *deterministic* hybrid model. The improvement compared to the pure mechanistic model seems quite large.

RMSE values for fitted fourth order hybrid model are shown below:

Basis weight	**Paper ash**	**Wire tray cons.**
0.18	0.19	0.0082

Figure 15 shows the validation results using the operational data set collected during March 8-11, 2001.

RMSE values for validation of fourth order hybrid model with operational data collected in March 8-11, 2001, are:

Basis weight	**Paper ash**	**Wire tray cons.**
0.78	0.56	0.047

The basis weight and paper ash validation results are better than for the pure mechanistic model, although this is not the case for the wire tray consistency where the result is poorer.

We mentioned earlier that only two measured disturbances were used in the empiric model, due to lack of excitation from other sources. This is true for the short

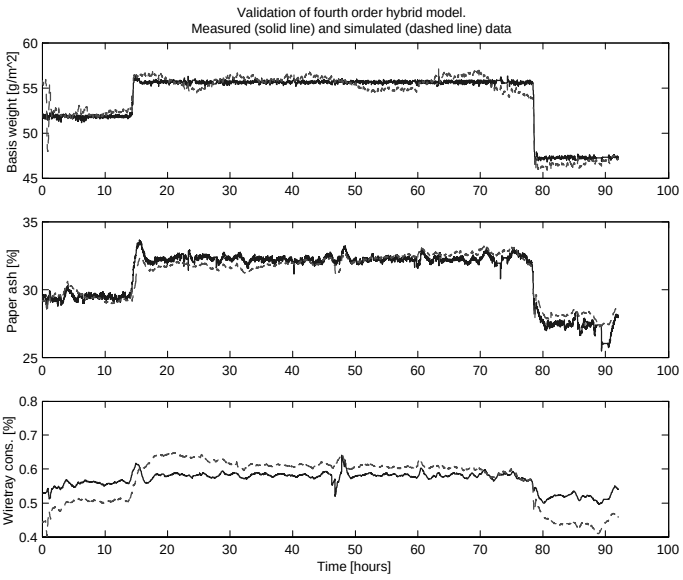

Figure 15: Validation of fourth order hybrid model by simulation. Operational data collected during March 8-11, 2001. Simulated data are bias corrected.

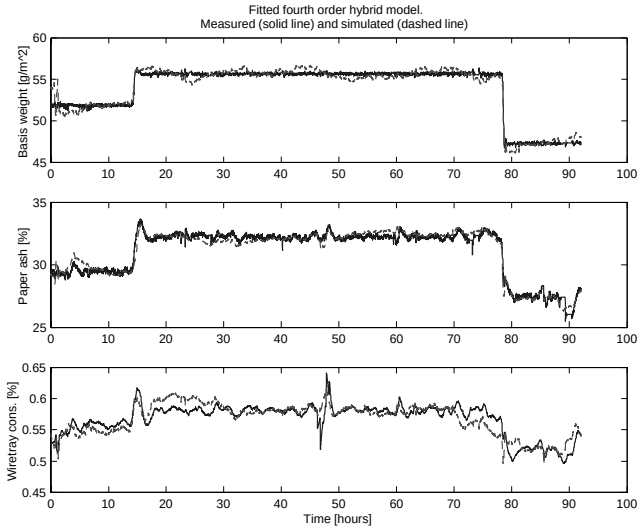

Figure 16: Fitted fourth order hybrid model. Only those elements in the empiric model of Equation 50, corresponding to measured disturbances (elements in E and F matrices), were tuned. Elements in other system matrices and parameters in mechanistic model are as identified with experimental data set collected at February 28, 2001. Operational data collected during March 8-11, 2001. Simulated data are bias corrected.

experimentation data set used to identify the models, but in the operational data sets which span several days, many measured disturbances vary quite a lot. We take advantage of this and identify the E and F matrices in the state space model of Equation 50 a new, and in addition augmenting the d vector such that $d \in \mathbb{R}^6$. The other system matrices are not altered. The measured disturbance vector used in the empiric model is equal to that of Equation 38, except that the last element (f) is not part of the empiric model. Figure 16 shows the fitted model and measured outputs.

RMSE values for fitted fourth order hybrid model with operational data collected during March 8-11, 2001, are:

Basis weight	**Paper ash**	**Wire tray cons.**
0.56	0.39	0.014

Two operational data sets were used for validation of the new hybrid model. The first validation data set is collected during May 11-16, 2001, and the bias corrected results can be seen in Figure 17. There appear to be problems with the basis weight and especially the wire tray concentration outputs, however compared to the model outputs when using the mechanistic model or the hybrid model with $d \in \mathbb{R}^2$, the re-

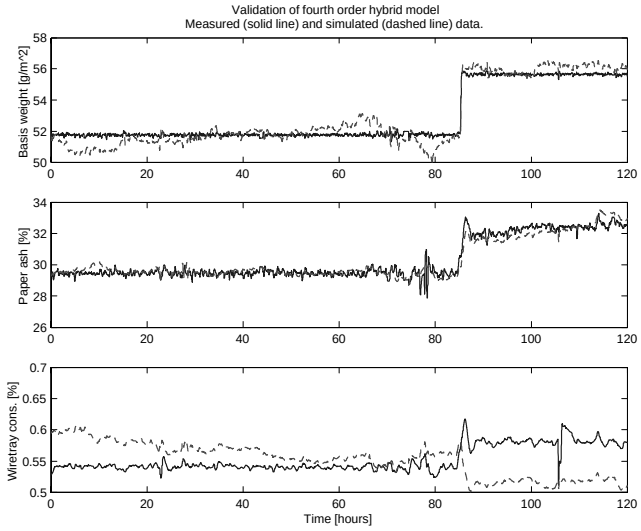

Figure 17: Validation of fourth order hybrid model identified from experimental data (February 28, 2001) and operational data (March 08-11, 2001). Operational validation data collected during May 11-16, 2001. Simulated data are bias corrected.

sults for the basis weight has improved while the result for the wire tray concentration is worse.

RMSE values for *validation* of the third order mechanistic model and two fourth order hybrid models with operational data collected during May 11-16, 2001, are:

	Basis weight	**Paper ash**	**W. t. cons.**
Third order mechanistic model	2.74	0.52	0.031
Fourth order hybrid model ($d \in \mathbb{R}^2$)	1.27	0.35	0.023
Fourth order hybrid model ($d \in \mathbb{R}^6$)	0.56	0.34	0.044

A second operational validation data set was collected during May 19-23, 2001, and the bias corrected results can be seen in Figure 18. This data set is rather special, because a filler used only a few times per year was added from around the 40th to the 60th hour. This filler has a significant effect on both the retention aid and on the measurement devices. In addition, extra chemicals are added in the pulping process due to high brightness demands on the finished paper. There are probably several errors in the data set, e.g. the low peaks around the 45th hour in the paper ash time series, and the large oscillations in the wire tray consistency during the 40-60th hour.

RMSE values for *validation* of the third order mechanistic model and two fourth order hybrid models with operational data collected during May 19-23, 2001, are:

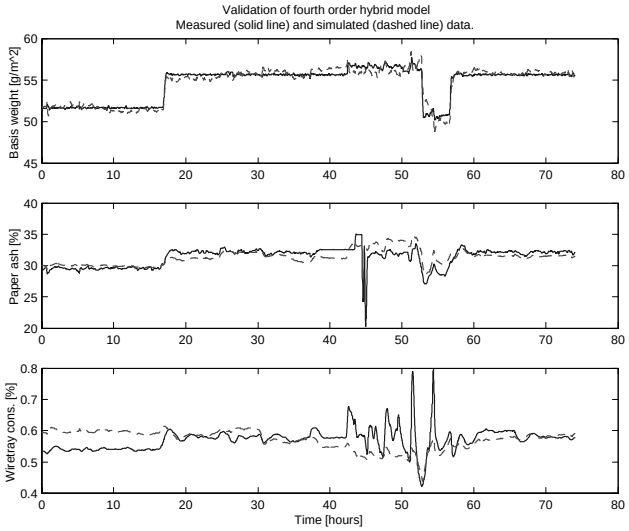

Figure 18: Validation of fourth order hybrid model identified from experimental data (February 28, 2001) and operational data (March 08-11, 2001). Operational validation data collected during May 19-23, 2001. Simulated data are bias corrected.

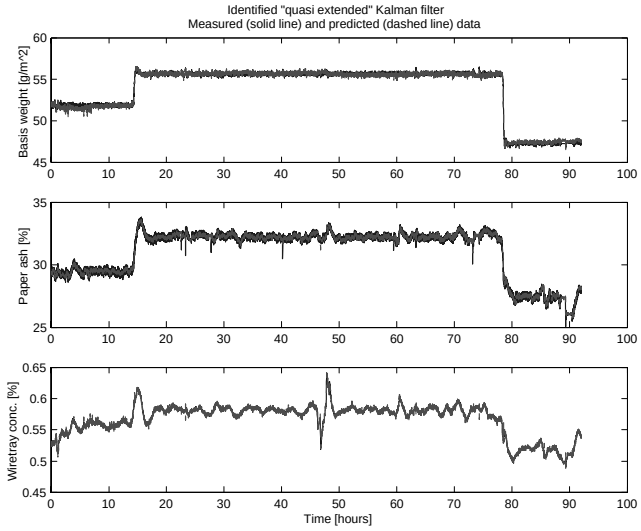

Figure 19: Identification of "quasi extended" Kalman filter for fourth order hybrid model. Operational data collected during March 08-11, 2001. Predictions are bias corrected.

	Basis weight	**Paper ash**	**W. t. cons.**
Third order mechanistic model	1.08	1.05	0.054
Fourth order hybrid model ($d \in \mathbb{R}^2$)	0.71	1.30	0.042
Fourth order hybrid model ($d \in \mathbb{R}^6$)	0.56	1.24	0.046

5.2 Identification and validation of "quasi extended" Kalman filter

Identification An extended Kalman filter normally updates the Kalman filter gain matrix at each sample, based on noise covariance matrices and a linearization of the model (see e.g. (Gelb 1974) and (Ergon 2001)). For simplicity we skip the linearization of the model and the identification or tuning of the covariance matrices, and identify the Kalman filter gain matrix directly from data as shown in Figure 19. Thus, the Kalman filter is not updated and therefore the name "quasi extended". Note that we do not use filtered data when we identify the Kalman filter.

One-step ahead validation Figure 20 and Figure 21 show validation results using the hybrid model with "quasi" extended Kalman filter. All in all, the Kalman filter seems to work properly for the two validation data sets. However, in Figure 21,

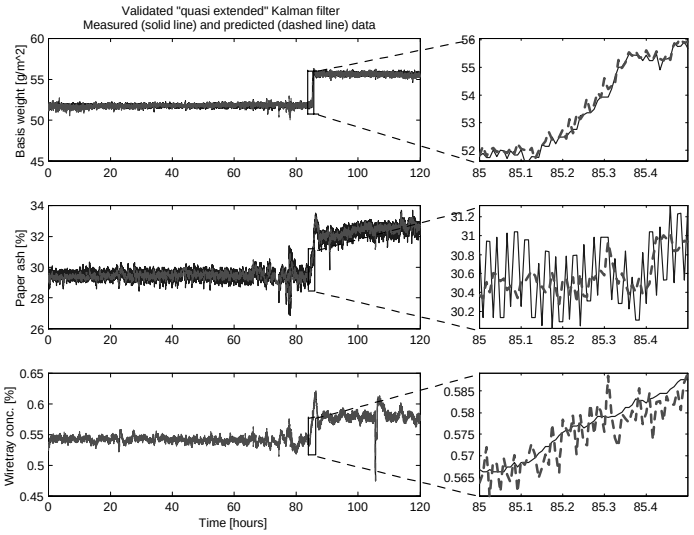

Figure 20: Validation of "quasi extended" Kalman filter for fourth order hybrid model. Operational data collected during May 11-16, 2001. Predictions are bias corrected.

several severe measurement errors in the paper ash time series around the 45th hour, cause large prediction errors for the basis weight and wire tray concentration. Before implementing this estimator on paper machine 6, some sort of outlier detection is needed.

RMSE values are based on bias corrected measured data and predicted data (one-step ahead predictions). RMSE values for identification (March 8-11, 2001,) and validation (May 11-16, 2001 and May 19-23, 2001) of the fourth order hybrid model with "quasi extended" Kalman filter, are:

	Basis weight	Paper ash	W. t. cons.
Identification, data set from March 8-11, 2001	0.21	0.23	0.0023
Validation, data set from May 11-16, 2001	0.20	0.32	0.0031
Validation, data set from May 19-23, 2001	0.46	0.67	0.0047

The poorer validation results for the May 19-23 dataset, is a result of the large measurement errors in the paper ash signal around the 45th hour.

Validation of prediction ability during sheet breaks The identification and validation carried out in the previous section assumed that all inputs and outputs are measured, and therefore known. A problem within the paper industry is that some of these measurements are lost when sheet breaks occur, and a standard solution to this

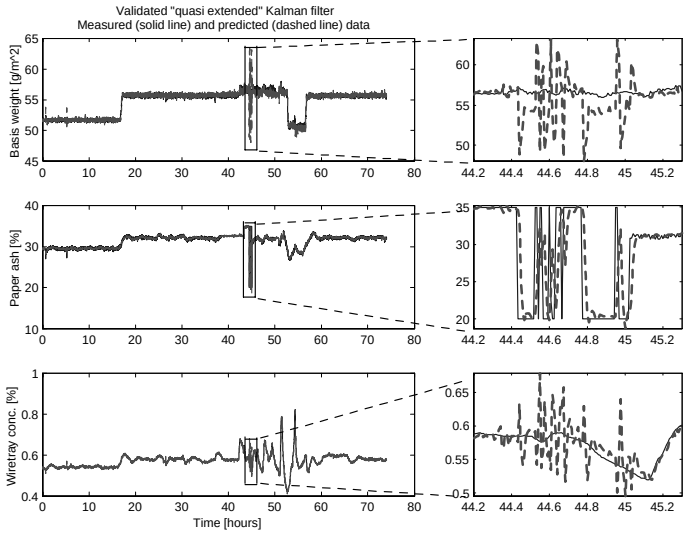

Figure 21: Validation of "quasi extended" Kalman filter for fourth order hybrid model. Operational data collected during May 19-23, 2001. Predictions are bias corrected.

problem is to "freeze" the corresponding inputs at their present values (the values at the time of the sheet break). At PM6, the basis weight and paper ash measurements are lost during sheet breaks, while we still measure the wire tray concentration. Thus, in Figure 22 and 23 we have validated the model, simulating sheet breaks of various lengths. The sheet breaks last from 30 minutes to 2 hours, and they take place during normal operation or during grade changes. The simulation is carried out such that at sheet breaks we use the identified constant gain Kalman filter matrix, and the innovation signal for basis weight and paper ash is "frozen" at the mean value of their ten values prior to the sheet break. The innovation signal for wire tray concentration is calculated at each sample as before. The paper ash seems to be predicted reasonably good during sheet breaks, while the result for the basis weight is more mixed considering the drift in the 40-41st hour in Figure 22.

An alternative, and perhaps more common, method for updating the states with missing measurements, is to set the innovation signal to zero for the lost measurements. The states will then only be updated through the available measurement.

Validation of prediction ability during grade changes Prior to grade changes, the operators must give information to the control system about the time of change, new basis weight, paper ash, and other variables. With this information the long term prediction ability of the model must be reasonably good. Figure 24 and 25 show validation results were we have validated the ability to predict the responses during

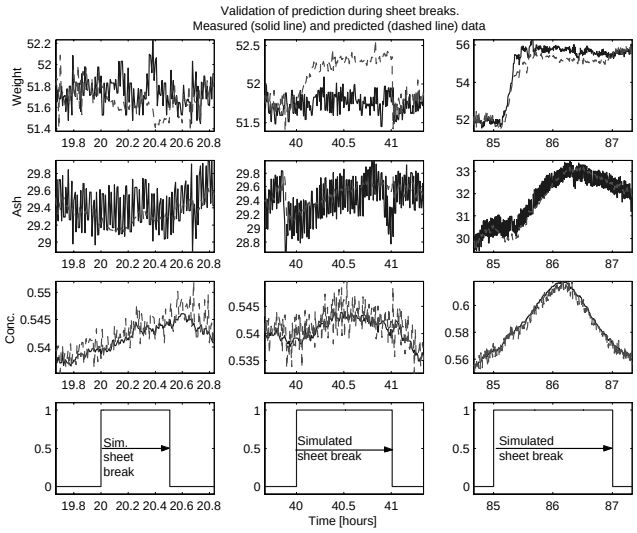

Figure 22: Three periods of simulated sheet breaks. The first and second column show simulated sheet breaks during normal operation, while the third column show a simulated sheet break just prior to a grade change. Operational data collected during May 11-16, 2001.

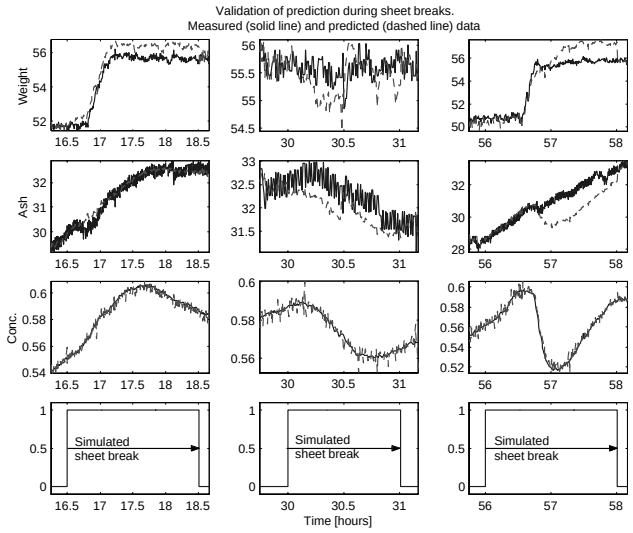

Figure 23: Three periods of simulated sheet breaks. The second column show a simulated sheet break during normal operation, while the first and third columns show simulated sheet breaks just prior to grade changes. Operational data collected during May 19-23, 2001.

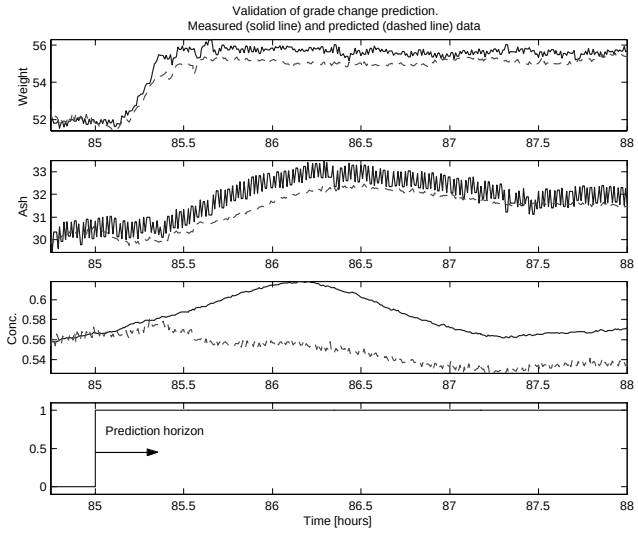

Figure 24: Prediction during a grade change. Operational data collected during May 11-16, 2001.

grade changes. The prediction horizon ranges from 2 to 3 hours. The innovation signal for all three model outputs is "frozen" at the mean value of their ten values prior to the long-term prediction.

6 Conclusions

In this paper we have presented a high order mechanistic model of paper machine 6 (PM6) at Norske Skog Saugbrugs in Halden, Norway. The model is simplified making it more suitable for control purposes, and a third order mechanistic model is outlined. The third order model is fitted to experimental data and validated with historical operational data. In the experimental data set only a few of the measured disturbances are properly excited, thus the data set is not ideal for fitting of the model. Fitting of the model to operational data sets, in which the measured disturbances were properly excited, were tested but failed due to lack of excitation of the manipulated inputs. One may consider merging several operational data sets, or merging data during grade changes such that both manipulated inputs and measured disturbances are properly exited. However, this approach may also fail because the process itself probably is time varying, and unmodelled disturbances, such as e.g. variations in the raw material, cause drifts and trends which are not accounted for in the model.

The fitting and validation reveals deficiencies in the model and perhaps in the experimentation, although it is not clear whether one can eliminate these deficiencies

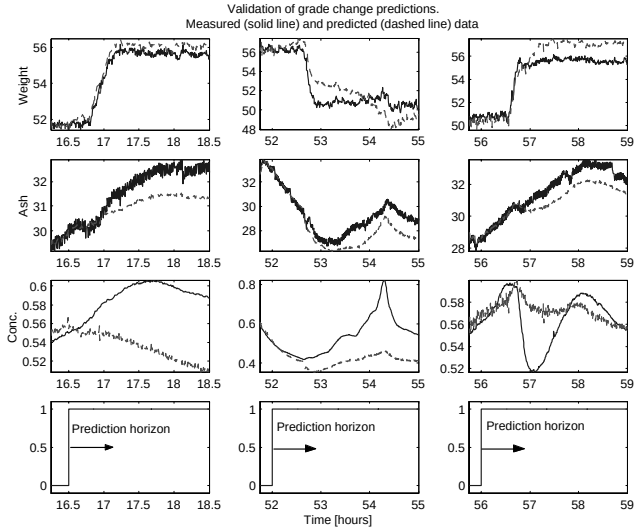

Figure 25: Predictions during three grade changes. Note that a rare filler is used during the grade changes in column two and three. Operational data collected during May 19-23, 2001.

without increasing the order of the model. Increased order models which were fitted to experimental data performed better than the lower order models, thus the choice of a third order model is a trade-off between e.g. complexity and accuracy.

A first order empiric model is added to the mechanistic model to capture neglected and unknown dynamics in the process. The resulting fourth order hybrid model gives much better validation results than the pure mechanistic model for the basis weight, while not a clear better/worse answer for the paper ash and wire tray concentration. The basis weight is perhaps the most important quality variable of the three outputs, and thus we choose to use the hybrid model in the sequel.

A "quasi extended" Kalman filter, in which the Kalman filter gain matrix is constant, is then identified from operational data. Validation of the hybrid model with Kalman filter on operational data seems to give good results. Finally the model is validated with respect to prediction ability during sheet breaks, and prediction ability during grade changes. The prediction ability during sheet breaks seems good for paper ash, but is more uncertain for the basis weight which have a tendency to drift away in some cases. Without improving the prediction ability during sheet breaks it seems that one might as well freeze the inputs at the value prior to the sheet break. However, one may consider using the predictions for operator support if e.g. changes in machine velocity and other variables occur during a sheet break. The prediction ability during grade changes seems reasonably good for the basis weight and paper ash, however for the wire tray concentration, the prediction ability seems poorer.

Let us finally point at a few topics which could be of interest for further research:

- Refining the model, especially focusing on improving the predictions of the wire tray concentration.
- Identify and validate covariance matrices, linearize the model, for implementation of extended Kalman filter.
- Online estimation of key parameters, i.e. an augmented Kalman filter.
- Compare with more traditional handling of measurement loss.

Acknowledgments The authors would like to thank the employees at PM6, and especially Process Engineer Roger Slora, for their cooperation in providing information and data for this paper and for their general helpfulness. The work of Tor Anders Hauge is financially supported by the Research Council of Norway (project number 134557/432), with additional financial support by Norske Skog Saugbrugs.

References

Bown, R. (1996), Physical and chemical aspects of the use of fillers in paper, *in* J. Roberts, ed., 'Paper Chemistry', 2 edn, Chapman and Hall, chapter 11.

Britt, K. W. & Unbehend, J. E. (1976), 'New methods for monitoring retention', *Tappi Journal* **59**(2), 6770.

Campbell, J. C. (1997), Modelling, Estimation, and Control of Sheet and Film Forming Processes, PhD thesis, University of Wisconsin-Madison.

Ergon, R. (2001), *Introduction to Kalman Filtering with some Industrial Application Areas*, Lecture notes, Telemark University College, Norway.

Featherstone, A. P., VanAntwerp, J. G. & Braatz, R. D. (2000), *Identification and Control of Sheet and Film Processes*, Springer-Verlag London.

Forssell, U. (1999), Closed-Loop Identification: Methods, Theory, and Applications, PhD thesis, Dep. of Electrical Engineering, Linköping University, Sweden.

Gelb, A., ed. (1974), *Applied Optimal Estimation*, The M.I.T. Press.

Gerald, C. F. & Wheatley, P. O. (1994), *Applied Numerical Analysis*, 5 edn, Addison-Wesley Publishing Company, Inc.

Goodwin, G. C. & Payne, R. L. (1977), *Dynamic System Identification: Experiment Design and Data Analysis*, Academic Press.

Gregory, J. (1988), 'Polymer adsorption and flocculation in sheared suspensions', *Colloids and Surfaces* **31**, 231–250.

Hagberg, M. & Isaksson, A. (1993), 'A paper machine benchmark for control systems 94', Available at ftp://ftp.e.kth.se/pub/control/benchmark/bench.ps.

Hauge, T. A., Ergon, R., Forsland, G. O., Slora, R. & Lie, B. (2000), Modeling, simulation and control of paper machine quality variables at norske skog saugbrugs, norway, *in* 'Scientific and Technological Advances in the Measurement and Control of Papermaking', Pira International.

Hauge, T. A. & Lie, B. (2000), Simulation for advanced control of a paper machine: Model complexity and model reduction, *in* '41. SIMS Simulation Conference, Kgs. Lyngby, Denmark', SIMS, Scandinavian Simulation Society, pp. 135–154.

Heaven, E. M., Manness, M. A., Vu, K. M. & Vyse, R. N. (1996), 'Application of systems identification to paper machine model development and simulation', *Pulp and Paper Canada* **97**(4), 49–54.

Hoppensteadt, F. C. (2000), *Analysis and Simulation of Chaotic Systems*, second edn, Springer, New York.

Horn, D. & Linhart, F. (1996), Retention aids, *in* J. Roberts, ed., 'Paper Chemistry', 2 edn, Chapman and Hall, chapter 5.

Koethe, J. L. & Scott, W. E. (1993), 'Polyelectrolyte interactions with papermaking fibers: The mechanism of surface-charge decay', *Tappi Journal* **76**(12), 123–133.

Larsson, J. E. & Olsson, T. (1996), Styrning av utstromningshastighet ur innloppslada, Master's thesis, Tekniska Hogskolan i Lulea.

Ljung, L. (1999), *System Identification, Theory for the User*, second edn, Prentice Hall PTR.

Menani, S., Koivo, H. N., Huhtelin, T. & Kuusisto, R. (1998), Dynamic modelling of paper machine from grade change data, *in* 'Control Systems 98, Helsinki', pp. 79–85.

Nissinen, A. (1999), Stability of Wet End for Paper Machines with Dilution Headboxes, PhD thesis, Tampere University of Technology.

Noreus, O. & Saltin, J. (1998), Dynamic modelling of wet-end on paper machine, *in* 'Control Systems 98, Helsinki', pp. 104–110.

Norske Skog (2000), Norske Skog internet page at www.norske-skog.com.

Pearson, R. K. & Ogunnaike, B. A. (1997), *Nonlinear Process Control*, Prentice Hall PTR.

Pelssers, E. G. M., Cohen Stuart, M. A. & Fleer, G. J. (1989), 'Kinetic aspects of polymer bridging: Equilibrium flocculation and nonequilibrium flocculation', *Colloids and Surfaces* **38**, 15–25.

Rao, M., Xia, Q. & Ying, Y. (1994), *Modeling and Advanced Control for Process Industries: Applications to Paper Making Processes*, Springer-Verlag London.

Roberts, J. C. (1996*a*), *The Chemistry of Paper*, The Royal Society of Chemistry.

Roberts, J. C., ed. (1996*b*), *Paper Chemistry*, 2 edn, Blackie, London.

Schiesser, W. E. (1991), *The Numerical Method of Lines: Integration of Partial Differential Equations*, Academic Press, Inc.

Shirt, R. W. (1997), Modelling and Identification of Paper Machine Wet End Chemistry, PhD thesis, The University of British Columbia, Dep. of Electrical and Computer Engineering, Canada.

Slora, R. (2001), Stabilization of the wet end at PM6. part 1: Developing controllers for the thick stock, Technical Report A-rapport RSL20001, Norske Skog Saugbrugs. (confidential and in Norwegian).

Söderström, T. & Stoica, P. (1989), *System Identification*, Prentice Hall International.

The MathWorks, Inc. (2000), 'Optimization toolbox for use with matlab, user's guide (version 2)'.

Tuladhar, A., Davies, M. S., Yim, C. & Woods, G. R. (1997), 'Headbox modelling and wet end pressure pulsation analysis', *Pulp and Paper Canada* **98**(9), 91–94.

Van de Ven, T. G. M. (1984), 'Theoretical aspects of drainage and retention of small particles on the fourdrinier', *Journal of Pulp and Paper Science* **10**(3), 57–63.

Van de Ven, T. G. M. (1993), 'Particle deposition on pulp fibers: The influence of added chemicals', *Nordic pulp and paper research journal* **8**(1), 130–134, 147.

Paper D

Model Predictive Control of a Norske Skog Saugbrugs Paper Machine: Preliminary Study

Hauge, T.A., Slora, R. and Lie, B. (2002). *Model Predictive Control of a Norske Skog Saugbrugs Paper Machine: Preliminary Study*, in proceedings of Control Systems 2002, June 3-5, Stockholm, Sweden, p 75-79.

Extended version.

Model Predictive Control of a Norske Skog Saugbrugs Paper Machine: Preliminary Study

Tor Anders Hauge*, Roger Slora†, and Bernt Lie‡

Abstract

In this paper we give an overview of some of the work, carried out in a project at Norske Skog Saugbrugs in order to stabilize the wet end of paper machine 6 (PM6). A nonlinear physical based model was developed and will be used in a model predictive control (MPC) application. Results from a controllability analysis is given, indicating the necessity of process operators acting on measured disturbances to avoid input saturation. A commercially available MPC algorithm based on a linear model is modified to handle the nonlinear model, and to allow for future setpoint changes.

1 Introduction

A project for stabilizing the wet end of paper machine 6 (PM6) at Norske Skog Saugbrugs was initiated in late 1999 (see e.g. (Hauge, Ergon, Forsland, Slora & Lie 2000)), and the project will continue throughout 2002. The present state of the project for stabilizing the wet end, is that a process model has been developed, fitted, and validated with mill data (Hauge & Lie 2002). The model is implemented in a commercially available MPC solution, and the vendor of this MPC is currently modifying the software based on inputs from PM6 engineers. In addition to implementing an MPC, several single-input single-output control loops and feed forward controllers are implemented at PM6 for stabilizing variables outside the scope of the MPC.

This paper is organized as follows. In Section 2 we briefly outline the preprocessing of data carried out before the model was fitted. The model is described and some fitting and validation results are discussed in Section 3. In Section 4 we analyze and discuss controllability (the ability to achieve acceptable control performance). The APIS software and APIS MPC is described in Section 5, and a simulation result is shown in Section 6. Finally, in Section 7, some conclusions are given.

*Telemark University College, P.b. 203, 3901 Porsgrunn, Norway. E-mail: Tor.A.Hauge@hit.no
†Norske Skog Saugbrugs, 1756 Halden, Norway. E-mail: Roger.Slora@norske-skog.com
‡Telemark University College, P.b. 203, 3901 Porsgrunn, Norway. E-mail: Bernt.Lie@hit.no

2 Preprocessing the data

When analyzing controllability we need to know something about the frequencies where the model is valid. An important aspect is the preprocessing of data which is discussed in this section.

The raw data collected from the paper machine has sampling rates of 5 s or 10 s. Those data sets having a sampling rate of 10 s are transformed into 5 s sampling rates by linear interpolation. The data have high frequency disturbances, particularly in the output variables: basis weight and paper ash. These disturbances have higher frequencies than the frequencies of interest, and we low-pass filter all data, prior to model fitting and identification, to put less weight on higher frequencies. All input and output series with 5 s sampling rate are filtered through a second order Butterworth filter

$$v_{\text{filtered}} = \frac{0.0055z^2 + 0.0111z + 0.0055}{z^2 - 1.7786z + 0.8008} v_{\text{raw data}}, \tag{1}$$

which has amplitude and phase characteristics as shown in the Bode diagram of Figure 1. This filter is realized in Matlab using the command

```
%2.order Butterworth filter, with normalized bandwidth equal to 0.05
[num,den]=butter(2,0.05);
```

The normalized bandwidth used here, corresponds to

$$w_f = w_{\text{Normalized}} \cdot w_{\text{Nyquist}} = w_{\text{Normalized}} \cdot \frac{\pi}{T} = 0.05 \cdot \frac{\pi}{5} = 0.0314\,\text{rad}/\,\text{s}\,, \tag{2}$$

where w_f is the filter bandwidth, w_{Nyquist} is the Nyquist frequency (the sampling frequency divided by two), $w_{\text{Normalized}}$ is the normalized filter frequency where $w_{\text{Normalized}} = 1$ corresponds to $w_f = w_{\text{Nyquist}}$.

The filtered data are resampled such that the sampling rate used for the model is $T = 30\,\text{s}$. The resampling is carried out simply by picking every 6'th sample from a data set with 5 s sampling rate. Figure 2 shows raw data versus filtered data for an experiment data set collected February 28, 2001.

3 The process model

The process model is described in detail in e.g. (Hauge & Lie 2002) and only a brief description will be given here.

The model was originally developed with several ordinary and partial differential equations. The model was then simplified, and eventually fitted to experimental and operational mill data. The "final" model consists of a third order nonlinear mechanistic model based on physical and chemical laws, and a first order linear empiric

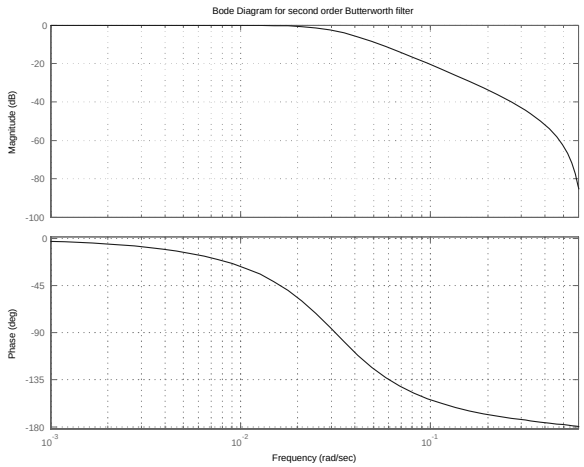

Figure 1: Bode diagram for 2.order Butterworth filter. The cut-off frequency or bandwidth of the filter is 0.0314 rad / s.

model added to the mechanistic model to compensate for neglected and unknown dynamics in the process. The structure of the developed process model is

$$\begin{aligned} \dot{x} &= f(x, u, d, \theta) \\ y &= g(x, u, d, \theta), \end{aligned} \tag{3}$$

with $x \in \mathbb{R}^n = \mathbb{R}^4$, $y \in \mathbb{R}^m = \mathbb{R}^3$, $u \in \mathbb{R}^r = \mathbb{R}^3$ and $d \in \mathbb{R}^d = \mathbb{R}^7$.

The states, manipulated inputs, outputs, and measured disturbances are

$$\begin{aligned} x^T &= [C_{R,fil}, \quad C_{WT,fil}, \quad C_{D,fib}, x_{\text{emp}}] \\ u^T &= [w_{TS}, \quad w_{filler}, \quad w_{\text{ret.aid}}] \\ y^T &= [y_{b.w.}, \quad y_{p.a.}, \quad C_{W,\text{total}}] \\ d^T &= [C_{\text{TS,tot}}, \quad C_{\text{TS,fil}}, \quad S_{\text{1.stage pump}}, \quad v, \quad P, \quad h_{\text{slice}}, \quad f], \end{aligned} \tag{4}$$

where $C_{R,fil}$ is the concentration of filler in a reject tank in the hydrocyclones, $C_{WT,fil}$ is the concentration of filler in the white water tank, $C_{D,fib}$ is the concentration of fiber in the deculator, and x_{emp} is the empiric state added to the mechanistic model to capture neglected and unknown dynamics. The manipulated inputs u are the flow of thick stock, filler, and retention aid. The outputs y are the basis weight, the paper ash content, and the total concentration in the wire tray. The measured disturbances accounted for in the model, are the total and filler thick stock concentrations $C_{\text{TS,tot}}$ and $C_{\text{TS,fil}}$, the speed of a pump between the white water tank and the first stage

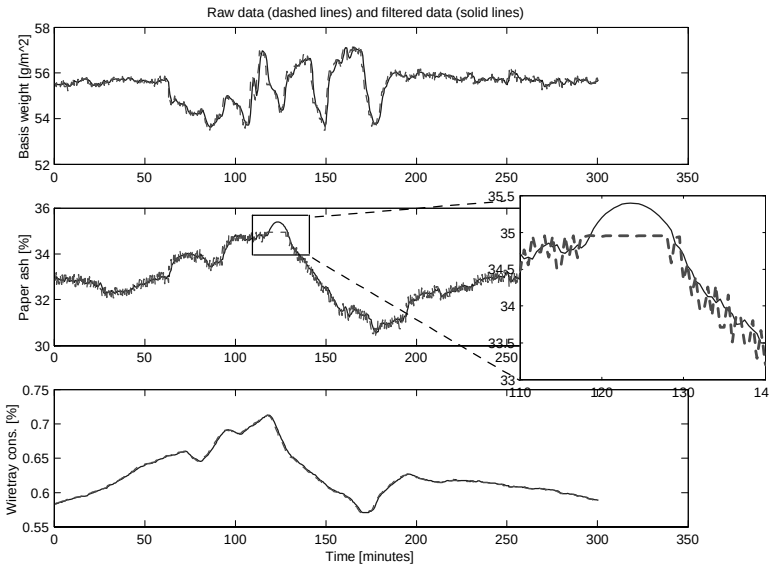

Figure 2: Process outputs during experimentation at February 28, 2001. Raw data, resampled at 30 s sampling rate, are in dashed lines and filtered data, also resampled at 30 s sampling rate, are shown in solid lines. Note the erronous paper ash data near the 125th minute. Cubic interpolation was applied to the data in the erronous region.

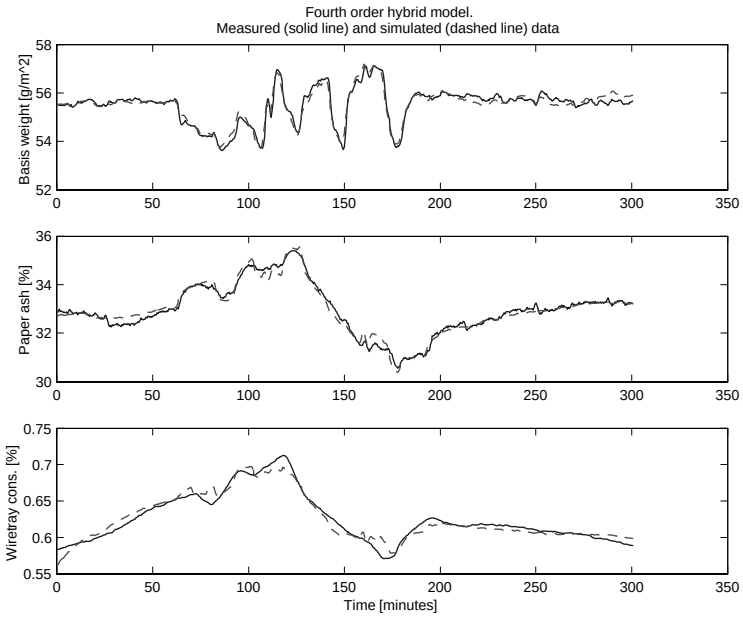

Figure 3: Process model fitted to experimental data.

of the hydrocyclones $S_{1.\text{stage pump}}$, the paper machine velocity v, the pressure inside the headbox P, the mean height of the slice opening h_{slice}, and the paper moisture percentage f.

θ consists of several model parameters, tuned to fit the model outputs to experimental and operational data. In Figure 3, the result from fitting the model to an experimental data set is shown, and Figure 4 shows the validation of the model by comparing simulated model outputs and process measurements during normal operation.

In Figure 5 we have validated the model with a Kalman filter. This Kalman filter is identified from another operational data set, and the filter gain is constant, thus this is a kind of "quasi extended" Kalman filter.

The nonlinear model in Equation 3 is linearized, giving

$$\begin{aligned} x_{k+1} &= Ax_k + Bu_k + Ed_k \\ y_k &= Cx_k + Du_k + Fd_k, \end{aligned} \tag{5}$$

where we for simplicity have used the same variable names as in the nonlinear model[1].

[1] We could e.g. used x^{nonlin} in the nonlinear model, x^o as the operating point, or point of linearization, thus giving the following equation for the linear model variable x^{lin}: $x^{lin} = x^{nonlin} - x^o$.

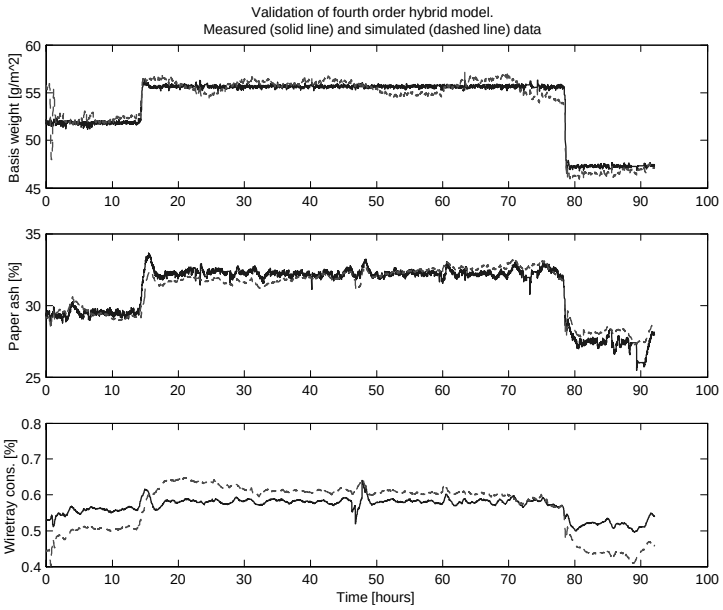

Figure 4: Validation of fourth order process model by simulation. Simulated data are bias corrected.

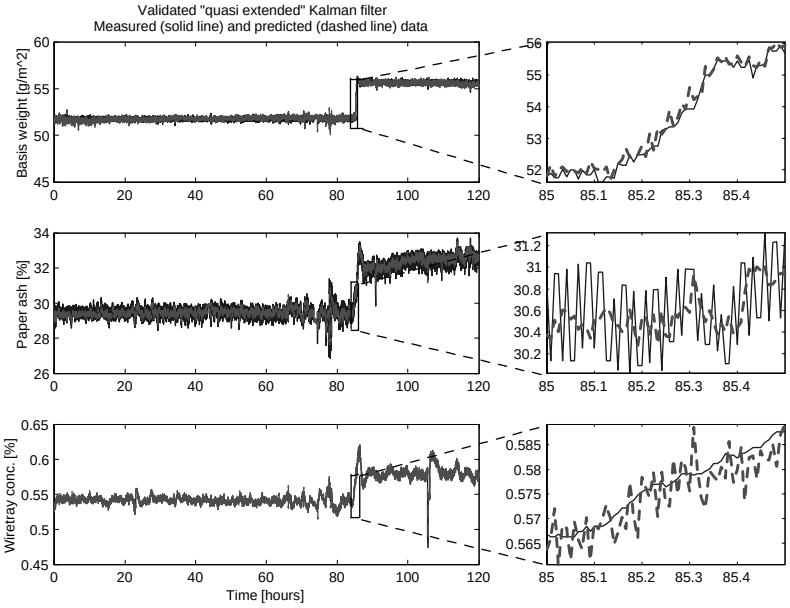

Figure 5: Validation of constant gain Kalman filter. Predictions are bias corrected.

Converting the linear discrete time model to a continuous time model, and then converting to a transfer matrix, we get

$$y(s) = G(s) \cdot u(s) + G_d \cdot d(s), \tag{6}$$

with $G(s) \in \mathbb{R}^{3x3}$ and $G_d(s) \in \mathbb{R}^{3x7}$. In the remainder of this paper we drop the use of the argument s.

4 Controllability

In this section we analyze and discuss the controllability of the paper machine, using techniques for linearized systems. The concept of state controllability will not be discussed, except that we have ascertained that the model is state controllable and observable, and thus a minimal realization. The controllability definition that we will use is one by (Skogestad & Postlethwaite 1996):

Definition 1 *(Input-output) controllability is the ability to achieve acceptable control performance; that is, to keep the outputs (y) within specified bounds or displacements from their references (r), in spite of unknown but bounded variations, such as disturbances (d) and plant changes, using available control inputs (u) and available measurements (y_m, or d_m).*

This concept of controllability is independent of the controller, and is a property of the process alone.

4.1 Model properties

In this subsection we discuss the model properties of the continuous time model, described by the transfer matrix equation 6.

4.1.1 Frequency responses

The frequency responses (magnitudes only) of the elements of G and G_d are shown in Figures 6 and 7. The model is fitted and identified with a direct input to output matrix D, and a direct measured disturbances to output matrix F. The reason for having these "non-physical" direct contributions is that it provided better validation results and model fit. The direct terms are seen on the frequency response plots, giving no roll-off at high frequencies. Some of the responses have their highest gain at higher frequencies, e.g. the response from the third manipulated input. This input is a retention aid, added to help flocculation amongst filler particles and fibers. The step response from this input is shown in Figure 8 and has a clear physical interpretation. The consistency of filler particles and fibers are at a certain level when the step input of retention aid is applied. The flocculation in the pipeline where the retention aid is added, will increase rapidly when the retention aid is increased causing more filler particles and fibers to be retained on the wire, and less to be drained through the

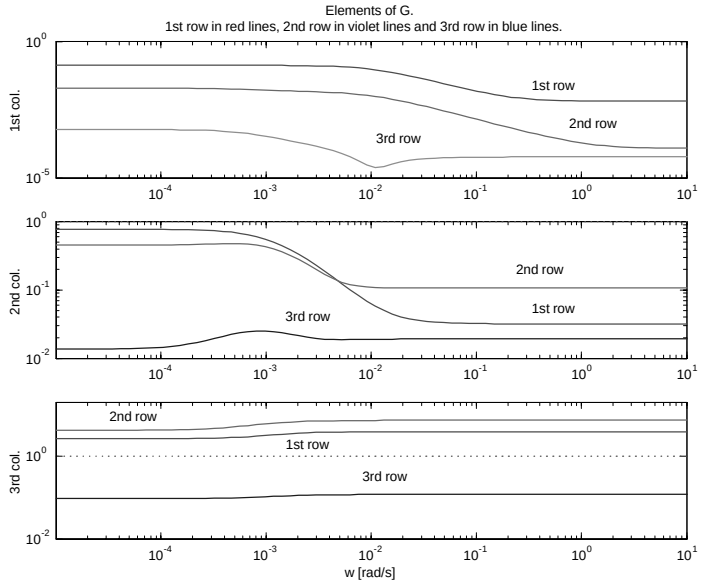

Figure 6: Frequency response of the elements of G. Upper plot is the response from the first column in G, i.e. from the first input to each of the three outputs. The lower plot is the response from the last column in G.

wire. The flow which is drained through the wire is recirculated back into the process and eventually cause a decrease in the consistency in the pipeline where the retention aid is added. This will cause less flocculation, but more flocculation will occur than prior to the step change in input. This means that the magnitude of the frequency response is lower in steady state than at high frequencies.

4.1.2 Poles and zeros

The poles and transmission zeros of the continuos time transfer matrix G (Equation 6) are

$$p = \{-0.0105\ ,\ -0.0038\ ,\ -0.0011\ ,\ -0.0007\}$$
$$z = \{-0.2252\ ,\ -0.0029\ ,\ -0.0013\ ,\ -0.0007\},$$

and we see that G is stable, and has no zeros in the complex right-half plane. G_d has the same poles as G, but has no transmission zeros. Thus, in the absence of right-half plane zeros and poles, we expect no particular controllability problems after studying the poles and transmission zeros.

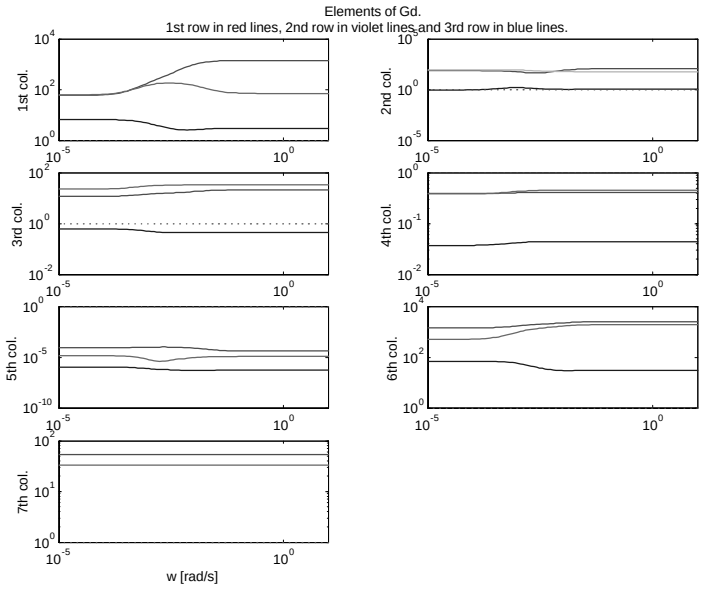

Figure 7: Frequency response of the elements of G_d. Upper left plot is the response from the first column in G_d, i.e. from the first measured disturbance to each of the three outputs.

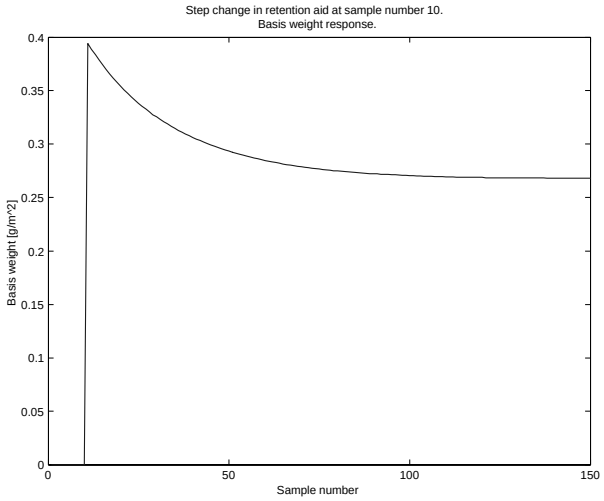

Figure 8: Response in basis weight, after step change in retention aid at the 10'th sample.

4.2 Scaling

To simplify the analysis of controllability with respect to tracking setpoints and suppressing disturbances, we scale the model. The scaling is done so that each input (manipulated input or measured disturbance) is less than one in magnitude, by dividing each variable by its maximum allowed or expected change from its nominal value. Also, the control error, e, and the reference, r, are scaled so that they are allowed to be maximum one in magnitude.

The following scaling matrices are applied

$$\begin{aligned} D_u &= \text{diag}([60\ ,\ 2.4\ ,\ 1.0]) \\ D_d &= \text{diag}([0.006\ ,\ 0.07\ ,\ 0.1\ ,\ 5\ ,\ 0.9 \cdot 10^5\ ,\ 0.0007\ ,\ 0.006]) \\ D_e &= \text{diag}([1.0\ ,\ 1.0\ ,\ 0.05]) \\ D_r &= \text{diag}([10\ ,\ 8\ ,\ 0.15]), \end{aligned} \tag{7}$$

where diag($[\cdot]$) is a diagonal matrix with the elements inside the square brackets on the diagonal. For the manipulated inputs we assume that the maximum allowed changes around the nominal value are ± 60 l / s for the thick stock pump, ± 2.4 l / s for the filler, and ± 1.0 l / s for the retention aid. The measured disturbances are expected to change at maximum ± 0.006 (thick stock total consistency), ± 0.07 (the thick stock filler consistency), ± 0.1 (the first stage pump), ± 5.0 m / s (the paper machine velocity), $\pm 0.9 \cdot 10^5$ Pa (headbox pressure), ± 0.0007 m (slice opening), ± 0.006 % (paper moisture), around the nominal values. The maximum allowed control error

is ± 1.0 g / m^2 for the basis weight, ± 1 % for the paper ash, and ± 0.05 % for the wire tray consistency. The maximum expected reference changes are ± 10 g / m^2 (basis weight), ± 8% (paper ash), and ± 0.15% (wire tray consistency).

In the sequel we denote the scaled transfer matrices by G, and G_d, and the un-scaled original matrices by $\hat{G}$ and $\hat{G}_d$ respectively. The scaled matrices are calculated by

$$G = D_e^{-1}\hat{G}D_u, \;\; G_d = D_e^{-1}\hat{G}_d D_d. \tag{8}$$

Also denote the un-scaled variables by $\hat{e}$, $\hat{y}$, and $\hat{r}$, and we have that

$$\hat{e} = \hat{y} - \hat{r} \implies D_e e = D_e y - D_r r \implies e = y - \underbrace{D_e^{-1} D_r}_{R} r,$$

and the scaled model and variables are

$$y = Gu + G_d d,\; e = y - Rr, \tag{9}$$

where $||u||_\infty \leq 1$, $||d|\,|_\infty \leq 1$, $||e||_\infty \leq 1$, and $||r||_\infty \leq 1$, for the frequencies of interest, and where $||\cdot||_\infty$ is the infinity or max norm (the largest element magnitude in the vector). Thus, the scaling is carried out so that each manipulated input, measured disturbance, control error and reference are less than one in magnitude by dividing each variable by its maximum allowed or expected change from the nominal value.

4.3 Tracking references

In this subsection we discuss the ability to track references, using the scaled continuous time model described by Equation 9

4.3.1 The singular values of the process model

For a given frequency, $G(jw)$ is a constant matrix. The singular value decomposition of $G(jw)$ gives

$$G(jw) = U(jw)S(jw)V^H(jw), \tag{10}$$

where superscript H denotes the conjugate transpose or Hermitian. The matrix $S(jw)$ is diagonal with the singular values in descending order. The largest singular value, $\bar{\sigma}(jw)$, corresponds to the largest gain at frequency w, and the smallest singular value, $\underline{\sigma}(jw)$ corresponds to the smallest gain[2] at frequency w. For a multivariable system, the gain varies with the direction of the input vector, although limited by the largest and smallest singular values. The matrix $U(jw)$ consists of output directions corresponding to the singular values, and $V(jw)$ consists of input directions corresponding to the singular values. Thus, at frequency w, we may find the largest gain as the first singular value, the input direction which gives the largest gain is the first column vector in $V(jw)$, and the output direction as the first column vector in $U(jw)$. Similarly we can find the input and output directions associated with the smallest gain.

[2] This is not true for a system with more inputs than outputs. In this case there will be input directions which will have no affect on the outputs, thus the smallest gain is always zero.

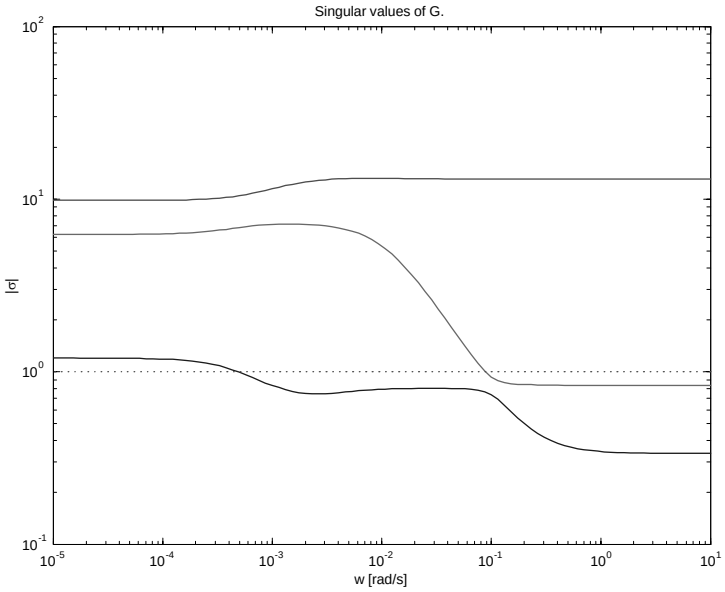

Figure 9: The singular values of G as a function of frequency.

Figure 9 shows the singular values as function of frequency. When the smallest singular value is less than 1, from $6 \cdot 10^{-4}$ rad / s to ∞ rad / s, this means that for some input directions of unit magnitude, the outputs will have less magnitude than one. In general we wish to have the smallest singular value as large as possible, especially within the desired bandwidth of the closed loop system. The singular values are very dependent on the scaling of the model, e.g. if we increase the scaling value for the filler input from 2.4 l / s to 3.4 l / s, then the smallest singular value is larger than one up till 0.1 rad / s. The reason for using 2.4 l / s in the scaling is that this is the operating point where the linear model is derived. Thus increasing the scaling above 2.4 l / s means that we allow a negative flow of filler. However, the physical limits for the filler flow is not symmetric about the operating point, so we may add more filler than the upper scaling limit (which is $2.4 + 2.4 = 4.8$ l / s).

4.3.2 Input saturation

We wish to study if, and at what frequencies, we can obtain perfect reference tracking. Perfect tracking, neglecting the measured disturbances, gives the input

$$\begin{aligned} e &= y - Rr \\ &\Downarrow \\ 0 &= Gu - Rr \\ &\Downarrow \\ u &= G^{\dagger}Rr, \end{aligned} \tag{11}$$

where $G^{\dagger} = G^H(GG^H)^{-1}$ is the pseudo-inverse. Figure 10 shows the frequency response of the elements of $G^{\dagger}R$ (magnitudes only). At frequencies were the magnitude exceeds one, we cannot achieve perfect tracking because $||u||_{\infty} = \left||G^{\dagger}Rr|\right|_{\infty} \leq 1$ is not satisfied for all $||r||_{\infty} \leq 1$. Note that we here study the references one by one, and not by means of e.g. a worst case scenario for all involved references.

The first column of $G^{\dagger}R$ corresponds to tracking the basis weight setpoint. In Figure 10 we see that none of the inputs saturate in steady state, however the element in the first row exceeds one in magnitude at a too low frequency. In the second and third columns of $G^{\dagger}R$ wee see that the elements in the second row are above one at all frequencies. Thus, we expect that the filler valve will saturate when operating in the outer regions of the paper ash and wire tray consistency setpoints.

The notion of a plant that can not be perfectly controlled, is even more clear if we study a combined reference change, limited by $||r(jw)||_2 \leq 1$, and $||u(jw)||_2 \leq 1$. The maximum expected reference change is ± 1 for each reference, and the maximum allowed input change is ± 1 for each input, however the limitations introduced here simplifies the calculation and is convenient for illustrating our main point: that the measured disturbances must be monitored, adjusted and related to the reference values. Using Equation 11 and the above limitation for u, we can write

$$\begin{aligned} ||u||_2 &= \left||G^{\dagger}Rr|\right|_2 \leq 1 \\ &\Downarrow \\ ||u||_2 &= \left||G^{\dagger}R|\right|_{i2} \cdot ||r||_2 \leq 1, \end{aligned} \tag{12}$$

where $||\cdot||_{i2}$ is the induced 2-norm, or the largest singular value. For $||r||_2 = 1$ we have that

$$\bar{\sigma}(G^{\dagger}R) \leq 1, \tag{13}$$

for perfect reference tracking, without input saturation. Figure 11 shows the singular values of $G^{\dagger}R$ plotted as function of frequency, and it is clear that perfect tracking is not obtained at any frequency with large combined reference changes.

Some comments on these results are necessary. First, for higher frequencies we will not expect nor want perfect tracking in most cases (large and rapid actuator movements). Based on knowledge of the process, it is expected that the bandwidth

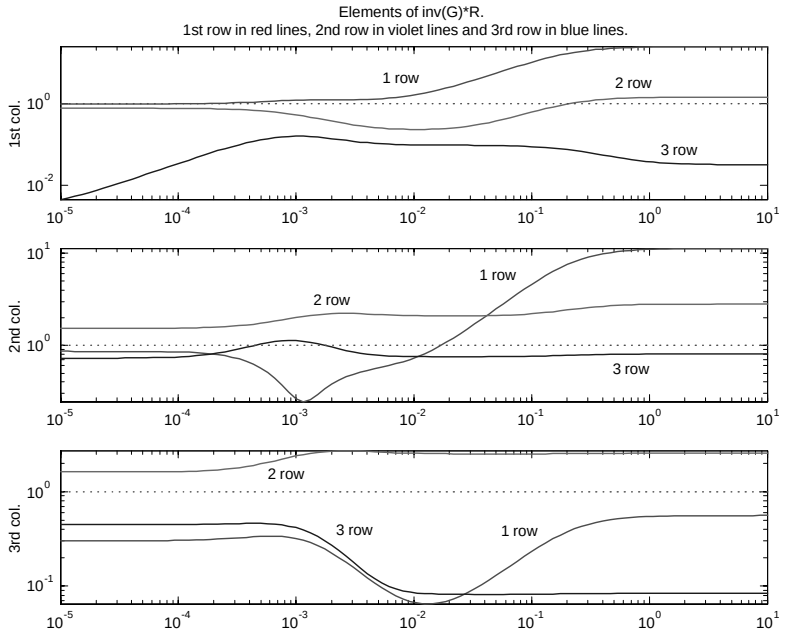

Figure 10: Magnitudes of the frequency response of the elements of $G^{\dagger}R$.

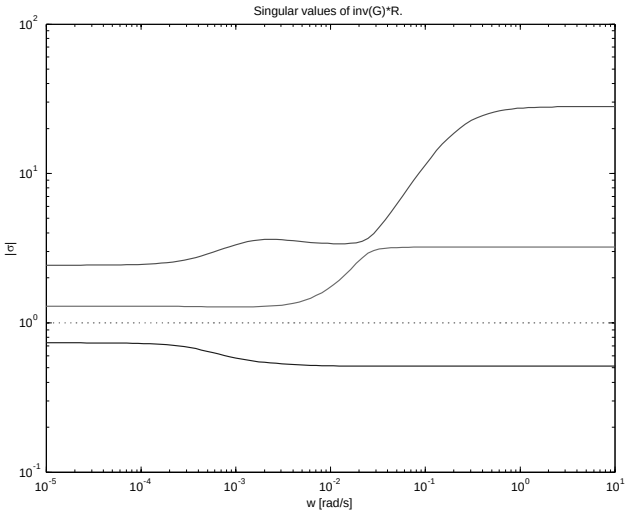

Figure 11: Singular values of $G^{\dagger}R$, as a function of frequency.

of the closed loop system should be around 0.01 - 0.1 rad/s. Second, for lower frequencies, at least for steady state conditions, one would normally expect to obtain perfect control. However, knowing that we neglected the measured disturbances in this particular analysis, we probably have a good explanation of the result in Figure 4. The conditions were the linearization was carried out was e.g. 50 g/m2 basis weight, 30% paper ash, 4% thick stock total consistency, and 1.48% thick stock filler consistency. The scaling of the model is carried out so that the entire product range of PM6 is reflected, e.g. the paper ash content can be as low as 20%. Given that the filler content in the thick stock is approximately 37%, as is the case here, the manipulated inputs would most certainly saturate trying to reach a paper ash level of 20%.

The comments above are supported by the fact that there are no known input saturation problems at PM6 today, however the process operators carefully adjusts e.g. thick stock consistencies to match the specifications on the finished paper. This analysis shows that without these adjustments from the process operators, off-spec paper would be produced. This would be the case independent of the controller which is used.

4.4 Rejecting disturbances

The model is scaled so that each disturbance should be less than one (absolute value), and we have also scaled the model with the allowed output error $(r-y)$. The frequency response of G_d will then show whether we need control or not, by studying the gain

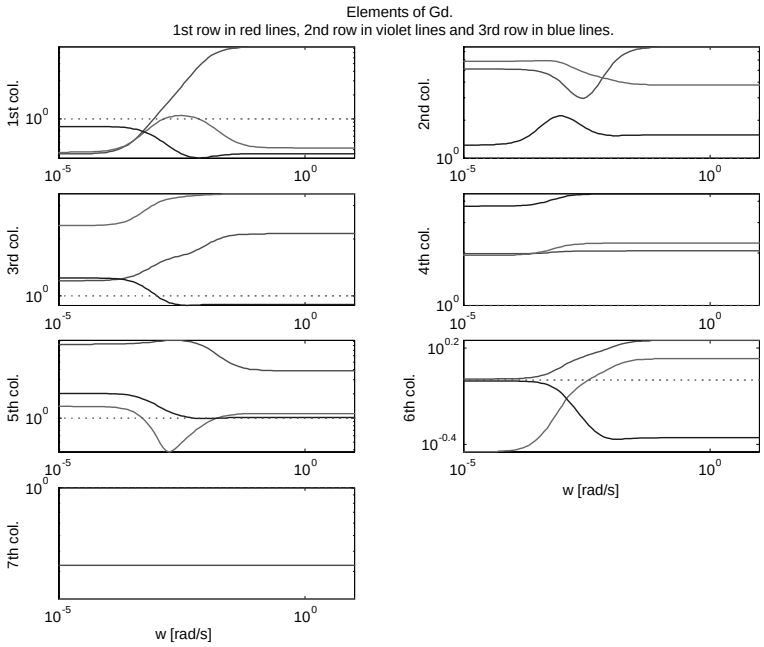

Figure 12: Magnitude of the frequency response of the elements of G_d.

from each disturbance to each output. At frequencies where the gain is larger than one, we need control. From Figure 12 we see that for most of the disturbances we need control, while the paper moisture disturbance, described by the seventh column in G_d, we do not need control in order to stay within the allowed control errors. We also see that for many of the disturbances we need control at high frequencies, however it is beyond the scope of most control loops to reject disturbances at very high frequencies.

4.4.1 Input saturation

Perhaps more interesting is the question of whether we can reject disturbances, while still maintaining acceptable manipulated inputs. Let us look at the possibility of achieving perfect control. That is, given some disturbance, can we keep $||e||_{\max} = 0$, and still maintain $||u||_{\max} \leq 1$? For simplicity, and without loss of generality, we set

$r = 0$

$$\begin{aligned} r - y &= r - Gu - G_d d \\ &\Downarrow \\ 0 &= Gu + G_d d \\ &\Downarrow \\ u &= -G^{\dagger} G_d d, \end{aligned}$$

and this is the input required for perfect control.

Figure 13 shows the frequency response of the elements of $G^{\dagger}G_d$ (magnitudes only). From this figure we see which disturbances can be controlled perfectly at which frequencies. Note that here we study the disturbances one by one, and not by means of e.g. a worst case scenario for all involved disturbances. For example in the upper left figure are the responses of the first column of $G^{\dagger}G_d$, corresponding to the first disturbance which is the thick stock total consistency. At low frequencies we see that the magnitudes are below one, which means that the outputs can be controlled perfectly even for a worst case disturbance in the thick stock total consistency (assuming other disturbances are zero). At higher frequencies the magnitude of the basis weight response (first row) crosses the saturation line (dashed line at magnitude equal to one), and at even higher frequencies the paper ash also exceeds one in magnitude. At frequencies were the magnitude exceeds one, we cannot achieve perfect control because $||u||_{\infty} = \left|\left|G^{\dagger}G_d d\right|\right|_{\infty} \leq 1$ is not satisfied for all $||d||_{\infty} \leq 1$.

In Figure 13 we do not worry very much about the higher frequencies, as we would not expect to achieve perfect control here any way. What is interesting is those cases where we have magnitudes larger than one, at lower frequencies. These are in particular the responses in the second column and second row, the fourth column and the second row, and the fifth column and the second row (referring to columns and rows in $G^{\dagger}G_d$). Consider e.g. the thick stock filler consistency (the second disturbance) and the inability to achieve perfect control of the paper ash even in steady state, as can be seen in the upper right corner in Figure 13. The paper ash originates from filler in the thick stock and filler added in the short circulation (the second manipulated input). The process operators make sure that when a high percentage of paper ash is required, then a high percentage of filler in the thick stock is present. Similarly, when a low paper ash percentage is required, then a lower percentage of filler is present in the thick stock. Thus, it is our opinion that the inability to achieve perfect control in steady state is a problem that is solved by the process operators. What can be learned here, is that in order to track the setpoints, also at low frequencies, it is necessary to either manually or automatically be able to influence some of the measured disturbances. As of today the process operators carefully adjust e.g. the thick stock composition to match the specifications on the finished paper, and without these adjustments off-spec paper would be produced as shown in Figure 13.

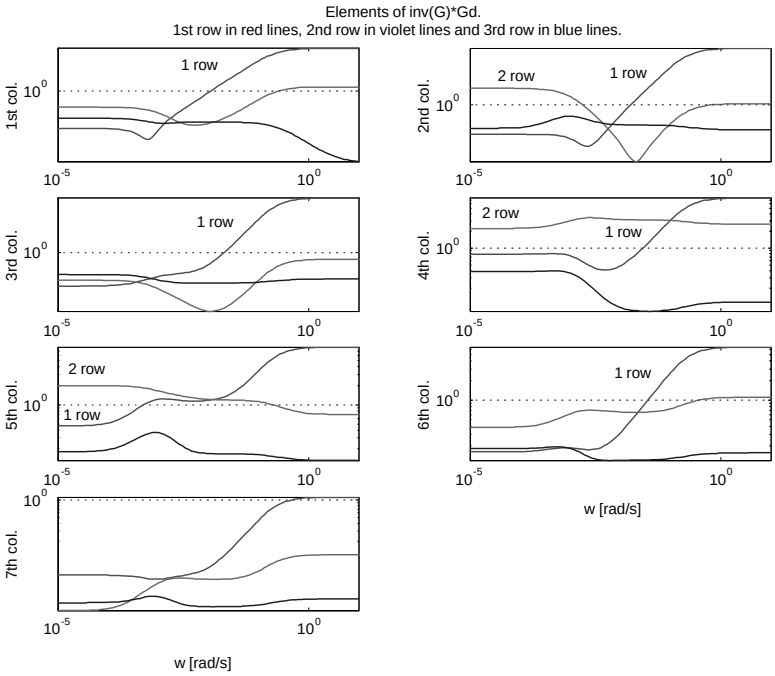

Figure 13: Magnitudes of the frequency response of the elements of $G^{\dagger}G_d$.

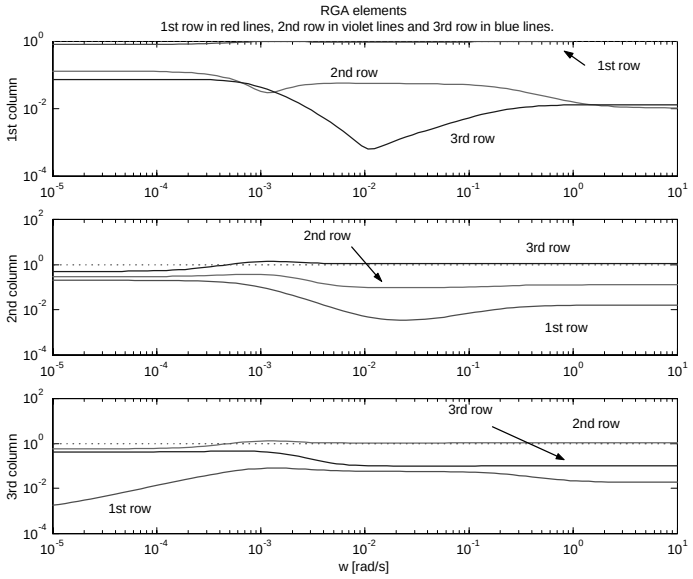

Figure 14: Frequency response of the RGA elements (only magnitudes), $\Lambda(G)$.

4.5 Sensitivity to uncertainty

4.5.1 Relative Gain Array (RGA)

The RGA is perhaps best known as a way to choose pairing between inputs and outputs for decentralized control. However, it also has an important application as an indicator of sensitivity to uncertainty (Skogestad & Postlethwaite 1996). The RGA is defined as

$$\Lambda(G) = G \times \left(G^{\dagger}\right)^{T}, \tag{14}$$

where $\times$ is the Hadamard product (an element by element multiplication). Figure 14 shows the frequency responses (only magnitudes) of the elements of the RGA matrix. Processes with large RGA elements (e.g. magnitude above 10) are fundamentally difficult to control due to sensitivity to input uncertainty (Skogestad & Postlethwaite 1996). Based on the frequency responses of Figure 14, there is no indication of such problems for the paper machine process.

It is interesting to note that the present choice of input-output pairing for decentralized control in the industry is not the choice that would be made based on the RGA frequency response. The rules of thumb for pairing are often given as: Choose pairing so that the corresponding RGA elements

1. in steady state, $\Lambda(G(0))$, are positive and as close to 1 as possible (Skogestad & Postlethwaite 1996).

2. near the desired bandwidth of the closed loop system, $\Lambda(G(w_b))$, are as close to 1 as possible (Skogestad & Postlethwaite 1996) (Seborg, Edgar & Mellichamp 1989).

In Figure 14 we see in the upper figure that we would choose to pair the thick stock pump (input 1) with the basis weight (output 1). This corresponds to the choice made in the industry. However, for the filler valve input (figure in the middle) we would choose to pair it with the wire tray consistency (output 3), and finally for the retention aid input (lower figure) we would choose to pair it with the paper ash (output 2). These last two pairings are not in correspondence with the industrial choice, as known by the authors of this paper.

4.5.2 Condition number

The condition number of the process is defined as

$$\gamma(G) = \frac{\bar{\sigma}(G)}{\underline{\sigma}(G)}, \tag{15}$$

and is an indicator of sensitivity to both diagonal and full-block input uncertainty (Skogestad & Postlethwaite 1996). A small condition number indicates robustness to the uncertainty. Figure 15 shows the condition number as a function of frequency. A rule of thumb states that a condition number larger than 10 may indicate sensitivity to uncertainty. In our case we do not expect very much sensitivity at lower frequencies, however at frequencies ranging from 10^{-3} to 10^{-1} rad / s there may be a problem with sensitivity to input uncertainty.

5 APIS (Advanced Process Improvement System)

APIS consists of a number of software components for process control, process data logging and presentation of process information on web pages, e.g. Apis MPC and Apis SoftSensor (a Kalman filter). Apis is a product of Prediktor AS (Norway) and more information is available at the company homepage at www.prediktor.no.

5.1 The "standard" APIS Model Predictive Controller (MPC)

The Apis MPC is based on an algorithm presented in (Muske & Rawlings 1993), although there are some modifications and extensions based on experience from MPC in industrial applications. The model is a linear state space model similar to Equation 5, with the following infinite horizon quadratic objective function

$$J_k = \sum_{j=0}^{\infty} \left[(y_{k+j} - y_s)^T Q (y_{k+j} - y_s) + (u_{k+j} - u_s)^T R (u_{k+j} - u_s) + \Delta u_{k+j}^T S \Delta u_{k+j} \right], \tag{16}$$

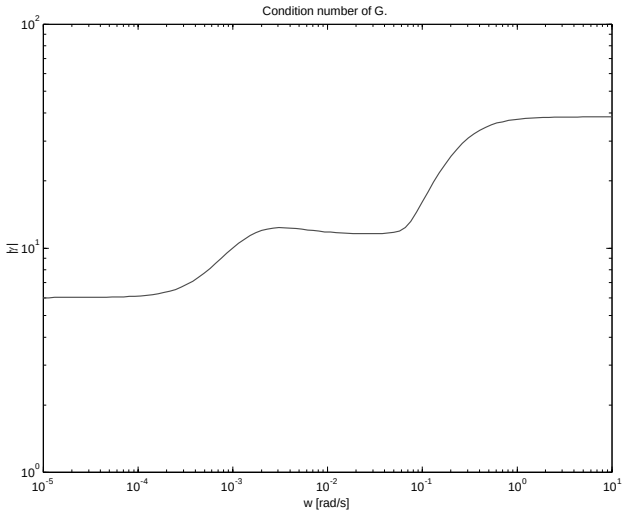

Figure 15: Condition number of G.

where $\Delta u_{k+j} = u_{k+j} - u_{k+j-1}$, y_s and u_s are target vectors for the inputs and outputs, Q and R are positive definite penalty matrices, and S is a positive semidefinite penalty matrix.

The MPC is based on minimization of the criterion subject to specified constraints. The model in Equation 5 gives a set of equality constraints, while the inequality constraints are

$$\begin{aligned} u_{\min} \leq u_{k+j} \leq u_{\max}, \;\; j = 0, 1, 2, ..., N-1 \\ y_{\min} \leq y_{k+j} \leq y_{\max}, \;\; j = j_1, j_1+1, ..., j_2 \\ \Delta u_{\min} \leq \Delta u_{k+j} \leq \Delta u_{\max}, \;\; j = 0, 1, 2, ..., N, \end{aligned} \tag{17}$$

where N is the horizon after which no control moves are allowed, and $[k+j_1, k+j_2]$ are the time interval where the output constraints are applied. The criterion is of infinite horizon, and this guarantees stability. Through the use of a Lyapunov equation the criterion can be reformulated as a finite horizon criterion which can be implemented.

5.2 A modified MPC for APIS

The APIS MPC described in the previous section can not handle nonlinear models or future setpoint changes. A modified MPC which handles these issues, is therefore currently being developed and implemented. The nonlinear model is linearized at each sample and used in the MPC.

At time k, suppose a reference vector and a measured disturbance vector for time $k, k+1, ..., k+N-1$ is given. These vectors may be provided by the process operators or simply taken as an expansion of the present values into the future. Using the linearized model at time k (as given by Equation 5) we calculate feasible target values at each sample up till $k+N-1$. The model of Equation 5, is then shifted, so that the origin of the model is the target value at time $k+N-1$. The shifted values are denoted by a bar (e.g. $\bar{x}$) in the remainder of this paper.

Assuming no control moves beyond sample $k+N-1$, and no change in target values beyond sample $k+N-1$, we can reformulate the infinite horizon criterion to the following finite horizon criterion

$$\begin{aligned} J_k = {} & \bar{x}_{k+N}^T \bar{Q}_k \bar{x}_{k+N} - 2\bar{u}_{k-1}^T S \bar{u}_k - \sum_{j=1}^{N-1} \left[2\bar{u}_{k+j}^T S \bar{u}_{k+j-1} \right] \\ & + \sum_{j=0}^{N-1} \left[\bar{y}_{k+j}^T Q \bar{y}_{k+j} - 2\left(\bar{y}_{k+j}^s\right)^T Q \bar{y}_{k+j} + \bar{u}_{k+j}^T \left(R+2S\right) \bar{u}_{k+j} - 2\left(\bar{u}_{k+j}^s\right)^T R \bar{u}_{k+j} \right] \\ & + \text{constant}\,. \end{aligned} \tag{18}$$

where $\bar{Q}$ is the solution of a Lyapunov equation, and the vector of unknowns is

$$z^T = \left[\bar{u}_k^T, \bar{u}_{k+1}^T, ..., \bar{u}_{k+N-1}^T, \bar{x}_{k+1}^T, \bar{x}_{k+2}^T, ..., \bar{x}_{k+N}^T, \bar{y}_k^T, \bar{y}_{k+1}^T, ..., \bar{y}_{k+N-1}^T \right], \tag{19}$$

The constraints are given by Equations 5 and 17. It is possible to reduce the number of unknowns in the z vector by inserting the model equations in the criterion. However, the formulation given here gives very sparse matrices, and sparse solvers quickly solve the optimization problem. Which method is more efficient is not studied in this paper.

6 A simulation result

For the process operators at PM6, the MPC will include some options not available previously. These include making future reference changes, control during sheet breaks and control during start up. The inclusion of the non-linear model in the controller makes it possible to rely on the model output when measurements are not available such as during start up and sheet breaks. The possibility of making future reference changes means that the controller can prepare the inputs and states for the forthcoming change, and calculate an optimal grade change. In Figure 16 the simulated outputs are shown, when the change in reference values is submitted to the MPC 50 minutes before the actual grade change.

For the simulation in Figure 16, control deviation caused by the basis weight is penalized hard, while the control deviation caused by the wire tray consistency is penalized relatively mild. Both the control increment (Δu) and the control deviation from the steady state value is penalized in the criterion. The control increment is

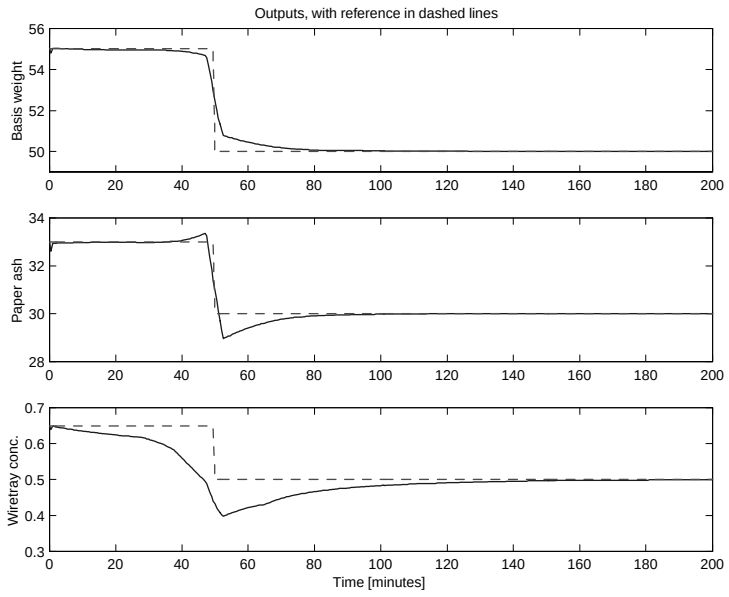

Figure 16: Model outputs and reference values (in dashed lines). The change in reference value at $t = 50$ minutes was submitted to the MPC at $t = 0$ minutes.

constrained by ± 2 liters per sample (the sampling time is 30 seconds) for the thick stock, ± 0.25 liters per sample for filler, and ± 0.05 liters per sample for the retention aid.

7 Conclusions

In this paper we gave a preliminary analysis of a developed paper machine model and its use in an MPC application. The process is non-linear and the analysis is carried out on a linearized model.

There are no strong indications of expected control problems, although the process to some extent may be sensitive to uncertainty. Input saturation may occur for large changes in disturbances and references. However, this can probably be compensated for by the process operators acting on measured disturbances (as is done today at PM6). A simulation result with a modified commercially available MPC algorithm is shown. The modifications include e.g. allowing future setpoint changes.

Acknowledgements The authors would like to thank the employees at PM6 for their cooperation in providing information and data for this paper, and for their general helpfulness. Steinar Sælid and Anders Veberg from Prediktor AS is acknowledged for information about APIS and APIS MPC. The work of Tor Anders Hauge is financially supported by the Research Council of Norway (project number 134557/432), with additional financial support by Norske Skog Saugbrugs.

References

Hauge, T. A., Ergon, R., Forsland, G. O., Slora, R. & Lie, B. (2000), Modeling, Simulation and Control of Paper Machine Quality Variables at Norske Skog Saugbrugs, Norway, *in* 'Scientific and Technological Advances in the Measurement and Control of Papermaking', Pira International.

Hauge, T. A. & Lie, B. (2002), 'Paper machine modeling at Norske Skog Saugbrugs: A mechanistic approach', *Modeling, Identification and Control* **23**(1), 27–52.

Muske, K. R. & Rawlings, J. B. (1993), 'Model predictive control with linear models', *AIChE Journal* **39**(2), 262–287.

Seborg, D. E., Edgar, T. F. & Mellichamp, D. A. (1989), *Process Dynamics and Control*, John Wiley & Sons, Inc.

Skogestad, S. & Postlethwaite, I. (1996), *Multivariable Feedback Control: Analysis and Design*, John Wiley & Sons Ltd.

Paper E

A Comparison of Implementation Strategies for MPC

Lie, B., Dueñas Díez, M., and Hauge, T. A. (2002). *A Comparison of Implementation Strategies for MPC*, in Proceedings of International Symposium on Advanced Control of Industrial Processes, June 10-11, 2002, Kumamoto, Japan.

A few corrections are made to the original paper.

A Comparison of Implementation Strategies for MPC

Bernt Lie*, Marta Dueñas Díez, and Tor Anders Hauge
Telemark University College, P.O. Box 203, N-3901 Porsgrunn, Norway

Abstract

Four quadratic programming (QP) formulations of model predictive control (MPC) are compared with regards to ease of formulation, memory requirement, and numerical properties. The comparison is based on two example processes: a paper machine model, and a model of the Tennessee Eastman challenge process; the number of free variables range from 150 – 1400. Five commercial QP solvers are compared. Preliminary results indicate that dense solvers still are the most efficient, but sparse solvers hold great promise.

Keywords: Model predictive control; Quadratic programming; Problem formulation; Analysis of formulation; Comparison of QP solvers

1 Introduction

Model based predictive control (MPC) is the repeated use of optimal control over a given horizon; many introductory books dealing with MPC exist, e.g. Maciejowski (2002), Camacho and Bordons (1999), and Seborg *et al.* (1989). Most of the work on MPC has been centered on the use of linear models and quadratic performance indices. Common model types are impulse and step response models, ARMAX/CARIMA models, and state space models. In many cases, such models are input-output equivalent, and the choice of model is less important for the resulting value of the control input.

The performance index typically puts quadratic weights on the control deviation, the control variable, and/or quadratic weight on the control increment. In practice, control inputs will be constrained to lie within lower and upper bounds, while it is also of interest to introduce constraints on response variables, e.g. that the outputs are constrained to lie in a given region, etc. The most common MPC formulations are thus posed as quadratic programming (QP) problems.

The development of the MPC algorithms typically include relatively lengthy formula manipulations in order to end up with a QP problem with future control inputs

*Corresponding author: Bernt.Lie@hit.no

as the unknowns. An alternative approach is to keep variables such as states, outputs, control deviations, etc. as unknowns, and include the model and various definitions as linear equality constraints in the QP problem.

In this paper, we compare various formulations of the QP problem. In section 2, we formulate a standard MPC problem using state space models, and pose it as QP problems with a complete set of variables, with an intermediate set of variables, and with the basic future control inputs as variables (the common formulation). In section 3, we analyze the various formulations via two case studies. In section 4, we compare the computation time for various optimization algorithms and various QP formulations. In section 5, we draw some conclusions.

2 The MPC problem

We consider the state space model

$$x_{k+1} = Ax_k + Bu_k \tag{1a}$$
$$y_k = Cx_k + Du_k, \tag{1b}$$

where $u_k \in \mathbb{R}^{m\times 1}$ is the control input, $y_k \in \mathbb{R}^{r\times 1}$ is the controlled output, $x_k \in \mathbb{R}^{n\times 1}$ is the state, and the performance index J_k is:

$$J_k = \sum_{i=0}^{\infty} \left(e_{k+i}^T Q e_{k+i} + u_{k+i}^T R u_{k+i} + \Delta u_{k+i}^T S \Delta u_{k+i} \right).$$

Here, the output error e_k is

$$e_k = y_k - s_k, \tag{2}$$

where s_k is the set point, and the control increment Δu_k is

$$\Delta u_k = u_{ki} - u_{k-1}. \tag{3}$$

For open loop stable systems and some mild additional conditions, we can transform the infinite performance index into the following finite horizon index, see e.g. Muske and Rawlings (1993):

$$\begin{aligned} J_k = {} & x_{k+N}^T \bar{Q} x_{k+N} + u_{k+N-1}^T S u_{k+N-1} \\ & + \sum_{i=0}^{N-1} \left(e_{k+i}^T Q e_{k+i} + u_{k+i}^T R u_{k+i} \right. \\ & \left. + \Delta u_{k+i}^T S \Delta u_{k+i} \right), \end{aligned} \tag{4}$$

where $\bar{Q}$ is found by solving the discrete Lyapunov equation:

$$\bar{Q} = C^T Q C + A^T \bar{Q} A. \tag{5}$$

With x_k known, denote the optimal input sequence by $u_{k+i|k}$, $i \in \{0, \ldots, N-1\}$. By repeatedly solving the optimal control problem for each time index k, letting the control input be $u_k = u_{k|k}$ leads to a nominally stable closed loop system, Rawlings and Muske (1993).

One of the main advantages of MPC is the direct handling of constraints in the calculation of the control input. This feature is importanct, since all processes are subject to constraints. Actuators have a limited range of action

$$u^\ell \leq u \leq u^u \tag{6}$$

and a limited control increment

$$\Delta u^\ell \leq \Delta u_k \leq \Delta u^u. \tag{7}$$

Ouput constraints are mainly introduced for safety and quality reasons. Such constraints also arise when the exact values of some output variables y are less important as long as they remain within specified boundaries or "zones". These constraints can be expressed as

$$y^\ell \leq y \leq y^u. \tag{8}$$

Other types of inequality constraints are viable, such as funnels and constraints on states. These extensions are in principle straightforward, and here we limit the discussion to the constraints discussed above.

3 The MPC problem formulated as QP problems

3.1 Standard QP problem

The general MPC formulation outlined above can be posed as a quadratic programming (QP) problem of the form

$$\begin{aligned} \min_z \quad & F(z) = \frac{1}{2} z^T H z + g^T z + k \\ \text{s.t.} \quad & \mathcal{A} z = a \\ & \mathcal{B} z \leq b \\ & z^\ell \leq z \leq z^u. \end{aligned} \tag{9}$$

where the value of k does not change the optimal solution z, and hence is not discussed further. If inequality constraints are passive, the solution can be found by solving the linear equation $\mathcal{L}\upsilon = \nu$ where

$$\mathcal{L} = \begin{pmatrix} H & \mathcal{A}^T \\ \mathcal{A} & 0 \end{pmatrix}, \quad \upsilon = \begin{pmatrix} z \\ \lambda \end{pmatrix}, \quad \nu = \begin{pmatrix} -g \\ a \end{pmatrix}, \tag{10}$$

and λ is the Lagrange multiplier.

Table 1: Notation used in MPC formulation.

Notation	Matlab form
$I_n \in \mathbb{R}^{n\times n}$	`eye(n)`
$I_{n,k} = \mathrm{diag}\left(1_{n-\lvert k\rvert\times 1}, k\right)$	`diag(ones(n-abs(k),1),k)`
$0_{m\times n} \in \mathbb{R}^{m\times n}$	`zeros(m,n)`
$1_{m\times n} \in \mathbb{R}^{m\times n}$	`ones(m,n)`
$A \in \mathbb{R}^{m\times n}: \begin{matrix}\dim_1 A = m \\ \dim_2 A = n\end{matrix}$	`[m,n] = dim(A)`
$A \otimes B$	`kron(A,B)`
$\mathrm{diag}\left(A_1, \ldots, A_n\right)$	— (block diagonal)
$\mathrm{rot}_{90}\, I_N$	`rot(eye(N),1)`

3.2 Complete set of variables

Although not the most common formulation, we first define the vector of unknowns z as:

$$\begin{aligned} z^T = \big(& u_k^T \quad \ldots \quad u_{k+N-1}^T \quad x_{k+1}^T \quad \ldots \quad x_{k+N}^T \\ & y_k^T \quad \ldots \quad y_{k+N-1}^T \quad e_k^T \quad \ldots \quad e_{k+N-1}^T \\ & \Delta u_k^T \quad \ldots \quad \Delta u_{k+N-1}^T \ \big) \end{aligned} \tag{11}$$

Matrix H and vector g of eq. 9 are determined from the requirement that J_k of eq. 4 should equal $F\left(z\right)$ in eq. 9. The constraints $\mathcal{A}z = a$ contain the dynamic model in eq. 1 and the definitions in eqs. 2 – 3. For the MPC problem defined here, inequality $\mathcal{B}z \leq b$ is empty, while physical, safety, and quality constraints of Section 2 is contained in z^ℓ and z^u.

In formulating the matrices, the notation of Table 1 is used. The following matrices result:

$$\begin{aligned} H = \mathrm{diag}\big(& 2\left(I_{N-1} \otimes R\right), 2\left(R+S\right), \\ & 0_{(N-1)\dim_1 \bar{Q}\times(N-1)\cdot\dim_2 \bar{Q}}, \\ & 0_{\dim_1 Q\times N\cdot\dim y}, 2\bar{Q}, 0_{N\dim y\times N\cdot\dim y}, \\ & 2\left(I_N \otimes Q\right), 2\left(I_N \otimes S\right)\big) \end{aligned} \tag{12}$$

$$g = 0_{N\cdot(2m+n+2r)x1} \tag{13}$$

$$\mathcal{A} = \begin{pmatrix} -\left(I_N \otimes B\right) & \mathcal{A}_{12} & 0 & 0 & 0 \\ -\left(I_N \otimes D\right) & \mathcal{A}_{22} & I_{N\cdot r} & 0 & 0 \\ 0 & 0 & I_{N\cdot r} & -I_{N\cdot r} & 0 \\ \mathcal{A}_{41} & 0 & 0 & 0 & I_{N\cdot m} \end{pmatrix} \tag{14}$$

where matrices $\mathcal{A}_{ij}$ are defined in Table 2.

Table 2: Matrices for complete variable set QP-formulation.

$$\underline{\mathcal{A}_{12} = I_{N\cdot n} - I_{N,-1} \otimes A}$$
$$\mathcal{A}_{22} = -I_{N,-1} \otimes C$$
$$\underline{\mathcal{A}_{41} = -I_{N\cdot m} + I_{N,-1} \otimes I_m}$$

$$a = \left(\begin{pmatrix} Ax_k \\ 0_{(N-1)\cdot n\times 1} \end{pmatrix}^T, \begin{pmatrix} Cx_k \\ 0_{(N-1)\cdot r\times 1} \end{pmatrix}^T, \right. \tag{15}$$
$$\left. \mathbf{s}^T, \begin{pmatrix} -u_{k-1} \\ 0_{(N-1)m\times 1} \end{pmatrix}^T \right)$$

$$z^\ell = \begin{pmatrix} 1_{N\times 1} \otimes u^\ell \\ -\infty \cdot 1^T_{N\cdot n\times 1} \\ 1_{N\times 1} \otimes y^\ell \\ -\infty \cdot 1^T_{N\cdot r\times 1} \\ 1_{N\times 1} \otimes \Delta u^\ell \end{pmatrix}, \quad z^u = \begin{pmatrix} 1_{N\times 1} \otimes u^u \\ \infty \cdot 1^T_{N\cdot n\times 1} \\ 1_{N\times 1} \otimes y^u \\ \infty \cdot 1^T_{N\cdot r\times 1} \\ 1_{N\times 1} \otimes \Delta u^u \end{pmatrix} \tag{16}$$

The dimensions of the complete variable set QP problem are given by $\dim z = N \cdot (n + 2m + 2r) \times 1$ and $\dim a = N \cdot (n + m + 2r) \times 1$. Typically, the definition of z as in eq. 11 leads to sparse matrices H and $\mathcal{A}$.

3.3 Intermediate set of variables

From the full QP formulation, we eliminate e_k, Δu_k, and y_k. The resulting vector of unknowns is:

$$z^T = \begin{pmatrix} u_k^T & \dots & u_{k+N-1}^T & x_{k+1}^T & \dots & x_{k+N}^T \end{pmatrix}. \tag{17}$$

The matrices and vectors in the QP formulation are

$$H = 2 \begin{pmatrix} H_{11} & H_{12} \\ H_{21} & H_{22} \end{pmatrix}, \tag{18}$$

$$g = \begin{pmatrix} 2\left(x_k^T C^T Q D - u_{k-1}^T S\right)^T \\ 0_{(N-1)m+Nn\times 1} \end{pmatrix} \tag{19}$$

$$\mathcal{A} = \begin{pmatrix} -I_N \otimes B & I_{N\cdot n} - I_{N,-1} \otimes A \end{pmatrix} \tag{20}$$

$$a = \begin{pmatrix} Ax_k \\ 0_{(N-1)n\times 1} \end{pmatrix} \tag{21}$$

$$z^\ell = \begin{pmatrix} 1_{N\times 1} \otimes u^\ell \\ -\infty \cdot 1_{N\cdot n\times 1} \end{pmatrix}, \qquad z^u = \begin{pmatrix} 1_{N\times 1} \otimes u^u \\ \infty \cdot 1_{N\cdot n\times 1} \end{pmatrix} \tag{22}$$

$$\mathcal{B} = \begin{pmatrix} \mathcal{B}_{11} & \mathcal{B}_{12} \\ -\mathcal{B}_{11} & -\mathcal{B}_{12} \\ \mathcal{B}_{31} & 0_{N\cdot m\times N\cdot n} \\ -\mathcal{B}_{31} & 0_{N\cdot m\times N\cdot n} \end{pmatrix}, \quad b = \begin{pmatrix} b_1 \\ b_2 \\ b_3 \\ b_4 \end{pmatrix}. \tag{23}$$

Table 3: Matrices for intermediate variable set QP formulation.

$$H_{11} = I_N \otimes \left(2S + R + D^T Q D\right) - I_{N,-1} \otimes S - I_{N,+1} \otimes S$$
$$H_{12} = I_{N,+1} \otimes D^T Q C = H_{21}^T$$
$$H_{22} = \begin{pmatrix} I_{N-1} \otimes C^T Q C \\ \bar{Q} \end{pmatrix}$$
$$\mathcal{B}_{11} = I_N \otimes D, \quad \mathcal{B}_{12} = I_{N,-1} \otimes C$$
$$\mathcal{B}_{31} = I_{N \cdot m} - I_{N,-1} \otimes I_m$$
$$b_1 = \begin{pmatrix} y^u - C x_k \\ 1_{N-1 \times 1} \otimes y^u \end{pmatrix}, \quad b_2 = \begin{pmatrix} -y^\ell + C x_k \\ -1_{N-1 \times 1} \otimes y^\ell \end{pmatrix}$$
$$b_3 = \begin{pmatrix} \Delta u^u + u_{k-1} \\ 1_{N-1 \times 1} \otimes \Delta u^u \end{pmatrix}, \quad b_4 = \begin{pmatrix} -\Delta u^\ell - u_{k-1} \\ -1_{N-1 \times 1} \otimes \Delta u^\ell \end{pmatrix}$$

The matrices encountered in equations 18 – 23 that have not been defined yet, are defined in Table 3. The dimensions of the intermediate variable set QP problem are given by $\dim z = N \cdot (n + r) \times 1$, $\dim a = N \cdot n \times 1$, and $\dim b = N\,(r + m)$. The definition of z as in eq. 17 leads to sparse matrices H, $\mathcal{A}$, and $\mathcal{B}$.

3.4 Basic set of variables

The most common QP formulation is found by using the equality constraints to eliminate all unknowns except the future control inputs, hence:

$$z^T = \begin{pmatrix} u_k^T & \dots & u_{k+N-1}^T \end{pmatrix}. \tag{24}$$

In this case, there are no equality constraints. The matrices and vectors of the QP formulation are

$$\begin{aligned} H = 2\,(&\mathcal{H}_{N-1}\,(I_N \otimes Q)\,\mathcal{H}_{N-1} + (I_N \otimes R) \\ &+ \Psi^T\,(I_N \otimes S)\,\Psi + \Omega + P^T \mathcal{C}_k^T \bar{Q} \mathcal{C}_k P\big), \end{aligned} \tag{25}$$

$$\begin{aligned} g^T = 2\,&(\mathcal{O}_N x_k - \mathbf{s})^T\,(I_N \otimes Q)\,\mathcal{H}_{N-1} \\ &+ 2u_{k-1}^T L^T\,(I_N \otimes S)\,\Psi + 2x_k^T \left(A^N\right)^T \bar{Q} \mathcal{C}_k P \end{aligned} \tag{26}$$

$$\mathcal{B} = \begin{pmatrix} \Psi \\ -\Psi \\ \mathcal{H}_{N-1} \\ -\mathcal{H}_{N-1} \end{pmatrix}, b = \begin{pmatrix} 1_{N \times 1} \otimes \Delta u^u - L u_{k-1} \\ -1_{N \times 1} \otimes \Delta u^\ell + L u_{k-1} \\ 1_{N \times 1} \otimes y^u - \mathcal{O}_N x_k \\ -1_{N \times 1} \otimes y^\ell + \mathcal{O}_N x_k \end{pmatrix} \tag{27}$$

$$z^\ell = 1_{N \times 1} \otimes u^\ell, \qquad z^u = 1_{N \times 1} \otimes u^u \tag{28}$$

The matrices encountered in equations 25 – 27 that have not been defined yet, are defined in Table 4.

The dimensions of the intermediate variable set QP problem are given by $\dim z = N \cdot r \times 1$ and $\dim b = 2N \cdot (m + r) \times 1$. The definition of z as in eq. 24 leads to dense matrices H and $\mathcal{B}$.

Table 4: Matrices for basic variable set QP formulation.

$$\Psi = I_{N\cdot m} - I_{N,-1} \otimes I_m,$$

$$L = \begin{pmatrix} -I_m \\ 0_{(N-1)\times m} \end{pmatrix}, \quad \mathbf{s}^T = \begin{pmatrix} s_k^T & \cdots & s_{k+N-1}^T \end{pmatrix}$$

$$\Omega = \begin{pmatrix} 0_{N-1\times N-1} & 0_{N-1\times 1} \\ 0_{1\times N-1} & 1 \end{pmatrix} \otimes S, P = \mathrm{rot}_{90}(I_{N\cdot m})$$

$$\mathcal{C}_k = \begin{pmatrix} B & AB & \dots & A^{k-1}B \end{pmatrix},$$

$$\mathcal{O}_k^T = \begin{pmatrix} C^T & (CA)^T & \dots & \left(CA^{k-1}\right)^T \end{pmatrix},$$

$$\mathcal{H}_k = \begin{pmatrix} D & 0_{\dim D} & \cdots & 0_{\dim D} \\ CB & D & \cdots & 0_{\dim D} \\ \vdots & \vdots & \ddots & \vdots \\ CA^{k-1}B & CA^{k-2}B & \cdots & D \end{pmatrix}$$

3.5 Basic variable set from QR factorization

It is possible to eliminate equality constraints by means of e.g. QR factorization. This is an alternative to the formula manipulation needed to reach the results in the previous section. Denoting the matrices in section 3.2 by subscript c, we have:

$$\mathcal{A}_c = \tilde{Q}\tilde{R}, \tag{29}$$

where $\tilde{Q}$ is orthogonal and $\tilde{R}$ is an upper triangular matrix, and $\dim \tilde{R} = \dim \mathcal{A}_c$. $\tilde{R}$ is then partitioned into:

$$\tilde{R} = \begin{pmatrix} R_{11} & R_{12} \end{pmatrix} \tag{30}$$

where $\tilde{R}_{11}$ is square and invertible for well posed MPC problems; z_c is partitioned into:

$$z_c^T = \begin{pmatrix} z_1^T & z_2^T \end{pmatrix} \tag{31}$$

where $\dim z_1$ is the number of columns in R_{11} and $\dim z_2 = N \cdot m$. This leads to

$$z_1 = R_{11}^{-1}\left(\tilde{Q}^T a_c - R_{12} z_2\right). \tag{32}$$

By eliminating the equality constraint, the matrices in the QP formulation become:

$$H = \begin{pmatrix} -R_{11}^{-1}R_{12} \\ I \end{pmatrix}^T H_c \begin{pmatrix} -R_{11}^{-1}R_{12} \\ I \end{pmatrix}$$

$$g^T = \begin{pmatrix} R_{11}^{-1}\tilde{Q}^T a_c \\ 0 \end{pmatrix}^T H_c \begin{pmatrix} -R_{11}^{-1}R_{12} \\ I \end{pmatrix}$$

$$\mathcal{B} = \begin{pmatrix} \mathcal{B}_1 \\ -\mathcal{B}_1 \end{pmatrix}, \qquad \mathcal{B}_1 = \begin{pmatrix} -R_{11}^{-1}R_{12} \\ I_{N\cdot m} \end{pmatrix}$$

Table 5: Case studies.

	1a	**1b**	**1c**	**2a**	**2b**	**2c**
Process	PM	PM	PM	TE	TE	TE
N	50	100	200	50	100	200

$$b = \begin{pmatrix} z_c^u - \begin{pmatrix} R_{11}^{-1}\tilde{Q}^T a_c \\ 0_{N\cdot m\times N\cdot m} \end{pmatrix} \\ -z_c^\ell + \begin{pmatrix} R_{11}^{-1}\tilde{Q}^T a_c \\ 0_{N\cdot m\times N\cdot m} \end{pmatrix} \end{pmatrix}$$

$$z_2^\ell = -\infty \cdot 1_{N\cdot m\times 1}, \qquad z_2^u = \infty \cdot 1_{N\cdot m\times 1}.$$

When z_2 is found, we can compute z_1 from eq. 32. However, since the first element of z_2 is Δu_k, we can find the desired u_k as $\Delta u_k + u_{k-1}$, hence z_1 is really not needed. The dimensions of the QR reduced basic variable set problem are given by $\dim z_2 = N \cdot m \times 1$ and $\dim b = 2 \cdot \dim z_c$. Since $\tilde{a}_c$ may change with time index k, it is necessary to also store $R_{11}^{-1}\tilde{Q}^T$ which is of dimension $\dim a_c \times \dim a_c$. This formulation leads to dense matrices H and $\mathcal{B}$, and a dense $\tilde{Q}$ matrix.

4 Analysis of QP problems

The formulations with a complete set of variables (**C**, section 3.2), an intermediate set of variables (**I**, section 3.3), the basic set of variables (**B**, section 3.4), and the basic set of variables as found via QR factorization (**QR**, section 3.5) are compared with regards to sparsity, the use of computer memory, and the conditioning of the formulations.

In the discussion of sparsity and conditioning, we assume that possible inequality constraints are passive, and thus consider the sparsity and condition number of matrix $\mathcal{L}$ in eq. 10.

The comparisons are based on two example processes. The first example process is a linearized fourth order paper machine (PM) model, with three inputs and three outputs; see Appendix A.1 for some details. The second example process is an identified 23 order model of the Tennessee Eastman (TE) Challenge Process, with seven inputs and ten outputs; see Appendix A.2 for some details. All computations in this paper are based on Intel Pentium III PCs running at 750 MHz, and with 256 Mbyte RAM.

The case studies are described in Table 5, where the first row is our reference name for the case study, the second row describes which process is used (Paper Machine or Tennessee Eastman), and the third row is the prediction horizon used in the formulation.

The **B** and **QR** formulations have totally dense Lagrange matrices $\mathcal{L}$, while the sparsity patterns for the **C** and **I** formulations are displayed in Table 6.

Table 7 displays the memory used by the matrices and vectors in the MPC formulation.

Table 6: Sparsity patterns for sparse QP formulations, case 2a.

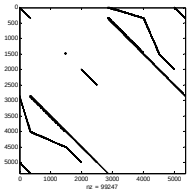

C

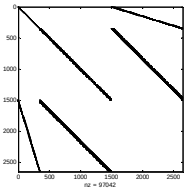

I

Table 7: Memory used (kbytes) for case studies.

	1a	**1b**	**1c**	**2a**	**2b**	**2c**
B	740	2919	11598	4962	19443	76965
QR	2888	11535	**	27380	**	**
I	79	158	317	955	1919	3846
C	78	154	308	722	1445	2892

Elements marked with "**" denotes that the computer ran out of memory during computation.

Table 8 displays the condition number of matrix $\mathcal{L}$.

5 Comparison of algorithms for solving the QP problems

The QP solvers used in this study are (i) `quadprog`, (The MathWorks, Inc. 2000); (ii) `qld`, available in Tomlab, Holmström (2001); as well as the following solvers which are available with a Tomlab interface: (iii) `lssol`, Gill *et al.* (1986); (iv) `qpopt`, Gill *et al.* (1995); and (iv) `sqopt`, Gill *et al.* (1997). The `sqopt` solver is the only one of these that fully handles sparse matrices. The `quadprog` solver can be used with

Table 8: Condition number for QP formulations. Some computations required virtual memory. Computations were terminated after 1 hour of computing time, and are marked with "**".

	B	**QR**	**I**	**C**
1a	2.1×10^3	8×10^5	1.3×10^{19}	8.9×10^{18}
1b	2.3×10^3	2.7×10^6	1.4×10^{19}	1.1×10^{19}
1c	2.3×10^3	**	1.4×10^{19}	1.1×10^{19}
2a	7×10^{12}	2.7×10^{15}	6.5×10^{13}	1.6×10^{14}
2b	7×10^{12}	**	6.6×10^{13}	**
2c	7×10^{12}	**	**	**

Table 9: Identification of solver and QP formulation.

Formulation	Solver	Notation
B	`lssol`	$\mathbf{B}_1$
B	`qpopt`	$\mathbf{B}_2$
B	`qld`	$\mathbf{B}_3$
B	`quadprog`	$\mathbf{B}_4$
QR	`lssol`	**QR**
I	`sqopt`	**I**
C	`sqopt`	**C**

Table 10: Total computation time (seconds) for case studies.

	1a	**1b**	**1c**	**2a**	**2b**	**2c**
$\mathbf{B}_1$	0.91	4.82	46.9	(7.84)*	(76.8)*	(592)*
$\mathbf{B}_2$	1.38	10.1	91.4	8.1	80.1	600
$\mathbf{B}_3$	1.42	7.45	54.5	15.4	97.1	3320
$\mathbf{B}_4$	15.3	49.7	283	19.5	96.9	**
QR	16.2	133	**	(754)*	**	**
I	3.86	20.3	85.8	96	(313)*	(994)*
C	7.10	32.1	119	196	(382)*	(139)*

sparse matrices only if there are no inequality constraints in the problem formulation.

We use the case studies of Table 5, with the notation of Table 9 to identify which solver is used in the formulations. In all cases, we simulate the controlled process for $T = 20$ time steps.

Table 10 displays the total time used by the computer to simulate the case studies with various MPC formulations and solvers. Table elements marked with "*" denotes that an optimization failure or optimization problem occured. Elements marked with "**" denotes that the computer ran out of memory during computation.

Table 11 displays the time spent on the first optimization. The reason for including these results is that most solvers solve the optimization problem much slower the first time than the remaining iterations. Typical computation times for the remaining

Table 11: Computation time for first iteration (seconds) for case studies.

	1a	**1b**	**1c**	**2a**	**2b**	**2c**
$\mathbf{B}_1$	0.12	0.4	2.6	(0.33)*	(3.22)*	(27.2)*
$\mathbf{B}_2$	0.13	1.3	11	0.35	4.4	27
$\mathbf{B}_3$	0.15	0.67	3.26	0.72	4.28	200
$\mathbf{B}_4$	1.75	6.5	40	1.13	4.5	**
QR	0.12	1.11	**	(4.6)*	**	**
I	0.82	3.29	11.3	10	(35)*	(88.7)*
C	0.72	3.2	11	21	(57)*	(266)*

Table 12: Typical computation time for remaining iterations (seconds) for case studies.

	1a	**1b**	**1c**	**2a**	**2b**	**2c**
$\mathbf{B}_1$	0.03	0.15	1.9	(0.29)*	(3.14)*	(23.9)*
$\mathbf{B}_2$	0.025	0.15	1.94	0.30	3.18	24.2
$\mathbf{B}_3$	0.05	0.29	2.28	0.67	4.14	150
$\mathbf{B}_4$	0.6	1.6	8.2	0.85	4.2	**
QR	0.05	0.26	**	(0.6)*	**	**
I	0.15	0.9	3.9	4.5	(14.6)*	(3)*
C	0.33	1.5	5.6	9.0	(17.2)*	(37)*

iterations are given in Table 12.

6 Conclusions

In this paper, we have discussed four formulations of a standard MPC problem. The formulation of section 3.2 (**C**) is, in our view, the most straightforward formulation from the pedagogical point of view. The formulation in section 3.5 (**QR**) only requires knowledge of linear algebra in addition to formulation **C**, and is also easy to present. The formulations in sections 3.3 (**I**) and 3.4 (**B**) utilize various degrees of elimination of equality constraints, where formulation **B** is the most demanding to present, yet it is also the most common formulation.

Formulations **C** and **I** both lead to sparse matrices, Table 6, and thus the memory requirement increases more or less linearly with the horizon N of the performance index, Table 7, while for the dense matrix formulations **B** and **QR** the memory requirement increases quadratically with N; the **QR** formulation is most demanding. In fact, the formulations **C** and **I** can be said to be *supersparse* in the sense that it is possible to introduce special sparse matrix structures that take advantage of the fact that the involved matrices are constructed from the Kronecker product, where typically the system matrices and horizon length N contain all necessary information, and the size becomes independent of N. To take advantage of this, it would, however, be necessary to develop special matrix libraries for such data structures. Table 8 indicates that the sparse formulations (**C**, **I**) may be poorly conditioned, but this may also be a result of how the conditioning is defined.

A number of commercially available QP solvers have been tested and compared. Overall, the best combination of formulation and solver in our investigation appears to be the **B** formulation of section 3.4 and the `qpopt` solver, which manages to solve all test problems where the number of free variables ranges from 150 to 1400, see Tables 10 – 12: the largest problem requires less than 30 s computation time for each iteration. The relatively poor performance of the **QR** formulation is mainly caused by the added memory requirement. The sparse solvers give relatively poor performance. With the memory advantage of the sparse formulations, it is to be hoped that sparse solvers will be tailor made to handle the (super-) sparse structures found in MPC

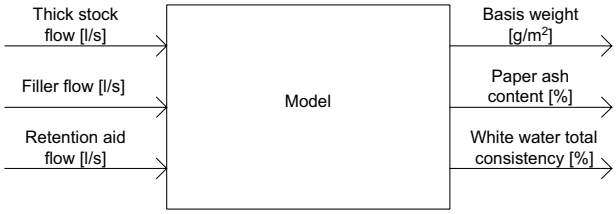

Figure 1: Inputs and outputs in PM6 model.

problems; such contributions are starting to appear, see Bartlett *et al.* (2002).

A Overview of example processes

A.1 Paper machine

A paper machine model has been developed for controlling certain key variables at paper machine 6 (PM6) at Norske Skog Saugbrugs, Norway. The original model is a fourth order nonlinear model with three inputs, three outputs and seven measured disturbances, and is described in detail in Hauge and Lie (2002). The model used in this paper is a linearized version where the measured disturbances are assumed constant. The inputs and outputs of the model are seen in Figure 1.

A.2 Tennessee Eastman Challenge Process

The Tennessee Eastman Challenge Process was defined in Downs and Vogel (1993), and a basic control structure for the process was suggested in McAvoy and Ye (1994). Recently, several subspace models for a part of this process were identified and compared, (Juricek, Seborg & Larimore 2001)Juricek *et al.* (2001). The subspace models all have 7 control inputs and 10 outputs, and the model that was found to give best predictions was based on the Canonical Variate Analysis (CVA) method and has 23 states. The seven inputs are (i) compressor recycle valve, (ii) condenser cooling water flow, (iii) setpoint for A feed, (iv) setpoint for D feed, (v) setpoint for C feed, (vi) set point for purge rate, and (vii) set point for reactor CW temp. The ten outputs are (i) recycle flow, (ii) reactor feed rate), (iii) reactor pressure, (iv) reactor temperature, (v) product separator temperature, (vi) product separator pressure, (vii) stripper pressure, (viii) stripper temperature, (ix) compressor work, and (x) separator CW temperature. The inputs and outputs have not been scaled, and the system that has been identified is rather stiff. The most promising prediction model from the subspace identification was graciously made available to the authors of this paper by the authors of (Juricek et al. 2001)Juricek *et al.* (2001).

References

Bartlett, R. A., Biegler, L. T., Backstrom, J. & Gopal, V. (2002), 'Quadratic programming algorithms for large-scale model predictive control', *Journal of Process Control* . In press.

Camacho, E. F. & Bordons, C. (1999), *Model Predictive Control*, Springer-Verlag London.

Downs, J. & Vogel, E. (1993), 'A plant-wide industrial process control problem', *Computers and chemical engineering* **17**(3), 245–255.

Gill, P. E., Hammarling, S. J., Murray, W., Saunders, M. A. & Wright, M. H. (1986), User's guide for lssol (version 1.0): A fortran package for constrained linear least-squares and convex quadratic programming, Technical Report SOL 86-1, Systems Optimization Laboratory (SOL), department of operations research, Stanford University.

Gill, P. E., Murray, W. & Saunders, M. A. (1995), User's guide for qpopt 1.0: A fortran package for quadratic programming, Technical Report SOL 95-4, Systems Optimization Laboratory, Dept. Operations Research, Stanford University.

Gill, P. E., Murray, W. & Saunders, M. A. (1997), 'User's guide for sqopt 5.3: A Fortran package for large-scale linear and quadratic programming'. (Draft, October 1997).

Hauge, T. A. & Lie, B. (2002), 'Paper machine modeling at Norske Skog Saugbrugs: A mechanistic approach', *Modeling, Identification and Control* **23**(1), 27–52.

Holmström, K. (2001), The TOMLAB optimization environment v3.0 user's guide, Technical report, HKH MatrisAnalys AB.

Juricek, B. C., Seborg, D. E. & Larimore, W. E. (2001), 'Identification of the tennessee eastman challenge process with subspace methods', *Control Engineering Practice* **9**, 1337–1351.

Maciejowski, J. (2002), *Predictive Control with Constraints*, Prentice Hall, Harlow, England.

McAvoy, T. & Ye, N. (1994), 'Base control for the tennessee eastman problem', *Computers and chemical engineering* **18**(5), 383–413.

Muske, K. R. & Rawlings, J. B. (1993), 'Model predictive control with linear models', *AIChE Journal* **39**(2), 262–287.

Rawlings, J. B. & Muske, K. R. (1993), 'The stability of constrained receding horizon control', *IEEE Transactions on Automatic Control* **38**(10), 1512–1516.

Seborg, D. E., Edgar, T. F. & Mellichamp, D. A. (1989), *Process Dynamics and Control*, John Wiley & Sons, Inc.

The MathWorks, Inc. (2000), 'Optimization toolbox for use with matlab, user's guide (version 2)'.

Paper F

Application of a Nonlinear Mechanistic Model and an Infinite Horizon Predictive Controller on Paper Machine 6 at Norske Skog Saugbrugs

Hauge, T.A., Slora, R., and Lie, B. (2002). *Application of a Nonlinear Mechanistic Model and an Infinite Horizon Predictive Controller on Paper Machine 6 at Norske Skog Saugbrugs*, Submitted to Journal of Process Control.

Extended version.

Application of a Nonlinear Mechanistic Model and an Infinite Horizon Predictive Controller to Paper Machine 6 at Norske Skog Saugbrugs

Tor Anders Hauge[*], Roger Slora[†], and Bernt Lie[‡]

Contents

[*]Telemark University College.
[†]Norske Skog Saugbrugs.
[‡]Corresponding author: Bernt.Lie@hit.no, Telemark University College, P.b. 203, 3901 Porsgrunn, Norway.

Abstract

A mechanistic nonlinear model of the wet end of paper machine 6 (PM6) at Norske Skog Saugbrugs, Norway has been developed, and used in an industrial MPC implementation. The MPC uses an infinite horizon criterion, successive linearization of the model, and estimation of states and parameters by an augmented Kalman filter. Variation in important quality variables and consistencies in the wet end have been reduced substantially, compared to the variation prior to the MPC implementation. The MPC also provides better efficiency through faster grade changes, control during sheet breaks and start ups, and better control during periods of poor measurements. From May 2002 the MPC has been the preferred controller choice for the process operators at PM6.

1 Introduction

Norske Skog Saugbrugs in Halden, Norway, is one of the largest manufacturers of uncoated super calendered magazine paper in the world. The total production capacity of the mill is $550,000$ ton per year. The largest paper machine (PM) at the Saugbrugs mill is PM6, accounting for more than half the total production capacity. PM6 was built in the early 1990s and produce paper with 8.62 meters width, and with a typical velocity of 1500 meters per minute.

Previous work A clear distinction is usually made between CD (Cross Direction) and MD (Machine Direction) control, when discussing the control of a paper machine. CD control refers to the profile across the paper web, while MD refers to the average value. In this paper we only consider the MD control problem.

Several MPC implementations using multivariable empiric paper machine models are reported, e.g. (McQuillin & Huizinga 1995), (Lang, Tian, Kuusisto & Rantala 1998), (Mack, Lovett, Austin, Wright & Terry 2001), (Kosonen, Fu, Nuyan, Kuusisto & Huhtelin 2002), and (Austin, Mack, Lovett, Wright & Terry 2002). To the best of the authors' knowledge, there exists no reported industrial MPC implementations utilizing a multivariable mechanistic model of the wet-end of the paper machine. Some industrial implementations of MPC with mechanistic models are known in other industry areas, e.g. (Qin & Badgwell 1998) and (Badgwell & Qin 2001) have reported a few implementations. Papers describing industrial implementations of MPC with mechanistic models are few, however (Hillestad & Andersen 1994) and (Glemmestad, Ertler & Hillestad 2002) report several applications to industrial polymer reactors. Several simulated examples exist, e.g. (Lee, Lee, Yang & Mahoney 2002), (Prasad, Schley, Russo & Bequette 2002), (Amin, Mehra & Arambel 2001), and (Schei & Singstad 1998), and also some applications to experimental test stands, e.g. (Ahn, Park & Rhee 1999) and (Park, Hur & Rhee 2002).

Process description A simplified drawing of PM6 is shown in Figure 1. Cellulose, TMP (thermomechanical pulp) and broke (repulped fibers and filler from sheet breaks and edge trimmings) are blended in the mixing chest. The stock is fed to the machine chest with a controlled total consistency[1]. Filler is added between the mixing and machine chests. The fillers used in paper production depend on the end-user requirements; typical fillers are kaolin, chalk, talc, and titanium dioxide (Bown 1996). About two thirds of the filler particles used at PM6 are added to the thick stock; the rest is added at the outlet of the white water tank. The flow to the machine chest is large in order to keep the level of the machine chest constant, and an overflow is returned to the mixing chest. The total consistency in the mixing and machine chests are typically around 3 – 4%, which is considerably higher than consistencies later on in the process, and thus the stock from the machine chest is denoted the "thick stock".

The thick stock enters the "short circulation" in the white water tank. Here, the thick stock is diluted to 1-1.5% total consistency by white water[2] and a recirculation flow from the deculator. Filler is added to the stock just after the white water tank. The first cleaning process is a five stage hydrocyclone arrangement, mainly intended to separate heavy particles (e.g. sand and stones) from the flow. The *accept* from the first stage of the hydrocyclones goes to the deculator where air is separated from the stock. The second cleaning process consists of two parallel screens, which separate larger particles (e.g. bark) from the stock. Retention aid is added to the stock at

[1] The total consistency is the weight of solids (i.e. filler particles and fiber) divided by the total weight of solids and water.

[2] White water, which is stored in the white water tank, is the drainage from the wire.

the outlet of the screens. The retention aid is a cationic polymer which, amongst others, adsorb onto anionic fibers and filler particles and cause them to flocculate. The flocculation is a key process for retaining small filler particles and small fiber fragments on the wire, although the significance of mechanical entrapment of non-flocculated filler and fines seems to be somewhat controversial in the literature. For example (Van de Ven 1984) found (theoretically) that mechanical entrapment was low, while (Bown 1996) reports that mechanical entrapment can be a dominant mechanism. In the headbox, the pulp is distributed evenly onto the finely meshed woven wire cloth. Most of the water in the pulp is recirculated to the white water tank, while a share of fiber material and filler particles form a network on the wire which will soon become the paper sheet. The pulp flow from the white water tank, through the hydrocyclones, deculator, screens, headbox, onto the wire and back to the white water tank is denoted the "short circulation".

In the wire section, most of the water is removed by drainage. In the press section, the paper sheet is pressed between rotating steel rolls, thus making use of mechanical forces for water removal. Finally, in the dryer section, the paper sheet passes over rotating and heated cast iron cylinders, and most of the water left in the sheet is removed by evaporation. The paper is then rolled up on the reel before it is moved on to further processing.

Motivation for multivariable model based control Magazine paper is characterized by its glossy appearance due to a high content of filler in the paper. The finished magazine paper typically consists of 65% fiber, 30% filler, and 5% water. The main difference between magazine paper and e.g. newsprint is the high content of filler. For newsprint the amount of filler is typically 0-10%. Due to the high filler content in magazine paper, the couplings between important input and output variables are relatively strong. A project called "Stabilization of the wet end at PM6" was initiated in 1999 based on the experience of strong couplings and oscillating behavior in the process. A key goal was to reduce variation in certain variables, such as consistencies in the short circulation, basis weight, filler content, and more. Based on experience and reported results from competitive mills (e.g. (McQuillin & Huizinga 1995), and (Lang et al. 1998)), it was decided to develop a model of the process and utilize this in a model predictive controller (MPC). Three input and three output variables were selected

$$\bar{u} = \begin{bmatrix} \bar{u}_{TS} \\ \bar{u}_{F} \\ \bar{u}_{RA} \end{bmatrix}, \ \bar{y} = \begin{bmatrix} \bar{y}_{BW} \\ \bar{y}_{PA} \\ \bar{y}_{WC} \end{bmatrix}, \tag{1}$$

where the inputs $\bar{u}$ are the amount of *thick stock*, *filler* added at the outlet of the white water tank, and *retention aid* added at the outlet of the screens, and where the outputs $\bar{y}$ are the *basis weight* (weight per area), *paper ash* content (content of filler in the paper), and *wire tray consistency* in the recirculation flow from the wire to the white water tank. The basis weight and paper ash outputs are direct quality variables, while the wire tray consistency is an indirect quality variable having significant effect on variation in other short circulation variables.

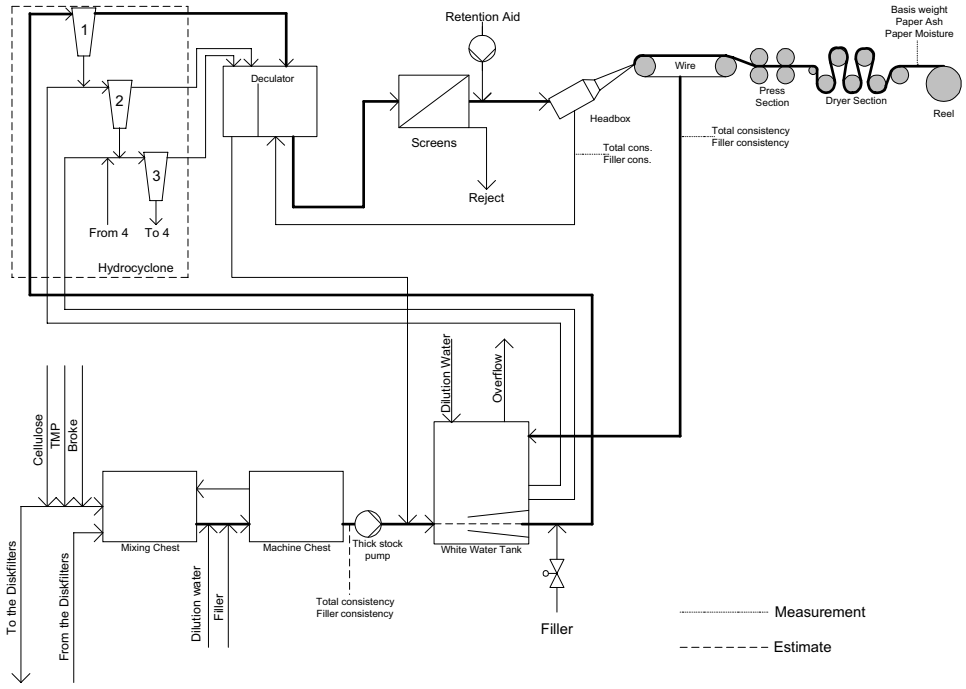

Figure 1: A simplified drawing of PM6. More details are available in (Hauge & Lie 2002).

Before the project started, single loop controllers and manual control were used. Grade changes were carried out manually or partly manually by the operators: the setpoints were changed a number of times before they were equal to the new grade. During start ups, the controllers were kept in manual mode until the measurements were close to the desired specifications. In addition, during sheet breaks the basis weight and paper ash measurements were lost and the inputs controlling these variables were set equal to the values that they had prior to the sheet break. The controllers were kept in manual mode until the paper was back on the reel. Thus, it was also a key goal in the project to be able to have the controllers in automatic mode during grade changes, sheet breaks, and start ups.

The process model The process model is described in detail in e.g. (Hauge & Lie 2002) and only a brief description will be given here. Note that some modifications have been introduced to the model detailed in (Hauge & Lie 2002), as compared to the model implemented at PM6. The most prominent modification is that a first order empiric model that was added to capture neglected and unknown dynamics in the process, has been removed.

The model was originally developed with several ordinary and partial differential equations. The model was then simplified, and eventually fitted to experimental and operational mill data. The implemented PM6 model consists of a third order nonlinear mechanistic model based on physical and chemical laws. The structure of the developed process model is

$$\begin{aligned} \dot{\bar{x}} &= \bar{f}(\bar{x}, \bar{u}, \bar{d}, \bar{\theta}) \\ \bar{y} &= \bar{g}(\bar{x}, \bar{u}, \bar{d}, \bar{\theta}), \end{aligned} \tag{2}$$

with $\bar{x} \in \mathbb{R}^n = \mathbb{R}^3$, $\bar{y} \in \mathbb{R}^m = \mathbb{R}^3$, $\bar{u} \in \mathbb{R}^r = \mathbb{R}^3$ and $\bar{d} \in \mathbb{R}^g = \mathbb{R}^4$. The bar above the variable names indicates that these are the variables in their original units and size. $\bar{\theta}$ consists of several model parameters, tuned to fit the model outputs to experimental and operational data.

The manipulated inputs $\bar{u}$ and the outputs $\bar{y}$ are shown in eq. 1, while the states and measured disturbances are

$$\begin{aligned} \bar{x}^T &= \begin{bmatrix} \bar{C}_{R,fil}, & \bar{C}_{WT,fil}, & \bar{C}_{D,fib} \end{bmatrix} \\ \bar{d}^T &= \begin{bmatrix} \bar{C}_{\mathrm{TS,tot}}, & \bar{C}_{\mathrm{TS,fil}}, & \bar{v}, & \bar{f} \end{bmatrix}, \end{aligned} \tag{3}$$

where $\bar{C}_{R,fil}$ is the concentration of filler in a *reject tank* in the hydrocyclones, $\bar{C}_{WT,fil}$ is the concentration of filler in the *white water tank*, and $\bar{C}_{D,fib}$ is the concentration of fiber in the *deculator*. The measured disturbances accounted for in the model, are the total and filler thick stock concentrations $\bar{C}_{\mathrm{TS,tot}}$ and $\bar{C}_{\mathrm{TS,fil}}$, the paper machine velocity $\bar{v}$, and the paper moisture percentage $\bar{f}$.

Note that the total- and filler concentrations in the thick stock flow are called "measured disturbances", although they are not measured. A model of the thick stock area has been developed (Slora 2001), and implemented at PM6, providing *estimates* of total- and filler concentrations in the thick stock.

Model Predictive Controller (MPC) A commercial MPC developed by Prediktor AS (www.prediktor.no), was chosen by Norske Skog for implementation. The choice of MPC was based on (i) cost, and (ii) the ability to add and develop certain features that were important. Important features were the abilities to

- utilize the non-linear model;
- specify future reference changes. This means that the process operators can specify a setpoint change some time into the future, see how the controller will respond, and let the controller do the grade change if they are satisfied with the response. In many systems, the setpoint is constant into the future, so once a change in setpoint is made, the controller will respond immediately, giving the operators no time to consider how wise the response is;
- make an interface suitable for gaining operator acceptance of the MPC;
- use the MPC during grade changes, sheet breaks, and start ups.

The commercial MPC is part of a software package named Apis (Advanced Process Improvement System), which also consists of a Kalman filter, subspace system identification, and more. The Apis MPC was intended for linear models, based on the infinite horizon objective function presented in (Muske & Rawlings 1993). For the predictive controller implemented at PM6, several extensions were made to the original MPC, such as

- on-line linearization at each sample;
- on-line estimation of key model parameters/biases;
- future setpoint changes, i.e. the process operators can submit new setpoints to the controller some time before the actual grade change;
- addition of a direct input to output term;
- inclusion of measured disturbances.

These extensions will be further discussed in later sections. Note that the extensions discussed in this paper are based on the authors' work, and the actual implementation in Apis may be based on other solutions and ideas. The use of MPC, a nonlinear model, extended Kalman filter, and linearization at each sample, has also been suggested by (Lee & Ricker 1994), although with a finite horizon criterion. Similarly, (Gattu & Zafiriou 1992) proposed an algorithm for nonlinear MPC, with linearization at each sample, but with computation of the steady state Kalman gain at each sample.

Organization of paper In Section 2 an overview of the algorithm for infinite horizon MPC with augmented Kalman filter is given. Linearization of the model is discussed in Section 3, and the MPC equations are outlined in Section 4. In Section 5 the augmented Kalman filter is discussed, and results from using MPC on paper machine 6 (PM6) at Norske Skog Saugbrugs is presented and discussed in Section 6. Finally, some conclusions are given in Section 7.

A few notes about the notation are given in Appendix A. Details on how to find the steady state values are given in Appendix B, and proofs for the finite horizon criteria are given in Appendix C. State and parameter estimation is detailed in Appendix D.

2 Overview of algorithm

At time k we have available the process model (eq. 2) in its discrete version

$$\begin{aligned} \bar{x}_{k+1} &= f(\bar{x}_k, \bar{u}_k, \bar{d}_k, \bar{\theta}_k) \\ \bar{y}_k &= g(\bar{x}_k, \bar{u}_k, \bar{d}_k, \bar{\theta}_k), \end{aligned} \tag{4}$$

as well as the following past measurements and estimates

$$\left.\begin{array}{c} \bar{u}_{k-i} \\ \bar{y}_{k-i} \\ \bar{d}_{k-i} \\ \widehat{\bar{x}}_{k-i+1} \end{array}\right\}, \forall i = 1, 2, 3..., \tag{5}$$

where $\widehat{\bar{x}}$ is an estimated state vector. The following step by step algorithm for controlling the process is suggested, assuming the present time to be k.

1) Linearization of model based on conditions at time $k-1$ For the chosen MPC we need a linear model. The linearization is based on the most up-to-date information about the process, i.e. the variable values at time $k-1$. Note that we have no information about $\bar{u}_k$ yet, so we can not linearize based on variable values at time k. The resulting model is

$$\begin{aligned} \overline{\bar{x}}_{k+1} &= A_k \overline{\bar{x}}_k + B_k \overline{\bar{u}}_k + E_k \overline{\bar{d}}_k \\ \overline{\bar{y}}_k &= C_k \overline{\bar{x}}_k + D_k \overline{\bar{u}}_k + F_k \overline{\bar{d}}_k. \end{aligned} \tag{6}$$

The linearization is discussed more thoroughly in Section 3. See also notes about notation in Appendix A.

2) Obtain current measured disturbances and future setpoints and disturbances The measured disturbances obtained from the process are $\bar{d}_k$. The future disturbances and references are

$$\begin{aligned} &\bar{r}_{k+j},\ j = 0, ..., N-1 \\ &\bar{d}_{k+j},\ j = 0, ..., N-1, \end{aligned} \tag{7}$$

which must be provided by the process operators or simply taken as an extention of the present values into the future.

3) Shift variables corresponding to the linearized model The references, disturbances, and constraints will be used with the linearized model in eq. 6 for calculation of target values. The references, disturbances, and constraints must then be shifted along with the model so that all variables have the same origin before the calculation of target values.

4) Calculate steady state values The calculation of steady state values is carried out for several reasons. The steady state values are used as targets in the optimization criterion. One could use e.g. reference values directly as targets in the criterion. However, the calculation of steady state values is a way of ensuring that the targets are feasible. In addition, by calculating steady state values one has the opportunity to add e.g. an economic type criterion if there are additional degrees of freedom. Finally, for the special case of an infinite horizon criterion with possibility of changing future references and measured disturbances, we need the steady state values at the end of the horizon in order to shift the origin of the model.

5) Shift the origin of the model to the steady state values at time $k+N-1$ This is a step taken in order to reformulate the criterion to a finite horizon criterion.

6) Shift measured and estimated variables The variables must be shifted along with the model so that they have the same origin.

7) Update MPC matrices and vectors The matrices and vectors in the MPC formulation that contain time variant variables, such as linear model matrices, input variables, estimated states, etc., must be updated.

8) Optimization An optimization algorithm is used to calculate optimal inputs.

9) Apply $\bar{u}_k$ **to the process** Note that only the first input is used.

10) Obtain $\bar{y}_k$ **from the process**

11) Estimate $\widehat{\bar{x}}_{k+1}$ Unless all states are measured, we need to estimate them (or some of them). Typically an extended Kalman filter is used for this purpose.

12) Set $k := k+1$ **and go to step 1**

3 Linearization of model

Consider perturbations $\bar{\bar{x}}_k$, $\bar{\bar{u}}_k$, and $\bar{\bar{d}}_k$ near the variable values at time $k-1$

$$\begin{aligned} \bar{x}_k &= \bar{x}_{k-1} + \bar{\bar{x}}_k \\ \bar{u}_k &= \bar{u}_{k-1} + \bar{\bar{u}}_k \\ \bar{d}_k &= \bar{d}_{k-1} + \bar{\bar{d}}_k. \end{aligned} \tag{8}$$

Inserting these perturbations into eq. 4, and neglecting the parameter vector $\bar{\theta}_k$, gives

$$\begin{aligned} \bar{x}_{k+1} &= f(\bar{x}_k, \bar{u}_k, \bar{d}_k) = f(\bar{x}_{k-1} + \bar{\bar{x}}_k, \bar{u}_{k-1} + \bar{\bar{u}}_k, \bar{d}_{k-1} + \bar{\bar{d}}_k) \\ \bar{y}_k &= g(\bar{x}_k, \bar{u}_k, \bar{d}_k) = g(\bar{x}_{k-1} + \bar{\bar{x}}_k, \bar{u}_{k-1} + \bar{\bar{u}}_k, \bar{d}_{k-1} + \bar{\bar{d}}_k). \end{aligned} \tag{9}$$

Define $s = \{\bar{x}_{k-1}, \bar{u}_{k-1}, \bar{d}_{k-1}\}$. A first order expansion, with center corresponding to s, then gives

$$\begin{aligned} \bar{x}_{k+1} \approx\ & f(\bar{x}_{k-1}, \bar{u}_{k-1}, \bar{d}_{k-1}) + \frac{\partial f}{\partial \bar{x}_k}|_s(\bar{x}_{k-1} + \bar{\bar{x}}_k - \bar{x}_{k-1}) \\ & + \frac{\partial f}{\partial \bar{u}_k}|_s(\bar{u}_{k-1} + \bar{\bar{u}}_k - \bar{u}_{k-1}) + \frac{\partial f}{\partial \bar{d}_k}|_s(\bar{d}_{k-1} + \bar{\bar{d}}_k - \bar{d}_{k-1}) \\ \bar{y}_k \approx\ & g(\bar{x}_{k-1}, \bar{u}_{k-1}, \bar{d}_{k-1}) + \frac{\partial g}{\partial \bar{x}_k}|_s(\bar{x}_{k-1} + \bar{\bar{x}}_k - \bar{x}_{k-1}) \\ & + \frac{\partial g}{\partial \bar{u}_k}|_s(\bar{u}_{k-1} + \bar{\bar{u}}_k - \bar{u}_{k-1}) + \frac{\partial g}{\partial \bar{d}_k}|_s(\bar{d}_{k-1} + \bar{\bar{d}}_k - \bar{d}_{k-1}) \end{aligned} \tag{10}$$

Defining

$$\begin{aligned} A_k &= \frac{\partial f}{\partial \bar{x}_k}|_s,\ B_k = \frac{\partial f}{\partial \bar{u}_k}|_s,\ E_k = \frac{\partial f}{\partial \bar{d}_k}|_s \\ C_k &= \frac{\partial g}{\partial \bar{x}_k}|_s,\ D_k = \frac{\partial g}{\partial \bar{u}_k}|_s,\ F_k = \frac{\partial g}{\partial \bar{d}_k}|_s \\ \bar{y}_k &= g(\bar{x}_{k-1}, \bar{u}_{k-1}, \bar{d}_{k-1}) + \bar{\bar{y}}_k \end{aligned} \tag{11}$$

and inserting the definitions in eq. 8 into eq. 10 gives

$$\begin{aligned} \bar{\bar{x}}_{k+1} &\approx A_k\bar{\bar{x}}_k + B_k\bar{\bar{u}}_k + E_k\bar{\bar{d}}_k \\ \bar{\bar{y}}_k &\approx C_k\bar{\bar{x}}_k + D_k\bar{\bar{u}}_k + F_k\bar{\bar{d}}_k, \end{aligned} \tag{12}$$

where we have assumed that $\bar{x}_k = f(\bar{x}_{k-1}, \bar{u}_{k-1}, \bar{d}_{k-1})$, in accordance with the original nonlinear model equation. In the remainder of this paper, eq. 12 will be used with equality sign ("=") instead of approximation ("≈").

Note that the linearization was carried out with center corresponding to variable values at time $k-1$. If the linearization is carried out before the computation of the optimal input $\bar{u}_k$, then the linearized model must have center corresponding to variable values at time $k-1$. If the input $\bar{u}_k$ is available at the time of linearization, the center can correspond to variable values at time k, however by the time the linearized model is used in the MPC the time is $k+1$. Thus, it is not important whether the linearization is carried out prior to, or after, the computation of optimal inputs since the linearized model will be centered on the variable values at the previous sample in any case.

The linear system matrices $A_k, B_k, ..., F_k$ can be found by analytic or numeric methods. These methods are presented next.

3.1 Analytic linearization

Analytic linearization is carried out e.g. by hand, automatic differentiation, see e.g. (Griewank 2000), (Griewank & Corliss 1991), and (Solberg 1988), or by software capable of symbolic computation, e.g. Maple, or Matlab with the symbolic toolbox. For small and not too complicated systems this is a convenient method. Consider e.g. matrices A_k and B_k, computed element by element according to

$$A_k = \frac{\partial f}{\partial \bar{x}_k}|_s = \begin{bmatrix} \frac{\partial f_1}{\partial \bar{x}_{k,1}}|_s & \frac{\partial f_1}{\partial \bar{x}_{k,2}}|_s & \cdots & \frac{\partial f_1}{\partial \bar{x}_{k,n}}|_s \\ \frac{\partial f_2}{\partial \bar{x}_{k,1}}|_s & \frac{\partial f_2}{\partial \bar{x}_{k,2}}|_s & \cdots & \frac{\partial f_2}{\partial \bar{x}_{k,n}}|_s \\ \vdots & \vdots & \ddots & \vdots \\ \frac{\partial f_n}{\partial \bar{x}_{k,1}}|_s & \frac{\partial f_n}{\partial \bar{x}_{k,2}}|_s & \cdots & \frac{\partial f_n}{\partial \bar{x}_{k,n}}|_s \end{bmatrix}$$

$$B_k = \frac{\partial f}{\partial \bar{u}_k}|_s = \begin{bmatrix} \frac{\partial f_1}{\partial \bar{u}_{k,1}}|_s & \frac{\partial f_1}{\partial \bar{u}_{k,2}}|_s & \cdots & \frac{\partial f_1}{\partial \bar{u}_{k,r}}|_s \\ \frac{\partial f_2}{\partial \bar{u}_{k,1}}|_s & \frac{\partial f_2}{\partial \bar{u}_{k,2}}|_s & \cdots & \frac{\partial f_2}{\partial \bar{u}_{k,r}}|_s \\ \vdots & \vdots & \ddots & \vdots \\ \frac{\partial f_n}{\partial \bar{u}_{k,1}}|_s & \frac{\partial f_n}{\partial \bar{u}_{k,2}}|_s & \cdots & \frac{\partial f_n}{\partial \bar{u}_{k,r}}|_s \end{bmatrix},$$

where $s = \bar{x}_{k-1}, \bar{u}_{k-1}, \bar{d}_{k-1}$ is the center of the linearization, $\bar{x}_{k,i}$ means the i'th state variable at time k in the nonlinear model, and similar for other variables. The other system matrices are computed similar to this. Note that the B matrix consists of n rows and r columns and is not in general a square matrix.

3.2 Numeric linearization

Numeric linearization is carried out by perturbing the variables and thus finding the derivatives in the system matrices, see e.g. (Dennis & Schnabel 1996) and (Gill, Murray & Wright 1981). Assuming $\bar{x}_{k-1}$, $\bar{u}_{k-1}$ and $\bar{d}_{k-1}$ are available, one would typically use an algorithm similar to the following:

1. Using the nonlinear model and known variables, compute $\bar{x}_k$ and $\bar{y}_{k-1}$.

2. For every state variable:

   (a) Perturb state variable $\bar{x}_{k-1,i}$, by adding a small number $\Delta\bar{x}_{k-1,i}$ to its value. For example one may increase its value by one percent, or a predetermined minimum perturbation (e.g. if the variable value is zero we can not use the one percent rule).

   (b) Using the nonlinear model, compute $\bar{x}_k^{\text{pert}}$ and $\bar{y}_{k-1}^{\text{pert}}$.

   (c) The i'th column in matrix A_k is then

   $$\frac{\bar{x}_k^{\text{pert}} - \bar{x}_k}{\Delta\bar{x}_{k-1,i}}$$

   and the i'th column in matrix C_k is

   $$\frac{\bar{y}_{k-1}^{\text{pert}} - \bar{y}_{k-1}}{\Delta\bar{x}_{k-1,i}}$$

3. For every input variable:

   (a) Perturb input variable $\bar{u}_{k-1,i}$, by adding a small number $\Delta\bar{u}_{k-1,i}$ to its value.

   (b) Using the nonlinear model, compute $\bar{x}_k^{\text{pert}}$ and $\bar{y}_{k-1}^{\text{pert}}$.

   (c) The i'th column in matrix B_k is then

   $$\frac{\bar{x}_k^{\text{pert}} - \bar{x}_k}{\Delta\bar{u}_{k-1,i}}$$

   and the i'th column in matrix D_k is

   $$\frac{\bar{y}_{k-1}^{\text{pert}} - \bar{y}_{k-1}}{\Delta\bar{u}_{k-1,i}}$$

4. For every measured disturbance variable:

   (a) Perturb measured disturbance variable $\bar{d}_{k-1,i}$, by adding a small number $\Delta\bar{d}_{k-1,i}$ to its value.

   (b) Using the nonlinear model, compute $\bar{x}_k^{\text{pert}}$ and $\bar{y}_{k-1}^{\text{pert}}$.

   (c) The i'th column in matrix E_k is then

   $$\frac{\bar{x}_k^{\text{pert}} - \bar{x}_k}{\Delta\bar{d}_{k-1,i}}$$

   and the i'th column in matrix F_k is

   $$\frac{\bar{y}_{k-1}^{\text{pert}} - \bar{y}_{k-1}}{\Delta\bar{d}_{k-1,i}}$$

3.3 Example: Linearization of a chemical reactor model

A model of a chemical reactor (Lie 1995) is

$$\dot{C}_A = \frac{q}{V} \cdot (C_{Ai} - C_A) - k_0 \cdot e^{-\frac{E}{R \cdot T}} \cdot C_A \tag{13}$$
$$\dot{T} = \frac{q}{V} \cdot (T_i - T) + \frac{1}{\bar{C}_V} \cdot \left(-\Delta U_r \cdot k_0 \cdot e^{-\frac{E}{R \cdot T}} \cdot C_A \cdot V + Q \right)$$

The A matrix in the linearized model is then

$$A = \begin{bmatrix} \frac{\partial \dot{C}_A}{\partial C_A} & \frac{\partial \dot{C}_A}{\partial T} \\ \frac{\partial \dot{T}}{\partial C_A} & \frac{\partial \dot{T}}{\partial T} \end{bmatrix}$$
$$= \begin{bmatrix} -\frac{q}{V} - k_0 e^{-\frac{E}{RT}}, & -\frac{E}{RT^2} k_0 C_A e^{-\frac{E}{RT}} \\ \frac{1}{\bar{C}_V} \cdot -\Delta U_r \cdot k_0 \cdot e^{-\frac{E}{R \cdot T}} \cdot V, & -\frac{q}{V} - \frac{1}{\bar{C}_V} \cdot \Delta U_r \cdot k_0 \cdot \frac{E}{RT^2} \cdot e^{-\frac{E}{R \cdot T}} \cdot C_A \cdot V \end{bmatrix}$$

With appropriate parameter values and operating point, as given in (Lie 1995), we have

$$A_{\text{analytic}} = \begin{bmatrix} -19.998 & -4.6209 \cdot 10^{-2} \\ 3824.4 & 8.3018 \end{bmatrix}$$

Numeric linearization, with a perturbation according to 1% of the state values, gives the following A matrix

$$A_{\text{numeric}} = \begin{bmatrix} -19.998 & -5.1131 \cdot 10^{-2} \\ 3824.4 & 9.2926 \end{bmatrix}$$

which is close to the analytic A matrix. The reactor is highly nonlinear and we try with a smaller perturbation corresponding to 0.1% of the state values. This gives

$$A_{\text{numeric},0.1\%} = \begin{bmatrix} -19.998 & -4.6675 \cdot 10^{-2} \\ 3824.4 & 8.3956 \end{bmatrix}$$

which is seen to be even closer to the analytic solution.

This example has shown the possibilities of analytic and numeric linearization, as well as the difficulty of choosing a proper perturbation for numeric linearization.

4 Model predictive controller (MPC)

Commercial MPC algorithms often consists of two stages (Qin & Badgwell 1997), first steady state values (or target values) are calculated, and then these values are used as targets in the calculation of the optimal input values. The calculation of steady state values is a way of ensuring that the targets are feasible. In addition, by calculating steady state values one has the opportunity to add e.g. an economic type criterion if there are additional degrees of freedom. Finally, for the special case of an infinite horizon criterion with the possibility of changing future references and

measured disturbances, we need the steady state values at the end of the horizon in order to shift the origin of the model. The model origin is shifted so that the variables in the criterion converges exponentially to a zero steady state, thus avoiding an infinite value of the criterion.

4.1 Steady state values

We assume that a linearized model (eq. 12) and the adjusted reference vector $\bar{\bar{r}}_{k+j}$ and disturbance vector $\bar{\bar{d}}_{k+j}$ are available (at time k):

$$\begin{aligned} \bar{\bar{r}}_{k+j} &= \bar{r}_{k+j} - \bar{y}_{k-1},\ j = 0, ..., N-1 \\ \bar{\bar{d}}_{k+j} &= \bar{d}_{k+j} - \bar{d}_{k-1},\ j = 0, ..., N-1, \end{aligned} \tag{14}$$

The future reference and disturbance vectors are provided by the process operators or simply taken as an extention of the present values into the future. N is a chosen control horizon where we allow input changes.

At each future time sample we calculate target values for the states and inputs of the process. The target values may be calculated using an economic criterion, or calculated as e.g.

$$\min_{\bar{x}^s_{k+j}, \bar{u}^s_{k+j}} \left(\bar{y}^s_{k+j} - \bar{\bar{r}}_{k+j}\right)^T Q_s \left(\bar{y}^s_{k+j} - \bar{\bar{r}}_{k+j}\right),\ \forall j = 0, ..., N-1, \tag{15}$$

constrained by the steady state solution of the model

$$\begin{bmatrix} (I - A_k) & -B_k \\ -C_k & -D_k \end{bmatrix} \begin{bmatrix} \bar{x}^s_{k+j} \\ \bar{u}^s_{k+j} \end{bmatrix} = \begin{bmatrix} E_k \bar{\bar{d}}_{k+j} \\ F_k \bar{\bar{d}}_{k+j} - \bar{y}^s_{k+j} \end{bmatrix},\ \forall j = 0, ..., N-1, \tag{16}$$

with bounds

$$\begin{aligned} \bar{u}^{\min}_{k+j} \le \bar{u}^s_{k+j} + \bar{u}_{k-1} \le \bar{u}^{\max}_{k+j},\ \forall j = 0, ..., N-1 \\ \bar{y}^{\min}_{k+j} \le \bar{y}^s_{k+j} + \bar{y}_{k-1} \le \bar{y}^{\max}_{k+j},\ \forall j = 0, ..., N-1, \end{aligned} \tag{17}$$

where $\bar{y}^{\min}_{k+j}$, $\bar{y}^{\max}_{k+j}$, $\bar{u}^{\min}_{k+j}$, and $\bar{u}^{\max}_{k+j}$ are minimum and maximum values corresponding to the original nonlinear model. If there are additional degrees of freedom we may specify an economic type criterion instead of eq. 15, and use eqs. 16-17 as constraints. In Appendix B it is shown how one may use the `lssol` algorithm (Gill, Hammarling, Murray, Saunders & Wright 1986) for calculating the steady state values.

The origin of the model is then shifted to the steady state values at time $N-1$

$$\left(\bar{\bar{x}}_{k+1} - \bar{x}^s_{k+N-1}\right) = A_k \left(\bar{\bar{x}}_k - \bar{x}^s_{k+N-1}\right) + B_k \left(\bar{\bar{u}}_k - \bar{u}^s_{k+N-1}\right) + E_k \left(\bar{\bar{d}}_k - \bar{\bar{d}}_{k+N-1}\right) \tag{18}$$

$$\left(\bar{\bar{y}}_k - \bar{y}^s_{k+N-1}\right) = C_k \left(\bar{\bar{x}}_k - \bar{x}^s_{k+N-1}\right) + D_k \left(\bar{\bar{u}}_k - \bar{u}^s_{k+N-1}\right) + F_k \left(\bar{\bar{d}}_k - \bar{\bar{d}}_{k+N-1}\right),$$

which gives the shifted model

$$\begin{aligned} x_{k+1} &= A_k x_k + B_k u_k + E_k d_k \\ y_k &= C_k x_k + D_k u_k + F_k d_k, \end{aligned} \tag{19}$$

where

$$\begin{aligned} x_{k+1} &= \bar{\bar{x}}_{k+1} - \bar{x}^s_{k+N-1} \\ x_k &= \bar{\bar{x}}_k - \bar{x}^s_{k+N-1} \\ u_k &= \bar{\bar{u}}_k - \bar{u}^s_{k+N-1} \\ d_k &= \bar{\bar{d}}_k - \bar{\bar{d}}_{k+N-1} \\ y_k &= \bar{\bar{y}}_k - \bar{y}^s_{k+N-1} \end{aligned} \tag{20}$$

The shifting of model origin to the steady state values at time $N-1$ makes the variables in the criterion converge exponentially to zero in steady state, thus ensuring a finite value of the criterion.

4.1.1 Shifting variables

The model origin is shifted twice, once during the linearization and once after the computation of steady state (target) values. The measured, estimated and calculated variables must be shifted along with the model as follows

$$\begin{aligned} \hat{x}_k &= \hat{\bar{x}}_k - \hat{\bar{x}}_{k-1} - \bar{x}^s_{k+N-1} \\ u_{k-1} &= \bar{u}_{k-1} - \bar{u}_{k-1} - \bar{u}^s_{k+N-1} = -\bar{u}^s_{k+N-1} \\ d_{k+i} &= \bar{d}_{k+i} - \bar{d}_{k-1} - \bar{\bar{d}}_{k+N-1},\ i = 0, ..., N-1 \\ u^s_{k+i} &= \bar{u}^s_{k+i} - \bar{u}^s_{k+N-1},\ i = 0, ..., N-1 \\ y^s_{k+i} &= \bar{y}^s_{k+i} - \bar{y}^s_{k+N-1},\ i = 0, ..., N-1 \end{aligned} \tag{21}$$

4.2 Optimal input values

This section is based on the algorithm presented in (Muske & Rawlings 1993), although several extensions are made, notably the inclusion of future reference and disturbance trajectories.

The infinite horizon criterion is

$$\min_{\mathcal{U}_k} J_k = \min_{\mathcal{U}_k} \sum_{j=0}^{\infty} \left[e^T_{k+j} Q e_{k+j} + \tilde{u}^T_{k+j} R \tilde{u}_{k+j} + \Delta u^T_{k+j} S \Delta u_{k+j} \right], \tag{22}$$

constrained by the model in eq. 19, i.e.

$$\begin{aligned} x_{k+1+j} &= A x_{k+j} + B u_{k+j} + E d_{k+j},\ \forall j = 0, 1, 2, ... \\ y_{k+j} &= C x_{k+j} + D u_{k+j} + F d_{k+j},\ \forall j = 0, 1, 2, ..., \end{aligned} \tag{23}$$

and the following inequality constraints

$$\begin{aligned} \bar{u}_{k+j}^{\min} \leq \bar{u}_{k+j} \leq \bar{u}_{k+j}^{\max},\ j = 0, 1, ..., N-1 \\ \bar{y}_{k+j}^{\min} \leq \bar{y}_{k+j} \leq \bar{y}_{k+j}^{\max},\ j = j_1, j_1+1, ..., j_2 \\ \Delta u_{k+j}^{\min} \leq \Delta u_{k+j} \leq \Delta u_{k+j}^{\max},\ j = 0, 1, ..., N, \end{aligned} \tag{24}$$

and where

$$\begin{aligned} e_{k+j} &= y_{k+j} - y_{k+j}^s \\ \tilde{u}_{k+j} &= u_{k+j} - u_{k+j}^s \\ \Delta u_{k+j} &= u_{k+j} - u_{k+j-1} \\ \mathcal{U}_k &= \left[u_k^T, u_{k+1}^T, ..., u_{k+N-1}^T\right]^T. \end{aligned} \tag{25}$$

The output constraints are active from sample $k+j_1$ to $k+j_2$. j_1 should be chosen so that feasibility is ensured from $k+j_1$, and j_2 should be chosen such that feasibility up to $k+j_2$ implies feasibility on the infinite horizon. Bounds for j_1 and j_2, so that feasibility is guaranteed, are developed in (Rawlings & Muske 1993).

Consider the Jordan decomposition of A_k

$$A_k = V_k J_k V_k^{-1} = \begin{bmatrix} V_k^u & V_k^s \end{bmatrix} \begin{bmatrix} J_k^u & 0 \\ 0 & J_k^s \end{bmatrix} \begin{bmatrix} \tilde{V}_k^u \\ \tilde{V}_k^s \end{bmatrix}, \tag{26}$$

where V_k^u and J_k^u are respectively the eigenvectors and Jordan blocks for the eigenvalues corresponding to the unstable modes of A_k, and V_k^s and J_k^s are respectively the eigenvectors and Jordan blocks for the eigenvalues corresponding to the stable modes of A_k. The following results can then be obtained.

Theorem 1 *Consider the model given by eq. 19, the criterion of eq. 22, and the definitions provided by eq. 25. Assume that*

$$u_{k+j} = 0, \forall j \in \{N, N+1, ...\}\text{, which is equivalent to } \bar{\bar{u}}_{k+j} = \bar{u}_{k+N-1}^s, \forall j \in \{N, N+1, ...\} \tag{27}$$

$$\begin{aligned} &d_{k+j} = 0, \forall j \in \{N, N+1, ...\}\text{, which is equivalent to } \bar{\bar{d}}_{k+j} = \bar{\bar{d}}_{k+N-1}, \forall j \in \{N, N+1, ...\} \\ &u_{k+j}^s = 0, \forall j \in \{N, N+1, ...\}\text{, which is equivalent to } \bar{u}_{k+j}^s = \bar{u}_{k+N-1}^s, \forall j \in \{N, N+1, ...\} \\ &y_{k+j}^s = 0, \forall j \in \{N, N+1, ...\}\text{, which is equivalent to } \bar{y}_{k+j}^s = \bar{y}_{k+N-1}^s, \forall j \in \{N, N+1, ...\}, \end{aligned}$$

thus there are no changes in the inputs, measured disturbances, or steady state inputs and outputs, from sample N and forward. If in addition we add the equality constraint (ref. eq. 26)

$$\tilde{V}_k^u x_{k+N} = 0, \tag{28}$$

which corresponds to bringing the unstable modes to zero at time $k+N$, then the

infinite horizon criterion can be written as the following finite horizon criterion

$$\min_{\mathcal{U}_k} J_k = \min_{\mathcal{U}_k} \left(x_{k+N}^T \left(\tilde{V}_k^s\right)^T \bar{Q}_k \tilde{V}_k^s x_{k+N} + \Delta u_{k+N}^T S \Delta u_{k+N} + \sum_{j=0}^{N-1} \left[e_{k+j}^T Q e_{k+j} + \tilde{u}_{k+j}^T R \tilde{u}_{k+j} + \Delta u_{k+j}^T S \Delta u_{k+j} \right] \right), \tag{29}$$

with $\bar{Q}_k$ given by the discrete Lyapunov equation

$$\bar{Q}_k = \left(V_k^s\right)^T C_k^T Q C_k V_k^s + \left(J_k^s\right)^T \bar{Q}_k J_k^s, \tag{30}$$

Proof. See Appendix C.1. ■

Proposition 2 *Consider the model given by eq. 19, the criterion of eq. 22, the inequality constraints given by eq. 24, the equality constraint given in eq. 28, and the definitions and assumptions provided by eqs. 25 and 27. This minimization problem can be formulated as the following standard constrained QP (Quadratic Programming) problem*

$$\min_{\mathcal{U}_k} J_k = \min_{\mathcal{U}_k} \left(\frac{1}{2} \mathcal{U}_k^T H_k \mathcal{U}_k + c_k^T \mathcal{U}_k \right), \tag{31}$$

subject to

$$b_{L,k} \leq \begin{bmatrix} \mathcal{U}_k \\ \bar{A}_k \mathcal{U}_k \end{bmatrix} \leq b_{U,k} \tag{32}$$

where

$$
\begin{aligned}
H_k &= 2\left(\left(P^u\right)^T \left(C_k^u\right)^T \left(\tilde{V}_k^s\right)^T \bar{Q}_k \tilde{V}_k^s C_k^u P^u + \mathcal{P}^T \left(I_{N+1} \otimes S\right) \mathcal{P} \right. \\
&\quad \left. + \left(\mathcal{H}_k^u\right)^T \left(I_N \otimes Q\right) \mathcal{H}_k^u + \left(I_N \otimes R\right) \right) \\
c_k^T &= 2\left(x_k^T \left(A_k^N\right)^T \left(\tilde{V}_k^s\right)^T \bar{Q}_k \tilde{V}_k^s C_k^u P^u + \mathcal{D}_k^T \left(P^d\right)^T \left(C_k^d\right)^T \left(\tilde{V}_k^s\right)^T \bar{Q}_k \tilde{V}_k^s C_k^u P^u \right. \\
&\quad + u_{k-1}^T \mathcal{L}^T \left(I_{N+1} \otimes S\right) \mathcal{P} + x_k^T \mathcal{O}_k^T \left(I_N \otimes Q\right) \mathcal{H}_k^u + \mathcal{D}_k^T \left(\mathcal{H}_k^d\right)^T \left(I_N \otimes Q\right) \mathcal{H}_k^u \\
&\quad \left. - \left(Y_k^s\right)^T \left(I_N \otimes Q\right) \mathcal{H}_k^u - \left(\mathcal{U}_k^s\right)^T \left(I_N \otimes R\right) \right) \\
\bar{A}_k &= \begin{bmatrix} \mathcal{H}_k^u \\ \mathcal{P} \\ \tilde{V}_k^u C_k^u P^u \end{bmatrix} \\
b_{L,k} &= \begin{bmatrix} \mathcal{U}_k^{min} - \bar{u}_{k-1} \otimes \mathbf{1}_N - \bar{u}_{k+N-1}^s \otimes \mathbf{1}_N \\ \mathcal{Y}_k^{min} - \bar{y}_{k-1} \otimes \mathbf{1}_N - \bar{y}_{k+N-1}^s \otimes \mathbf{1}_N - \mathcal{O}_k x_k - \mathcal{H}_k^d \mathcal{D}_k \\ \Delta \mathcal{U}_k^{min} - \mathcal{L} u_{k-1} \\ -\tilde{V}_k^u \left(A_k^N x_k + C_k^d P^d \mathcal{D}_k\right) \end{bmatrix} \\
b_{U,k} &= \begin{bmatrix} \mathcal{U}_k^{max} - \bar{u}_{k-1} \otimes \mathbf{1}_N - \bar{u}_{k+N-1}^s \otimes \mathbf{1}_N \\ \mathcal{Y}_k^{max} - \bar{y}_{k-1} \otimes \mathbf{1}_N - \bar{y}_{k+N-1}^s \otimes \mathbf{1}_N - \mathcal{O}_k x_k - \mathcal{H}_k^d \mathcal{D}_k \\ \Delta \mathcal{U}_k^{max} - \mathcal{L} u_{k-1} \\ -\tilde{V}_k^u \left(A_k^N x_k + C_k^d P^d \mathcal{D}_k\right) \end{bmatrix}
\end{aligned} \tag{33}
$$

and definitions of $\mathcal{P}$ *,*$\mathcal{H}_k^u$*,* $\mathcal{D}_k$*,* $\mathcal{H}_k^d$*,* $\mathcal{O}_k$*, etc. are provided in Appendix C.2.* $\otimes$ *denotes the Kronecker product.*

Proof. See Appendices C.1-C.2. ■

A possible choice of QP solver is `sqopt` which solves problems in the form of eqs. 31–32. The `sqopt` algorithm for solving constrained linear and quadratic problems (Gill, Murray & Saunders 1997), is available with a Matlab interface in the Tomlab environment (Holmström 2001). Other formulations, choice of QP solvers, and variables are investigated more thoroughly in (Lie, Dueñas Díez & Hauge 2002).

5 Estimating the states and parameters

Using a state space model in an MPC application, as in the previous section, requires estimation of the states unless all states are measured. A Kalman filter is used at PM6 for estimating the states in the paper machine model. The Kalman filter equations for a linear time variant process are derived in Appendix D.1. The paper machine model is nonlinear and thus an extended Kalman filter is used for estimating the states in the model. An algorithm for estimating the states in a nonlinear model is reviewed in Appendix D.2.

Due to disturbances and model errors, the MPC presented in previous sections is likely to exhibit steady state offset from the setpoints. The most common way

to handle this problem is to assume a step disturbance at the model outputs and estimate the size of the step in a deadbeat fashion (Qin & Badgwell 1997), (Muske & Rawlings 1993). Other methods also exist, such as assuming the disturbance to originate from the process inputs (Muske & Rawlings 1993). In (Muske & Badgwell 2002) various disturbance models which provide offset-free control are discussed, and conditions for offset-free control are developed. In Appendix D.3 we have shown how the MPC and Kalman filter can be redesigned to prevent steady state offset by estimating the bias and adding this to the model outputs. Although this is the most commonly used method for removing steady state offset, it is often a poor method for solving the problem, notably if the disturbances enters the inputs or states (Muske & Rawlings 1993), (Muske & Badgwell 2002). The main point is that offset-free control can be obtained with many different disturbance models, however to obtain best possible performance the disturbance should be included in the model where it enters in the real process.

The question of where the disturbances enter in a real process is easy to answer: everywhere. As pointed out in (Muske & Badgwell 2002), only a limited number of biases or parameters can be estimated on-line, thus the choice of which parameters or biases to estimate must be based on experience with the process and model. Three biases have been selected for on-line estimation in the paper machine model. The first two are biases on the estimated total- and filler thick stock consistencies (see eq. 3). These disturbances are estimated using a ballistic estimator (Slora 2001), and thus they are assumed to be good candidates for having time-varying biases. The third bias estimated on-line is for the total wire tray concentration, i.e. a bias in one of the outputs. In Appendix D.4 we have shown how arbitrary parameters and biases in the model can be estimated on-line by an augmented Kalman filter. It is also shown how the linearization, calculation of steady state values, and optimization may be carried out on the augmented system.

5.1 Tuning and validation

In theory, and in the true Kalman filter, the noise characteristics of the process should be found and used in the Kalman filter equations. However, these characteristics are hard, if not impossible, to find. Thus, one often aims for a suboptimal Kalman filter, where the noise characteristics are used as tuning parameters until satisfactory Kalman filter performance is obtained. Specifically, the tuning parameters are the process noise covariance matrix Q_k and the measurement noise covariance matrix R_k. In the augmented Kalman filter (as described in section D.4), the augmented process noise covariance matrix $\tilde{Q}_k$ is used. Often, it is assumed that only diagonal elements are non-zero. Thus, for the paper machine model there are three diagonal elements in R_k (three outputs), and six diagonal elements in $\tilde{Q}_k$ (three states plus three estimated parameters). The first element (upper left corner) in R_k corresponds to the variance of the basis weight measurement, the second element (the element on the second row and second column) in R_k corresponds to the variance of the paper ash measurement, etc. Similarly for the diagonal elements in $\tilde{Q}_k$, the first diagonal element corresponds to the variance of the first state variable (the concentration of filler in the reject

tank), and e.g. the last element on the diagonal corresponds to the variance of the last parameter to be estimated (bias in the wire tray total concentration).

When tuning and validating the (suboptimal) Kalman filter, we have used a few facts and rules of thumb, e.g.:

- The tuning and validation (with different data sets) should aim at good tracking properties (i.e. the estimated outputs should follow the measured outputs to some extent), good filtering properties (i.e. the estimated outputs should not track measurement noise), and a sound balance between the updating of states and updating of parameters (e.g. the parameters should not vary a lot while the states are more or less resting).

- It can be shown that it is the ratio of the various variances that determines the performance of the Kalman filter. Thus, one need not be careful about finding realistic variance values.

- It is possible to estimate the variances, using a parameter estimation method. This is done for a constant gain Kalman filter (i.e. the individual variances are not estimated, but the Kalman filter gain matrix is estimated) in (Hauge & Lie 2002). The drawback with this method is that the Kalman filter will be rather aggressive, and some de-tuning procedure is needed (but it may give a good starting point).

- Start the tuning by finding approximate values for the various variances. The measurement variances can be approximately found by visually studying the random variations in the measurements. It is harder to find suitable starting values for the process noise variances and the parameter estimate variances. However, the expected state and parameter values will give good indications of reasonable starting values. Consider e.g. a concentration that is expected to have a value around 0.05 (5%). If one assumes that the noise entering this state is approximately 1% of the state value, we see that the variance will be a very small number. In the Kalman filter used at PM6, the measurement variances are much larger than the process and parameter variances (around 10^8 larger).

- In general, increasing the measurement variances leads to a slower updating of state estimates. The same result is obtained by decreasing the process variance. Thus, decreasing the process variance leads to a slower updating of state estimates.

- Since the parameters are augmented states, changing the parameter variances has much of the same effect as changing the state variances. Increasing the parameter variances leads to a faster updating of parameter estimates, thus also leading to a faster elimination of estimation error (the difference between estimated outputs and measured outputs).

Validation results for the augmented Kalman filter are shown in Figures 2-4 .

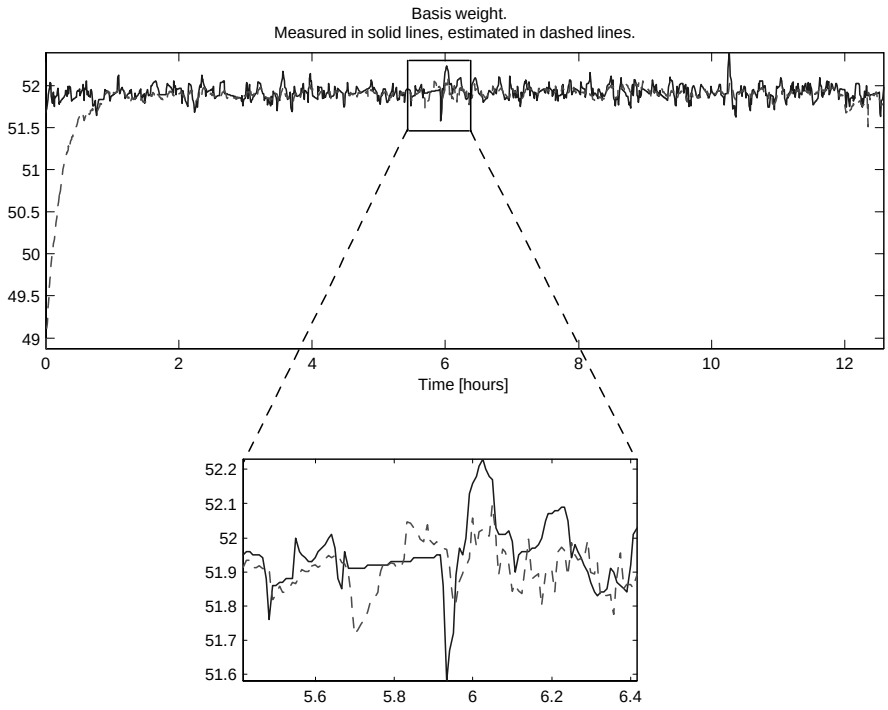

Figure 2: Validation of Kalman filter performance. The measured basis weight is shown in solid line and the estimated is shown in dashed line.

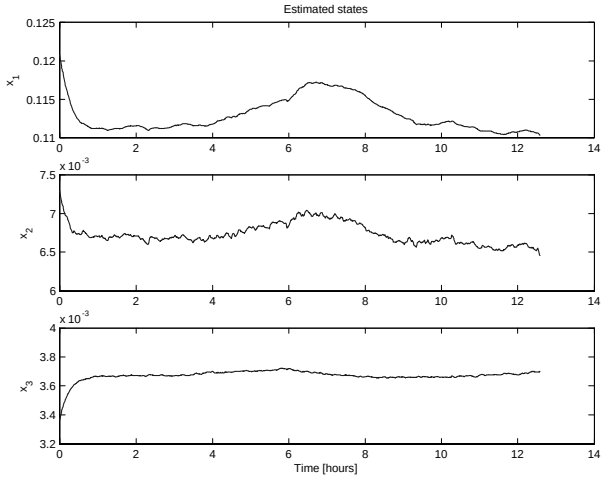

Figure 3: The estimated states for the validation shown in Figure 2.

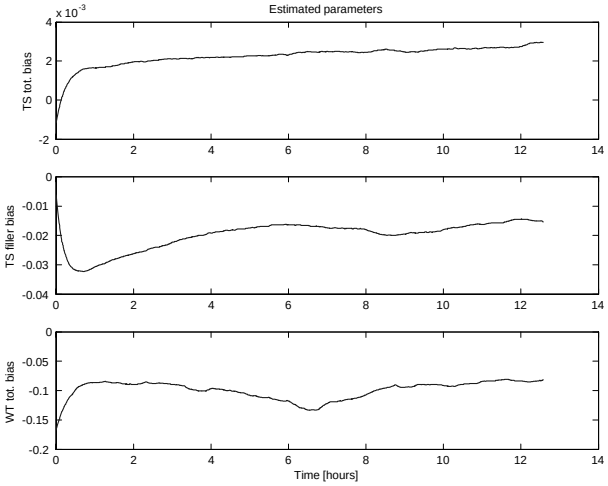

Figure 4: The estimated parameters for the validation shown in Figure 2.

6 Results

6.1 Implementation and interface

The MPC was installed at PM6 in March 2002. During the first two months, the MPC, the Kalman filter and the model were continuously tuned, retuned, and validated in open and closed loop. Some structural changes were also made during these months. From May 2002, the MPC has been in operation more or less continuously. The process operators still have the original "pre-MPC era" control configuration available, but the MPC has been the preferred choice from the beginning. Furthermore, the operators have been very active in making suggestions for improvements and new features in the system. Some of these suggestions are implemented, and others are being considered for implementation.

In addition to discussing and involving the operators in the project from the beginning, it is our opinion that the MPC interface has been very important for the positive operator attitude. Figure 5 shows part of the MPC interface at PM6. The upper row in the figure shows the basis weight, setpoint for basis weight, and the flow of thick stock. The middle row shows the paper ash, setpoint for paper ash, and the flow of filler added to the short circulation. The lower row shows the total concentration in the wire tray, the corresponding setpoint, and the flow of retention aid added to the short circulation. The interface and pairing of inputs and outputs are based on the pre-MPC control configuration, basically because this is how the operators and engineers at PM6 are used to see it. The vertical dashed line in the middle of each row is the current time. When Figure 5 was captured, the paper machine was in the middle of a grade change, and studying the figure carefully, one may see the setpoints change at the current time. The setpoints for the new grade were submitted to the MPC some time before the grade change, so at the time of the grade change the outputs are actually half way to the new setpoints. In terms of gaining operator acceptance for the MPC, this feature of previewing the action taken by the controller has been very helpful. The operators can specify a grade change e.g. half an hour into the future, and see how the MPC will achieve the change: how the inputs will be manipulated to reach the new setpoints.

6.2 Reduction of variation

An important objective with the MPC was to reduce variation in consistencies, basis weigh, paper ash, paper moisture, and more. Figure 6 shows and example with the wire tray concentration and the paper ash. The bottom line indicates whether the MPC is on (at 1) or off (at 0). When the controller is off, the original control configuration is used. The MPC provides a distinct effect of reduced variation in these two outputs.

The main objective of the project "Stabilization of the wet end at PM6" was to increase the total efficiency by 0.47%. This is an objective that is unmeasurable, due to many factors affecting the total efficiency. Thus, several sub-goals were defined which were assumed easier to measure and validate. The sub-goals, and results,

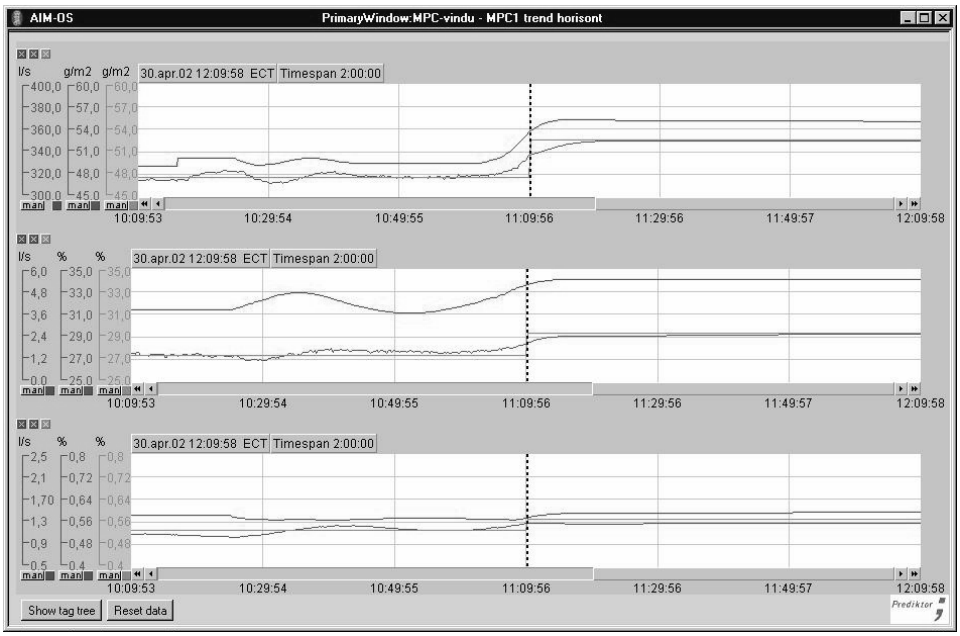

Figure 5: Part of the MPC interface at PM6.

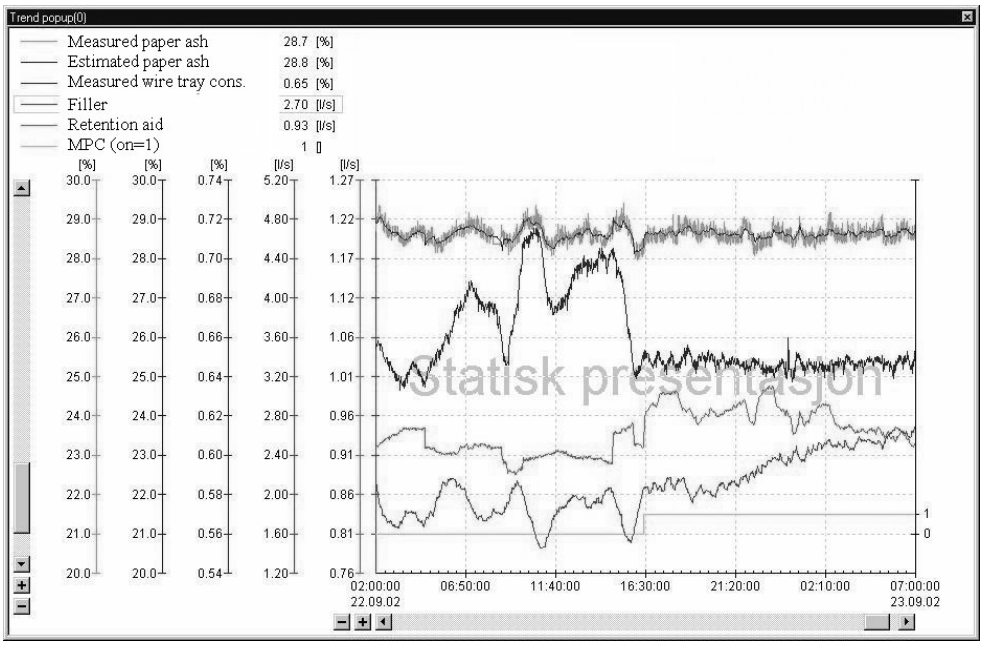

Figure 6: Wire tray concentration and paper ash, with (bottom line is 1) and without (bottom line is 0) MPC. From top to bottom the following variables are shown: Measured and estimated paper ash (overlapping), wire tray total concentration, retention aid, filler, and MPC on/off indication.

concerning reduced variability are:

Variable	Sub-goal (red. std. dev.)	Result
Total cons. in the wire tray	60%	OK
Filler cons. in the wire tray	50%	OK
Total cons. in the headbox	50%	OK
Filler cons. in the headbox	35%	OK
Basis weight	20%	No change achieved
Paper ash	20%	OK
Paper moisture	20%	OK

These sub-goals were defined in 1999 when the project was initiated. In 2001 a new scanning device for measuring e.g. basis weight and paper ash was installed at PM6. This significantly improved the control of the basis weight using the "old" controllers. The results in the table above are calculated with the measurement devices as of 2002, comparing the old control configuration with the MPC control configuration. Exact numbers for the reduction in standard deviation are not given, as they vary from day to day, and from operator to operator.

6.3 Other benefits of MPC

In addition to reducing the variation in key paper machine variables, several other benefits are obtained using MPC. Some of these benefits arise from utilizing the developed model, not only for control purposes, but also as a replacement for measurements when these are not available or not trustworthy.

Grade changes in automatic mode Previously, grade changes were carried out manually or partly manually (the setpoints were changed a number of times before they were equal to the new grade) by the operators. With a mechanistic model, applicable over a wide range of operating conditions, the grade changes are carried out using the MPC (see Figure 5). This has resulted in faster grade changes and operator independent grade changes. During larger grade changes, the use of MPC results in less off-spec paper being produced during the change. Using one mechanistic model, the grade change is handled in a straight forward fashion, as there is no need to switch between various local models.

Control during sheet breaks The basis weight and paper ash outputs can not be measured during sheet breaks. Previously, during sheet breaks the flow of thick stock and filler were frozen at the value they had immediately prior to the break. Usually the sheet breaks last less than half an hour, and the output variables are not far from target values when the paper is back on the reel. However, occasionally the sheet breaks last longer periods and there may be e.g. velocity changes during the break, leading to off-spec paper being produced for a period following the break. Another frequently experienced problem are large measurement errors immediately

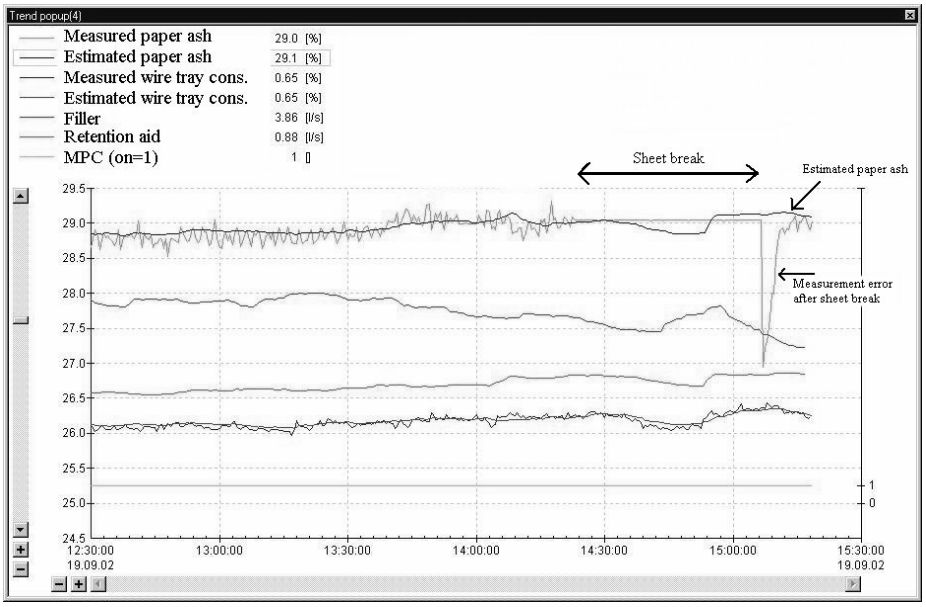

Figure 7: Sheet break. From top to bottom the following variables are shown: Measured and estimated paper ash (overlapping), filler, retention aid, measured and estimated wire tray total concentration (overlapping),and MPC on/off indication.

after a sheet break. With the MPC, the Kalman filter estimates the basis weight and paper ash during sheet breaks, and these estimates are used in the MPC as if no break had taken place. Thus, when the paper is back on the reel, the outputs are close to their setpoints.

In Figure 7 a sheet break, followed by a large measurement error, is shown. The two lines at the top are the measured and estimated paper ash (the lines are overlapping to some extent). During the sheet break the measured value is lost, and thus frozen at the value immediately prior to the break. When the paper is back on the reel, a large measurement error occurs giving a difference between measured and estimated value above 2%. The measured value converges to the estimated value before the estimate is updated in the Kalman filter. The MPC use the estimated values and is thus unaffected by the erroneous measurement. Studying the inputs, it is obvious that it is the measurement that is erroneous, and not the estimate. The rise in measured paper ash from approximately 27% to 29% in less than 10 minutes is too fast to be realistic by itself, and the fact that this happens during a period when the dosage of retention aid is constant and the filler is decreasing is very hard to explain.

Control during start ups Previously, the controllers were not set to automatic mode before the outputs were close to the setpoints, following a start up. With a model based controller using a mechanistic model with a wide operating range, the MPC is set to automatic mode early during start ups. This results in faster start ups, and less off-spec paper being produced.

Control during periods with poor measurements Occasionally a special filler is added to the stock, to increase the brightness of the paper. During these periods the consistency measurements are not trustworthy as they are based on optical measurement methods. This problem is solved within the MPC / Kalman filter framework by neglecting the updates of the consistency estimate, relying on the estimate alone. For each output, there is an option within the MPC to neglect the updating of states based on this output. This is done based on experience with periods of poor measurements, even when only standard filler is used. Figures 8–9 show an example of a period of poor wire tray consistency measurement. There are large variations in all outputs in the first half of the period shown in the figures. When the MPC was switched on, the updating of states from the wire tray consistency measurement was switched off. The effect is pronounced, as the paper ash, basis weight, moisture, and also all inputs vary considerably less in this latter half. Note that the measurement of wire tray consistency is the only variable that varies equally much in the first and second halves.

Filtering of measurements The Kalman filter estimates are used in the MPC instead of the measurements. This leads to smoother controller action, and eliminates the need for additional filtering.

Updating of model parameters The model is augmented so that some key parameters/biases are updated automatically. This reduces the need for model maintenance off-line. However, should there be larger changes in the process, such as if the white water tank is removed, or a new retention aid is used, then it will probably be necessary to re-tune the model and controller.

7 Conclusions

A mechanistic nonlinear model of the wet end of PM6 at Norske Skog Saugbrugs has been developed and used in an MPC application. The MPC uses an infinite horizon criterion, successive linearization of the model, and estimation of states and parameters by an augmented Kalman filter.

Variation in important quality variables and consistencies in the wet end have been reduced substantially, compared to the variation prior to the MPC implementation. The MPC also provides better efficiency through faster grade changes, control during sheet breaks and start ups, and better control during periods of poor measurements.

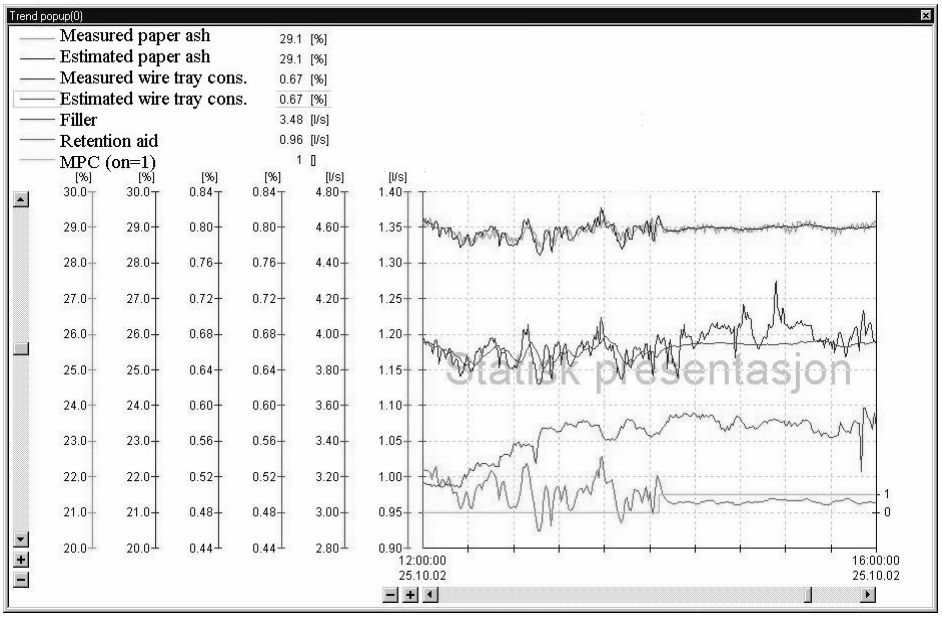

Figure 8: Period of poor wire tray consistency measurement. During the second half, the controller relies on the estimated consistency, rather than the measured. From top to bottom the following variables are shown: Measured and estimated paper ash (overlapping), measured and estimated wire tray total concentration (overlapping), filler, retention aid, and MPC on/off indication.

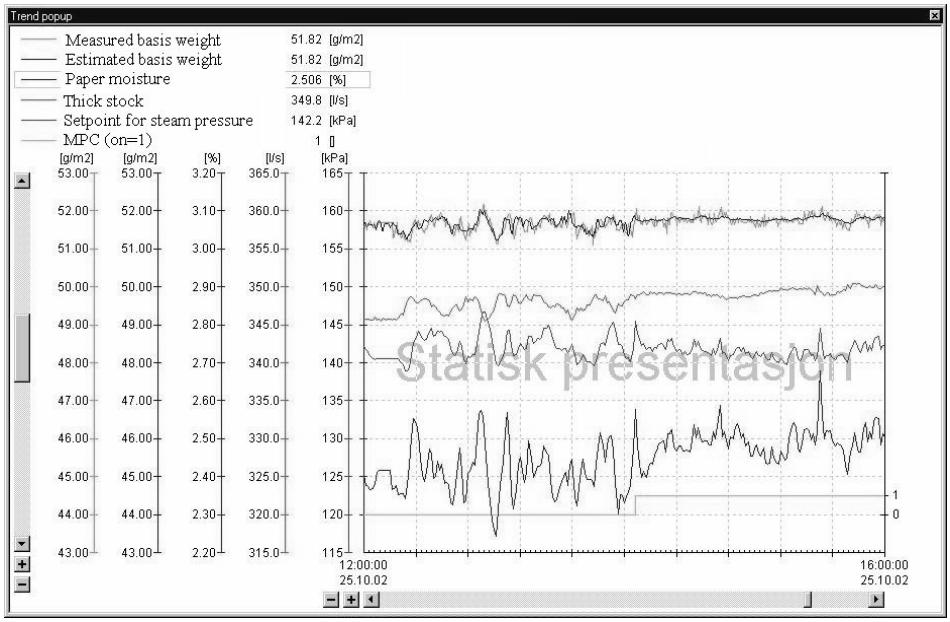

Figure 9: Period of poor wire tray consistency measurement. During the second half, the controller relies on the estimated consistency, rather than the measured. From top to bottom the following variables are shown: Measured and estimated basis weight (overlapping), flow of thick stock, setpoint for steam pressure, paper moisture, and MPC on/off indication.

Acknowledgements The authors would like to thank the employees at PM6 for their cooperation in providing information and data for this paper, and for their general helpfulness. Steinar Sælid and Anders Veberg from Prediktor AS are acknowledged for information about Apis and Apis MPC. The work of Tor Anders Hauge is financially supported by the Research Council of Norway (project number 134557/432), with additional financial support by Norske Skog Saugbrugs.

A Notes about notation

Variables in original units, i.e. unscaled and unshifted, are denoted by a bar above the variable, e.g. $\bar{x}$ and $\bar{u}$. Variables in the linearized model, i.e. variables that have origin corresponding to the center of linearization are denoted by a double bar above the variable, e.g. $\bar{\bar{x}}$ and $\bar{\bar{u}}$. Finally, variables shifted first by linearization and then by the steady state values at time $k+N-1$ are shown as e.g. x and u.

B Example: Finding the steady state values with `lssol`

The solution to eqs. 15-17 can be found by using standard optimization software. The `lssol` algorithm (Gill et al. 1986) for solving constrained linear least squares problems, is available with a Matlab interface in the Tomlab environment (Holmström 2001). The algorithm solves the following problems (amongst others)

$$\min_{z^s_{k+j}} J^s_{k+j} = \min_{z^s} \frac{1}{2}(b^s_{k+j} - A^s_{k+j} z^s_{k+j})^T (b^s_{k+j} - A^s_{k+j} z^s_{k+j}), \tag{34}$$

with constraints

$$b_{L,k+j} \leq \begin{bmatrix} z^s_{k+j} \\ \bar{A}_k z^s_{k+j} \end{bmatrix} \leq b_{U,k+j}, \tag{35}$$

where $j = 0, ..., N-1$ so that the optimization must in principle be carried out at each sample in the future horizon. In practice one would only calculate the steady state values once for every change in the future reference values, measured disturbance values, or max/min values.

The matrix A^s_{k+j} is then found in eq. 16 as

$$A^s_{k+j} = \begin{bmatrix} (I - A_k) & -B_k \\ -C_k & -D_k \end{bmatrix}, \tag{36}$$

while b^s_{k+j} is

$$b^s_{k+j} = \begin{bmatrix} E_k \bar{\bar{d}}_{k+j} \\ F_k \bar{\bar{d}}_{k+j} - \bar{y}^s_{k+j} \end{bmatrix}. \tag{37}$$

The constraints on $\bar{u}^s_{k+j}$ is

$$\bar{u}^{\min}_{k+j} - \bar{u}_{k-1} \leq \bar{u}^s_{k+j} \leq \bar{u}^{\max}_{k+j} - \bar{u}_{k-1},\ j = 0, ..., N-1 \tag{38}$$

and the constraints on $\bar{y}^s_{k+j}$ can be formulated as

$$\begin{aligned}
&\bar{y}^{\min}_{k+j} - \bar{y}_{k-1} \leq \bar{y}^s_{k+j} \leq \bar{y}^{\max}_{k+j} - \bar{y}_{k-1},\ j = 0, ..., N-1 \\
&\qquad\qquad \Downarrow \\
&\bar{y}^{\min}_{k+j} - \bar{y}_{k-1} \leq C_k \bar{x}^s_{k+j} + D_k \bar{u}^s_{k+j} \leq \bar{y}^{\max}_{k+j} - \bar{y}_{k-1},\ j = 0, ..., N-1 \\
&\qquad\qquad \Downarrow \\
\bar{y}^{\min}_{k+j} - \bar{y}_{k-1} - F_k \overline{\overline{d}}_{k+j} \leq &\begin{bmatrix} C_k & D_k \end{bmatrix} \begin{bmatrix} \bar{x}^s_{k+j} \\ \bar{u}^s_{k+j} \end{bmatrix} \leq \bar{y}^{\max}_{k+j} - \bar{y}_{k-1} - F_k \overline{\overline{d}}_{k+j} \\
&, j = 0, ..., N-1.
\end{aligned} \tag{39}$$

The constraints can then be written, as in eq. 35, as

$$\begin{aligned}
b_{L,k+j} &= \begin{bmatrix} -\infty \\ \bar{u}^{\min}_{k+j} - \bar{u}_{k-1} \\ \bar{y}^{\min}_{k+j} - \bar{y}_{k-1} - F_k \overline{\overline{d}}_{k+j} \end{bmatrix},\ j = 0, ..., N-1 \\
b_{U,k+j} &= \begin{bmatrix} \infty \\ \bar{u}^{\max}_{k+j} - \bar{u}_{k-1} \\ \bar{y}^{\max}_{k+j} - \bar{y}_{k-1} - F_k \overline{\overline{d}}_{k+j} \end{bmatrix},\ j = 0, ..., N-1 \\
\bar{A}_k &= \begin{bmatrix} C_k & D_k \end{bmatrix}.
\end{aligned} \tag{40}$$

C Proofs for finite horizon criterion

C.1 Reduction to finite horizon criterion

We split the infinite horizon criterion in two sums

$$\begin{aligned}
\min_{\mathcal{U}_k} J_k &= \min_{\mathcal{U}_k} \sum_{j=0}^{\infty} \left[e^T_{k+j} Q e_{k+j} + \tilde{u}^T_{k+j} R \tilde{u}_{k+j} + \Delta u^T_{k+j} S \Delta u_{k+j} \right] \\
&= \min_{\mathcal{U}_k} \left(\sum_{j=N}^{\infty} \left[e^T_{k+j} Q e_{k+j} + \tilde{u}^T_{k+j} R \tilde{u}_{k+j} + \Delta u^T_{k+j} S \Delta u_{k+j} \right] \right. \\
&\quad \left. + \sum_{j=0}^{N-1} \left[e^T_{k+j} Q e_{k+j} + \tilde{u}^T_{k+j} R \tilde{u}_{k+j} + \Delta u^T_{k+j} S \Delta u_{k+j} \right] \right),
\end{aligned} \tag{41}$$

where the sum from zero to $N-1$ can be easily calculated, while the infinite sum from N to infinity must be studied carefully. We take a closer look at each of the

three terms in that part of the criterion where the sum is infinite. First we study the $\tilde{u}$ term:

$$\sum_{j=N}^{\infty} \tilde{u}_{k+j}^T R \tilde{u}_{k+j} = \sum_{j=N}^{\infty} \left(u_{k+j} - u_{k+j}^s\right)^T R \left(u_{k+j} - u_{k+j}^s\right) = 0 \tag{42}$$

which is a direct consequence of the definition of $\tilde{u}_{k+j}$ in eq. 25, and the assumptions in eq. 27. We then study the Δu term:

$$\sum_{j=N}^{\infty} \Delta u_{k+j}^T S \Delta u_{k+j} = \Delta u_{k+N}^T S \Delta u_{k+N}, \tag{43}$$

because of assumptions made in eq. 27. Finally we study the e term:

$$\begin{aligned}
\sum_{j=N}^{\infty} e_{k+j}^T Q e_{k+j} &= \sum_{j=N}^{\infty} \left(y_{k+j} - \overbrace{y_{k+j}^s}^{0}\right)^T Q \left(y_{k+j} - \overbrace{y_{k+j}^s}^{0}\right) \\
&= \sum_{j=N}^{\infty} \left(C_k x_{k+j} + D_k \overbrace{u_{k+j}}^{0} + F_k \overbrace{d_{k+j}}^{0}\right)^T Q \left(C_k x_{k+j} + D_k \overbrace{u_{k+j}}^{0} + F_k \overbrace{d_{k+j}}^{0}\right) \\
&= \sum_{j=N}^{\infty} x_{k+j}^T C_k^T Q C_k x_{k+j},
\end{aligned} \tag{44}$$

where we have used eqs. 23, 25 and 27. Eq. 44 needs to be studied further, but first we will establish some facts needed. Consider a decomposition of the A_k matrix into its Jordan form

$$A_k = V_k J_k V_k^{-1} = \begin{bmatrix} V_k^u & V_k^s \end{bmatrix} \begin{bmatrix} J_k^u & 0 \\ 0 & J_k^s \end{bmatrix} \begin{bmatrix} \tilde{V}_k^u \\ \tilde{V}_k^s \end{bmatrix}, \tag{45}$$

where V_k^u and J_k^u are respectively the eigenvectors and Jordan blocks for the eigenvalues corresponding to the unstable modes of A_k, and V_k^s and J_k^s are respectively the eigenvectors and Jordan blocks for the eigenvalues corresponding to the stable modes of A_k.Consider x_{k+j}, $\forall j = N, ...\infty$

$$\begin{aligned}
x_{k+N} &= x_{k+N} \\
x_{k+N+1} &= A_k x_{k+N} + B_k \overbrace{u_{k+N}}^{0} + E_k \overbrace{d_{k+N}}^{0} \\
x_{k+N+2} &= A_k^2 x_{k+N} + B_k \overbrace{u_{k+N+1}}^{0} + E_k \overbrace{d_{k+N+1}}^{0} \\
&\dots
\end{aligned}$$

which gives

$$x_{k+j} = A_k^{j-N} x_{k+N}, \; \forall j = N, N+1, N+2, ... \tag{46}$$

Inserting eq. 45 into 46 gives

$$\begin{aligned} x_{k+j} &= A_k^{j-N} x_{k+N} = \left(V_k J_k V_k^{-1}\right)^{j-N} x_{k+N} \\ &= V_k J_k^{j-N} V_k^{-1} x_{k+N} \\ &= \begin{bmatrix} V_k^u & V_k^s \end{bmatrix} \begin{bmatrix} (J_k^u)^{j-N} & 0 \\ 0 & (J_k^s)^{j-N} \end{bmatrix} \begin{bmatrix} \tilde{V}_k^u \\ \tilde{V}_k^s \end{bmatrix} x_{k+N} \\ &= V_k^u \left(J_k^u\right)^{j-N} \tilde{V}_k^u x_{k+N} + V_k^s \left(J_k^s\right)^{j-N} \tilde{V}_k^s x_{k+N}, \, \forall j = N, N+1, N+2, ... \end{aligned} \quad (47)$$

At this point we introduce a new constraint, i.e. we force the unstable modes to zero at time $k+N$

$$\tilde{V}_k^u x_{k+N} = 0, \quad (48)$$

and this gives then

$$x_{k+j} = V_k^s \left(J_k^s\right)^{j-N} \tilde{V}_k^s x_{k+N}, \, \forall j = N, N+1, N+2, ...$$

This result is inserted into eq. 44:

$$\begin{aligned} &\sum_{j=N}^{\infty} x_{k+j}^T C_k^T Q C_k x_{k+j} \\ &= \sum_{j=N}^{\infty} \left(V_k^s \left(J_k^s\right)^{j-N} \tilde{V}_k^s x_{k+N}\right)^T C_k^T Q C_k \left(V_k^s \left(J_k^s\right)^{j-N} \tilde{V}_k^s x_{k+N}\right) \\ &= x_{k+N}^T \left(\tilde{V}_k^s\right)^T \left[\sum_{j=N}^{\infty} \left(\left(J_k^s\right)^{j-N}\right)^T \left(V_k^s\right)^T C_k^T Q C_k V_k^s \left(J_k^s\right)^{j-N}\right] \tilde{V}_k^s x_{k+N} \\ &= x_{k+N}^T \left(\tilde{V}_k^s\right)^T \left[\sum_{j=0}^{\infty} \left(\left(J_k^s\right)^{j}\right)^T \left(V_k^s\right)^T C_k^T Q C_k V_k^s \left(J_k^s\right)^{j}\right] \tilde{V}_k^s x_{k+N} \\ &= x_{k+N}^T \left(\tilde{V}_k^s\right)^T \bar{Q}_k \tilde{V}_k^s x_{k+N}, \end{aligned} \quad (49)$$

where $\bar{Q}_k$ is given by the discrete Lyapunov equation

$$\bar{Q}_k = \left(V_k^s\right)^T C_k^T Q C_k V_k^s + \left(J_k^s\right)^T \bar{Q}_k J_k^s, \quad (50)$$

because

$$\begin{aligned} &\overbrace{\sum_{j=0}^{\infty} \left(\left(J_k^s\right)^{j}\right)^T \left(V_k^s\right)^T C_k^T Q C_k V_k^s \left(J_k^s\right)^{j}}^{\bar{Q}_k} \\ &= \left(V_k^s\right)^T C_k^T Q C_k V_k^s + \left(J_k^s\right)^T \overbrace{\sum_{j=0}^{\infty} \left(\left(J_k^s\right)^{j}\right)^T \left(V_k^s\right)^T C_k^T Q C_k V_k^s \left(J_k^s\right)^{j}}^{\bar{Q}_k} \left(J_k^s\right). \end{aligned}$$

From eq. 41, 42, 43, and 49, we have the criterion

$$\begin{aligned}\min_{\mathcal{U}_k} J_k &= \min_{\mathcal{U}_k} \left(\sum_{j=N}^{\infty} \left[e_{k+j}^T Q e_{k+j} + \tilde{u}_{k+j}^T R \tilde{u}_{k+j} + \Delta u_{k+j}^T S \Delta u_{k+j} \right] \right. \\ &\quad \left. + \sum_{j=0}^{N-1} \left[e_{k+j}^T Q e_{k+j} + \tilde{u}_{k+j}^T R \tilde{u}_{k+j} + \Delta u_{k+j}^T S \Delta u_{k+j} \right] \right) \\ &= \min_{\mathcal{U}_k} \left(x_{k+N}^T \left(\tilde{V}_k^s \right)^T \bar{Q}_k \tilde{V}_k^s x_{k+N} + \Delta u_{k+N}^T S \Delta u_{k+N} \right. \\ &\quad \left. + \sum_{j=0}^{N-1} \left[e_{k+j}^T Q e_{k+j} + \tilde{u}_{k+j}^T R \tilde{u}_{k+j} + \Delta u_{k+j}^T S \Delta u_{k+j} \right] \right),\end{aligned} \tag{51}$$

with $\bar{Q}_k$ given by eq. 50, $\tilde{V}_k^s$ found from the Jordan decomposition of A_k (see eq. 45), and with the additional equality constraint given by eq. 48.

C.2 Formulation as standard QP problem

Define

$$\begin{aligned}\mathcal{U}_k &= \begin{bmatrix} u_k \\ \vdots \\ u_{k+N-1} \end{bmatrix}, \mathcal{U}_k^s = \begin{bmatrix} u_k^s \\ \vdots \\ u_{k+N-1}^s \end{bmatrix}, \mathcal{Y}_k = \begin{bmatrix} y_k \\ \vdots \\ y_{k+N-1} \end{bmatrix}, \\ \mathcal{Y}_k^s &= \begin{bmatrix} y_k^s \\ \vdots \\ y_{k+N-1}^s \end{bmatrix}, \mathcal{D}_k = \begin{bmatrix} d_k \\ \vdots \\ d_{k+N-1} \end{bmatrix}, \Delta\mathcal{U}_k = \begin{bmatrix} \Delta u_k \\ \vdots \\ \Delta u_{k+N} \end{bmatrix}.\end{aligned} \tag{52}$$

Using the model in eq. 19 to predict future state and output values, we have the following results

$$\begin{aligned}x_{k+1} &= A_k x_k + B_k u_k + E_k d_k \\ x_{k+2} &= A_k x_{k+1} + B_k u_{k+1} + E_k d_{k+1} \\ &= A_k^2 x_k + A_k B_k u_k + A_k E_k d_k + B_k u_{k+1} + E_k d_{k+1} \\ x_{k+3} &= A_k x_{k+2} + B_k u_{k+2} + E_k d_{k+2} \\ &= A_k^3 x_k + A_k^2 B_k u_k + A_k^2 E_k d_k + A_k B_k u_{k+1} + A_k E_k d_{k+1} + B_k u_{k+2} + E_k d_{k+2} \\ &\vdots \\ x_{k+i} &= A_k^i x_k + \sum_{j=1}^{i} A_k^{i-j} B_k u_{k+j-1} + \sum_{j=1}^{i} A_k^{i-j} E_k d_{k+j-1},\end{aligned} \tag{53}$$

and

$$y_{k+i} = C_k x_{k+i} + D_k u_{k+i} + F_k d_{k+i} \tag{54}$$
$$= C_k A_k^i x_k + \sum_{j=1}^{i} C_k A_k^{i-j} B_k u_{k+j-1} + \sum_{j=1}^{i} C_k A_k^{i-j} E_k d_{k+j-1} + D_k u_{k+i} + F_k d_{k+i}.$$

We then derive equations for $\mathcal{Y}_k$ and $\Delta\mathcal{U}_k$ in terms of $\mathcal{U}_k$, $\mathcal{D}_k$, x_k and u_{k-1}

$$\begin{aligned} \mathcal{Y}_k &= \mathcal{O}_k x_k + \mathcal{H}_k^u \mathcal{U}_k + \mathcal{H}_k^d \mathcal{D}_k \\ \Delta\mathcal{U}_k &= \mathcal{P}\mathcal{U}_k + \mathcal{L}u_{k-1}, \end{aligned} \tag{55}$$

where

$$\mathcal{O}_k = \begin{bmatrix} C_k \\ C_k A_k \\ C_k A_k^2 \\ \vdots \\ C_k A_k^{N-1} \end{bmatrix} \tag{56}$$

$$\mathcal{H}_k^u = \begin{bmatrix} D_k & 0 & \cdots & 0 & 0 \\ C_k B_k & D_k & \cdots & 0 & 0 \\ \vdots & \vdots & \ddots & \vdots & \vdots \\ C_k A_k^{N-3} B_k & C_k A_k^{N-4} B_k & \cdots & D_k & 0 \\ C_k A_k^{N-2} B_k & C_k A_k^{N-3} B_k & \cdots & C_k B_k & D_k \end{bmatrix}$$

$$\mathcal{H}_k^d = \begin{bmatrix} F_k & 0 & \cdots & 0 & 0 \\ C_k E_k & F_k & \cdots & 0 & 0 \\ \vdots & \vdots & \ddots & \vdots & \vdots \\ C_k A_k^{N-3} E_k & C_k A_k^{N-4} E_k & \cdots & F_k & 0 \\ C_k A_k^{N-2} E_k & C_k A_k^{N-3} E_k & \cdots & C_k E_k & F_k \end{bmatrix}$$

$$\mathcal{P} = \begin{bmatrix} I & 0 & \cdots & 0 \\ -I & I & \cdots & 0 \\ \vdots & \ddots & \ddots & \vdots \\ 0 & \cdots & -I & I \\ 0 & \cdots & 0 & -I \end{bmatrix}$$

$$\mathcal{L} = \begin{bmatrix} -I \\ 0 \\ \vdots \\ 0 \\ 0 \end{bmatrix}$$

Each term in the criterion in eq. 51, and in the constraints in eqs. 24 and 48 is now written in terms of the unknown variable $\mathcal{U}_k$, and the known variables $\mathcal{U}_k^s$, $\mathcal{Y}_k^s$, $\mathcal{D}_k$, $\mathcal{U}_k^{\min}$, $\mathcal{U}_k^{\max}$, $\mathcal{Y}_k^{\min}$, $\mathcal{Y}_k^{\max}$, $\Delta\mathcal{U}_k^{\min}$, $\Delta\mathcal{U}_k^{\max}$, x_k and u_{k-1}.

C.2.1 The criterion

We start with the first term in the criterion in eq. 51, using the result in eq. 53

$$
\begin{aligned}
& x_{k+N}^T \left(\tilde{V}_k^s\right)^T \bar{Q}_k \tilde{V}_k^s x_{k+N} \qquad (57)\\
&= \left(A_k^N x_k + \sum_{j=1}^{N} A_k^{N-j} B_k u_{k+j-1} + \sum_{j=1}^{N} A_k^{N-j} E_k d_{k+j-1} \right)^T \left(\tilde{V}_k^s\right)^T \bar{Q}_k \tilde{V}_k^s \left(\cdot\right) \\
&= \left(A_k^N x_k + C_k^u P^u \mathcal{U}_k + C_k^d P^d \mathcal{D}_k\right)^T \left(\tilde{V}_k^s\right)^T \bar{Q}_k \tilde{V}_k^s \left(A_k^N x_k + C_k^u P^u \mathcal{U}_k + C_k^d P^d \mathcal{D}_k\right) \\
&= \left(x_k^T \left(A_k^N\right)^T + \mathcal{U}_k^T \left(P^u\right)^T \left(C_k^u\right)^T + \mathcal{D}_k^T \left(P^d\right)^T \left(C_k^d\right)^T\right) \\
&\quad \cdot \left(\tilde{V}_k^s\right)^T \bar{Q}_k \tilde{V}_k^s \left(A_k^N x_k + C_k^u P^u \mathcal{U}_k + C_k^d P^d \mathcal{D}_k\right) \\
&= \overbrace{\mathcal{U}_k^T \left(P^u\right)^T \left(C_k^u\right)^T \left(\tilde{V}_k^s\right)^T \bar{Q}_k \tilde{V}_k^s C_k^u P^u \mathcal{U}_k}^{\text{quadratic}} \\
&\quad + \overbrace{2 x_k^T \left(A_k^N\right)^T \left(\tilde{V}_k^s\right)^T \bar{Q}_k \tilde{V}_k^s C_k^u P^u \mathcal{U}_k + 2 \mathcal{D}_k^T \left(P^d\right)^T \left(C_k^d\right)^T \left(\tilde{V}_k^s\right)^T \bar{Q}_k \tilde{V}_k^s C_k^u P^u \mathcal{U}_k}^{\text{linear}} \\
&\quad + \overbrace{\left(A_k^N x_k + C_k^d P^d \mathcal{D}_k\right)^T \left(\tilde{V}_k^s\right)^T \bar{Q}_k \tilde{V}_k^s \left(A_k^N x_k + C_k^d P^d \mathcal{D}_k\right)}^{\text{constant}}
\end{aligned}
$$

where

$$
\begin{aligned}
C_k^u &= \begin{bmatrix} B_k & A_k B_k & \cdots & A_k^{N-1} B_k \end{bmatrix} \qquad (58)\\
C_k^d &= \begin{bmatrix} E_k & A_k E_k & \cdots & A_k^{N-1} E_k \end{bmatrix} \\
P^u &= I_N^{\text{rot90}} \otimes I_r \\
P^d &= I_N^{\text{rot90}} \otimes I_g
\end{aligned}
$$

and I_N^{rot90} is an $N \times N$ identity matrix rotated 90 degrees, I_m and I_g are identity matrices of size m and g respectively, and $\otimes$ is the Kronecker product.

We then study the two Δu terms in the criterion (eq. 51), using the result obtained

in eq. 55

$$
\begin{aligned}
&\sum_{j=0}^{N} \Delta u_{k+j}^T S \Delta u_{k+j} \\
&= \Delta \mathcal{U}_k^T \left(I_{N+1} \otimes S\right) \Delta \mathcal{U}_k \\
&= \left(\mathcal{P}\mathcal{U}_k + \mathcal{L}u_{k-1}\right)^T \left(I_{N+1} \otimes S\right) \left(\mathcal{P}\mathcal{U}_k + \mathcal{L}u_{k-1}\right) \\
&= \left(\mathcal{U}_k^T \mathcal{P}^T + u_{k-1}^T \mathcal{L}^T\right) \left(I_{N+1} \otimes S\right) \left(\mathcal{P}\mathcal{U}_k + \mathcal{L}u_{k-1}\right) \\
&= \overbrace{\mathcal{U}_k^T \mathcal{P}^T \left(I_{N+1} \otimes S\right) \mathcal{P}\mathcal{U}_k}^{\text{quadratic}} + \overbrace{2u_{k-1}^T \mathcal{L}^T \left(I_{N+1} \otimes S\right) \mathcal{P}\mathcal{U}_k}^{\text{linear}} + \overbrace{u_{k-1}^T \mathcal{L}^T \left(I_{N+1} \otimes S\right) \mathcal{L}u_{k-1}}^{\text{constant}}.
\end{aligned}
\tag{59}
$$

Next, the control error term is studied, using the definitions in eqs. 25 and 52, and the results from eq. 55

$$
\begin{aligned}
&e_{k+j}^T Q e_{k+j} \\
&= \left(\mathcal{Y}_k - \mathcal{Y}_k^s\right)^T \left(I_N \otimes Q\right) \left(\mathcal{Y}_k - \mathcal{Y}_k^s\right) \\
&= \left(\mathcal{O}_k x_k + \mathcal{H}_k^u \mathcal{U}_k + \mathcal{H}_k^d \mathcal{D}_k - Y_k^s\right)^T \left(I_N \otimes Q\right) \left(\mathcal{O}_k x_k + \mathcal{H}_k^u \mathcal{U}_k + \mathcal{H}_k^d \mathcal{D}_k - Y_k^s\right) \\
&= \overbrace{\mathcal{U}_k^T \left(\mathcal{H}_k^u\right)^T \left(I_N \otimes Q\right) \mathcal{H}_k^u \mathcal{U}_k}^{\text{quadratic}} \\
&+ \overbrace{2x_k^T \mathcal{O}_k^T \left(I_N \otimes Q\right) \mathcal{H}_k^u \mathcal{U}_k + 2\mathcal{D}_k^T \left(\mathcal{H}_k^d\right)^T \left(I_N \otimes Q\right) \mathcal{H}_k^u \mathcal{U}_k - 2\left(Y_k^s\right)^T \left(I_N \otimes Q\right) \mathcal{H}_k^u \mathcal{U}_k}^{\text{linear}} \\
&+ \overbrace{\left(\mathcal{O}_k x_k + \mathcal{H}_k^d \mathcal{D}_k - Y_k^s\right)^T \left(I_N \otimes Q\right) \left(\mathcal{O}_k x_k + \mathcal{H}_k^d \mathcal{D}_k - Y_k^s\right)}^{\text{constant}}
\end{aligned}
\tag{60}
$$

The last term in the criterion to be studied, using the definitions in eqs. 25 and 52, is

$$
\begin{aligned}
&\sum_{j=0}^{N-1} \tilde{u}_{k+j}^T R \tilde{u}_{k+j} \\
&= \left(\mathcal{U}_k - \mathcal{U}_k^s\right)^T \left(I_N \otimes R\right) \left(\mathcal{U}_k - \mathcal{U}_k^s\right) \\
&= \left(\mathcal{U}_k^T - \left(\mathcal{U}_k^s\right)^T\right) \left(I_N \otimes R\right) \left(\mathcal{U}_k - \mathcal{U}_k^s\right) \\
&= \overbrace{\mathcal{U}_k^T \left(I_N \otimes R\right) \mathcal{U}_k}^{\text{quadratic}} - \overbrace{2\left(\mathcal{U}_k^s\right)^T \left(I_N \otimes R\right) \mathcal{U}_k}^{\text{linear}} + \overbrace{\left(\mathcal{U}_k^s\right)^T \left(I_N \otimes R\right) \mathcal{U}_k^s}^{\text{constant}}
\end{aligned}
\tag{61}
$$

C.2.2 The constraints

First we define the following

$$\mathcal{U}_k^{\min} = \begin{bmatrix} \bar{u}_k^{\min} \\ \vdots \\ \bar{u}_{k+N-1}^{\min} \end{bmatrix}, \mathcal{U}_k^{\max} = \begin{bmatrix} \bar{u}_k^{\max} \\ \vdots \\ \bar{u}_{k+N-1}^{\max} \end{bmatrix} \tag{62}$$

$$\mathcal{Y}_k^{\min} = \begin{bmatrix} -\infty \\ \vdots \\ -\infty \\ \bar{y}_{k+j_1}^{\min} \\ \vdots \\ \bar{y}_{k+j_2}^{\min} \\ -\infty \\ \vdots \\ -\infty \end{bmatrix}, \mathcal{Y}_k^{\max} = \begin{bmatrix} \infty \\ \vdots \\ \infty \\ \bar{y}_{k+j_1}^{\max} \\ \vdots \\ \bar{y}_{k+j_2}^{\max} \\ \infty \\ \vdots \\ \infty \end{bmatrix}$$

$$\Delta\mathcal{U}_k^{\min} = \begin{bmatrix} \Delta\bar{u}_k^{\min} \\ \vdots \\ \Delta\bar{u}_{k+N}^{\min} \end{bmatrix}, \Delta\mathcal{U}_k^{\max} = \begin{bmatrix} \Delta\bar{u}_k^{\max} \\ \vdots \\ \Delta\bar{u}_{k+N}^{\max} \end{bmatrix}$$

The constraints are given in eqs. 24 and 48. These are now written in terms of the unknown variable $\mathcal{U}_k$, and the known variables $\mathcal{U}_k^s$, $\mathcal{Y}_k^s$, $\mathcal{D}_k$, $\mathcal{U}_k^{\min}$, $\mathcal{U}_k^{\max}$, $\mathcal{Y}_k^{\min}$, $\mathcal{Y}_k^{\max}$, $\Delta\mathcal{U}_k^{\min}$, $\Delta\mathcal{U}_k^{\max}$, x_k and u_{k-1}. The constraints on the inputs are reformulated using eqs. 8, 20, 52, and 62

$$\begin{aligned}
&\bar{u}_{k+j}^{\min} \leq \bar{u}_{k+j} \leq \bar{u}_{k+j}^{\max},\ j = 0, 1, ..., N-1 \\
&\quad\Downarrow \\
&\bar{u}_{k+j}^{\min} \leq u_{k+j} + \bar{u}_{k-1} + \bar{u}_{k+N-1}^s \leq \bar{u}_{k+j}^{\max},\ j = 0, 1, ..., N-1 \\
&\quad\Downarrow \\
&\mathcal{U}_k^{\min} \leq \mathcal{U}_k + \bar{u}_{k-1} \otimes \mathbf{1}_N + \bar{u}_{k+N-1}^s \otimes \mathbf{1}_N \leq \mathcal{U}_k^{\max} \\
&\quad\Downarrow \\
\mathcal{U}_k^{\min} - \bar{u}_{k-1} \otimes \mathbf{1}_N - \bar{u}_{k+N-1}^s \otimes \mathbf{1}_N \leq \mathcal{U}_k \leq \mathcal{U}_k^{\max} - \bar{u}_{k-1} \otimes \mathbf{1}_N - \bar{u}_{k+N-1}^s \otimes \mathbf{1}_N,
\end{aligned} \tag{63}$$

where $\mathbf{1}_N$ is an N dimensional vector with 1 in all elements. Next the constraints on the outputs are reformulated using eqs. 11, 20, 52, 55, and 62

$$\begin{aligned}
&\bar{y}_{k+j}^{\min} \leq \bar{y}_{k+j} \leq \bar{y}_{k+j}^{\max},\ j = j_1, j_1+1, ..., j_2 \\
&\quad \Downarrow \\
&\bar{y}_{k+j}^{\min} \leq y_{k+j} + \bar{y}_{k-1} + \bar{y}_{k+N-1}^{s} \leq \bar{y}_{k+j}^{\max},\ j = j_1, j_1+1, ..., j_2 \\
&\quad \Downarrow \\
&\mathcal{Y}_k^{\min} \leq \mathcal{Y}_k + \bar{y}_{k-1} \otimes \mathbf{1}_N + \bar{y}_{k+N-1}^{s} \otimes \mathbf{1}_N \leq \mathcal{Y}_k^{\max} \\
&\quad \Downarrow \\
&\quad \mathcal{Y}_k^{\min} - \bar{y}_{k-1} \otimes \mathbf{1}_N - \bar{y}_{k+N-1}^{s} \otimes \mathbf{1}_N \\
&\quad \leq \mathcal{O}_k x_k + \mathcal{H}_k^u \mathcal{U}_k + \mathcal{H}_k^d \mathcal{D}_k \\
&\quad \leq \mathcal{Y}_k^{\max} - \bar{y}_{k-1} \otimes \mathbf{1}_N - \bar{y}_{k+N-1}^{s} \otimes \mathbf{1}_N \\
&\quad \Downarrow \\
&\quad \mathcal{Y}_k^{\min} - \bar{y}_{k-1} \otimes \mathbf{1}_N - \bar{y}_{k+N-1}^{s} \otimes \mathbf{1}_N - \mathcal{O}_k x_k - \mathcal{H}_k^d \mathcal{D}_k \\
&\quad \leq \mathcal{H}_k^u \mathcal{U}_k \\
&\quad \leq \mathcal{Y}_k^{\max} - \bar{y}_{k-1} \otimes \mathbf{1}_N - \bar{y}_{k+N-1}^{s} \otimes \mathbf{1}_N - \mathcal{O}_k x_k - \mathcal{H}_k^d \mathcal{D}_k
\end{aligned} \tag{64}$$

The constraints on the input moves are reformulated using eqs. 25, 52, 55, and 62

$$\begin{aligned}
\Delta u_{k+j}^{\min} \leq \Delta u_{k+j} \leq \Delta u_{k+j}^{\max},\ j = 0, 1, ..., N \\
\Downarrow \\
\Delta \mathcal{U}_k^{\min} \leq \Delta \mathcal{U}_k \leq \Delta \mathcal{U}_k^{\max} \\
\Downarrow \\
\Delta \mathcal{U}_k^{\min} \leq \mathcal{P}\mathcal{U}_k + \mathcal{L}u_{k-1} \leq \Delta \mathcal{U}_k^{\max} \\
\Downarrow \\
\Delta \mathcal{U}_k^{\min} - \mathcal{L}u_{k-1} \leq \mathcal{P}\mathcal{U}_k \leq \Delta \mathcal{U}_k^{\max} - \mathcal{L}u_{k-1}
\end{aligned} \tag{65}$$

Finally, we reformulate the constraint in eq. 48, using eqs. 57, and 58

$$\begin{aligned}
\tilde{V}_k^u x_{k+N} &= 0 \\
&\Downarrow \\
\tilde{V}_k^u \left(A_k^N x_k + C_k^u P^u \mathcal{U}_k + C_k^d P^d \mathcal{D}_k \right) &= 0 \\
&\Downarrow \\
\tilde{V}_k^u C_k^u P^u \mathcal{U}_k &= -\tilde{V}_k^u \left(A_k^N x_k + C_k^d P^d \mathcal{D}_k \right) \\
&\Downarrow \\
-\tilde{V}_k^u \left(A_k^N x_k + C_k^d P^d \mathcal{D}_k \right) &\leq \tilde{V}_k^u C_k^u P^u \mathcal{U}_k \leq -\tilde{V}_k^u \left(A_k^N x_k + C_k^d P^d \mathcal{D}_k \right)
\end{aligned} \tag{66}$$

C.2.3 Summary of standard QP problem

From eqs. 51, 57, 59, 60, and 61, we can write the criterion as

$$\min_{\mathcal{U}_k} J_k = \min_{\mathcal{U}_k} \left(\frac{1}{2} \mathcal{U}_k^T H_k \mathcal{U}_k + c_k^T \mathcal{U}_k + \kappa \right), \tag{67}$$

and using eqs. 24, 48, 63, 64, 65 and 66, we can write the constraints as

$$b_{L,k} \leq \begin{bmatrix} \mathcal{U}_k \\ \bar{A}_k \mathcal{U}_k \end{bmatrix} \leq b_{U,k}, \tag{68}$$

where

$$\begin{aligned}
H_k &= 2 \Big((P^u)^T (C_k^u)^T \left(\tilde{V}_k^s \right)^T \bar{Q}_k \tilde{V}_k^s C_k^u P^u + \mathcal{P}^T (I_{N+1} \otimes S) \mathcal{P} \\
&\quad + (\mathcal{H}_k^u)^T (I_N \otimes Q) \mathcal{H}_k^u + (I_N \otimes R) \Big) \\
c_k^T &= 2 \Big(x_k^T \left(A_k^N \right)^T \left(\tilde{V}_k^s \right)^T \bar{Q}_k \tilde{V}_k^s C_k^u P^u + \mathcal{D}_k^T \left(P^d \right)^T \left(C_k^d \right)^T \left(\tilde{V}_k^s \right)^T \bar{Q}_k \tilde{V}_k^s C_k^u P^u \\
&\quad + u_{k-1}^T \mathcal{L}^T (I_{N+1} \otimes S) \mathcal{P} + x_k^T \mathcal{O}_k^T (I_N \otimes Q) \mathcal{H}_k^u \\
&\quad + \mathcal{D}_k^T \left(\mathcal{H}_k^d \right)^T (I_N \otimes Q) \mathcal{H}_k^u - (Y_k^s)^T (I_N \otimes Q) \mathcal{H}_k^u - (\mathcal{U}_k^s)^T (I_N \otimes R) \Big) \\
\kappa &= \left(A_k^N x_k + C_k^d P^d \mathcal{D}_k \right)^T \left(\tilde{V}_k^s \right)^T \bar{Q}_k \tilde{V}_k^s \left(A_k^N x_k + C_k^d P^d \mathcal{D}_k \right) + u_{k-1}^T \mathcal{L}^T (I_{N+1} \otimes S) \mathcal{L} u_{k-1} \\
&\quad + \left(\mathcal{O}_k x_k + \mathcal{H}_k^d \mathcal{D}_k - Y_k^s \right)^T (I_N \otimes Q) \left(\mathcal{O}_k x_k + \mathcal{H}_k^d \mathcal{D}_k - Y_k^s \right) + (\mathcal{U}_k^s)^T (I_N \otimes R) \mathcal{U}_k^s \\
\bar{A}_k &= \begin{bmatrix} \mathcal{H}_k^u \\ \mathcal{P} \\ \tilde{V}_k^u C_k^u P^u \end{bmatrix} \\
b_{L,k} &= \begin{bmatrix} \mathcal{U}_k^{\min} - \bar{u}_{k-1} \otimes \mathbf{1}_N - \bar{u}_{k+N-1}^s \otimes \mathbf{1}_N \\ \mathcal{Y}_k^{\min} - \bar{y}_{k-1} \otimes \mathbf{1}_N - \bar{y}_{k+N-1}^s \otimes \mathbf{1}_N - \mathcal{O}_k x_k - \mathcal{H}_k^d \mathcal{D}_k \\ \Delta \mathcal{U}_k^{\min} - \mathcal{L} u_{k-1} \\ -\tilde{V}_k^u \left(A_k^N x_k + C_k^d P^d \mathcal{D}_k \right) \end{bmatrix} \\
b_{U,k} &= \begin{bmatrix} \mathcal{U}_k^{\max} - \bar{u}_{k-1} \otimes \mathbf{1}_N - \bar{u}_{k+N-1}^s \otimes \mathbf{1}_N \\ \mathcal{Y}_k^{\max} - \bar{y}_{k-1} \otimes \mathbf{1}_N - \bar{y}_{k+N-1}^s \otimes \mathbf{1}_N - \mathcal{O}_k x_k - \mathcal{H}_k^d \mathcal{D}_k \\ \Delta \mathcal{U}_k^{\max} - \mathcal{L} u_{k-1} \\ -\tilde{V}_k^u \left(A_k^N x_k + C_k^d P^d \mathcal{D}_k \right) \end{bmatrix}
\end{aligned} \tag{69}$$

The criterion and constraints given by eqs. 67 and 68 are in the form used by e.g. the `sqopt` algorithm[3] (Gill et al. 1997). The `sqopt` algorithm is available with a Matlab interface in the Tomlab environment (Holmström 2001).

[3] The constant term κ in the criterion is not part of the `sqopt` algorithm (or any QP solver), and can be omitted without affecting the result of the optimization.

D State and parameter estimation

In this appendix we do not follow the notation used in other parts of this paper. For example $\bar{x}$ is here the a-priori state estimate, and not a state variable in original "global" units.

D.1 Kalman filter equations for linear time variant processes

In this section we derive the Kalman filter equations for a linear time variant system with colored process noise. The derivations are in particular based on (Ergon 2001) and to some extent on (Gelb 1974). We assume that the process is described by

$$\begin{aligned} x_{k+1} &= A_k x_k + B_k u_k + E_k d_k + G_k w_k \\ y_k &= C_k x_k + D_k u_k + F_k d_k + v_k \end{aligned} \tag{70}$$

where $x_k \in \mathbb{R}^n$ is the state vector, $u_k \in \mathbb{R}^r$ is the (manipulated) input vector, $d_k \in \mathbb{R}^s$ is the measured disturbance vector, $y_k \in \mathbb{R}^m$ is the output vector, and k is the discrete time variable. w_k and v_k are zero mean uncorrelated white noise

$$\begin{aligned} E\left[w_k\right] = 0,\, E\left[v_k\right] = 0, \\ E\left[w_k v_j^T\right] = 0,\, \forall k, j, \\ E\left[w_k w_j^T\right] = 0,\, E\left[v_k v_j^T\right] = 0,\, \forall k \neq j \\ E\left[w_k w_k^T\right] = Q_k,\, E\left[v_k v_k^T\right] = R_k, \end{aligned} \tag{71}$$

where $E\left[\cdot\right]$ is the expectation operator, and $Q_k \in \mathbb{R}^{n \times n}$ and $R_k \in \mathbb{R}^{m \times m}$ are covariance matrices. In Figure 10 the Kalman filter structure is shown.

From Figure 10 we find the following equations for the Kalman filter

$$\begin{aligned} \bar{x}_{k+1} &= A_k \hat{x}_k + B_k u_k + E_k d_k \\ \hat{x}_k &= \bar{x}_k + K_k \cdot \varepsilon_k = \bar{x}_k + K_k \left(y_k - \bar{y}_k\right) \\ \bar{y}_k &= C_k \bar{x}_k + D_k u_k + F_k d_k. \end{aligned} \tag{72}$$

Define the covariance matrices

$$Z_k = E\left[\left(x_k - \hat{x}_k\right)\left(x_k - \hat{x}_k\right)^T\right] \text{ and } P_k = E\left[\left(x_k - \bar{x}_k\right)\left(x_k - \bar{x}_k\right)^T\right], \tag{73}$$

where

$$\begin{aligned} \hat{x}_k &= \bar{x}_k + K_k \left(y_k - \bar{y}_k\right) \\ &= \bar{x}_k + K_k \left(C_k x_k + D_k u_k + F_k d_k + v_k - C_k \bar{x}_k - D_k u_k - F_k d_k\right) \\ &= \bar{x}_k + K_k C_k x_k + K_k v_k - K_k C_k \bar{x}_k \\ &= (I - K_k C_k)\bar{x}_k + K_k C_k x_k + K_k v_k. \end{aligned}$$

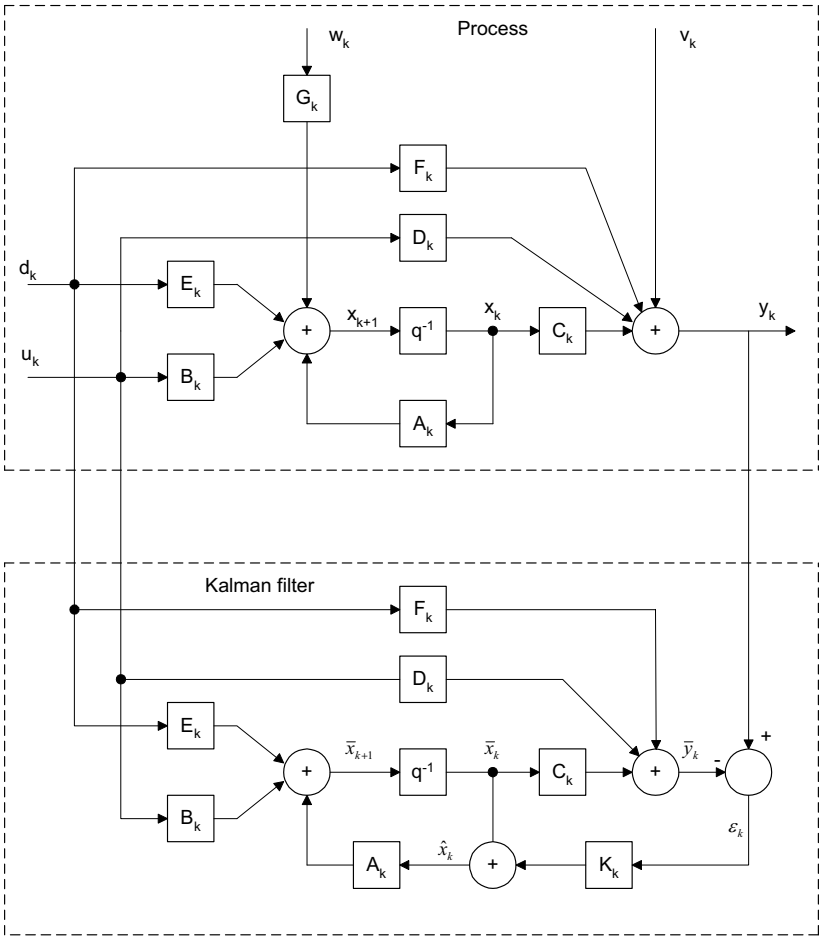

Figure 10: Structure of Kalman filter for linear time variant process with colored noise.

Then

$$\begin{aligned}
Z_k &= E\left[(x_k - (I - K_kC_k)\bar{x}_k - K_kC_kx_k - K_kv_k)\,(\cdot)^T\right] \\
&= E\left[((I - K_kC_k)(x_k - \bar{x}_k) - K_kv_k)\,((I - K_kC_k)(x_k - \bar{x}_k) - K_kv_k)^T\right] \\
&= E\left[(I - K_kC_k)(x_k - \bar{x}_k)(x_k - \bar{x}_k)^T(I - K_kC_k)^T - (I - K_kC_k)(x_k - \bar{x}_k)v_k^TK_k^T\right. \\
&\left.-K_kv_k(x_k - \bar{x}_k)^T(I - K_kC_k)^T + K_kv_kv_k^TK_k^T\right] \\
&= (I - K_kC_k)E\left[(x_k - \bar{x}_k)(x_k - \bar{x}_k)^T\right](I - K_kC_k)^T - (I - K_kC_k)E\left[(x_k - \bar{x}_k)v_k^T\right]K_k^T \\
&- K_kE\left[v_k(x_k - \bar{x}_k)^T\right](I - K_kC_k)^T + K_kE\left[v_kv_k^T\right]K_k^T \\
&= (I - K_kC_k)P_k(I - K_kC_k)^T + K_kR_kK_k^T, \qquad (74)
\end{aligned}$$

and where $E\left[(x_k - \bar{x}_k)v_k^T\right] = 0$ is a reasonable assumption since

$$\begin{aligned}
x_k - \bar{x}_k &= A_{k-1}x_{k-1} + G_{k-1}w_{k-1} - A_{k-1}\bar{x}_{k-1} - K_{k-1}(y_{k-1} - \bar{y}_{k-1}) \\
&= A_{k-1}x_{k-1} + G_{k-1}w_{k-1} - A_{k-1}\bar{x}_{k-1} - K_{k-1}(C_{k-1}x_{k-1} + v_{k-1} - C_{k-1}\bar{x}_{k-1}) \\
&= (A_{k-1} - K_{k-1}C_{k-1})(x_{k-1} - \bar{x}_{k-1}) + G_{k-1}w_{k-1} - K_{k-1}v_{k-1},
\end{aligned}$$

where we see that the state estimation error $x_k - \bar{x}_k$ only depends on past noise sequences.

We now seek to find the gain matrix K_k which minimizes the covariance Z_k, noting that $\min(Z_k)$ implies $\min(\text{trace}(Z_k))$ and that for a symmetric matrix B we have the following rule

$$\frac{\partial}{\partial A}\text{trace}(ABA^T) = 2AB.$$

Then the optimal gain matrix, or the Kalman filter gain matrix, is

$$\begin{aligned}
&\frac{\partial}{\partial K_k}(Z_k) = 0 \\
&\qquad\Downarrow \\
&K_k = P_kC_k^T\left(R_k + C_kP_kC_k^T\right)^{-1}. \qquad (75)
\end{aligned}$$

Using the Kalman filter on-line we must find P_{k+1}

$$\begin{aligned}
P_{k+1} &= E\left[(x_{k+1} - \bar{x}_{k+1})\,(x_{k+1} - \bar{x}_{k+1})^T\right] \\
&= E\left[(A_kx_k + G_kw_k - A_k\hat{x}_k)\,(A_kx_k + G_kw_k - A_k\hat{x}_k)^T\right] \\
&= E\left[(A_k(x_k - \hat{x}_k) + G_kw_k)\,(A_k(x_k - \hat{x}_k) + G_kw_k)^T\right] \\
&= E\left[A_k(x_k - \hat{x}_k)(x_k - \hat{x}_k)^TA_k^T + A_k(x_k - \hat{x}_k)w_k^TG_k^T\right. \\
&\quad\left.+G_kw_k(x_k - \hat{x}_k)^TA_k^T + G_kw_kw_k^TG_k^T\right] \\
&= A_kE\left[(x_k - \hat{x}_k)(x_k - \hat{x}_k)^T\right]A_k^T + A_kE\left[(x_k - \hat{x}_k)w_k^T\right]G_k^T \\
&\quad + G_kE\left[w_k(x_k - \hat{x}_k)^T\right]A_k^T + G_kE\left[w_kw_k^T\right]G_k^T \qquad (76) \\
&= A_kZ_kA_k^T + G_kQ_kG_k^T. \qquad (77)
\end{aligned}$$

We see from this last equation that the K_k that minimized Z_k also minimizes P_{k+1}.

D.2 Extended Kalman filter for nonlinear processes

Assume the process is nonlinear

$$\begin{aligned} x_{k+1} &= f(x_k, u_k, d_k) + G_k w_k \\ y_k &= g(x_k, u_k, d_k) + v_k, \end{aligned} \tag{78}$$

with noise characteristics as given by Equation 71. Then the extended Kalman filter algorithm can be written as (Ergon 2001)

1. At time k, given y_k, u_k, $\bar{x}_k$,P_k, $A_k = \frac{\partial f}{\partial x_k}|_s$ and $C_k = \frac{\partial g}{\partial x_k}|_s$.

2. Compute the Kalman filter gain matrix as given by Equation 75

$$K_k = P_k C_k^T \left(R_k + C_k P_k C_k^T\right)^{-1}.$$

3. Compute updated state estimate

$$\hat{x}_k = \bar{x}_k + K_k \left(y_k - g(\bar{x}_k, u_k, d_k)\right).$$

4. Compute updated covariance matrix for state error, as given by Equation 74

$$Z_k = (I - K_k C_k) P_k (I - K_k C_k)^T + K_k R_k K_k^T.$$

5. Compute state estimate at time $k+1$

$$\bar{x}_{k+1} = f(\hat{x}_k, u_k, d_k).$$

6. Compute covariance matrix for state error, as given by Equation 77

$$P_{k+1} = A_k Z_k A_k^T + G_k Q_k G_k^T.$$

7. Set $k \to k+1$ and go to step 2.

Note that when there is a direct input to output term in the model, and the model is used in a control loop, we must know the input u_k before we can estimate $\hat{x}_k$ or $\bar{x}_{k+1}$. This means that the controller must rely on the estimate $\bar{x}_{k|k-1}$ when computing the inputs u_k.

D.3 Offset free control by bias estimation

We will in this section show how the MPC and Kalman filter developed in previous sections and appendices can be redesigned to prevent steady state offset by estimating the bias and adding this to the model outputs.

Assume the following augmented process model

$$\begin{aligned} \begin{bmatrix} x_{k+1}^{\text{nonlin}} \\ p_{k+1}^{\text{nonlin}} \end{bmatrix} &= \begin{bmatrix} f(x_k^{\text{nonlin}}, u_k^{\text{nonlin}}, d_k^{\text{nonlin}}) \\ p_k^{\text{nonlin}} \end{bmatrix} \\ y_k^{\text{nonlin}} &= g(x_k^{\text{nonlin}}, u_k^{\text{nonlin}}, d_k^{\text{nonlin}}) + p_k^{\text{nonlin}}, \end{aligned} \tag{79}$$

where the bias p_k^{nonlin} is added to the process outputs. We will now review some of the stages in the algorithm described in Section 2.

D.3.1 Linearization

The linearization can be carried out on the augmented system, the same way as was done for the original model in Section 3. However, by studying the structure of the augmented system we may carry out the linearization in a more efficient way

$$\begin{aligned} \begin{bmatrix} x_{k+1}^{\text{lin}} \\ p_{k+1}^{\text{lin}} \end{bmatrix} &= \begin{bmatrix} A_k^x & 0 \\ 0 & I \end{bmatrix} \begin{bmatrix} x_k^{\text{lin}} \\ p_k^{\text{lin}} \end{bmatrix} + \begin{bmatrix} B_k \\ 0 \end{bmatrix} u_k^{\text{lin}} + \begin{bmatrix} E_k \\ 0 \end{bmatrix} d_k^{\text{lin}} \\ y_k^{\text{lin}} &= \begin{bmatrix} C_k^x & I \end{bmatrix} \begin{bmatrix} x_k^{\text{lin}} \\ p_k^{\text{lin}} \end{bmatrix} + D_k u_k^{\text{lin}} + F_k d_k^{\text{lin}}. \end{aligned} \tag{80}$$

The linearization can thus be carried out on the original non-augmented system, and augmentation of the A and C matrices can be done after the linearization.

D.3.2 Steady state values, shifting the model and variables

Assuming the steady state value of p to be known and equal to p_k^{lin} we may calculate the steady state values as follows

$$\min_{\bar{x}_{k+j}^s, \bar{u}_{k+j}^s} \left(\bar{y}_{k+j}^s - r_{k+j}^{\text{lin}}\right)^T Q_s \left(\bar{y}_{k+j}^s - r_{k+j}^{\text{lin}}\right), \forall j = 0, ..., N-1, \tag{81}$$

constrained by the steady state solution to the model

$$\begin{bmatrix} (I - A_k^x) & -B_k \\ -C_k^x & -D_k \end{bmatrix} \begin{bmatrix} \bar{x}_{k+j}^s \\ \bar{u}_{k+j}^s \end{bmatrix} = \begin{bmatrix} E_k d_{k+j}^{\text{lin}} \\ F_k d_{k+j}^{\text{lin}} - \bar{y}_{k+j}^s + p_k^{\text{lin}} \end{bmatrix}, \forall j = 0, ..., N-1, \tag{82}$$

and

$$\begin{aligned} \bar{u}_{k+j}^{\min} \leq \bar{u}_{k+j}^s + u_{k-1}^{\text{nonlin}} \leq \bar{u}_{k+j}^{\max}, \forall j = 0, ..., N-1 \\ \bar{y}_{k+j}^{\min} \leq \bar{y}_{k+j}^s + y_{k-1}^{\text{nonlin}} \leq \bar{y}_{k+j}^{\max}, \forall j = 0, ..., N-1, \end{aligned} \tag{83}$$

and

$$\bar{y}_{k+j}^s = C_k^x \bar{x}_{k+j}^s + p_{k+j}^{\text{lin}} + D_k \bar{u}_{k+j}^s + F_k d_{k+j}^{\text{lin}}, \forall j = 0, ..., N-1, \tag{84}$$

When shifting the augmented model to the steady state values at time $N-1$, all bias terms are set to zero since we assume the bias is constant into the future. Thus, there is no point in using the augmented model in the MPC.

D.3.3 Optimization

The optimization is carried out the same way as was done in Section 4, due to the fact that the augmented model reduces to the original model when assuming a constant bias term, and shifting it to the steady state values at time $N-1$.

D.3.4 Estimating the states

The process model is given by the augmented model of Equation 79, and we assume the real process is given by

$$\begin{aligned} \tilde{x}_{k+1}^{\text{nonlin}} &= \tilde{f}(x_k^{\text{nonlin}}, u_k^{\text{nonlin}}, d_k^{\text{nonlin}}, p_k^{\text{nonlin}}) + \tilde{G}_k \tilde{w}_k \\ y_k^{\text{nonlin}} &= g(x_k^{\text{nonlin}}, u_k^{\text{nonlin}}, d_k^{\text{nonlin}}) + p_k^{\text{nonlin}} + v_k, \end{aligned} \tag{85}$$

where

$$\tilde{x}_{k+1}^{\text{nonlin}} = \begin{bmatrix} x_{k+1}^{\text{nonlin}} \\ p_{k+1}^{\text{nonlin}} \end{bmatrix} \tag{86}$$

$$\tilde{f}(x_k^{\text{nonlin}}, u_k^{\text{nonlin}}, d_k^{\text{nonlin}}, p_k^{\text{nonlin}}) = \begin{bmatrix} f(x_k^{\text{nonlin}}, u_k^{\text{nonlin}}, d_k^{\text{nonlin}}) \\ p_k^{\text{nonlin}} \end{bmatrix}$$

$$\tilde{G}_k = \begin{bmatrix} G_k^x & 0 \\ 0 & G_k^p \end{bmatrix} \tag{87}$$

$$\tilde{w}_k = \begin{bmatrix} w_k^x \\ w_k^p \end{bmatrix}, \tag{88}$$

and where the noise characteristics are as given by Equation 71 (with tilde above appropriate elements).

We study the covariance matrices

$$\tilde{Z}_k = E\left[\left(\tilde{x}_k^{\text{nonlin}} - \widetilde{\hat{x}}^{\text{nonlin}}\right)\left(\tilde{x}_k^{\text{nonlin}} - \widetilde{\hat{x}}^{\text{nonlin}}\right)^T\right] \tag{89}$$

$$\tilde{P}_k = E\left[\left(\tilde{x}_k^{\text{nonlin}} - \widetilde{\bar{x}}^{\text{nonlin}}\right)\left(\tilde{x}_k^{\text{nonlin}} - \widetilde{\bar{x}}^{\text{nonlin}}\right)^T\right], \tag{90}$$

where

$$\begin{aligned} \tilde{x}_k^{\text{nonlin}} &= \begin{bmatrix} x_k^{\text{nonlin}} \\ p_k^{\text{nonlin}} \end{bmatrix} \\ \widetilde{\hat{x}}^{\text{nonlin}} &= \begin{bmatrix} \hat{x}_k^{\text{nonlin}} \\ \hat{p}_k^{\text{nonlin}} \end{bmatrix} \\ \widetilde{\bar{x}}^{\text{nonlin}} &= \begin{bmatrix} \bar{x}_k^{\text{nonlin}} \\ \bar{p}_k^{\text{nonlin}} \end{bmatrix} \end{aligned} \tag{91}$$

For a linearized model we then have

$$\begin{aligned}\tilde{\hat{x}}^{\text{lin}} &= \tilde{\bar{x}}^{\text{lin}} + \tilde{K}_k\left(y_k^{\text{lin}} - \bar{y}_k^{\text{lin}}\right) \\ &= \tilde{\bar{x}}^{\text{lin}} + \tilde{K}_k\left(\tilde{C}_k\tilde{x}_k^{\text{lin}} + D_k u_k^{\text{lin}} + F_k d_k^{\text{lin}} + v_k - \tilde{C}_k\tilde{\bar{x}}^{\text{lin}} - D_k u_k^{\text{lin}} - F_k d_k^{\text{lin}}\right) \\ &= \tilde{\bar{x}}^{\text{lin}} + \tilde{K}_k\left(\tilde{C}_k\tilde{x}_k^{\text{lin}} + v_k - \tilde{C}_k\tilde{\bar{x}}^{\text{lin}}\right) \\ &= \left(I - \tilde{K}_k\tilde{C}_k\right)\tilde{\bar{x}}^{\text{lin}} + \tilde{K}_k\tilde{C}_k\tilde{x}_k^{\text{lin}} + \tilde{K}_k v_k\end{aligned} \tag{92}$$

where

$$\tilde{K}_k = \begin{bmatrix} K_k^x \\ K_k^p \end{bmatrix}, \text{ and } \tilde{C}_k = \begin{bmatrix} C_k & I \end{bmatrix} \tag{93}$$

Then

$$\begin{aligned}\tilde{Z}_k &= E\left[\left(\tilde{x}_k^{\text{lin}} - \left(I - \tilde{K}_k\tilde{C}_k\right)\tilde{\bar{x}}^{\text{lin}} - \tilde{K}_k\tilde{C}_k\tilde{x}_k^{\text{lin}} - \tilde{K}_k v_k\right)(\cdot)^T\right] \\ &= E\left[\left(\left(I - \tilde{K}_k\tilde{C}_k\right)\left(\tilde{x}_k^{\text{lin}} - \tilde{\bar{x}}^{\text{lin}}\right) - \tilde{K}_k v_k\right)(\cdot)^T\right] \\ &= \left(I - \tilde{K}_k\tilde{C}_k\right)\tilde{P}_k\left(I - \tilde{K}_k\tilde{C}_k\right)^T + \tilde{K}_k R_k^T\tilde{K}_k^T,\end{aligned} \tag{94}$$

and

$$\tilde{K}_k = \tilde{P}_k^T\tilde{C}_k^T\left(R_k + \tilde{C}_k\tilde{P}_k^T\tilde{C}_k^T\right)^{-1}, \tag{95}$$

and finally

$$\tilde{P}_{k+1} = \tilde{A}_k\tilde{Z}_k\tilde{A}_k^T + \tilde{G}_k\tilde{Q}_k\tilde{G}_k^T, \tag{96}$$

where

$$\tilde{Q}_k = E\left[\tilde{w}_k\tilde{w}_k^T\right]. \tag{97}$$

Then the augmented Kalman filter algorithm can be written as

1. At time k, given y_k^{nonlin}, u_k^{nonlin},$\tilde{\bar{x}}_k^{\text{nonlin}}$, C_k, A_k and $\tilde{P}_k$. Augment model matrices
$$\tilde{A}_k = \begin{bmatrix} A_k & 0 \\ 0 & I \end{bmatrix}, \text{ and } \tilde{C}_k = \begin{bmatrix} C_k & I \end{bmatrix}$$
2. Compute the Kalman filter gain matrix
$$\tilde{K}_k = \tilde{P}_k^T\tilde{C}_k^T\left(R_k + \tilde{C}_k\tilde{P}_k^T\tilde{C}_k^T\right)^{-1}.$$
3. Compute updated state estimate
$$\tilde{\hat{x}}^{\text{nonlin}} = \tilde{\bar{x}}^{\text{nonlin}} + \tilde{K}_k\left(y_k^{\text{nonlin}} - g(\bar{x}_k^{\text{nonlin}}, u_k^{\text{nonlin}}, d_k^{\text{nonlin}}) - \bar{p}_k^{\text{nonlin}}\right)$$
4. Compute updated covariance matrix for state error
$$\tilde{Z}_k = \left(I - \tilde{K}_k\tilde{C}_k\right)\tilde{P}_k\left(I - \tilde{K}_k\tilde{C}_k\right)^T + \tilde{K}_k R_k^T\tilde{K}_k^T.$$

5. Compute state estimate at time $k+1$

$$\widetilde{\hat{x}}_{k+1}^{\text{nonlin}} = \widetilde{\hat{f}}(\hat{x}_k^{\text{nonlin}}, u_k^{\text{nonlin}}, d_k^{\text{nonlin}}, \hat{p}_k^{\text{nonlin}}) = \begin{bmatrix} f(\hat{x}_k^{\text{nonlin}}, u_k^{\text{nonlin}}, d_k^{\text{nonlin}}) \\ \hat{p}_k^{\text{nonlin}} \end{bmatrix}.$$

6. Compute covariance matrix for state error

$$\tilde{P}_{k+1} = \tilde{A}_k \tilde{Z}_k \tilde{A}_k^T + \tilde{G}_k \tilde{Q}_k \tilde{G}_k^T.$$

7. Set $k \to k+1$ and go to step 2.

D.4 Online parameter estimation by augmented Kalman filter

An alternative to bias estimation to obtain offset free control may be to estimate parameters and biases in the model on-line. The estimation can be done by augmenting the state vector by parameters and biases that we wish to estimate. The procedure is similar, but not equal, to the procedure in the previous section where only the (output) bias was estimated. We will in this section show how the MPC and Kalman filter developed in previous sections can be redesigned to prevent steady state offset by estimating parameters and/or biases in the model.

Assume the following augmented process model

$$\begin{bmatrix} x_{k+1}^{\text{nonlin}} \\ \theta_{k+1}^{\text{nonlin}} \end{bmatrix} = \begin{bmatrix} f(x_k^{\text{nonlin}}, u_k^{\text{nonlin}}, d_k^{\text{nonlin}}, \theta_k^{\text{nonlin}}) \\ \theta_k^{\text{nonlin}} \end{bmatrix} \tag{98}$$
$$y_k^{\text{nonlin}} = g(x_k^{\text{nonlin}}, u_k^{\text{nonlin}}, d_k^{\text{nonlin}}, \theta_k^{\text{nonlin}}),$$

We will now review some of the stages in the algorithm described in Section 2.

D.4.1 Linearization

The linearization can be carried out on the augmented system, the same way as was done for the original model in Section 3. However, by studying the structure of the augmented system we may carry out the linearization in a more efficient way

$$\begin{bmatrix} x_{k+1}^{\text{lin}} \\ \theta_{k+1}^{\text{lin}} \end{bmatrix} = \begin{bmatrix} A_k^x & A_k^\theta \\ 0 & I \end{bmatrix} \begin{bmatrix} x_k^{\text{lin}} \\ \theta_k^{\text{lin}} \end{bmatrix} + \begin{bmatrix} B_k \\ 0 \end{bmatrix} u_k^{\text{lin}} + \begin{bmatrix} E_k \\ 0 \end{bmatrix} d_k^{\text{lin}} \tag{99}$$
$$y_k^{\text{lin}} = \begin{bmatrix} C_k^x & C_k^\theta \end{bmatrix} \begin{bmatrix} x_k^{\text{lin}} \\ \theta_k^{\text{lin}} \end{bmatrix} + D_k u_k^{\text{lin}} + F_k d_k^{\text{lin}}.$$

D.4.2 Steady state values, shifting the model and variables

Assuming the steady state value of θ to be known and equal to θ_k^{lin} we may calculate the steady state values as follows

$$\min_{\bar{x}_{k+j}^s, \bar{u}_{k+j}^s} \left(\bar{y}_{k+j}^s - r_{k+j}^{\text{lin}}\right)^T Q_s \left(\bar{y}_{k+j}^s - r_{k+j}^{\text{lin}}\right), \forall j = 0, ..., N-1, \tag{100}$$

constrained by the steady state solution to the model

$$\begin{bmatrix} (I - A_k^x) & -B_k \\ -C_k^x & -D_k \end{bmatrix} \begin{bmatrix} \bar{x}_{k+j}^s \\ \bar{u}_{k+j}^s \end{bmatrix} = \begin{bmatrix} A_k^\theta \theta_k^{\text{lin}} + E_k d_{k+j}^{\text{lin}} \\ C_k^\theta \theta_k^{\text{lin}} + F_k d_{k+j}^{\text{lin}} - \bar{y}_{k+j}^s \end{bmatrix}, \forall j = 0, ..., N-1, \tag{101}$$

and

$$\begin{aligned} \bar{u}_{k+j}^{\min} \leq \bar{u}_{k+j}^s + u_{k-1}^{\text{nonlin}} \leq \bar{u}_{k+j}^{\max}, \forall j = 0, ..., N-1 \\ \bar{y}_{k+j}^{\min} \leq \bar{y}_{k+j}^s + y_{k-1}^{\text{nonlin}} \leq \bar{y}_{k+j}^{\max}, \forall j = 0, ..., N-1, \end{aligned} \tag{102}$$

and

$$\bar{y}_{k+j}^s = C_k^x \bar{x}_{k+j}^s + C_k^\theta \theta_{k+j}^{\text{lin}} + D_k \bar{u}_{k+j}^s + F_k d_{k+j}^{\text{lin}}, \forall j = 0, ..., N-1, \tag{103}$$

When shifting the augmented model to the steady state values at time $N-1$, all augmented states are set to zero since we assume the parameter values are constant into the future. Thus, there is no point in using the augmented model in the MPC.

D.4.3 Optimization

The optimization is carried out the same way as was done in Section 4, due to the fact that the augmented model reduces to the original model when assuming constant parameters and biases into the future, and when the model is shifted to the steady state values at time $N-1$.

D.4.4 Estimating the states

The process model is given by the augmented model of Equation 98, and we assume the real process is given by

$$\begin{aligned} \tilde{x}_{k+1}^{\text{nonlin}} &= \tilde{f}(x_k^{\text{nonlin}}, u_k^{\text{nonlin}}, d_k^{\text{nonlin}}, \theta_k^{\text{nonlin}}) + \tilde{G}_k \tilde{w}_k \\ y_k^{\text{nonlin}} &= g(x_k^{\text{nonlin}}, u_k^{\text{nonlin}}, d_k^{\text{nonlin}}, \theta_k^{\text{nonlin}}) + v_k, \end{aligned} \tag{104}$$

where

$$\begin{aligned} \tilde{x}_{k+1}^{\text{nonlin}} &= \begin{bmatrix} x_{k+1}^{\text{nonlin}} \\ \theta_{k+1}^{\text{nonlin}} \end{bmatrix} \\ \tilde{f}(x_k^{\text{nonlin}}, u_k^{\text{nonlin}}, d_k^{\text{nonlin}}, \theta_k^{\text{nonlin}}) &= \begin{bmatrix} f(x_k^{\text{nonlin}}, u_k^{\text{nonlin}}, d_k^{\text{nonlin}}, \theta_k^{\text{nonlin}}) \\ \theta_k^{\text{nonlin}} \end{bmatrix} \\ \tilde{G}_k &= \begin{bmatrix} G_k^x & 0 \\ 0 & G_k^\theta \end{bmatrix} \\ \tilde{w}_k &= \begin{bmatrix} w_k^x \\ w_k^\theta \end{bmatrix}, \end{aligned} \tag{105}$$

and where the noise characteristics are as given by Equation 71 (with tilde above appropriate elements).

We study the covariance matrices

$$\tilde{Z}_k = E\left[\left(\tilde{x}_k^{\text{nonlin}} - \widetilde{\hat{x}}^{\text{nonlin}}\right)\left(\tilde{x}_k^{\text{nonlin}} - \widetilde{\hat{x}}^{\text{nonlin}}\right)^T\right] \tag{106}$$

$$\tilde{P}_k = E\left[\left(\tilde{x}_k^{\text{nonlin}} - \widetilde{\bar{x}}^{\text{nonlin}}\right)\left(\tilde{x}_k^{\text{nonlin}} - \widetilde{\bar{x}}^{\text{nonlin}}\right)^T\right], \tag{107}$$

where

$$\begin{aligned}\tilde{x}_k^{\text{nonlin}} &= \begin{bmatrix} x_k^{\text{nonlin}} \\ \theta_k^{\text{nonlin}} \end{bmatrix} \\ \widetilde{\hat{x}}^{\text{nonlin}} &= \begin{bmatrix} \hat{x}_k^{\text{nonlin}} \\ \hat{\theta}_k^{\text{nonlin}} \end{bmatrix} \\ \widetilde{\bar{x}}^{\text{nonlin}} &= \begin{bmatrix} \bar{x}_k^{\text{nonlin}} \\ \bar{\theta}_k^{\text{nonlin}} \end{bmatrix}\end{aligned} \tag{108}$$

For a linearized model we then have

$$\begin{aligned}\widetilde{\hat{x}}^{\text{lin}} &= \widetilde{\bar{x}}^{\text{lin}} + \tilde{K}_k\left(y_k^{\text{lin}} - \bar{y}_k^{\text{lin}}\right) \\ &= \widetilde{\bar{x}}^{\text{lin}} + \tilde{K}_k\left(\tilde{C}_k\tilde{x}_k^{\text{lin}} + D_k u_k^{\text{lin}} + F_k d_k^{\text{lin}} + v_k - \tilde{C}_k\widetilde{\bar{x}}^{\text{lin}} - D_k u_k^{\text{lin}} - F_k d_k^{\text{lin}}\right) \\ &= \widetilde{\bar{x}}^{\text{lin}} + \tilde{K}_k\left(\tilde{C}_k\tilde{x}_k^{\text{lin}} + v_k - \tilde{C}_k\widetilde{\bar{x}}^{\text{lin}}\right) \\ &= \left(I - \tilde{K}_k\tilde{C}_k\right)\widetilde{\bar{x}}^{\text{lin}} + \tilde{K}_k\tilde{C}_k\tilde{x}_k^{\text{lin}} + \tilde{K}_k v_k\end{aligned} \tag{109}$$

where

$$\tilde{K}_k = \begin{bmatrix} K_k^x \\ K_k^\theta \end{bmatrix}, \text{ and } \tilde{C}_k = \begin{bmatrix} C_k^x & C_k^\theta \end{bmatrix} \tag{110}$$

Then

$$\begin{aligned}\tilde{Z}_k &= E\left[\left(\tilde{x}_k^{\text{lin}} - \left(I - \tilde{K}_k\tilde{C}_k\right)\widetilde{\bar{x}}^{\text{lin}} - \tilde{K}_k\tilde{C}_k\tilde{x}_k^{\text{lin}} - \tilde{K}_k v_k\right)(\cdot)^T\right] \\ &= E\left[\left(\left(I - \tilde{K}_k\tilde{C}_k\right)\left(\tilde{x}_k^{\text{lin}} - \widetilde{\bar{x}}^{\text{lin}}\right) - \tilde{K}_k v_k\right)(\cdot)^T\right] \\ &= \left(I - \tilde{K}_k\tilde{C}_k\right)\tilde{P}_k\left(I - \tilde{K}_k\tilde{C}_k\right)^T + \tilde{K}_k R_k^T \tilde{K}_k^T,\end{aligned} \tag{111}$$

and

$$\tilde{K}_k = \tilde{P}_k^T\tilde{C}_k^T\left(R_k + \tilde{C}_k\tilde{P}_k^T\tilde{C}_k^T\right)^{-1}, \tag{112}$$

and finally

$$\tilde{P}_{k+1} = \tilde{A}_k\tilde{Z}_k\tilde{A}_k^T + \tilde{G}_k\tilde{Q}_k\tilde{G}_k^T, \tag{113}$$

where

$$\tilde{A}_k = \begin{bmatrix} A_k^x & A_k^\theta \\ 0 & I \end{bmatrix} \tag{114}$$

$$\tilde{Q}_k = E\left[\tilde{w}_k\tilde{w}_k^T\right]. \tag{115}$$

Then the augmented Kalman filter algorithm can be written as

1. At time k, given y_k^{nonlin}, u_k^{nonlin}, $\widetilde{\bar{x}}_k^{\text{nonlin}}$, C_k^x, C_k^θ, A_k^x, A_k^θ and $\tilde{P}_k$. Augment model matrices

$$\tilde{A}_k = \begin{bmatrix} A_k^x & A_k^\theta \\ 0 & I \end{bmatrix}, \text{ and } \tilde{C}_k = \begin{bmatrix} C_k^x & C_k^\theta \end{bmatrix}$$

2. Compute the Kalman filter gain matrix

$$\tilde{K}_k = \tilde{P}_k^T \tilde{C}_k^T \left(R_k + \tilde{C}_k \tilde{P}_k^T \tilde{C}_k^T \right)^{-1}.$$

3. Compute updated state estimate

$$\widetilde{\hat{x}}^{\text{nonlin}} = \widetilde{\bar{x}}^{\text{nonlin}} + \tilde{K}_k \left(y_k^{\text{nonlin}} - g(\bar{x}_k^{\text{nonlin}}, u_k^{\text{nonlin}}, d_k^{\text{nonlin}}, \bar{\theta}_k^{\text{nonlin}}) \right)$$

4. Compute updated covariance matrix for state error

$$\tilde{Z}_k = \left(I - \tilde{K}_k \tilde{C}_k \right) \tilde{P}_k \left(I - \tilde{K}_k \tilde{C}_k \right)^T + \tilde{K}_k R_k^T \tilde{K}_k^T.$$

5. Compute state estimate at time $k+1$

$$\widetilde{\bar{x}}_{k+1}^{\text{nonlin}} = \widetilde{\hat{f}}(\hat{x}_k^{\text{nonlin}}, u_k^{\text{nonlin}}, d_k^{\text{nonlin}}, \hat{\theta}_k^{\text{nonlin}}) = \begin{bmatrix} f(\hat{x}_k^{\text{nonlin}}, u_k^{\text{nonlin}}, d_k^{\text{nonlin}}, \hat{\theta}_k^{\text{nonlin}}) \\ \hat{\theta}_k^{\text{nonlin}} \end{bmatrix}.$$

6. Compute covariance matrix for state error

$$\tilde{P}_{k+1} = \tilde{A}_k \tilde{Z}_k \tilde{A}_k^T + \tilde{G}_k \tilde{Q}_k \tilde{G}_k^T.$$

7. Set $k \to k+1$ and go to step 2.

References

Ahn, S., Park, M. & Rhee, H. (1999), 'Extended Kalman filter-based nonlinear model predictive control for a continuous MMA polymerization reactor', *Ind. Eng. Chem. Res.* **38**(10), 3942–3949.

Amin, J., Mehra, R. K. & Arambel, P. (2001), Coordinated dynamic positioning of a multi-platform mobile offshore base using nonlinear model predictive control, *in* 'Eleventh (2001) International Offshore and Polar Engineering Conference'. Stavanger, Norway, June 17-22, 2001.

Austin, P., Mack, J., Lovett, D., Wright, M. & Terry, M. (2002), Improved wet end stability of a paper machine using model predictive control, *in* 'Control Systems 2002', STFi and SPCI, pp. 80–84. June 3-5, 2002, Stockholm, Sweden.

Badgwell, T. A. & Qin, S. J. (2001), Review of nonlinear model predictive control applications, *in* 'IEE Control Engineering Series', Vol. 61, pp. 3–32.

Bown, R. (1996), Physical and chemical aspects of the use of fillers in paper, *in* J. Roberts, ed., 'Paper Chemistry', 2 edn, Chapman and Hall, chapter 11.

Dennis, J. E. & Schnabel, R. B. (1996), *Numerical Methods for Unconstrained Optimization and Nonlinear Equations*, Classics in Applied Mathematics, 16, SIAM, Philadelphia.

Ergon, R. (2001), *Introduction to Kalman Filtering with some Industrial Application Areas*, Lecture notes, Telemark University College, Norway.

Gattu, G. & Zafiriou, E. (1992), 'Nonlinear quadratic dynamic matrix control with state estimation', *Ind. Eng. Chem. Res.* **31**(4), 1096–1104.

Gelb, A., ed. (1974), *Applied Optimal Estimation*, The M.I.T. Press.

Gill, P. E., Hammarling, S. J., Murray, W., Saunders, M. A. & Wright, M. H. (1986), User's guide for lssol (version 1.0): A fortran package for constrained linear least-squares and convex quadratic programming, Technical Report SOL 86-1, Systems Optimization Laboratory (SOL), department of operations research, Stanford University.

Gill, P. E., Murray, W. & Saunders, M. A. (1997), 'User's guide for sqopt 5.3: A Fortran package for large-scale linear and quadratic programming'. (Draft, October 1997).

Gill, P. E., Murray, W. & Wright, M. H. (1981), *Practical Optimization*, Academic Press.

Glemmestad, B., Ertler, G. & Hillestad, M. (2002), Advanced process control in a Borstar PP plant, *in* 'ECOREPII, 2nd European Conference on the Reaction Engineering of Polyolefins. Lyon, France, 1-4 July 2002'.

Griewank, A. (2000), *Evaluating Derivatives: Principles and Techniques of Algorithmic Differentiation*, SIAM, Philadelphia.

Griewank, A. & Corliss, G. F., eds (1991), *Automatic Differentiation of Algorithms: Theory, Implementation, and Application*, SIAM, Philadelphia. Proceedings of the first SIAM Workshop on automatic differentiation, held in Breckenridge, Colorado, January 6-8, 1991.

Hauge, T. A. & Lie, B. (2002), 'Paper machine modeling at Norske Skog Saugbrugs: A mechanistic approach', *Modeling, Identification and Control* **23**(1), 27–52.

Hillestad, M. & Andersen, K. S. (1994), Model predictive control for grade transitions of a polypropylene reactor, *in* 'ESCAPE4, 4th European Symposioum on Computer Aided Process Engineering, Dublin, March 1994'.

Holmström, K. (2001), The TOMLAB optimization environment v3.0 user's guide, Technical report, HKH MatrisAnalys AB.

Kosonen, M., Fu, C., Nuyan, S., Kuusisto, R. & Huhtelin, T. (2002), Narrowing the gap between theory and practice: Mill experiences with multivariable predictive control, *in* 'Control Systems 2002', STFi and SPCI, pp. 54–59. June 3-5, 2002, Stockholm, Sweden.

Lang, D., Tian, L., Kuusisto, R. & Rantala, T. (1998), Multivariable predictive control for the wet end, *in* 'Measurement and Control of Papermaking, Edinburgh, Scotland', Pira International.

Lee, J. H. & Ricker, N. L. (1994), 'Extended Kalman filter based nonlinear model predictive control', *Ind. Eng. Chem. Res.* **33**(6), 1530–1541.

Lee, K., Lee, J. H., Yang, D. R. & Mahoney, A. W. (2002), 'Integrated run-to-run and on-line model-based control of particle size distribution for a semi-batch precipitation reactor', *Computers and chemical engineering* **26**(7-8), 1117–1131.

Lie, B. (1995), Kompendium i prosessmodellering, Lecture notes, Telemark University College. (in norwegian).

Lie, B., Dueñas Díez, M. & Hauge, T. A. (2002), A comparison of implementation strategies for MPC, *in* 'International Symposium on Advanced Control of Industrial Processes'. June 10-11, 2002, Kumamoto, Japan.

Mack, J., Lovett, D., Austin, P., Wright, M. & Terry, M. (2001), Connoisseur model predictive control of a paper machine's wet-end., *in* 'ICHEME - Advances in Process Control'. York, UK, 24-25 September 2001.

McQuillin, D. L. & Huizinga, P. W. (1995), Reducing grade change time through the use of predictive multi-variable cotrol, *in* 'ECOPAPERTECH', pp. 73–82. Helsinki, Finland.

Muske, K. R. & Badgwell, T. A. (2002), 'Disturbance modeling for offset-free linear model predictive control', *Journal of Process Control* **12**, 617–632.

Muske, K. R. & Rawlings, J. B. (1993), 'Model predictive control with linear models', *AIChE Journal* **39**(2), 262–287.

Park, M. J., Hur, S. M. & Rhee, H. K. (2002), 'Online estimation and control of polymer quality in a copolymerization reactor', *AIChE Journal* **48**(5), 1013–1021.

Prasad, V., Schley, M., Russo, L. P. & Bequette, B. W. (2002), 'Product property and production rate control of styrene polymerization', *Journal of Process Control* **12**(3), 353–372.

Qin, S. J. & Badgwell, T. A. (1997), An overview of industrial model predictive control technology, *in* 'AIChE Symposium Series, No. 316', pp. 232–256.

Qin, S. J. & Badgwell, T. A. (1998), An overview of nonlinear model predictive control applications, *in* 'Nonlinear Model Predictive Control Workshop - Assessment and Future Directions'. Ascona, Switzerland, June 3-5, 1998.

Rawlings, J. B. & Muske, K. R. (1993), 'The stability of constrained receding horizon control', *IEEE Transactions on Automatic Control* **38**(10), 1512–1516.

Schei, T. S. & Singstad, P. (1998), Nonlinear model predictive control of a batch polymerization process, *in* 'American Control Conference'. Philadelphia, Pennsylvania, June 1998.

Slora, R. (2001), Stabilization of the wet end at PM6. part 1: Developing controllers for the thick stock, Technical Report A-rapport RSL20001, Norske Skog Saugbrugs. (confidential and in Norwegian).

Solberg, I. (1988), A Modular Implementation of the Extended Kalman Filter with Application to a Crushing and Screening Circuit, PhD thesis, Norwegian University of Science and Technology.

Van de Ven, T. G. M. (1984), 'Theoretical aspects of drainage and retention of small particles on the fourdrinier', *Journal of Pulp and Paper Science* **10**(3), 57–63.

Paper G

Roll-out of model based control with application to paper machines

Hauge, T.A., Slora, R., and Lie, B. (2002). *Roll-out of model based control with application to paper machines*, Submitted to Journal of Process Control.

Extended version.

Roll-out of Model Based Control with Application to Paper Machines

Tor Anders Hauge*, Roger Slora† and Bernt Lie‡

Contents

Abstract

A mechanistic nonlinear model of the wet end of paper machine 6 (PM6) at Norske Skog Saugbrugs, Norway has been developed, and used in an MPC application. In this paper we study if the model can be applied to other paper machines (roll-out), and we discuss advantages and disadvantages of different modeling approaches. The paper machines studied are PM4 at Norske Skog

*Telemark University College, P.b. 203, 3901 Porsgrunn, Norway.
†Norske Skog Saugbrugs, 1756 Halden, Norway.
‡Telemark University College, P.b. 203, 3901 Porsgrunn, Norway. E-mail: Bernt.Lie@hit.no

Saugbrugs, and PM3 at Norske Skog Skogn, Norway. PM6 is a new and modern paper machine producing SC (Super Calendered) magazine paper. PM4 also produces SC paper but the machine is older and smaller than PM6. PM3 produces newsprint and has a size comparable with PM6. Fitting and validation of the model to PM4 and PM3 are very promising. No structural changes to the model were introduced, and still the validation results were good. The time spent on fitting and validating the PM6 model to PM4 and PM3 are approximately 1% of the time spent on developing the original model. This should be a strong incentive for focusing on mechanistic modeling in industries were there are many similar production lines or units.

1 Introduction

Many large- and medium sized industry companies have a number of more or less similar process-units for processing of raw materials or production of finished products. An industrial company which has invested, or is about to invest, in advanced model based control in one of their units / factories, would benefit economically if the model and controller could be efficiently rolled-out at similar units. The main idea of this paper is to investigate how a model and controller developed for a specific industrial process can be applied to similar processes. A mechanistic model of paper machine 6 (PM6) at Norske Skog Saugbrugs, Norway, has been developed in (Hauge & Lie 2002), and used in a model predictive control (MPC) implementation (Hauge, Slora & Lie 2002). In this paper we investigate if and how the model can be reused at PM4, Norske Skog Saugbrugs, and PM3, Norske Skog Skogn, Norway.

The papermaking process is the only process studied in this paper, however the field of roll-out should be of interest also to other industries. For example Borealis (www.borealisgroup.com) has many polymer reactors for producing plastics raw materials, Norsk Hydro (www.hydro.com) has many plants for fertilizer production, and Icopal (www.icopal.com) has many production lines for extrusion of plastic pipes.

The control method chosen for PM6 is model predictive control (MPC). The reason for choosing MPC is that it is perhaps the only advanced model based control scheme used to any extent in the industry, there are commercially available software systems for implementation, and the reported payback time is low (e.g. 3 months in (Bassett & Van Wijck 1999)).

A model of the process is the foundation for every advanced control algorithm. Given a good model of a process, there are probably a number of algorithms that will provide excellent control of the process, and given a poor model of a process, there are probably no algorithms that will provide good control of the process. Also, given a good advanced control algorithm, there are often no models available for the specific process or process unit of concern. Thus, today the key factor for success in advanced control is the development of a reliable and good process model, or as the following closing sentence in a paper put it:

> Nowadays control is easy, modelling will always be the nut to crack...
> (Richalet, Estival & Fiani 1995, page 942).

It should be emphasized that even if a perfect model is available, several limitations to control performance may occur. These limitations may arise from e.g. input constraints, and right half plane (RHP) zeros (Skogestad & Postlethwaite 1996). In practice, the model is not perfect, and additional limitations due to model uncertainty are always present.

There exists very little published material focusing on how to efficiently roll-out models and controllers in the industry. However, the idea of efficient roll-out of models is not entirely new, e.g. (Glemmestad, Ertler & Hillestad 2002) emphasize the advantage of reusing the models developed at Borealis, and many commercial simulators include model libraries of process units intended for reuse.

This paper is organized as follows. In Section 2, various approaches to modeling, with advantages and disadvantages, are discussed. Section 3 summarizes the work on modeling and model predictive control (MPC) carried out at paper machine 6 (PM6), Norske Skog Saugbrugs. Roll-out of the model on PM4, Norske Skog Saugbrugs, is described in Section 4, and similarly for PM3, Norske Skog Skogn, in Section 5. Finally, some conclusions are given in Section 6.

2 Modeling approaches

Two basic modeling approaches are *mechanistic* modeling and *empiric* modeling. An empiric model is entirely based on experimental data and an appropriate model structure, and often requires little knowledge of the system to be modeled. In the literature one often encounter terms like black box modeling, system identification, time series analysis, and behavioral modeling. All these terms basically mean the same as empiric modeling. Introductory and advanced text books on empiric modeling are e.g. (Nelles 2001), (Ljung 1999), (Walter & Pronzato 1997), (Söderström & Stoica 1989), and (Box, Jenkins & Reinsel 1994). A mechanistic model is a model built from basic principles of physics, chemistry, biology, etc., by writing down conservation or balance equations. Obviously this requires extensive knowledge of the process to be modeled. In the literature one sometimes encounters terms like white-, and grey box modeling, see e.g. (Sohlberg 1998). White box models are mechanistic models based on complete knowledge of the process, i.e. where both equations governing the behavior and the associated parameters are known *a priori*. Obviously, such models are rarely found. A grey box model is a mechanistic model where the equations governing the behavior are assumed known, but parameter values need to be estimated using experimental or historical data. Throughout this paper we include grey box models whenever we speak of mechanistic models.

Table 1 summarizes some general properties of mechanistic and empiric models, although exceptions can easily be found.

The perhaps strongest argument for using an empiric model is that the time for building such a model is much lower than for a mechanistic model. In (Foss, Lohmann & Marquardt 1998) it is indicated that the development cost for an empiric model is about 1/10 compared to a mechanistic model. Another positive feature of empiric models is that they often have a simple structure (linear and time invariant) which

Table 1: Mechanistic versus empiric models. Partly reproduced from Støle-Hansen 1998, and Walter & Pronzato 1997.

Properties	**Mechanistic**	**Empiric**
Utilize physical knowledge and insight	yes	no
The parameters have known range	yes	no
Number of unknown parameters	low	high
Time needed to develop a model	high	low
Resources needed to maintain a model	low	high
Easy to use for complex/unknown processes	no	yes
Amount of data needed	low	high
Applicability to control and training	yes	yes
Applicability to design	yes	no
Extrapolation properties	good*	bad
Increases process knowledge	yes	no
Complex	yes (non-linear)	no (often linear)
Simulation	long/difficult	quick/easy
Possible roll-out of model	yes	no

*if structure is correct.

leads to quick and easy simulation, analysis, and design of control algorithms. If one has access to experimental data, and the operating region of the process is only moderately nonlinear, then it seems reasonable to first try an empiric model.

The strength of a mechanistic model lies in its ability to capture known nonlinear phenomena and thereby having extraordinary extrapolating properties, and the possible reuse of the model on similar processes. This and other features are emphasized in the following quotation:

> ..., a model based on first principles can operate in a larger domain than a black-box model. A model based on first principles will in general contain fewer parameters and will therefore be more parsimonious. From the parsimony principle we know that the best model is the simplest model that adequately describes the process, since overparameterization will in general lead to poor generalization. A consequence of fewer parameters, a model based on first principles will need fewer experiments to be identified. On the other hand, a black-box structure is easier to develop. ... To identify our model (a mechanistic model – authors note) we have only used history data from the plant. (Hillestad & Andersen 1994, page 42 and 45)

Consider the paper machine model implemented at PM6. This model has 19 parameters, including two biases and three initial ODE values, which are tuned to fit the model to data. The model has three inputs, three outputs, three states, and four measured disturbances. A linear (empiric) state space model of the same dimension would consist of 63 parameters, including the direct input to output matrix and three

initial ODE values. An empiric transfer matrix model would consist of *minimum* 42 parameters, corresponding to pure first order elements. That is one parameter for the time constant, and one for the gain, in each element. If a step response model or impulse response model is used, the number of parameters would increase even more. In addition, the empiric models mentioned here have a limited operating range and must either be adaptive or a set of models is needed. In (Kosonen, Fu, Nuyan, Kuusisto & Huhtelin 2002), an approach where a set of adaptive empiric models are used to cover the operating region of the paper machine, is described.

A point made by (Ogunnaike & Wright 1997, page 49), is that mechanistic modeling results in a small number of parameters that can intuitively be understood, thus reducing long term support cost. Industrial processes do not remain static and it is likely that the model, whether empiric or mechanistic, will degrade with time. Another point, which is often neglected in the literature, is that the un-manipulatable nature of most measured disturbances makes it hard to model their effect on the model outputs empirically. Submodels from measured disturbances to model outputs can in some cases be identified from experimental data, however in most cases the data will not be informative enough and physical knowledge and insight must be used.

3 Modeling and MPC at PM6, Norske Skog Saugbrugs

Norske Skog Saugbrugs in Halden, Norway, is one of the largest manufacturers of uncoated super calendered magazine paper in the world. The total production capacity of the mill is 550,000 ton per year. The largest paper machine (PM) at the Saugbrugs mill is PM6, accounting for more than half the total production capacity. PM6 was build in the early 1990's and produce paper with width of 8.62 meters, and with a typical velocity of 1550 meters per minute.

Magazine paper is characterized by its glossy appearance due to a high content of filler in the paper. The finished magazine paper typically consists of 65% fiber, 30% filler, and 5% water. The main difference between magazine paper and e.g. newsprint is the content of filler. For newsprint the amount of filler is typically between 0-10%. Due to the high filler content in magazine paper, the couplings between important input and output variables are rather dominant.

3.1 Process description

A simplified drawing of PM6 is shown in Figure 1. Cellulose, TMP (thermomechanical pulp) and broke (repulped fibers and filler from sheet breaks and edge trimmings) are blended in the mixing chest. The stock is fed to the machine chest with a controlled total consistency[1]. Between the mixing and machine chests, filler is added at a

[1] The total consistency is the weight of solids (i.e. filler particles and fiber) divided by the total weight of solids and water.

constant rate. The fillers used in paper production depends on the end-user requirements, however some of the typical fillers are kaolin, chalk, talc, and titanium dioxide (Bown 1996). About two thirds of the filler particles used at PM6 is added to the thick stock, the rest at the outlet of the white water tank. The flow to the machine chest is large in order to keep the level of the machine chest constant, and an overflow is returned to the mixing chest. The total consistency in the mixing and machine chests are typically around 3 to 4%, which is considerably higher than consistencies later on in the process, and thus the stock from the machine chest is denoted the "thick stock".

The thick stock enters the "short circulation" in the white water tank. Here, the thick stock is diluted to 1-1.5% total consistency by white water[2] and a recirculation flow from the deculator. Filler is added to the stock just after the white water tank. The first cleaning process is a five stage hydrocyclone arrangement, mainly intended to separate heavy particles (e.g. sand and stones) from the flow. The accept from the first stage of the hydrocyclones goes to the deculator where air is separated from the stock. The second cleaning process is two parallel screens, which separates larger particles (e.g. bark) from the stock. Retention aid is added to the stock at the outlet of the screens. The retention aid is a cationic polymer which, amongst others, adsorb onto anionic fibers and filler particles and cause them to flocculate. The flocculation process is a key for retaining small filler particles (and small fiber fragments) on the wire, although the significance of mechanical entrapment of non-flocculated filler and fines seems to be somewhat controversial in the literature. For example (Van de Ven 1984) found (theoretically) that mechanical entrapment was low, while (Bown 1996) reports that mechanical entrapment can be a dominant mechanism. In the headbox the pulp is distributed evenly onto the fine mesh, woven wire cloth. Most of the water in the pulp is recirculated to the white water tank, while a share of fiber material and filler particles form a network on the wire which will soon become the paper sheet. The pulp flow from the white water tank, through the hydrocyclones, deculator, screens, headbox, onto the wire and back to the white water tank is denoted the "short circulation".

In the wire section, most of the water is removed by draining. In the press section, the paper sheet is pressed between rotating steel rolls, thus making use of mechanical forces for water removal. Finally, in the dryer section the paper sheet passes over rotating and heated cast iron cylinders, and most of the water left in the sheet is removed by evaporation. The paper is then accumulated on the reel before it is moved on to further processing.

3.2 The process model

The process model is described in detail in e.g. (Hauge & Lie 2002) and only a brief description will be given here. Note that some modifications have been carried out to the model detailed in (Hauge & Lie 2002), as compared to the model implemented at PM6. The most prominent modification is that a first order empiric model that was

[2] White water is the drainage from the wire. It is stored in the white water tank.

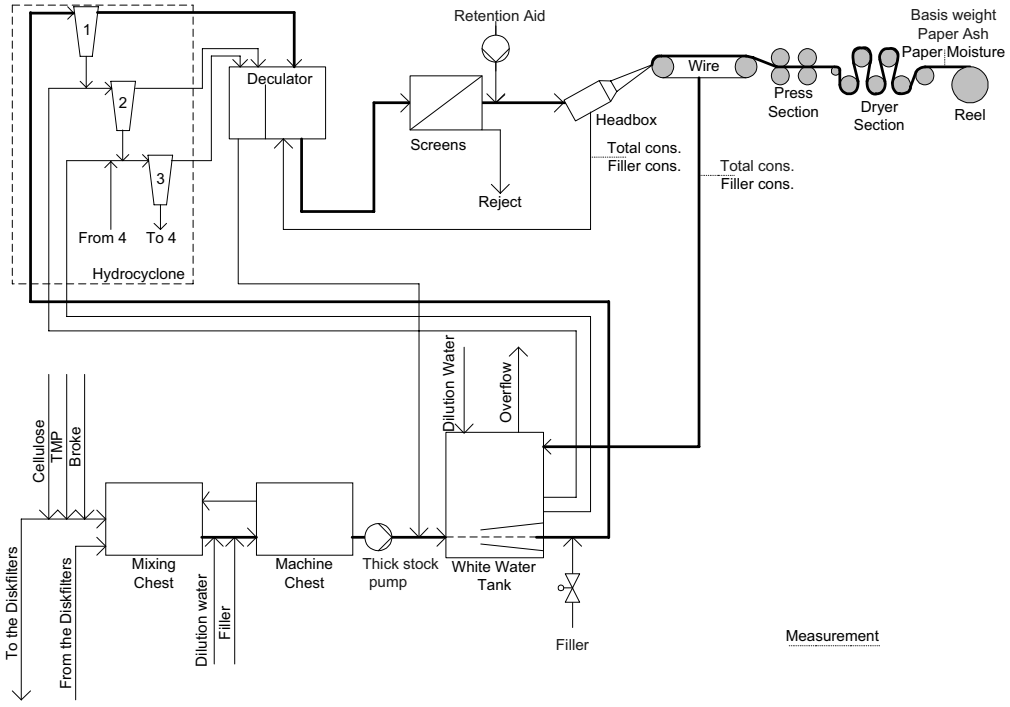

Figure 1: Simplified drawing of PM6, Norske Skog Saugbrugs.

added to capture neglected and unknown dynamics in the process, has been removed.

The model was originally developed with several ordinary and partial differential equations. The model was then simplified, and eventually fitted to experimental and operational mill data. The "final" model consists of a third order nonlinear mechanistic model based on physical and chemical laws. The structure of the developed process model is

$$\begin{aligned} \dot{\bar{x}} &= \bar{f}(\bar{x}, \bar{u}, \bar{d}, \bar{\theta}) \\ \bar{y} &= \bar{g}(\bar{x}, \bar{u}, \bar{d}, \bar{\theta}), \end{aligned} \tag{1}$$

with $\bar{x} \in \mathbb{R}^n = \mathbb{R}^3$, $\bar{y} \in \mathbb{R}^m = \mathbb{R}^3$, $\bar{u} \in \mathbb{R}^r = \mathbb{R}^3$ and $\bar{d} \in \mathbb{R}^g = \mathbb{R}^4$. The bar above the variable names indicate that these are the variables in their original units and coordinate system. $\bar{\theta}$ consists of several model parameters, tuned to fit the model outputs to experimental and operational data.

The manipulated inputs $\bar{u}$, the outputs $\bar{y}$, the states $\bar{x}$, and the measured disturbances $\bar{d}$ are

$$\begin{aligned} \bar{u}^T &= [\bar{u}_{TS}, \ \bar{u}_F, \ \bar{u}_{RA}] \\ \bar{y}^T &= [\bar{y}_{BW}, \ \bar{y}_{PA}, \ \bar{y}_{WC}] \\ \bar{x}^T &= \left[\bar{C}_{R,fil}, \ \bar{C}_{WT,fil}, \ \bar{C}_{D,fib}\right] \\ \bar{d}^T &= \left[\bar{C}_{\mathrm{TS,tot}}, \ \bar{C}_{\mathrm{TS,fil}}, \ \bar{v}, \ \bar{f}\right], \end{aligned} \tag{2}$$

where the inputs are the amount of thick stock, filler added at the outlet of the white water tank, and retention aid added at the outlet of the screens, and where the outputs are the basis weigh (weight per area), paper ash content (content of filler in the paper), and wire tray consistency in the recirculation flow from the wire to the white water tank. The basis weight and paper ash outputs are direct quality variables, while the wire tray consistency is an indirect quality variable having significant effect on variability of other short circulation variables. $\bar{C}_{R,fil}$ is the concentration of filler in a reject tank in the hydrocyclones, $\bar{C}_{WT,fil}$ is the concentration of filler in the white water tank, and $\bar{C}_{D,fib}$ is the concentration of fiber in the deculator. The measured disturbances accounted for in the model, are the total and filler thick stock concentrations $\bar{C}_{\mathrm{TS,tot}}$ and $\bar{C}_{\mathrm{TS,fil}}$, the paper machine velocity $\bar{v}$, and the paper moisture percentage $\bar{f}$.

Note that the total- and filler concentrations in the thick stock flow are called "measured disturbances", although they are not measured. A model of the thick stock area has been developed (Slora 2001), and implemented at PM6, providing estimates of total- and filler concentrations in the thick stock.

3.3 Model fitting from experimental data

The developed model has many parameters. These parameters have physical interpretations and thus it should be possible to measure them (e.g. the volumes) or estimate them one by one from local measurements (e.g. measure the flows and concentrations

in each stage of the hydrocyclones and calculate the associated parameters). This approach would require a very large and detailed model, probably not suitable for on-line use. The model used at PM6 is a simple approximation of a complex process and the parameters in the model, although they have a physical interpretation, should not be measured and/or estimated one by one due to the poor input-output properties of the resulting model. Consider e.g. the deculator volume, which is important for characterizing the time constant for the sub-model between the thick stock and the basis weight. The real volume of the deculator is approximately $17\,\mathrm{m}^3$ (right chamber), however in the model it is many times larger. The deculator volume in the model should be regarded as a lumped volume and not a single physical volume. The most important properties of the model are the input-output properties, i.e. the response on the outputs from changes in inputs. Thus, we want to estimate the parameters in the model so that these properties are good. In principle we would therefore like to tune the parameters so that the model outputs are equal to measured outputs. However, due to the large number of parameters in the model we set some parameters equal to values that seem reasonable, and estimate the rest, i.e. we estimate 19 parameters including two biases and three initial ODE values.

The function `lsqnonlin` in the Matlab Optimization toolbox is used for solving the minimization problem

$$\hat{\theta} = \arg\min_{\theta} J(\theta), \tag{3}$$

subject to the constraints

$$\theta_{\min} \leq \hat{\theta} \leq \theta_{\max}, \tag{4}$$

where θ is the parameter vector and $\hat{\theta}$ is the estimated parameter vector. Thus, we wish to find the parameter values (arguments) $\hat{\theta}$ that minimize the criterion $J(\theta)$. The criterion used is

$$J(\theta) = e^T(\theta) \cdot Q \cdot e(\theta), \tag{5}$$

where e is a vector of errors, and Q is a diagonal weighting matrix. The function relies on the Levenberg-Marquardt algorithm in its search for the optimal parameter values (The MathWorks, Inc. 2000). The errors e are calculated by simulating the system, with only the initial conditions given. The error is then

$$\varepsilon(t) = \hat{y}(t|0) - y(t), \tag{6}$$

where $y(t)$ is the measured output at time t, and $\hat{y}(t|0)$ is the model output at time t given only the initial conditions. The error vector for output i is then

$$e_i^T(\theta) = \begin{bmatrix} \varepsilon_i(1) & \varepsilon_i(2) & \cdots & \varepsilon_i(t) & \cdots & \varepsilon_i(N-1) & \varepsilon_i(N) \end{bmatrix}. \tag{7}$$

where N is the number of samples in the data set.

Traditional system identification (see e.g. (Ljung 1999)) is in most cases carried out using a one-step-ahead predictor (corresponding to $\varepsilon(t) = \hat{y}(t|t-1) - y(t)$), however in our case we wish to emphasize the need for a model with good long term prediction

abilities. The reason for this is that the model is used for model predictive control (MPC). Then, it seems natural to use the simulation approach in the parameter estimation algorithm. The simulation approach results in a deterministic model, and it is also necessary to identify or model the noise.

The concept of scaling is very important for robust and rapid convergence to the optimal parameter values (Betts 2001). Here, we will point at two simple methods for scaling: scaling of parameters and scaling of the simulation error. Scaling of the parameters can be achieved by introducing

$$\theta = S \times \tilde{\theta}, \tag{8}$$

where $\tilde{\theta}$ is the scaled parameter vector, θ is the original non-scaled parameter vector, S is a scaling vector, and $\times$ is the Hadamard product (an element by element multiplication). The scaling vector S may be chosen so that the assumed scaled parameter values are close to unity. Consider e.g. the following assumed parameter vector

$$\theta = [10^{-5}, 10^{8}].$$

Choosing

$$S = [10^{-5}, 10^{8}],$$

gives the following scaled parameter vector

$$\tilde{\theta} = [1, 1].$$

Any constraints or bounds on the parameters must be scaled accordingly.

The simulation error is defined in equation 6. The basis weight is measured in $\mathrm{g/m^2}$ and has a value typically around $50\,\mathrm{g/m^2}$, paper ash is measured in % and has a value typically around 30%, and the wire tray concentration in measured in % has a value of approximately 0.6%. Based on this, it is easy to understand that the error for the wire tray concentration is very small compared to the other to errors, thus any model fitting routine would more or less ignore the wire tray concentration and concentrate on fitting the basis weight and paper ash. To compensate for this one may scale the simulation error or outputs, simply by multiplying with a weight. If all outputs are regarded equally important, one may weight them so that the outputs are approximately equal. For example, the wire tray could be multiplied by 50 to make it approximately equal to the paper ash. However, in our case we define the most important output to be the basis weight, the second most important output to be the paper ash, and the least important output is the wire tray concentration. This ranking of importance should thus also be reflected in the weighting of the outputs.

3.4 Validation and re-tuning of model

Validation is the method of checking how good the model really is. One may find a model fitted almost perfectly to one data set, and totally failing to explain another data set (failing to simulate outputs close to measured outputs). Many methods for validation exist, however in our opinion any proper validation method should at least

include testing of the model with a new data set. Using one half of the data set for model fitting and one half for validation is not in our opinion a proper validation method, as one will e.g. not discover whether slow varying disturbances, drifts and trends, eventually will ruin the properties of the model. Ideally, data sets spanning all operating conditions of the process should be used for validation, thus one would have a fair chance to find areas where the model is not functioning properly.

Validating a model by comparing simulated and real outputs, is in general not enough when the model should be used for control. The individual responses from each input to each output are also very important. A procedure is presented next, which is used and found to work well, for model fitting, validation and re-tuning of the model. The procedure is also pictorially presented in Figure 2.

1. Make model.

2. Collect several data sets, at least one for model fitting and one for validation. The data set used for model fitting should contain well excited data. The data set for validation must also to some extent be excited. The length of the data sets obviously depends on the process and size of the model. For the PM6 work, the data sets ranged from 2 hours to several days. It is usually not important whether the data are collected in open or closed loop since "*a directly applied prediction error method – applied as if any feedback did not exist – will work well and give optimal accuracy if the true system can be described within the chosen model structure*" (Ljung 1999, page 434). Check the data for outliers and that the units are correct, and also consider filtering of the data.

3. Set up tables of approximately expected gains and time constants from inputs and measured disturbances, to outputs. These gains and time constants could be found from discussions with process operators and engineers alone, but should be supported by step tests carried out on the process, if possible.

4. Choose initial parameter values and fit the model to the data. Several re-optimizations may be needed. For example if the optimal parameter values are very different from the initial values, then the optimal values should be used as initial values and optimized again (thus, a re-scaling is also carried out). Other reasons for re-optimizing may be to try other initial parameter values, or other parameter bounds. If reasonably good model fit is *not* obtained, changing the model equations may eventually be necessary.

5. Validate the model by comparing simulated and measured outputs, using a different data set than the one used for model fitting. If the result is not satisfactory one should probably return to point 4, and try different initial values or parameter bounds. Eventually one may need to change the model equations if reasonable validation results are not obtained.

6. Simulate step tests on the fitted model, and compare the gains and time constants with the expected results as found in point 3. If the gains and time

constants are reasonably close to the expected ones, the model fitting and validation is finished.

7. If the gains and time constants in point 6 are too far from the expected values, re-tune the model by changing parameter values that move the gains and time constants towards the expected ones. When reasonable gains and time constants are found, go to point 5 and compare simulated and measured outputs. Eventually one may need to change the model equations if reasonable gains and time constants are not found.

3.5 Model Predictive Controller (MPC)

A commercial MPC developed by Prediktor AS (www.prediktor.no), was chosen by Norske Skog for implementation. The choice of MPC was based on (i) cost, and (ii) the ability to add and develop certain features that were important. Special features that were important were the abilities to

- utilize the non-linear model;
- specify future reference changes. This means that the process operators can specify a setpoint change some time into the future, see how the controller will respond, and let the controller do the grade change if they are satisfied with the response. In many other systems, the setpoint is constant into the future, so once a change in the setpoint is made, the controller will respond immediately, giving the operators no time to consider how wise the response is;
- develop an interface that will gain operator acceptance of the MPC;
- use the MPC during grade changes, sheet breaks, and start ups.

The commercial MPC is part of a software package named Apis (Advanced Process Improvement System), which also consists of a Kalman filter, subspace system identification, and more. The Apis MPC was intended for linear models, based on the infinite horizon objective function presented in (Muske & Rawlings 1993). For the predictive controller implemented at PM6, several extensions were made to the original MPC, such as

- online linearization at each sample;
- online estimation of key model parameters/biases;
- future setpoint changes, i.e. the process operators can submit new setpoints to the controller some time ahead of the actual grade change;
- addition of a direct input to output term;
- inclusion of measured disturbances.

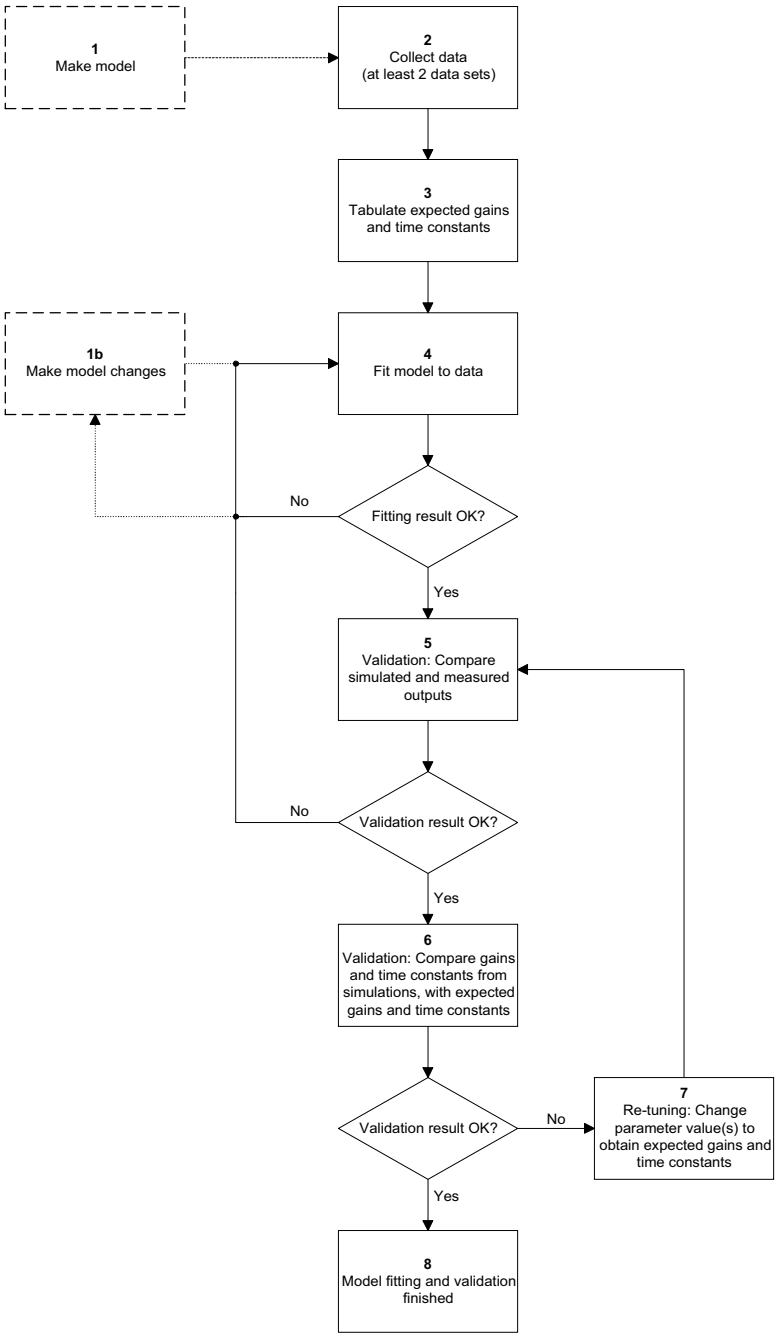

Figure 2: Procedure for model fitting and validation.

The use of MPC, a nonlinear model, an extended Kalman filter, and linearization at each sample, has also been suggested by (Lee & Ricker 1994), although with a finite horizon criterion. Similarly, (Gattu & Zafiriou 1992) proposed an algorithm for nonlinear MPC, with linearization at each sample, but with computation of the steady state Kalman gain at each sample.

3.6 Results

The main objective of the project "Stabilization of the wet end at PM6" was to increase the total efficiency by 0.47%. This objective can hardly be validated, due to many factors affecting the total efficiency. Thus, several sub-goals were defined which were assumed easier to measure and validate. The sub-goals and results concerning reduced variability are:

Variable	**Sub-goal (red. std. dev.)**	**Result**
Total cons. in the wire tray	60%	Achieved
Filler cons. in the wire tray	50%	Achieved
Total cons. in the headbox	50%	Achieved
Filler cons. in the headbox	35%	Achieved
Basis weight	20%	Not achieved
Paper ash	20%	Achieved
Paper moisture	20%	Achieved

These sub-goals were defined in 1999 when the project was initiated. In 2001 a new scanning device for measuring e.g. basis weight and paper ash was installed at PM6. This significantly improved the control of the basis weight using the "old" controllers. The results in the table above are calculated with the measurement devices as of 2002, comparing the old control configuration with the MPC control configuration. Exact numbers for the reduction in standard deviation are not given, as they vary from day to day, and from operator to operator.

In addition to reducing the variation in key paper machine variables, several other benefits are obtained using MPC. Some of these benefits arise from utilizing the developed model, not only for control purposes, but also as a replacement for measurements when these are not available or not trustworthy.

Previously, grade changes were carried out manually or partly manually (the set-points were changed a number of times before they were equal to the new grade) by the operators. With a mechanistic model, applicable over a wide range of operating conditions, the grade changes are carried out using the MPC. This has resulted in faster grade changes and operator independent grade changes. During larger grade changes, the use of MPC results in less off-spec paper being produced during the change. Using a single mechanistic model, the grade change is handled in a straight forward fashion, as there is no need to switch between various local models.

The basis weight and paper ash outputs can not be measured during sheet breaks. Previously during sheet breaks, the flow of thick stock and filler were frozen at the value they had immediately prior to the break. Usually the sheet breaks last less

than half an hour, and the output variables are not far from target values when the paper is back on the reel. However, occasionally the sheet breaks last longer periods and there may be e.g. velocity changes during the break, leading to off-spec paper being produced for a period after the paper is back on the reel. Another frequently experienced problem are large measurement errors immediately after a sheet break. With the MPC, the Kalman filter estimates the basis weight and paper ash during sheet breaks, and these estimates are used in the MPC as if no break had taken place. Thus, when the paper is back on the reel, the outputs are close to their setpoints.

Previously, the controllers were not set to automatic mode before the outputs were close to the setpoints, following a start up. With a model based controller using a mechanistic model with a wide operating range, the MPC is set to automatic mode early during start ups. This results in faster start ups, and less off-spec paper being produced.

Occasionally a special filler is added to the stock, to increase the brightness of the paper. During these periods the consistency measurements are not trustworthy as they are based on optical measurement methods. This problem is solved within the MPC / Kalman filter framework by neglecting the measured consistency, relying on the estimate alone. For each output, there is an option within the MPC to neglect the updating of states based on this output. This is done based on experience with periods of poor measurements, even when only standard filler is used.

The Kalman filter estimates are used in the MPC instead of the measurements. This leads to smoother controller action, and eliminates the need for additional filtering.

The model is augmented so that some key parameters/biases are updated automatically. This reduces the need for model maintenance off-line. However, should there be larger changes in the process, such as if the white water tank is removed, or a new retention aid is used, then it will probably be necessary to re-tune the model and controller.

4 Roll-out at PM4, Norske Skog Saugbrugs

PM4 at Norske Skog Saugbrugs in Halden, Norway, produce super calendered magazine paper. PM4 started up in 1963 and was rebuild during a period between 1987 to 1993. The production capacity is $125,000$ ton per year, with paper width of 4.65 meters and with a typical velocity of $1,250$ meters per minute (Sandersen 1999).

4.1 Process description

A simplified drawing of PM4 at Norske Skog Saugbrugs is shown in Figure 3. Only differences between PM4 and PM6, described in subsection 3.1, will be commented on. Note that both PM6 and PM4 at Norske Skog Saugbrugs produce super calendered magazine paper, but PM6 is 30 years younger, and has more than twice the production capacity of PM4.

The largest differences between PM4 and PM6 are probably found in the thick stock area. At PM4, no filler is added to the thick stock. Thus the only filler present in the thick stock area comes with the flow of broke and recovered stock. At PM6 disc filters are used to reclaim usable fiber and filler particles from the white water tank overflow, while another technology is used at PM4. Starch is a polymer of glucose derived from e.g. corn and potatoes (Scott 1996). Starch is added to the thick stock of PM4 through the TMP flow, while no starch is added at PM6. Starch is mainly added to improve the dry-strength of the paper, however it may also improve fines retention and drainage on the wire, and it may have a negative effect on paper formation[3] (Marton 1996).

At PM6 the thick stock pump is manipulated to control the flow of thick stock, while at PM4 the thick stock pump is set at a constant speed and a thick stock valve is manipulated. This difference should be of no concern since the measured flow of thick stock is the flow entering the white water tank in both cases, and the MPC calculates the setpoint for this flow. Whether the lower level controller manipulates a pump or valve to obtain the setpoint, is irrelevant for the MPC.

The accept from the second and third stages of the hydrocyclone arrangement goes to the inlet of the white water tank via the deculator (left chamber) at PM6. At PM4 the accept goes straight to the inlet of the white water tank. This is probably not an important difference since the volume of the left chamber of the deculator is very small. Finally, a difference in the number of stages in the hydrocyclone arrangement can be found; at PM6 a five stage arrangement is used, while it is a seven stage arrangement at PM4.

4.2 Model fitting results

Figure 4 shows the first attempt to fit the PM6 model to a noisy and oscillating operational data set collected from PM4 during October 18-19, 2002. Based on this first attempt to fit the model, it was decided to carry out experiments to obtain more informative data.

Open loop experiments were carried out during a 5-hour period on the 10th of December 2002. These experiments were used to find approximate values for gains and time constants in the process, and for model fitting, as described in Section 3.4 and Figure 2. Another data set was collected on the 12th of December 2002 for validation of the model. The validation data set was collected partly in open loop and with the process operators manually carrying out some step changes and a grade change. The inputs are shown in Figure 5, and the measured and simulated outputs are shown in Figure 6. Note that no state updating takes place during the validation, and only the initial values are given. Some statistics from the validation are given in Table 2. The term RMSE in Table 2 denotes the Root Mean Square Error value defined by

[3] The distribution of fibres in the paper sheet.

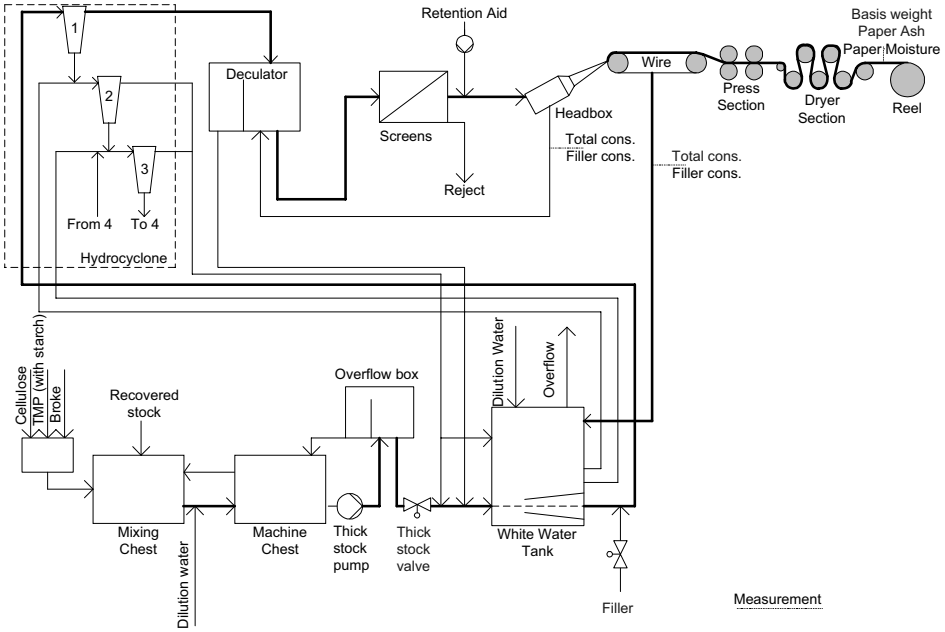

Figure 3: Simplified drawing of PM4, Norske Skog Saugbrugs.

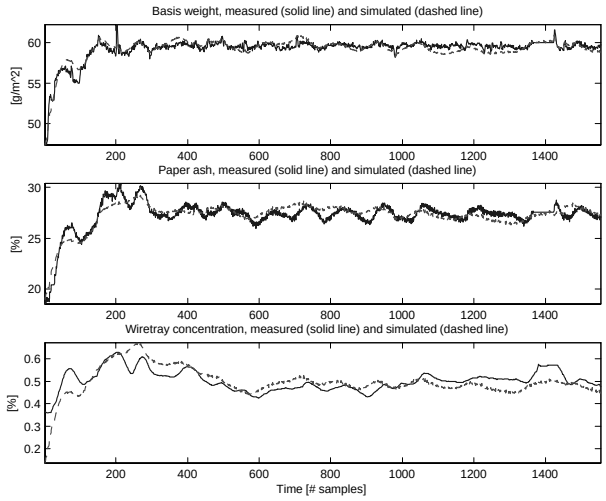

Figure 4: First trial fitting of PM6 model to data from PM4.

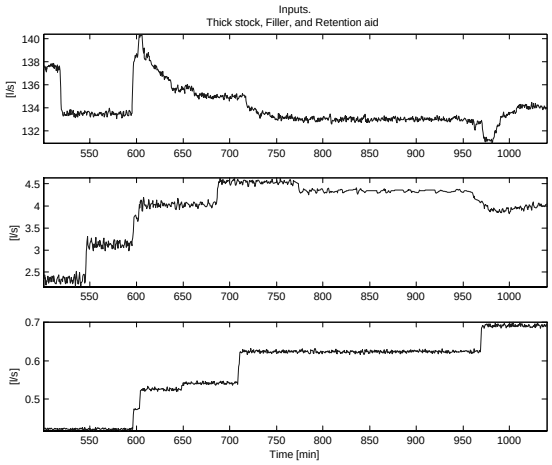

Figure 5: Inputs at PM4 on the 12th of December 2002. The data set were used for validation of the fitted model.

Table 2: Statistics from validation of model with PM4 data.

Properties	**Basis weight**	**Paper ash**	**W.t. conc.**
Bias	-0.52	0.97	0.04
RMSE*	0.37	0.19	0.013

*Bias corrected

$$\mathrm{RMSE}_i = \sqrt{\frac{1}{N}\sum_{t=1}^{N}\left(y_i(t) - \hat{y}_i(t)\right)^2}, \tag{9}$$

where N is the number of observations, $y_i(t)$ is the measured value of output i at time t, and $\hat{y}_i(t)$ is the predicted or simulated value of output i at time t.

5 Roll-out at PM3, Norske Skog Skogn

Norske Skog Skogn is the largest producer of newsprint in Norway. The production of newsprint started in 1966, and the mill has three paper machines as of today. PM3 is the largest and most modern paper machine at the Skogn mill. The production capacity of PM3 is $227,000$ ton per year, with paper width of 8.47 meters, and with a typical velocity of $1,350$ meters per minute. The basis weight has a more limited range than the Saugbrugs machines; typical values are 42.5, 45, and 48.8 $\mathrm{g/m^2}$. PM3 started up in 1981 and had a major rebuild/updating in 1995. PM3 is the only paper

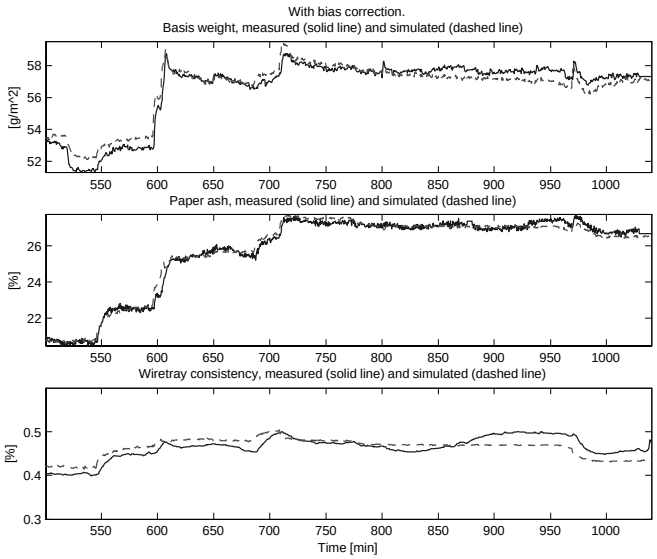

Figure 6: Validation of fitted model. The outputs were collected at PM4 on the 12th of December 2002. The validation is carried out by simulating the system with only the initial state values given.

machine in Norway using DIP[4] for production of newsprint. The DIP content, or the amount of recycled fiber, is approximately 50-55% (Norske Skog 2002), (Heggli 2002).

5.1 Process description

A simplified drawing of PM3 at Norske Skog Skogn is shown in Figure 7. Only differences between PM3 at Skogn and PM6 and PM4 at Saugbrugs, described in subsection 3.1, will be commented on. Note that PM3 in Skogn produce newsprint while both PM6 and PM4 at Saugbrugs produce super calendered magazine paper. In terms of production capacity and paper width, PM3 at Skogn, and PM6 at Saugbrugs are comparable.

Filler is added via the DIP and broke flows, thus no other filler is added to the thick stock or short circulation. The thick stock flow is manipulated through the thick stock valve, with the thick stock pump set to a constant speed. The number of stages in the hydrocyclones are 6. The accept from the second stage of the hydrocyclones goes to the inlet of the white water tank, and the accept from the third stage goes to the white water tank. At PM6, the accept from the second and third stage goes to the left chamber of the deculator. The screens and the deculator appear in reverse order at PM3, compared to PM6 and PM4 at Saugbrugs. Also, the retention aid is added before the screens, and not after as is done at PM6.

5.2 Model fitting results

Figure 8 shows the first attempt to fit the PM6 Saugbrugs model to data collected at PM3 Skogn during December, 4th, 2002. The basis weight is the only output excited to any extent in this data set, the paper ash and wire tray concentration being more or less at rest. This is a general feature of PM3 due to the low filler content in the stock. Thus, the multivariable PM6 model does not come to full appraisal at PM3 yet, however there is an increasing trend of using more filler in newsprint, and test runs at PM3 with filler added to the short circulation will soon take place (Heggli 2002).

Studying data from PM3, it is clear that there is not much to gain in terms of stabilizing the process during normal operation. However, during start ups, sheet breaks, and grade changes, efficiency may be improved. Figure 9 shows the inputs during a grade change. Note that the filler input is zero throughout the data set because no filler is added to the short circulation. At the beginning of the grade change a sheet break occur. This is recognized in Figure 10 by the basis weight and paper ash outputs being frozen at the values that they had immediately prior to the break. When the paper is back on the reel, the measured basis weight is $52\,\mathrm{g/m^2}$, while the setpoint is $48.8\,\mathrm{g/m^2}$. The simulated basis weight is close to the measured basis weight when the paper is back on the reel, and the simulated basis weight follows the measured basis weight closely during the whole simulation. The bias in the basis weight is approximately $0.25\,\mathrm{g/m^2}$. If the controller had relied on the simulated model output during the combined grade change and sheet break, the basis weight would

[4] DIP = De-Inked Pulp, i.e. pulp produced from recovered paper.

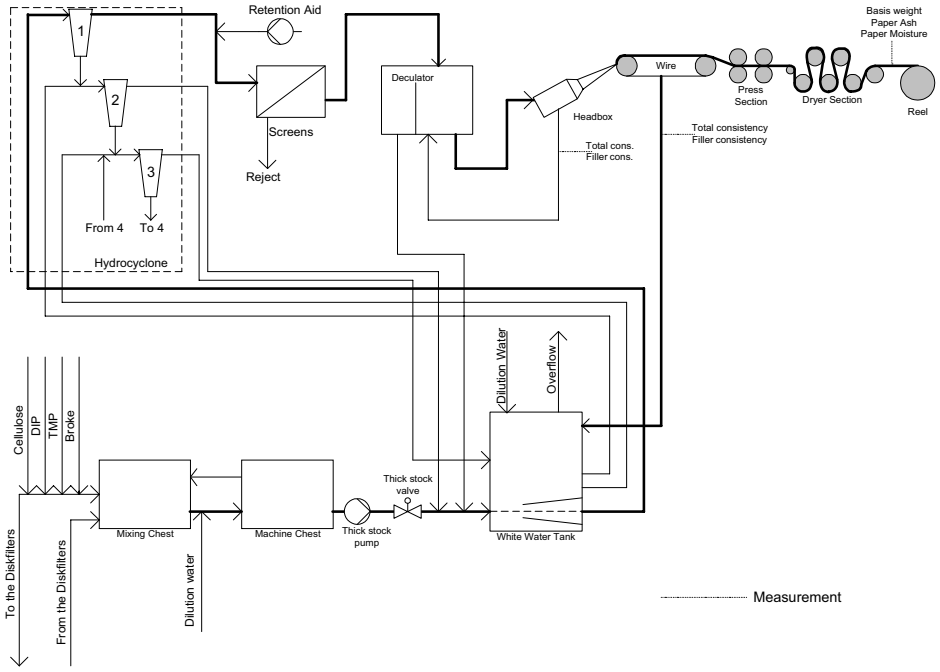

Figure 7: Simplified drawing of PM3, Norske Skog Skogn.

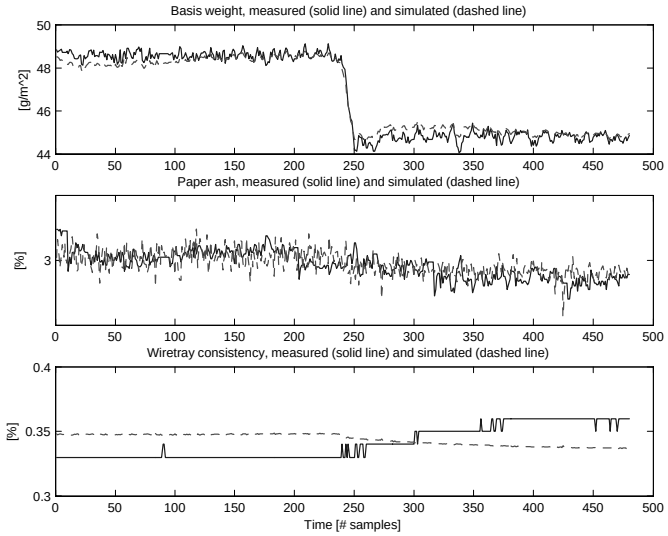

Figure 8: First trial fitting of PM6 Saugbrugs model to data from PM3 Skogn. Data collected at 4th of December, 2002, with 30 seconds sampling time (resampled from 5 seconds sampling time).

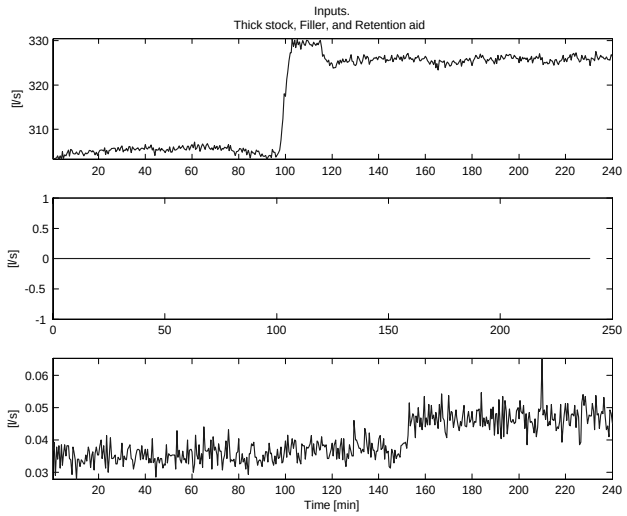

Figure 9: Inputs at Norske Skog Skogn PM3 on the 12th of December 2002 during a grade change. The data set were used for validation of the fitted model.

probably have been close to the setpoint when the paper was back on the reel. Thus, less off-spec paper would be produced.

Figure 11 shows the inputs during a start up, and Figure 12 shows the basis weight and wire tray concentration outputs. The basis weight measurement is frozen at $44.8\,\mathrm{g/m^2}$ during the first 330 minutes. In Figure 13, it is shown in detail what happens to the basis weight measurement and simulated output when the paper is back on the reel for the first time after the start up. The measured basis weight is close to $49\,\mathrm{g/m^2}$, with the setpoint being $45\,\mathrm{g/m^2}$. This deviation was more or less predicted by the model simulation, thus the basis weight could have been much closer to the setpoint after the start up if the controller had relied on the simulated model outputs when the measurements were not available.

6 Conclusions

A mechanistic nonlinear model of the wet end of PM6 at Norske Skog Saugbrugs has been developed, and used in an MPC application. Variability in important quality variables and consistencies in the wet end have been reduced substantially, compared to the variability prior to the MPC implementation. The MPC also provides better efficiency through faster grade changes, control during sheet breaks and start ups, and better control during periods of poor measurements.

Data and information from PM4 at Norske Skog Saugbrugs, and PM3 at Norske

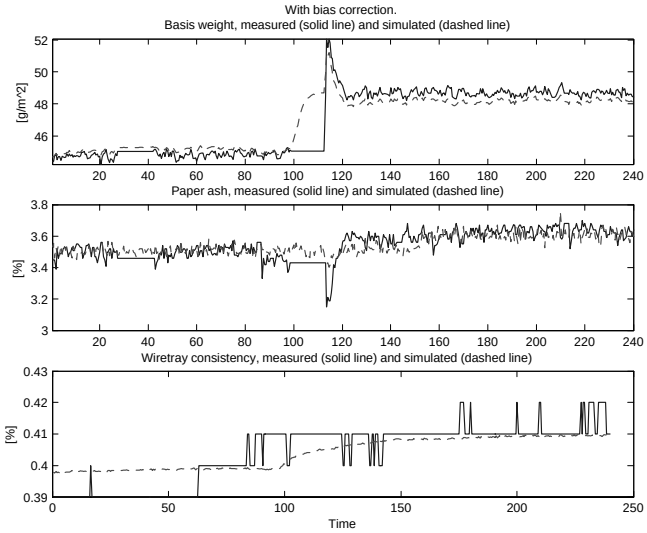

Figure 10: Validation of fitted model. The outputs were collected at Norske Skog Skogn PM3 on the 12th of December 2002 during a grade change. The validation is carried out by simulating the system with only the initial state values given.

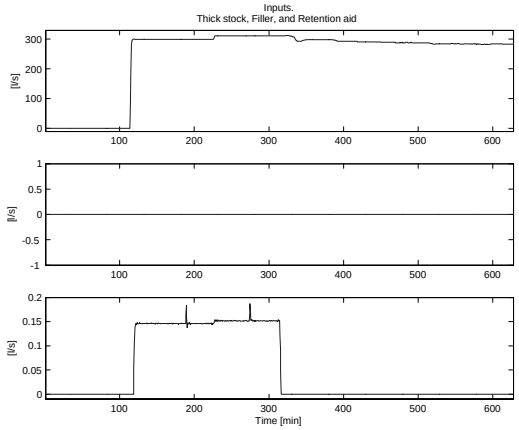

Figure 11: Inputs at Norske Skog Skogn PM3 on the 11th and 12th of December 2002 during a start up. The data set were used for validation of the fitted model.

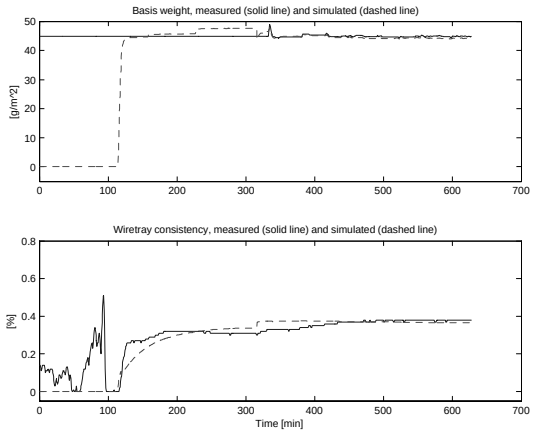

Figure 12: Validation of fitted model. The outputs were collected at Norske Skog Skogn PM3 on the 11th and 12th of December 2002 during a start up. The validation is carried out by simulating the system with only the initial state values given. During the first 330 minutes paper is not produced and the basis weight measurement is frozen at $44.8\,\mathrm{g}/\,\mathrm{m}^2$.

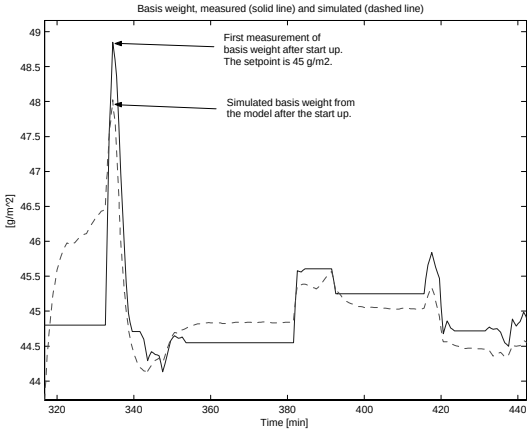

Figure 13: Validation of basis weight during start up. The outputs were collected at Norske Skog Skogn PM3 on the 11th and 12th of December 2002. The validation is carried out by simulating the system with only the initial state values given. During the first 330 minutes paper is not produced and the basis weight measurement is frozen at $44.8\,\mathrm{g}/\,\mathrm{m}^2$.

Skog Skogn were gathered in order to investigate the possibility to roll-out the model and controller on other paper machines. Fitting and validation of the model were very promising. No changes to the model were carried out, except for tuning of parameter values, and still the validation results were good. The time spent on fitting and validating the PM6 model to PM4 and PM3 are approximately 1% of the time spent on developing the original model. This should be a strong incentive for focusing on mechanistic modeling in industries were there are many similar production lines or units.

Acknowledgements The authors would like to thank the employees at Norske Skog Saugbrugs and Norske Skog Skogn for their cooperation in providing information and data for this paper, and for their general helpfulness. In particular we would like to thank process engineer Tor Gunnar Heggli at Norske Skog Skogn. The work of Tor Anders Hauge is financially supported by the Research Council of Norway (project number 134557/432), with additional financial support by Norske Skog Saugbrugs.

References

Bassett, S. & Van Wijck, M. (1999), 'Application of predictive control technology at BP's crude oil terminal at grangemouth', *IEE Colloquium Digest* (95).

Betts, J. T. (2001), *Practical Methods for Optimal Control Using Nonlinear Programming*, SIAM.

Bown, R. (1996), Physical and chemical aspects of the use of fillers in paper, *in* J. Roberts, ed., 'Paper Chemistry', 2 edn, Chapman and Hall, chapter 11.

Box, G. E. P., Jenkins, G. M. & Reinsel, G. C. (1994), *Time Series Analysis, Forecasting and Control*, third edn, Prentice-Hall, Inc.

Foss, B. A., Lohmann, B. & Marquardt, W. (1998), 'A field study of the industrial modeling process', *Journal of Process Control* **8**, 325–338.

Gattu, G. & Zafiriou, E. (1992), 'Nonlinear quadratic dynamic matrix control with state estimation', *Ind. Eng. Chem. Res.* **31**(4), 1096–1104.

Glemmestad, B., Ertler, G. & Hillestad, M. (2002), Advanced process control in a Borstar PP plant, *in* 'ECOREPII, 2nd European Conference on the Reaction Engineering of Polyolefins. Lyon, France, 1-4 July 2002'.

Hauge, T. A. & Lie, B. (2002), 'Paper machine modeling at Norske Skog Saugbrugs: A mechanistic approach', *Modeling, Identification and Control* **23**(1), 27–52.

Hauge, T. A., Slora, R. & Lie, B. (2002), 'Application of a nonlinear mechanistic model and an infinite horizon predictive controller to paper machine 6 at norske skog saugbrugs', *Submitted to Journal of Process Control* .

Heggli, T. G. (2002). Personal communication with process engineer T. G. Heggli at Norske Skog Skogn.

Hillestad, M. & Andersen, K. S. (1994), Model predictive control for grade transitions of a polypropylene reactor, *in* 'ESCAPE4, 4th European Symposioum on Computer Aided Process Engineering, Dublin, March 1994'.

Kosonen, M., Fu, C., Nuyan, S., Kuusisto, R. & Huhtelin, T. (2002), Narrowing the gap between theory and practice: Mill experiences with multivariable predictive control, *in* 'Control Systems 2002', STFi and SPCI, pp. 54–59. June 3-5, 2002, Stockholm, Sweden.

Lee, J. H. & Ricker, N. L. (1994), 'Extended Kalman filter based nonlinear model predictive control', *Ind. Eng. Chem. Res.* **33**(6), 1530–1541.

Ljung, L. (1999), *System Identification, Theory for the User*, second edn, Prentice Hall PTR.

Marton, J. (1996), Dry-strength additives, *in* J. C. Roberts, ed., 'Paper Chemistry', Chapman and Hall, chapter 6.

Muske, K. R. & Rawlings, J. B. (1993), 'Model predictive control with linear models', *AIChE Journal* **39**(2), 262–287.

Nelles, O. (2001), *Nonlinear System Identification*, Springer.

Norske Skog (2002), Norske Skog internet page at www.norske-skog.com.

Ogunnaike, B. A. & Wright, R. A. (1997), Industrial applications of nonlinear control, *in* 'AIChE Symposium Series; 1997; Issue 316', pp. 46–59.

Richalet, J., Estival, J. L. & Fiani, P. (1995), Industrial applications of predictive functional control to metallurgical industries, *in* 'In Proceedings of the 4th IEEE Conference on Control Applications', pp. 934–942. Albany, N.Y.

Sandersen, E. (1999), 'Guide. Norske Skog Saugbrugs'. (Booklet).

Scott, W. E. (1996), *Principles of Wet End Chemistry*, Tappi Press, Atlanta.

Skogestad, S. & Postlethwaite, I. (1996), *Multivariable Feedback Control: Analysis and Design*, John Wiley & Sons Ltd.

Slora, R. (2001), Stabilization of the wet end at PM6. part 1: Developing controllers for the thick stock, Technical Report A-rapport RSL20001, Norske Skog Saugbrugs. (confidential and in Norwegian).

Söderström, T. & Stoica, P. (1989), *System Identification*, Prentice Hall International.

Sohlberg, B. (1998), *Supervision and Control for Industrial Processes*, Springer.

Støle-Hansen, K. (1998), Studies of some Phenomena in Control Engineering Projects - With Application to Precipitation Processes, PhD thesis, Norwegian University of Science and Technology.

The MathWorks, Inc. (2000), 'Optimization toolbox for use with matlab, user's guide (version 2)'.

Van de Ven, T. G. M. (1984), 'Theoretical aspects of drainage and retention of small particles on the fourdrinier', *Journal of Pulp and Paper Science* **10**(3), 57–63.

Walter, E. & Pronzato, L. (1997), *Identification of Parametric Models from Experimental Data*, Springer.